

HIGH ENERGY PHYSICS AT UCR

Table of Contents

I. PHYSICS RESEARCH	
A. Experimental High Energy Physics	1
1. Hadron Collider Physics - Task A1	1
a) Overview/Personnel/Talks/Publications	1
b) DØ : Proton-Antiproton Interactions at 2 TeV	10
c) SDC : Proton-Proton Interactions at 20 TeV	27
d) Nucleon Structure Functions	32
2. Task A2	51
2.1 Overview/Personnel/Talks/Publications	51
2.2 OPAL at LEP	69
2.3 The Compact Muon Solenoid at LHC	136
2.4 Neutrino Physics at LAMPF	144
2.5 TPC/2γ at PEP	148
2.6 Budget Justification	149
B. Theory	155
a) Introduction	155
b) Research Program	155
c) Publications	159
d) Travel and Consultants	161
e) Personnel and needs	162
f) Future Research Plans	162
II. BUDGET	164
III. VITAE AND PUBLICATIONS	182

MASTER

hg

TASK A1

DISCLAIMER

This report was prepared as an account of work sponsored by an agency of the United States Government. Neither the United States Government nor any agency thereof, nor any of their employees, makes any warranty, express or implied, or assumes any legal liability or responsibility for the accuracy, completeness, or usefulness of any information, apparatus, product, or process disclosed, or represents that its use would not infringe privately owned rights. Reference herein to any specific commercial product, process, or service by trade name, trademark, manufacturer, or otherwise does not necessarily constitute or imply its endorsement, recommendation, or favoring by the United States Government or any agency thereof. The views and opinions of authors expressed herein do not necessarily state or reflect those of the United States Government or any agency thereof.

DISCLAIMER

Portions of this document may be illegible in electronic image products. Images are produced from the best available original document.

9. Descriptive Summary of Work

The hadron collider group (Task A1) is studying proton-antiproton interactions at the world's highest collision energy 2 TeV. Data-taking with the DØ detector is in progress at Fermilab and we have begun the search for the top quark. S. Wimpenny is coordinating the effort to detect $t\bar{t}$ decaying to two leptons, the most readily identifiable channel. At UC Riverside design and testing for a silicon tracker for the DØ upgrade is in progress; a parallel development for the SDC detector at SSC is also underway.

The major group effort of Task A2 will be devoted to the OPAL experiment at LEP. We will continue to focus on data-taking to improve the quality and quantity of our data sample. A large number of papers has been published based on approximately 500,000 events taken so far. We will concentrate on physics analysis which provides stringent tests of the Standard Model. We are continuing our participation in the RD5 experiment at the SPS to study muon triggering and tracking. The results of this experiment will provide critical input for the design of the Compact Muon Solenoid experiment being proposed for the LHC.

The theory group (Task B) has been working on problems concerning the possible violation of e - μ - τ universality, effective Lagrangians, neutrino physics, as well as quark and lepton mass matrices.

10. "A New VME Based High Voltage Power Supply for Large Experiments", S.J.Wimpenny, M.-J. Yang, et al. Proceedings of the 1991 IEEE Nuclear Science Symposium, Santa Fe, Nov., 1991, pp. 984-989 (1992).

"A Measurement of the Strong Coupling Constant α_s at the CERN SPS Collider", M. Lindgren, M. Ikeda, D. Joyce, A. Kernan, J.-P. Merlo, D. Smith, and S.J. Wimpenny, Phys. Rev. D45, No. 9, 3038-3041 (1992).

"A Direct Measurement of the Z^0 Invisible Width by Single Photon Counting", M. Dittmar, W. Gorn, E.G. Heflin, C. Ho, W.J. Larson, J.G. Layter, J. Ma, B.P. O'Neill, H. Oh, K. Riles, B.C. Shen, G.J. VanDalen, Y. Yang et al. (OPAL Collaboration), Zeitschrift f. Physik C50, 373-384 (1991).

"A Direct Observation of Quark-Gluon Jet Differences at LEP", M. Dittmar, W. Gorn, E.G. Heflin, C. Ho, W.J. Larson, J.G. Layter, J. Ma, B.P. O'Neill, H. Oh, K. Riles, B.C. Shen, G.J. VanDalen, Y. Yang et al. (OPAL Collaboration), Phys. Lett. B265, 462-474 (1991).

"Measurement of Branching Ratios and τ Polarization from $\tau \rightarrow e\nu\bar{\nu}$, $\tau \rightarrow \mu\nu\bar{\nu}$, and $\tau \rightarrow \pi(K)\nu$ Decays at LEP", M. Dittmar, W. Gorn, E.G. Heflin, C. Ho, W.J. Larson, J.G. Layter, J. Ma, B.P. O'Neill, H. Oh, K. Riles, B.C. Shen, G.J. VanDalen, Y. Yang et al. (OPAL Collaboration), Phys. Lett. B266, 201-217 (1991).

10. (continued publications)

"Generation Nonuniversality and Precision Electroweak Measurements", X. Li and E. Ma, Phys. Rev. D46, Rapid Communications (in press).

"Screening in the QCD Instanton Gas and the U(1) problem", H. Kikuchi and J. Wudka, Phys. Lett. B284, 111 (1992).

1a.

TASK A1: HADRON COLLIDER PHYSICS OVERVIEW

The DØ detector moved into the Tevatron ring on February 14, 1992 and first collisions were observed shortly after the collider turn-on May 12. Commissioning of DØ has gone smoothly and no major problems have been encountered in either the detector or the data-acquisition system. The luminosity passed $10^{30} \text{ cm}^{-2} \text{ s}^{-1}$ in mid-July. We are scheduled to run until the end of March '93 with the expectation of collecting 25 pb^{-1} of data. Most of our group will be based at Fermilab for the duration of the run.

The group's primary responsibilities in the detector and data acquisition area are: the operation of the muon trigger system and the reconstruction of the muon momentum. An increasing effort will be devoted to physics analysis. S. Wimpenny is co-ordinator of the group which will look for evidence of the top quark in dilepton channels, and this will be the thesis topic of graduate student R. Hall. J. Ellison and A. Klatchko have initiated a project to measure directly the three vector boson coupling $WW\gamma$ and the W magnetic moment by studying the process $p\bar{p} \rightarrow W^\pm\gamma$; this will constitute the thesis research of graduate student A. Khachatourian. A. Kernan and graduate student T. Huehn are working on inclusive muon production and the b-quark production cross section.

A major upgrade of the DØ detector is required to match the increased luminosity ($5 \times 10^{31} \text{ cm}^{-2}\text{s}^{-1}$) and decreased bunch crossing time (132 ns) projected for Tevatron collider runs beyond 1995. Stage 1 of this upgrade involves replacement of the inner tracking system with a silicon microstrip detector covering the rapidity range $|\eta| < 3.3$. The silicon tracker will be a hybrid consisting of a central barrel and forward disks using both single- and double-sided silicon detector technology. The UCR group (Ellison, Heinson and Wimpenny) is playing a major role in the design and, together with LBL and Fermilab, will be responsible for its construction.

Our work on the SDC silicon tracker will continue, concentrating on radiation damage studies and R&D on the forward disk system. At UCR, we will work on the mask design for the double-sided AC-coupled wedge detectors, and then evaluate the prototypes produced. A test bench for testing approximately 500 production detector modules will be set up at UCR based on a computer controlled laser and x-y translation table.

The budget contains a request for \$44K for a laser scanner, which will be used for DØ silicon detector module testing. We plan a major upgrade to this system for use in SDC module testing and are submitting a TNRLC proposal for funding for this upgrade.

S. Wimpenny reported on "A New QCD Analysis of the EMC Hydrogen and Deuterium Data" in an invited talk to the Joint Lepton and Photon Symposium and Europhysics Conference, Geneva, July 1991. At Fermilab he presented a series of lectures on Hadron Collider Physics to DØ students and postdocs in Summer and Fall 1991. J. Ellison presented an invited talk:

"Temperature Effects on Radiation Damage to Silicon Detectors" at the sixth European Symposium on Semiconductor Detectors, Milan, February 1992.

Publications 3 (Double Pomeron Exchange in Proton-Antiproton Interactions at 630 GeV) and 7 (A Measurement of the Strong Coupling Constant α_s at the CERN SPS Collider) are based on the Ph. D. theses of graduate students D. Joyce and M. Lindgren. These are our final results from the UA1 experiment. The Double Pomeron Exchange results will be presented by A. Kernan at the Fermilab Workshop on "Small-x and Diffractive Physics at the Tevatron" in September 1992.

In August 1991 A. Kernan accepted the position of Vice-Chancellor for Research and Dean of the Graduate Division at UCR. She will continue to do research in particle physics. To compensate for her reduced effort the university has provided a new assistant professor position in experimental physics and support for a postdoc for two years. J. Ellison, formerly assistant research physicist, has been appointed to the assistant professor position; we are currently seeking his replacement. B. Choudhary is filling the UC funded postdoctoral position. Postgraduate researcher and former graduate student, D. Joyce, has accepted a postdoctoral position at UCLA. Ann Heinson, formerly of UCI, has joined the group.

Overall, the number of graduate students and postdoctoral researchers in the budget is unchanged. One additional undergraduate helper is requested. And for the additional faculty, J. Ellison, we are requesting summer salary and support for one quarter of leave to work on the collider run at Fermilab.

TASK A1: PERSONNEL

FACULTY

J. Ellison : assistant professor
A. Kernan : professor
S.J. Wimpenny : associate professor

POSTDOCTORAL RESEARCHERS

K. Bazizi : post graduate researcher
B. Choudhary : post graduate researcher
A. Heinson : post graduate researcher
A. Klatchko : post graduate researcher

GRADUATE STUDENTS

R. Hall
T. Huehn
A. Khachatourian

UNDERGRADUATE STUDENTS

T. Reed
J. Fleming
M. Mason

TALKS- HADRON COLLIDER TASK
8-91 to 8-92

1. "Calibration Plans"
J. Ellison
Silicon Tracker Subsystem Meeting, Univ. of California at Santa Cruz, August 1, 1991.
2. "A New QCD Analysis of the EMC Hydrogen and Deuterium Data"
S.J. Wimpenny
Invited talk, Joint International Lepton-Photon Symposium and Europhysics Conference on High Energy Physics, Geneva, 25th July-1st August 1991.
3. "The Reanalysis of the EMC Structure Function Data"
S.J. Wimpenny
Seminar to New Muon Collaboration, CERN, 3rd August, 1991.
4. "Review of W^\pm and Z^0 Physics from the 1991 Lepton-Photon Symposium"
S.J. Wimpenny
Review talk, Fermilab, 21st September 1991.
5. "Radiation Damage Results from 1991 LAMPF Run"
J. Ellison
Talk given at the SDC Silicon Tracker Subsystem Meeting
Santa Fe, New Mexico, Nov. 4, 1991.
6. "A New QCD Analysis of the EMC Hydrogen and Deuterium Data"
S.J. Wimpenny
D-Zero Seminar, Fermilab, November 14, 1991.
7. "Experimental Hadron Collider Physics"
S.J. Wimpenny
Series of 13 lectures given at Fermilab between September and December 1991.
8. "Top Quark Search via the Dimuon Decay Channel in $p\bar{p}$ Collisions at $\sqrt{s} = 1.8$ TeV"
R. Hall
DØ Collaboration Meeting, Fermilab, December 5, 1991.
9. "Temperature Effects on Radiation Damage to Silicon Detectors"
J. Ellison
Invited talk, Sixth European Symposium on Semiconductor Detectors,
Milan, Italy February 24-26, 1992.

10. "EMC and QCD - A New Analysis of the EMC Structure Function Data"
S. J. Wimpenny
Seminar, Univ. of California, Los Angeles, April 29, 1992.
11. "Silicon Detectors and the $WW\gamma$ Coupling: Two Topics in $p\bar{p}$ Physics Research at UCR"
J. Ellison
Seminar, UC Riverside, April 29, 1992.

**Publications - Hadron Collider Task
8-91 to 8-92**

1. "Radiation-Hard Frontend Electronics and Silicon Microstrip Detectors". J. Ellison and SDC Collaboration, Proceedings of the Symposium on Detector Research and Development for the SSC, Forth Worth, TX, Oct. 15-18, 1990, World Scientific Publishing, Singapore, pp. 166-168 (1991).
2. "A New QCD Analysis of the EMC Hydrogen and Deuterium Data", S.J. Wimpenny. Proceedings of the Joint International Lepton-Photon Symposium and Europhysics Conference on High Energy Physics, Geneva, July 1991, World Scientific Publishing, 145-146 (1992).
3. "Double Pomeron Exchange in Proton-Antiproton Interactions at 630 GeV", D. Joyce, A. Kernan, M. Lindgren, B.C. Shen, D. Smith, S.J. Wimpenny (UC Riverside) and M.G. Albrow, B. Denby, G. Grayer (Rutherford-Appleton Lab, U.K.), Proceedings of the XXIth International Symposium on Multiparticle Dynamics, Wuhan, China, 23-27 September 1991, (in press).
4. "A New VME Based High Voltage Power Supply for Large Experiments", S.J. Wimpenny, M.-J. Yang, et al., Proceedings of the 1991 IEEE Nuclear Science Symposium, Santa Fe, Nov., 1991, pp. 984-989 (1992).
5. "Parametrization of the Multiple Coulomb Scattering Error in High Energy Physics Detectors", A. Klatchko, Fermilab Pub. 92/46, UCR/D0/92-01, Nucl. Instr. Meth., (in press).
6. "Temperature Effects on Radiation Damage to Silicon Detectors", J. Ellison, J.K. Fleming, S. Jerger, D. Joyce, C. Lietzke, E. Reed, S.J. Wimpenny, et al., Proceedings of the Sixth European Symposium on Semiconductor Detectors, Milan, Italy, Feb. 1992, Nucl. Instr. Meth., (in press).
7. "A Measurement of the Strong Coupling Constant α_s at the CERN SPS Collider", M. Lindgren, M. Ikeda, D. Joyce, A. Kernan, J.-P. Merlo, D. Smith, and S.J. Wimpenny, Phys. Rev. D45, No. 9, 3038-3041 (1992).
8. "Beam Tests of the DØ Uranium Liquid Argon End Calorimeters", K. Bazizi, J. Ellison, R. Hall, T. Huehn, A. Kernan, A. Klatchko, D. Smith, S.J. Wimpenny, M.-J. Yang and DØ Collaboration (1992), 66 pp., Nucl. Instr. Meth., (in press).

PAPERS SUBMITTED TO CONFERENCES

1. "A QCD Analysis of the Proton Structure Function $F_2(x, Q^2)$ ", K. Bazizi, S.J. Wimpenny, UCR/DIS/91-03. Submitted to Joint International Lepton and Photon Symposium and Europhysics Conference on High Energy Physics, Geneva, 25th July-1st August, 1991.
2. "A Comparative Study of Structure Function Measurements from Hydrogen and Deuterium", K. Bazizi, S.J. Wimpenny, UCR/DIS/91-02. Submitted to Joint International Lepton and Photon Symposium and Europhysics Conference on High Energy Physics, Geneva, 25th July-1st August, 1991.
3. "Double Pomeron Exchange in $p\bar{p}$ Interactions at 0.63 TeV", D. Joyce, A. Kernan, M. Lindgren, D. Smith, S.J. Wimpenny, et al., Submitted to XXVI International Conference on High Energy Physics, Dallas, TX, Aug. 5-12, 1992.

Technical Notes - Hadron Collider Task
8-91 to 8-92

D-Zero Notes

1. "The Kalman Filter Technique and Multiple Coulomb Scattering Error for the DØ User", A. Klatchko, T. Fahland, DØ Note 1160, UCR/DØ/91-05, (1991).
2. "Radiation Levels in DØ and Effects on Silicon Detectors", J. Ellison, DØ Note 1155, UCR/DØ/91-06 (1991).
3. "A Search for the $t\bar{t} \mu\mu$ in the Double Blind 100K Challenge Events", R. Hall, DØ Note, 1189, UCR/DØ/91-07 (1991).
4. "Review of W^\pm and Z^0 Physics from 1991 Lepton-Photon Symposium", S.J. Wimpenny, DØ Note 1187, UCR/DØ/91-08.
5. " $Z^0 \rightarrow \mu^+\mu^-$ with MUFITS", A. Klatchko, DØ Note 1198, UCR/DØ/91-09.
6. "The Physics of W^\pm and Z^0 Production and Decay - I. Mass and Width of the W^\pm and Z^0 ", S.J. Wimpenny, DØ Note 1252, UCR/DØ/91-10.
7. "The Physics of W^\pm and Z^0 Production and Decay - II. Production Cross-Sections, - Production and Decay Asymmetries", S.J. Wimpenny, DØ Note 1253, UCR/DØ/91-11.
8. "Heavy Flavor Production I - General Features of $O(\alpha_s^2)$ and $O(\alpha_s^3)$ Processes - J/ψ Production, ψ' Production", S.J. Wimpenny, DØ Note 1254, UCR/DØ/91-12.
9. "Heavy Flavor Production II - Υ Production - Drell-Yan $\mu^+\mu^-$ Pairs - Charm Fragmentation in Jets", S.J. Wimpenny, DØ Note 1255, UCR/DØ/91-13.
10. "Neutrino Counting", S.J. Wimpenny, DØ Note 1260, UCR/DØ/91-14.
11. "Heavy Flavor Physics III - Inclusive Muon Cross-Section, b-quark Cross-Section - B-hadron Cross Section", S.J. Wimpenny, DØ Note 1256, UCR/DØ/91-15.
12. "Heavy Flavor Production IV - b-quark Total Cross-Section, Evidence for b-quark Production", S.J. Wimpenny, DØ Note 1261, UCR/DØ/91-16.
13. "Heavy Flavor Production V - B^0 - \bar{B}^0 Mixing", S. J. Wimpenny, DØ Note 1263, UCR/DØ/91-17.
14. "Missing Energy Analysis I", S.J. Wimpenny, DØ Note 1267, UCR/DØ/91-18.

15. "Missing Energy Analysis II - UA2 $W \rightarrow \tau\nu$ Analysis, - CDF $W \rightarrow \tau\nu$ Analysis", S.J. Wimpenny, DØ Note 1268, UCR/DØ/91-19.
16. "A New QCD Analysis of the EMC Hydrogen and Deuterium Data", S.J. Wimpenny, DØ Note 1269, UCR/DØ/91-20.
17. "Missing Energy Analysis III - What remains after $W \rightarrow \tau\nu$ is removed?", S.J. Wimpenny, DØ Note 1275, UCR/DØ/91-21.
18. "A Study of $\pi/K \rightarrow \mu\nu$ in-flight Decay Backgrounds in the Central Region, $|\eta| < 0.76$ ", T. Huehn, DØ Note 1288, UCR/DØ/91-22.
19. "The Search for Something New - Part I - The Top Quark", S.J. Wimpenny, DØ Note 1286, UCR/DØ/91-23.
20. "Level 1.0 Muon Trigger Test in the Spring Cosmic Ray Run", K. Bazizi, DØ Note 1145, UCR/DØ/91-25.
21. "Discovering Top at DØ", R. Hall, DØ Note 1305, UCR/DØ/91-26.
22. "Estimation of the Multiple Coulomb Scattering Error for a Large Number of Radiation Lengths", B.C. Choudhary, A. Klatchko, and T. Huehn, DØ Note 1406, Fermilab Pub. 92/116, UCR/DØ/92-02, Nucl. Instr. Meth., (in press) 1992.
23. "Testing the $WW\gamma$ Vertex by DØ - Measurements of the Magnetic Dipole moment of the W boson", H. Aihara, T. Spadatoro (LBL), J. Ellison, A. Klatchko (UCR), DØNote 1368, UCR/DØ/92-03.

1b. DØ : PROTON-ANTIPROTON INTERACTIONS AT 2 TeV

1. Introduction

Riverside joined the DØ collaboration at Fermilab in late 1986. Our work to date spans four areas: the implementation of the high voltage system, hardware/software development for the DØ muon system, R&D studies for a silicon microstrip detector for the DØ upgrade and Monte Carlo studies of various physics scenarios. Seven UCR physicists are currently stationed at Fermilab.

Work on the high voltage system is essentially completed. Our primary responsibilities in the detector and data reconstruction area are: the operation and continuing development of the muon trigger system and the muon reconstruction software. An increasing effort will be devoted to physics analysis. We are focussing on the top quark in dilepton channels, the W magnetic moment and the b-quark production cross section; these topics will constitute the thesis research of our graduate students. R&D studies for a silicon microstrip detector for the DØ upgrade are in progress at UCR; these are being done in parallel with similar studies for the SSC.

Section 2 outlines the physics goals and general features of the DØ detector. Section 3 details the activities of the Riverside group.

2. Physics and detector

DØ is a 4π non-magnetic hermetic detector designed for the Tevatron Collider at Fermilab. The evolution of the DØ design has benefitted substantially from the experience with the UA1 and UA2 detectors at CERN and the CDF detector at Fermilab. Additional input from the ongoing SSC R&D program has also proved valuable especially in the areas of readout and tracking designs for the projected Tevatron upgrades. In overall concept DØ complements the strengths of the CDF detector.

The dominant emerging areas for new physics at the Tevatron are the search for the top quark and exploration of the B-physics sector. In addition the general themes of the Tevatron program include: (i) precision measurements of W and Z properties (mass differences, decay widths, production mechanisms, rare decays, decay asymmetries, study of trilinear boson couplings); (ii) tests of QCD at very large Q^2 (jet topological cross sections, searches for parton compositeness, direct photon studies, searches for quark-gluon phase transitions, measurement of fragmentation functions); (iii) searches for new states which could direct the extension and evolution of the standard model (manifestations of supersymmetry - squarks, gluinos, winos, zinos, sleptons), technicolor particles, heavy leptons, additional gauge bosons, or massive quasistable objects; (iv) measurement of the characteristics of the large cross-section, low p_T processes (multiplicity distributions, multiparton collisions, emergences of some new phenomena

glimpsed in cosmic ray experiments); and (v) sensitivity to qualitatively new phenomena in the heretofore unexplored high energy, large Q^2 domain.

These physics issues dictated the basic design choices for $D\bar{O}$:

i.) No central magnetic field is provided. Since the relevant particles to be detected are jets (partons), leptons and non-interacting secondaries (neutrinos, photinos etc.) at large momentum, calorimetric measurement of energies are superior to momentum determination by track curvature. Moreover, a non-magnetic tracking system can be compressed, giving the opportunity for enhanced calorimetry and muon detection.

ii.) Lepton identification is of fundamental importance in searching for most high mass states, due to the relative cleanliness of leptonic decay modes of W,Z and heavy quarks. Measurement of both electrons and muons over the fullest possible solid angle is highly desirable; electron and muon measurements have quite different systematics so confirmation of new effects in both channels is highly beneficial. Electron channels are superior for precision mass measurements, while muons offer the possibility of seeing a lepton within a jet.

iii.) Measurement of the missing transverse energy in an event is crucial for many studies, and achievement of the best possible E_T resolution is a dominant goal. It is of particular importance to prevent unknown large fluctuations in measured event E_T , particularly far out in the tails of the distribution, in order to avoid having common event types simulate new physics. Good missing E_T resolution involves optimization of several features of the detector. Calorimeter coverage should cover the full solid angle with minimal cracks or hot spots. Holes for beam entrance and exit should be limited to $\theta < 1^\circ$ ($\eta \geq 5$). Good energy resolution helps control the rms width of the E_T distribution; of more importance here is the near equality of response to electrons and hadrons so that fluctuations in hadron shower composition are of minimal importance. Fig 1 is a schematic of the $D\bar{O}$ detector.

The completed $D\bar{O}$ detector was moved into the Tevatron ring on February 14th 1992 and first collisions were observed shortly after the collider turn-on on May 12th. The period immediately following May 12th was used to tune the Tevatron optics (initial instantaneous luminosity was only 10^{27}) and to commission the $D\bar{O}$ detector. A significant fraction of the detector was commissioned prior to 'roll-in' during two Cosmic Ray runs in the fall of 1991 and spring of 1992 and no major problems were found in either the detector or the data-acquisition system. For the first two months of running the Tevatron luminosity remained low and the machine reliability poor. Initial physics studies have concentrated on the optimization of the Level 1 and Level 2 trigger algorithms and the search for W and Z decays into electrons and muons. Both have been observed at rates consistent with the measured production cross-sections from the CDF Collaboration [1,2]. By mid-July many of the problems with the Tevatron and anti-proton

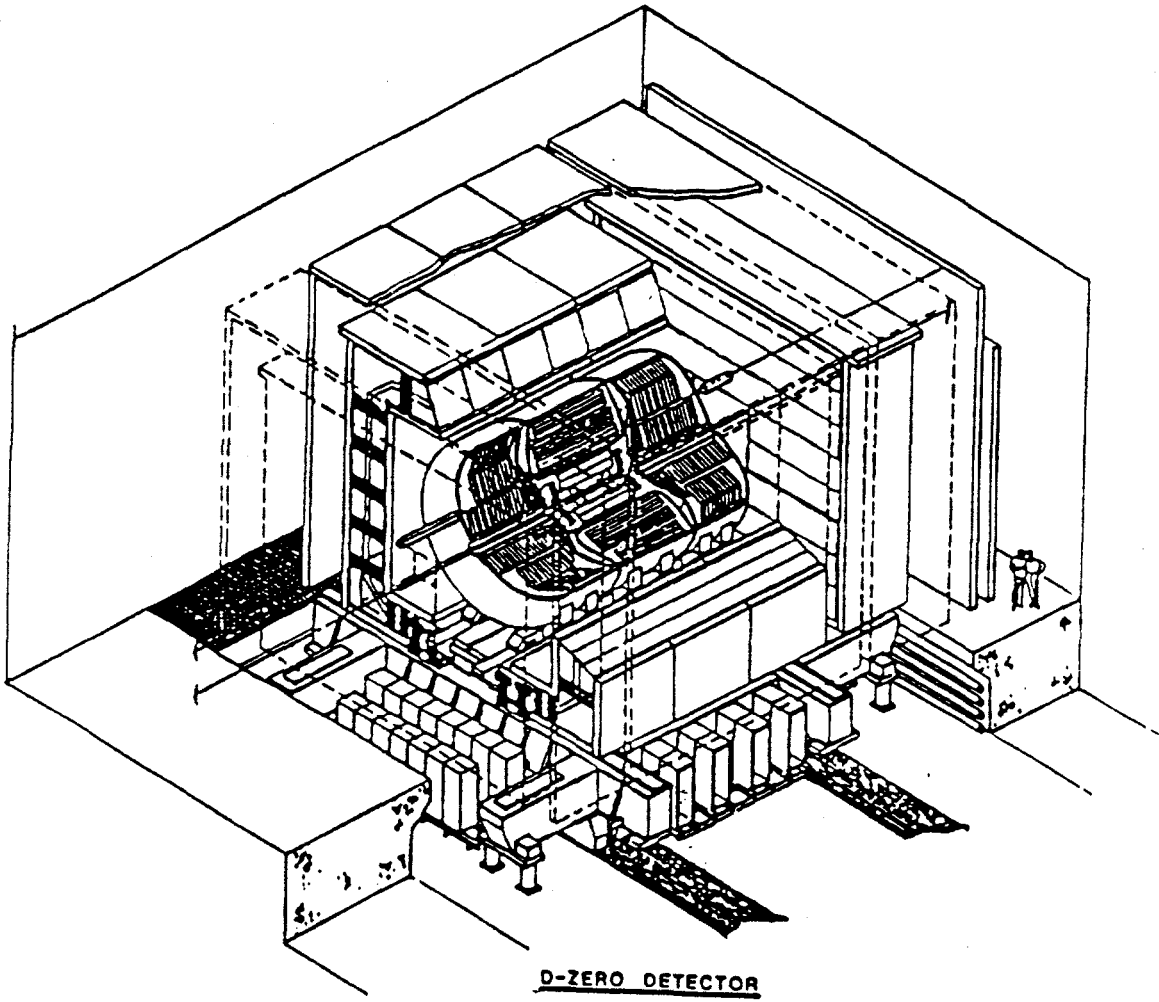


Fig. 1 Schematic View of the D-Zero Detector

accumulator optics have been corrected and we anticipate the first high luminosity running (instantaneous luminosity $> 10^{30}$) in mid-August after the current shutdown.

References

- [1] F. Abe et al. (CDF Collaboration) Phys. Rev. D44 (1991) 29.
- [2] F. Abe et al. (CDF Collaboration) Phys. Rev. Lett. 69 (1992) 28.

3. Riverside Activities

Following DØ 'roll-in' we have a major responsibility for the operation of the muon trigger system and the reconstruction of muon data (section 3.1). This is shared with the Arizona, Fermilab and Northern Illinois groups. Work on the design and implementation of the DØ high voltage system for which S.J. Wimpenny was largely responsible is completed and the full system is operational (section 3.2). Physics analysis activities include i) a search for associated $W + \gamma$ production (section 3.3.1), ii) the measurement of the inclusive muon cross-section (section 3.3.2) and iii) the search for the top quark (section 3.3.3). Following the Stage 1 approval of the DØ detector upgrade, the Riverside group is playing a major role in the design and construction of the new central silicon tracking system (section 3.4). This is a joint project between Riverside, Fermilab and LBL.

Six UCR people are currently fulltime at Fermilab: postdocs K. Bazizi, A. Klatchko and B. Choudhary and grad students R. Hall, A. Khachatourian and T. Huehn; in addition S. Wimpenny will be at Fermilab from July through December 1992.

3.1 The DØ Muon System

In DØ the muon detection system covers the entire solid angle to within 2.5° of the circulating beams. It consists of two toroidal magnetic spectrometer systems: WAMUS and SAMUS. WAMUS, the Wide Angle Muon Spectrometer, consists of one central and two endcap iron toroids instrumented with planes of proportional drift tubes (PDT) for tracking; angular coverage extends from within 10° to 170° of each beam. The Small Angle Muon Spectrometer extends coverage down to 2.5° using two iron toroids and PDT planes. An elevation view of the combined system is shown in Fig. 2.

About 80% of large-angle PDT's were commissioned during cosmic ray runs in the Spring and Fall of 1991 cosmic ray run with the detector outside of the collision hall. This work was completed following 'roll-in' in February 1992 and the muon detector was integrated into the central DØ trigger framework. Figure 3 shows a cosmic ray muon traversing the various sub-systems.

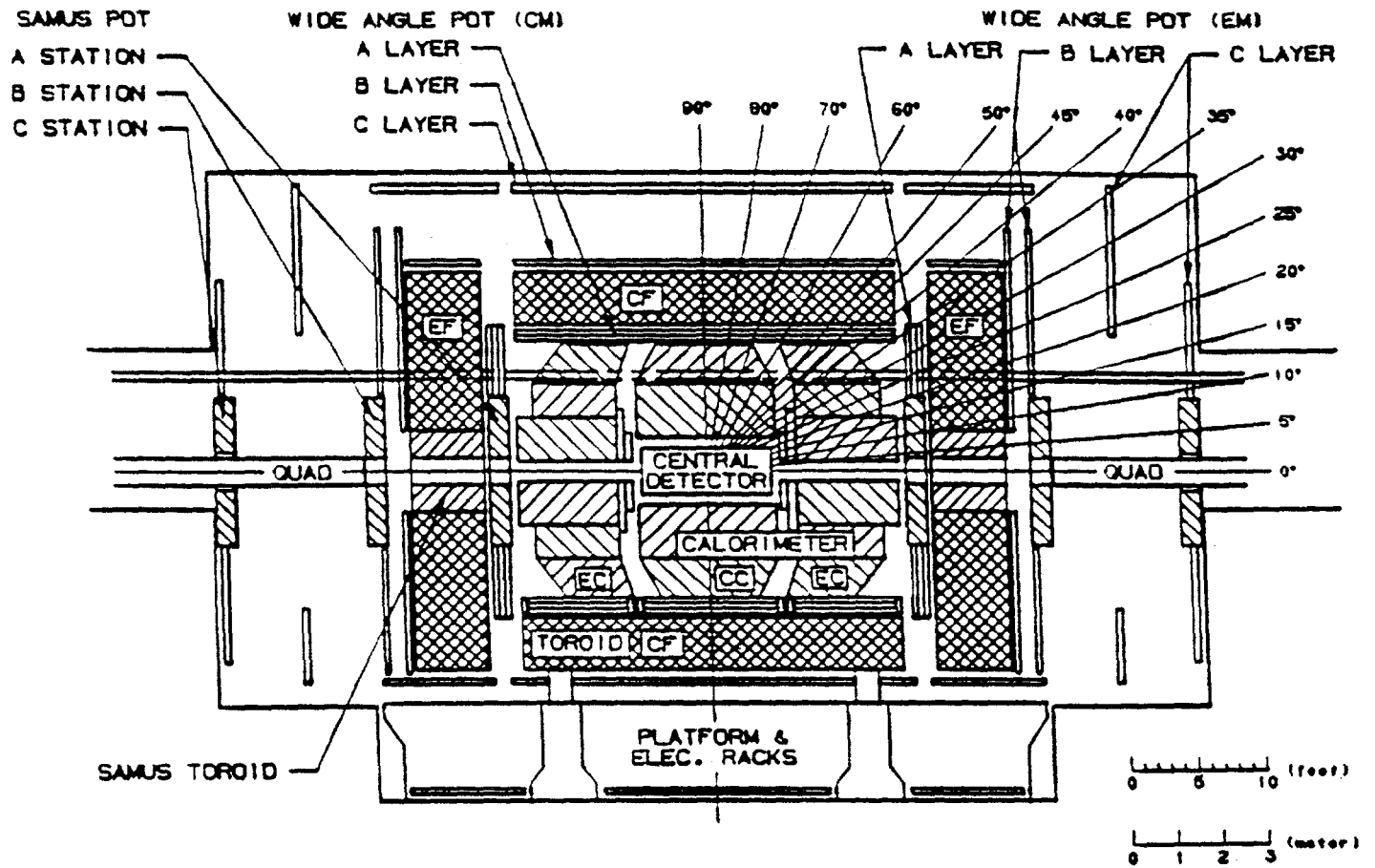


Fig.2 Side Elevation of the D-Zero Muon System

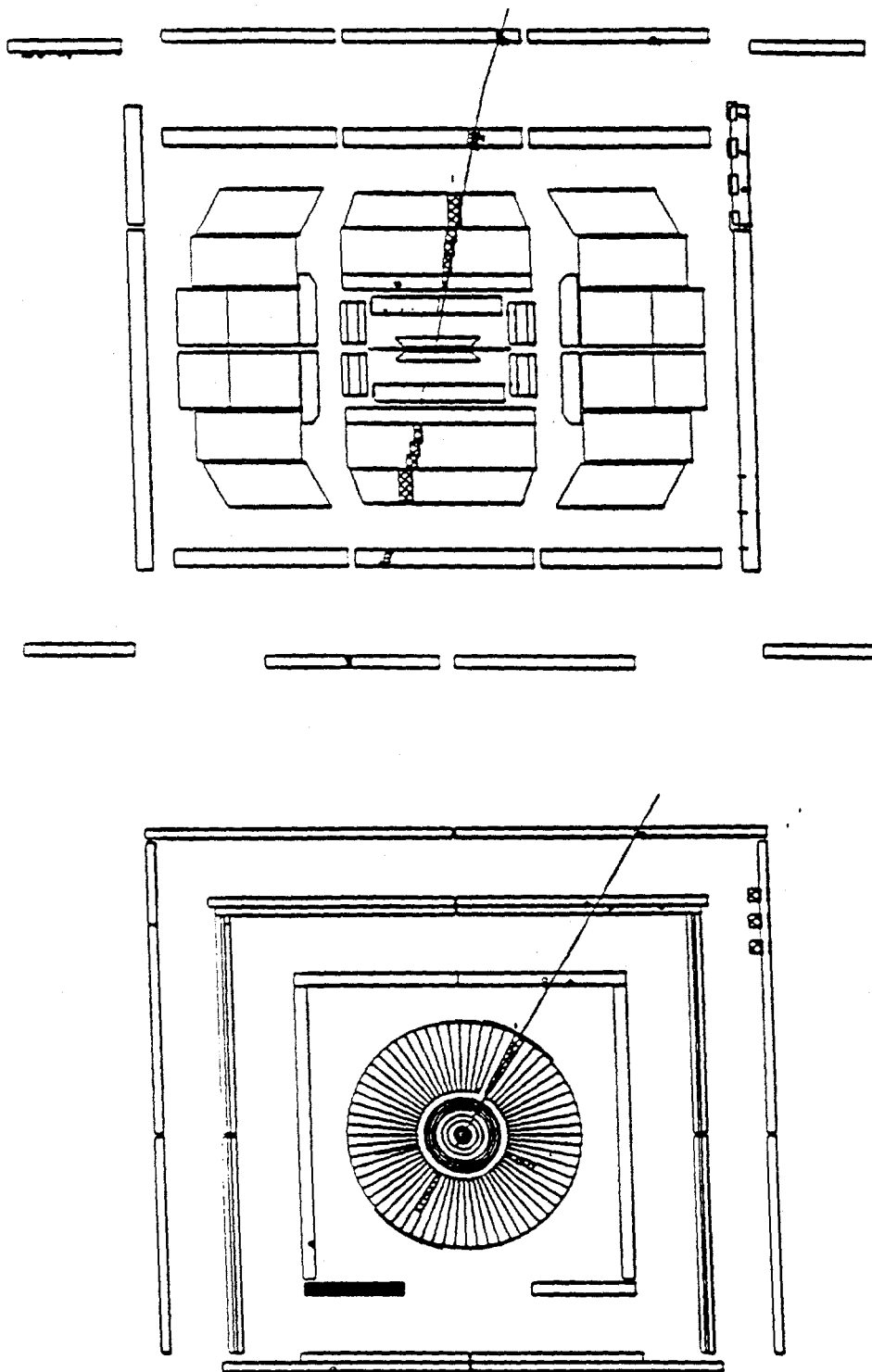


Fig.3 A Cosmic Ray Event from the Spring Run

At present and throughout most of the coming year the major UCR hardware effort will be devoted to optimizing the muon trigger and to running the DØ muon system.

3.1.1 Hardware

During the last year K. Bazizi has been coordinating the muon trigger group, consisting of 13 physicists, graduate students and engineers. He led the UCR effort in developing, installing and testing the level 1 muon trigger for all elements of the DØ system. In addition UCR has played a major role in upgrading the data acquisition hardware for compatibility with the higher level muon triggers, which are in the process of integration. UCR graduate students made a significant contribution to these efforts: R. Hall through his expertise on the Module Address cards and T. Huehn in testing and installing the Coarse Centroid Trigger cards.

The level 1 muon trigger is a fast hardware trigger which signals a track traversing the muon detector. It has been extensively used for recording calibration and alignment data; it also provided triggers for the other DØ subsystems such as the calorimeter and the central tracking chambers during the Winter-Spring 92 cosmic ray commissioning run. The muon trigger is currently operational at $\theta > 20^\circ$ for $p\bar{p}$ collisions. However at luminosities around 10^{30} the high rates restrict the trigger range to $\theta > 40^\circ$.

In the coming year the UCR group will work on extending the level 1 muon trigger below θ of 20° . This will be a challenging task since no $p\bar{p}$ experiment to date has been able to trigger on muons in this region. Due to the higher multiplicity of charged particles in the forward direction new trigger cards with better centroid resolution must be designed for this region. K. Bazizi will lead this effort; he will also continue to be responsible for the muon trigger simulator and its interface with the DØ trigger simulator package. This software has been used extensively in developing trigger schemes and in trigger efficiency and rate studies.

3.1.2 Software

As shown in Fig. 4 a muon track is registered by the A layer (4 space points) of PDT's before the toroid, and by the B and C layers (3 space points each) after the toroid. The expected spatial resolution is 2.0 mm along the wire and 0.5 mm perpendicular to the wire. Momentum resolution is limited to 18% by multiple Coulomb scattering in the toroid.

UCR is working on the online and offline muon reconstruction programs. A. Klatchko assumed responsibility for the muon online software at the start of 1992. Since then he has combined the WAMUS and SAMUS routines and integrated them into the global DØEXAMINE. He is writing routines for online examination of the muon data as well as maintaining/debugging existing routines.

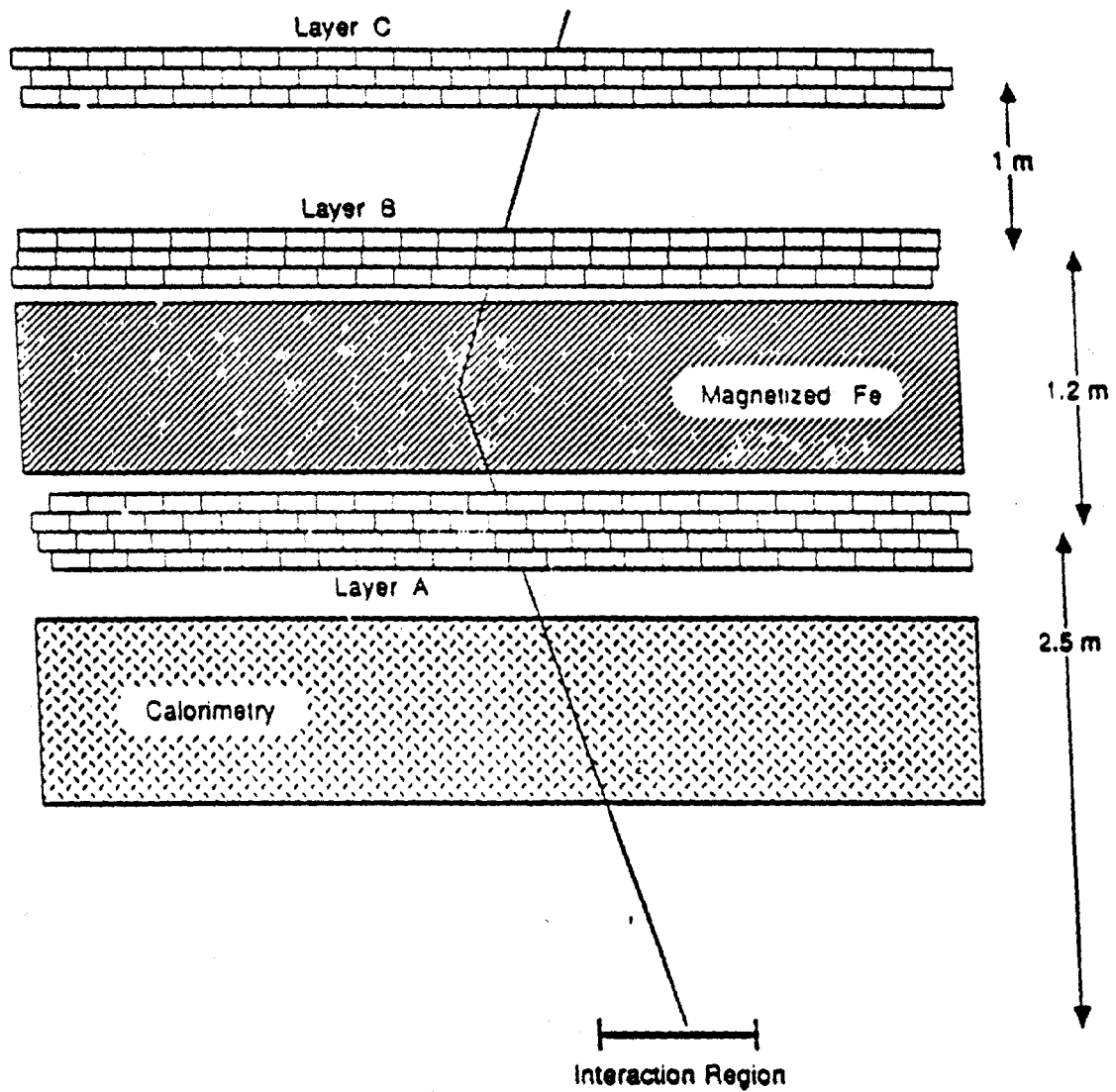


Fig.4 Schematic View of a Muon traversing the PDT Chambers

In offline reconstruction B. Choudhary and A. Klatchko are responsible for the final muon track reconstruction through the muon chambers and are working with the Fermilab group on the global muon fit based on all available tracking information. Their current studies include:

- reconstruction of muonic W decays,
- optimizing the muon momentum reconstruction algorithm,
- improving the magnetic field map,
- parametrization of multiple Coulomb scattering errors.

3.2 DØ High Voltage System

The DØ high voltage system is a computer controlled power system which provides high voltage power to all of the parts of the detector. It consists of a VME power supply and control system which are mounted in the moveable counting house, a remote control system which operates from the main control room and a passive splitter and distribution system. Each of these items has been custom designed for DØ by a joint UCR and Fermilab team.

The full system has been installed and commissioned and is used to power and monitor the DØ detector. A small amount of additional software development is needed to implement some additional features in the central VAX-based control system. At present one UCR person is working on this project: S.J. Wimpenny who will be based at Fermilab for the second half of 1992.

3.2.1 Hardware

We have coordinated work on the design of the DØ high voltage system since early 1987. The system is built around a 6U x 160 mm VME module which contains 8 independent high voltage power supplies (Fig.5). These can be run as either 0 to ± 5.6 kV at 1mA (for the central tracking chambers, muon system and calorimeters) and or 0 to ± 2 kV at 3mA (for the Level 0 trigger and Inter Cryostat Detector scintillation counters). Apart from the wide dynamic range these units are also required to be low noise and to have fast response for current and trip monitoring[1]. The design, fabrication and implementation of the system is completed and we are in the process of refining the documentation [2] and monitoring system.

Work on the distribution system is completed and all of the cabling, and splitter systems have been installed and are in use in the collision hall. The cabling and connector system are now available as off-the-shelf commercial products. The high voltage power supply module will follow later this year.

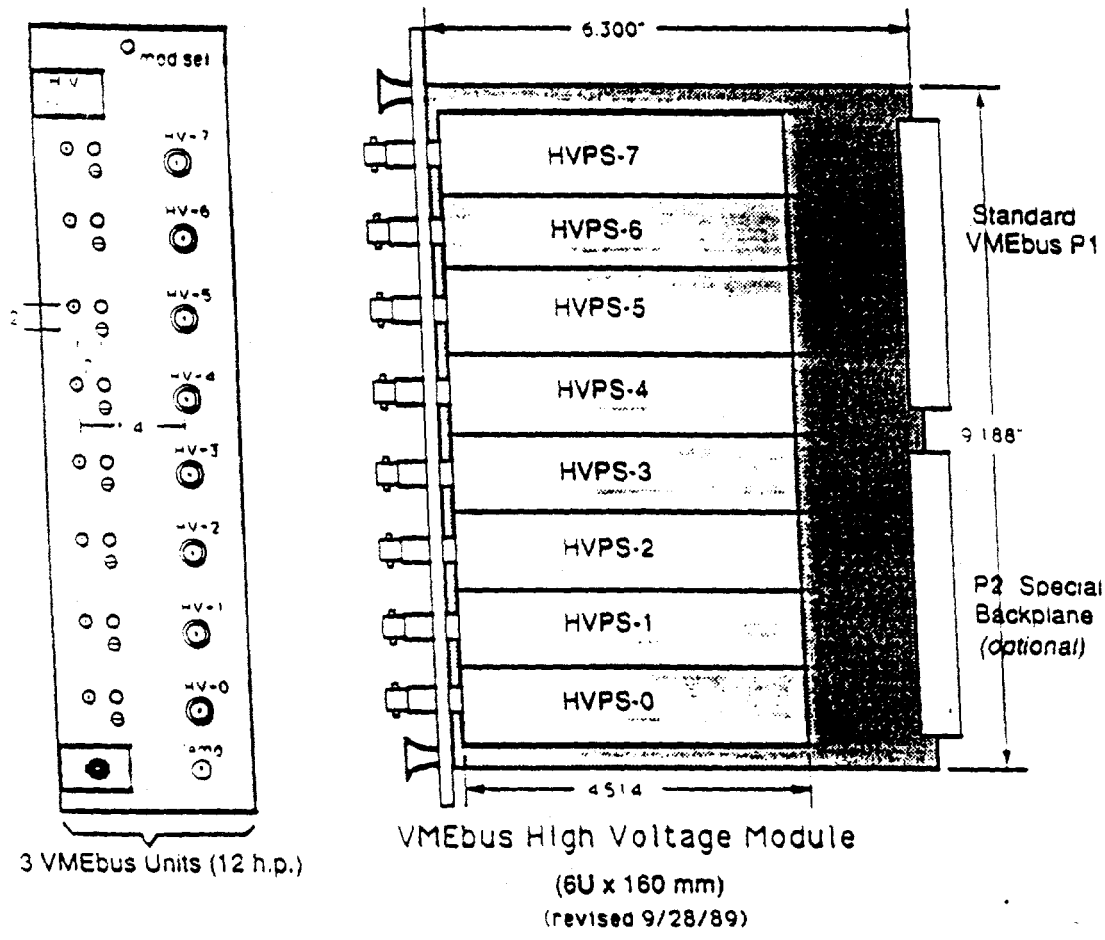


Fig. 5 Schematic of the D-Zero VMEbus High Voltage Power Supply

3.2.2 Software

Control of the power system is provided either locally via a PC or remotely from a VaxStation in the DØ Control Room (Fig.6). The microprocessor and PC software have been implemented by S.J. Wimpenny and M-J. Yang and were commissioned during the Fall 1991 cosmic ray run [2]. In addition to the basic control functions the system has a suite of diagnostic routines for use in studying time stability and noise levels (eg. Fig.7). The Vax system is also operational and was debugged during the commissioning studies of the spring and early summer of 1992.

References

- [1] S.J. Wimpenny, M.-J. Yang, "A New VME Based High Voltage Power Supply for Large Experiments". Proceedings of the IEEE Nuclear Science Symposium, Santa Fe, Nov. 91, 984-989.
M.-J. Yang, Nucl. Phys. B. Vol. 23A, pp. 402-408, 1991.
T. Droege et al., Nucl. Instr. Meth., A279, 3359- (1989).
- [2] "The DØ High Voltage System Users Guide", M-J. Yang and DØ Group , DØ Note 1175.

3.3 Physics Analysis

With the first data-taking now in progress we are working on data analysis and the development of software tools for the level 2 trigger and the offline analysis packages. As a group we are concentrating our efforts on the search for the top quark, muonic decays of the b-quark and the W magnetic moment. The studies in progress are summarized below.

3.3.1 Testing the $WW\gamma$ coupling in DØ

At the Tevatron, the process $p\bar{p} \rightarrow W^\pm\gamma$ provides an opportunity to measure directly the three vector boson coupling $WW\gamma$. In the Standard Model (SM), at the tree level, this coupling is completely fixed by the gauge theory structure of the model. The experimental observation of the $WW\gamma$ coupling is therefore a crucial test of the SM, and has so far been measured only by UA2 with very limited accuracy. In runs Ia and Ib of the DØ experiment we expect to collect a data sample of about 100 pb^{-1} and therefore make a much more sensitive measurement.

At the parton level the principal processes are:

$$\begin{aligned} q + \bar{q}' &\rightarrow \gamma + W^- (W^- \rightarrow l^- + \bar{\nu}) && \text{"production"} \\ q + \bar{q}' &\rightarrow W^- \rightarrow \gamma + l^- + \bar{\nu} && \text{"decay"} \end{aligned}$$

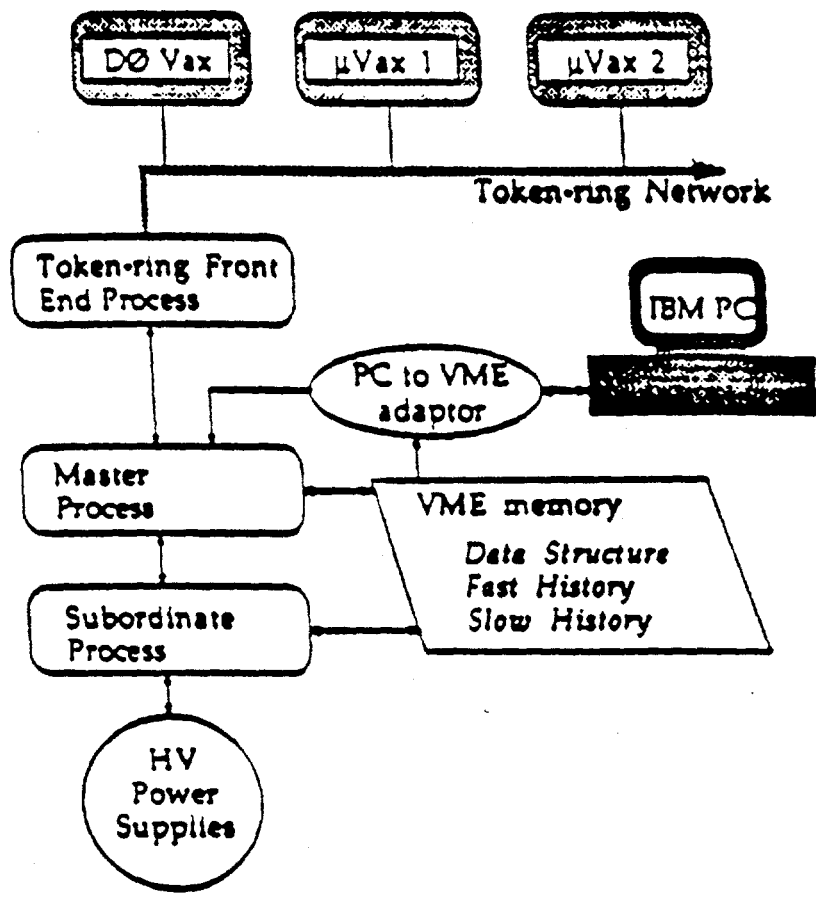


Fig. 6 Software Configuration of the High Voltage Control System

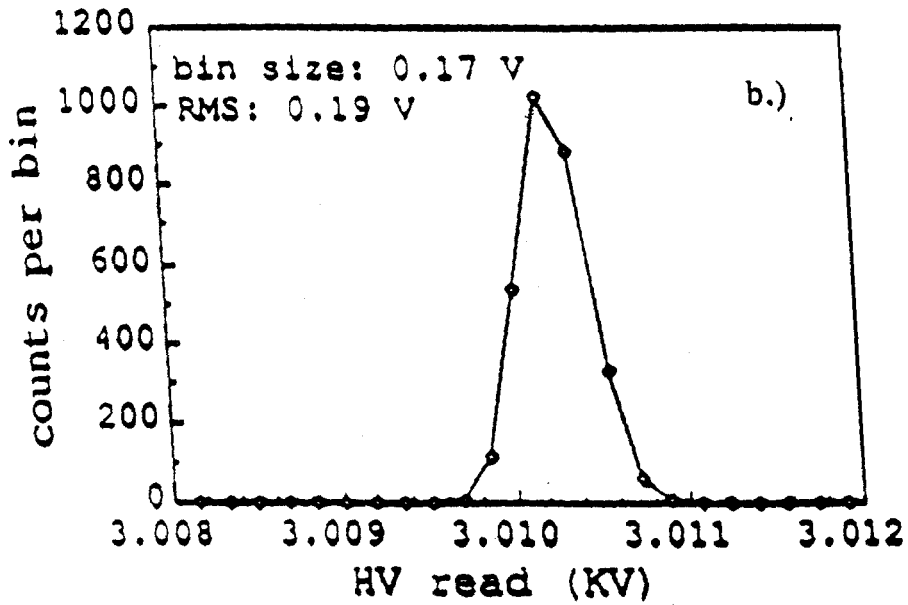
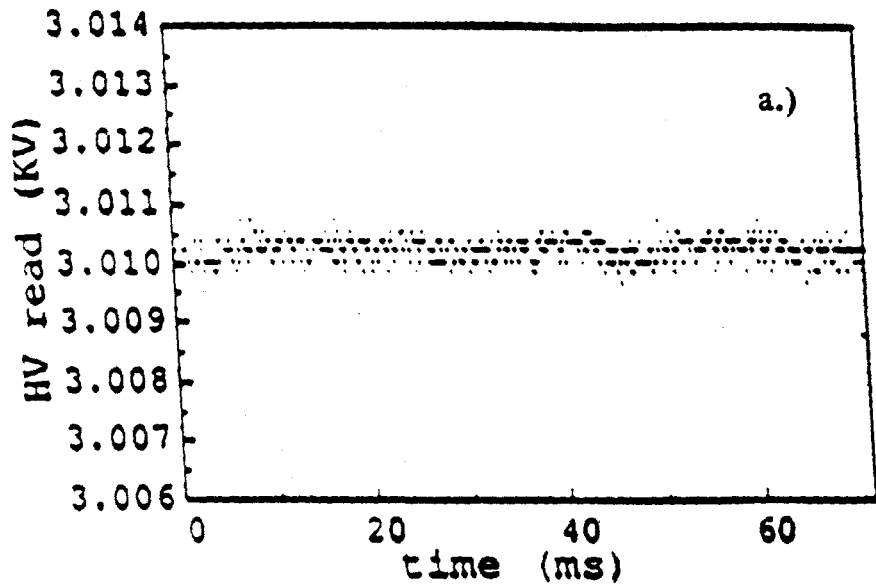


Fig. 7 Displays of the ADC Readback of High Voltage Output Signal
 a.) Time Stability
 b.) Resolution Histogram

The general WW γ coupling can be described by four free parameters and is given by the effective Lagrangian

$$\begin{aligned} \mathcal{L}_{WW\gamma} = & -ie [(W_{\mu\nu}^\dagger W^{\mu A\nu} - W_{\mu}^\dagger A_{\nu} W^{\mu\nu}) \\ & + \kappa W_{\mu}^\dagger W_{\nu} F^{\mu\nu} + \frac{\lambda}{m_W^2} W_{\lambda\nu}^\dagger W_{\nu}^{\mu} \tilde{F}^{\nu\lambda} \\ & + \tilde{\kappa} W_{\mu}^\dagger W_{\nu} \tilde{F}^{\mu\nu} + \frac{\tilde{\lambda}}{m_W^2} W_{\lambda\nu}^\dagger W_{\nu}^{\mu} \tilde{F}^{\nu\lambda}] \end{aligned} \quad (1)$$

where A_{μ} is the photon field W^{μ} is the W^- field, $W^{\mu\nu} = \partial_{\mu} W_{\nu} - \partial_{\nu} W_{\mu}$, $F^{\mu\nu} = \partial_{\mu} A_{\nu} - \partial_{\nu} A_{\mu}$ and, $\tilde{F}_{\mu\nu} = \frac{1}{2} \epsilon_{\mu\nu\rho\sigma} F^{\rho\sigma}$.

The first term in equation 1 is the so-called "minimal" coupling term, and the second coefficient κ is conventionally called the "anomalous" magnetic moment of the W . This term and the third coefficient λ are related to the magnetic dipole moment μ_W and the electric quadrupole moment Q_W of the W by

$$\mu_W = \frac{e}{2m_W} (1 + \kappa + \lambda) \quad (2)$$

$$Q_W = \frac{e}{m_W^2} (\kappa - \lambda) \quad (3)$$

While κ and λ do not violate any discrete symmetries, the $\tilde{\kappa}$ and $\tilde{\lambda}$ terms are P odd and CP violating. They are related to the electric dipole moment d_W and the magnetic quadrupole moment \tilde{Q}_W of the W by

$$d_W = \frac{e}{2m_W} (\tilde{\kappa} + \tilde{\lambda}) \quad (4)$$

$$\tilde{Q}_W = \frac{e}{m_W^2} (\tilde{\kappa} - \tilde{\lambda}) \quad (5)$$

In the SM at tree level, $\kappa = 1$, $\lambda = 0$, $\tilde{\kappa} = 0$ and $\tilde{\lambda} = 0$. The consequences of deviations of these parameters from their SM values are:

- The cross-section for the process $p\bar{p} \rightarrow W^\pm\gamma$ increases and thus any excess of events measured will be an indication for physics beyond the SM.
- The differential distributions for some kinematical variables depend strongly on κ , λ , $\tilde{\kappa}$ and $\tilde{\lambda}$. Such variables are, for example, the transverse momentum of the photon ($p_{T\gamma}$), the invariant mass of the $W\gamma$ system ($M_{W\gamma}$) and the angular distribution of the photon in the partonic center of mass system ($\cos\theta^*$).

By comparison with theoretical predictions for the above quantities we expect to achieve 25% accuracy in the measurement of these parameters. This study will constitute the thesis project of graduate student A. Khachatourian. He has already started the generation and analysis of $W\gamma$ events at the parton level.

Two Monte Carlo programs, Papageno and Baur and Zeppenfeld have been used to generate $p\bar{p} \rightarrow W^\pm\gamma$ events. We have found good agreement between the two programs. Fig. 8 shows the variation of the cross-section with κ when the other parameters are fixed at their SM values. With the cuts given in the figure, the minimum cross-section is $10.2 pb^{-1}$ for $\kappa = 0$. After accounting for detection efficiency, we expect to see about 357 events in $D\bar{D}$ for an integrated luminosity of $100 pb^{-1}$.

$W\gamma$ production events were selected by making a cut on the cluster transverse mass $m_T(\gamma l; \nu)$, where

$$m_T^2(\gamma l; \nu) = [(m_\gamma^2 + |\mathbf{p}_{T\gamma} + \mathbf{p}_{Tl}|^2)^{1/2} + |\mathbf{p}_{T\nu}|]^2 - |\mathbf{p}_{T\gamma} + \mathbf{p}_{Tl} + \mathbf{p}_{T\nu}|^2 \quad (6)$$

A cut of 90 GeV eliminates almost all of the decay events for which $m_T(\gamma l; \nu)$ is bounded by the W mass. Fig. 9 shows the photon p_T distribution obtained after making this cut on the generated events.

A remarkable test of the SM can be made by measuring the angular distribution of the photon in the partonic rest frame. The non-abelian gauge theory predicts (for $W^-\gamma$ production) a radiation zero at $\cos\theta^*_{d\gamma} = \frac{1}{3}$. The angular distribution is shown in Fig. 10.

The principal experimental background comes from high p_T gluon jets in which a π^0 has been misidentified as a photon. We have started a study of this background by generating W + jets events and estimating the fraction of events which pass the isolated photon identification criteria.

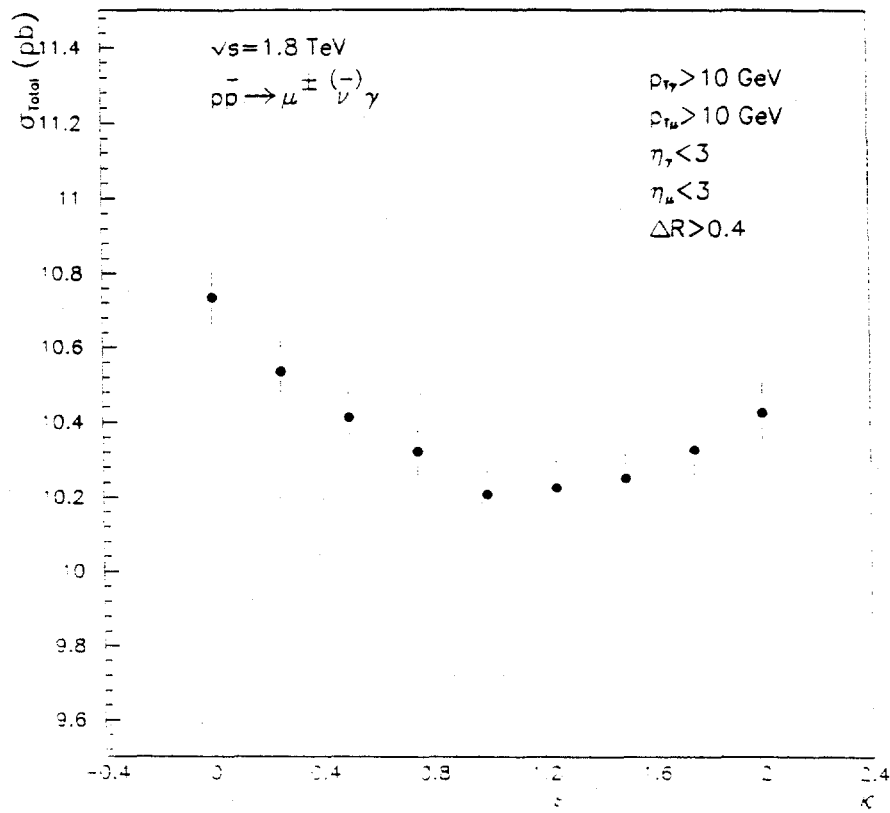


Fig. 8 Total cross-section as a function of κ . The cuts used are indicated in the figure.

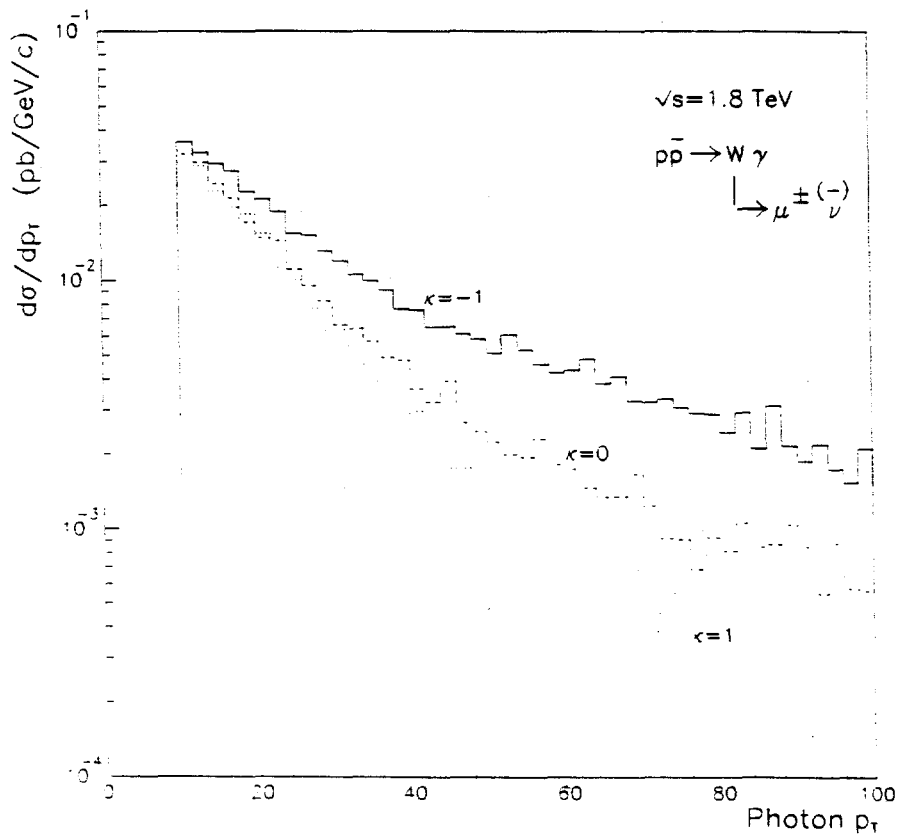


Fig. 9 Transverse momentum distribution of the photon in $p\bar{p} \rightarrow W^\pm \gamma$.

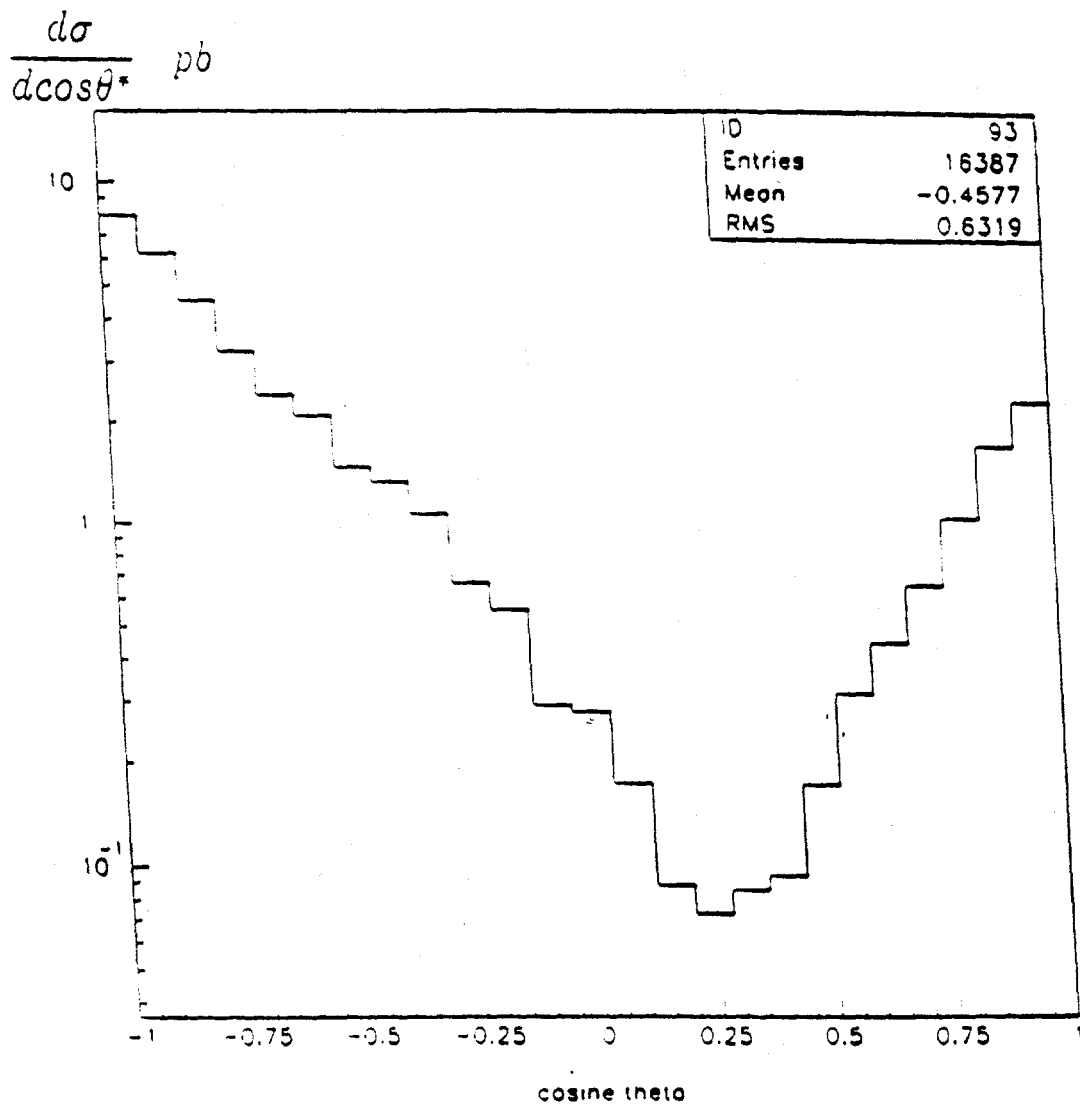


Fig. 10 Angular distribution ($\cos\theta^*$) of the photon in the partonic rest frame for production events, showing the expected dip at $\cos\theta^* = \frac{1}{3}$.

We estimate this fraction to be about 10^{-4} , which, together with γ/π^0 separation techniques, will be sufficient to suppress the background well below the signal.

Future work will concentrate on the further analysis (including detector simulation) of the $W\gamma$ events, the background estimate and on the selection of the $D\bar{D} W + \gamma$ event sample.

3.3.3 Inclusive Muon Production and the b-Quark Cross-Section

Many processes contribute to muon production in hadron-hadron collisions at high energy. These include Drell-Yan, J/ψ and Υ production, W and Z^0 decays into muons and the semi-leptonic decays of C and B hadrons. All these processes give rise to "prompt" muon production. In addition non-prompt muons from pion and kaon decay-in-flight are expected to contribute strongly at low p_T .

The measurement and analysis of the inclusive muon cross section in proton-antiproton interactions at 1.8 TeV is an important goal of the first run of the $D\bar{D}$ detector for the following reasons :

- it will be the first such measurement at the Fermilab Collider.
- it will be important to verify Monte Carlo calculations of the decay-in-flight background to prompt muons and our understanding of muon detection efficiency.
- since the prompt muon p_T spectrum below 15 GeV/c is dominated by b-quark production it will provide a measurement of the total b-quark cross section.
- the b-quark differential cross section can be measured out to large values of p_T since the B decay muon, being in a jet, can be readily separated from the isolated muons from W and Z^0 decay.
- the $c\bar{c} / b\bar{b}$ cross section ratio can be estimated from the shape of the transverse momentum of muons relative to the axis of the accompanying jet.

Finally it is essential to account for all known muon sources before we can search for new phenomena involving leptons, in particular the top quark.

This study will constitute the thesis project of graduate student T. Huehn. His preliminary ISAJET studies suggest that decay-in-flight muons dominate muon production below p_T of 5 GeV/c.

3.3.4 The Search for the Top Quark

One of the primary objectives for $D\bar{D}$ is detection and study of the top quark. The CDF Collaboration has established that the top quark mass exceeds $91 \text{ GeV}/c^2$, while theoretical considerations set an upper bound around $200 \text{ GeV}/c^2$. Thus top will decay to a real W and a b quark :

$$t \rightarrow W + b$$

$$\begin{array}{l} | \\ \rightarrow l \nu \\ \rightarrow q \bar{q} \end{array}$$

and $t\bar{t}$ final states will be characterized by multiple leptons and/or jets. $D\bar{O}$ is ideally suited for such studies since it is hermetic and has precise and uniform muon, electron and jet capability covering almost 4π in solid angle.

To date no group has been able to reliably tag W boson decays into quark final states. Also the $\tau\nu$ decay has been observed but is difficult to tag with any efficiency so that the most promising decay channels will be $e\nu$ and $\mu\nu$. Thus a $t\bar{t}$ event will be tagged using either one or both of the daughter W decays into a high p_T lepton and missing energy, and the experimental signatures will be :

- two high p_T leptons (e^+e^- , $\mu^+\mu^-$, $e^+\mu^-$, $e^-\mu^+$), missing energy and two quark jets ;
- one high p_T lepton (e or μ), missing energy and four quark jets .

Each channel has a different admixture of conventional backgrounds and to establish a top signal it will be necessary to understand each of these in detail and to find a signal in at least two decay channels.

As a group we are concentrating our efforts onto the dilepton + jets + missing energy channels for the first collider run. The Monte Carlo (section 3.2.0) and Inclusive Muon Cross-Section (section 3.2.3) studies will each contribute to this.

S. Wimpenny is leading the $D\bar{O}$ group searching for $t\bar{t}$ events decaying to give ee $e\mu$ or $\mu\mu$ final states. Work currently in progress includes the development of an analysis structure, the implementation of algorithms for background rejection and the generation of large Monte Carlo event samples to study trigger and software acceptances.

R. Hall has been studying the optimization of the level 2 trigger algorithm for $t\bar{t} \rightarrow \mu\mu$ events and is also contributing to the development of software algorithms for rejection of QCD $\rightarrow \mu\mu$ background events. The search for top via the $\mu\mu$ decay channel will constitute his thesis project. He is also responsible for the MAC cards in the muon trigger system (section 3.1.1).

3.4 $D\bar{O}$ Upgrade

A major upgrade of the $D\bar{O}$ detector is required for running with the increased luminosity ($5 \times 10^{31} \text{ cm}^{-2}\text{s}^{-1}$) and decreased bunch crossing time (132 ns) projected for the Tevatron collider runs beyond 1995 [1-3]. To meet these requirements, it is proposed to replace all of the present central and forward tracking chambers with a new system consisting of silicon microstrip detectors covering the pseudorapidity range $|\eta| \leq 3.3$, surrounded by a scintillating fiber outer

tracker. The new tracker will be enclosed in a 2 T solenoidal magnetic field. The proposed upgrade will be phased to match the Tevatron upgrade schedule. Step I will be installed by 1995 in time for run II. Step II (the full upgrade including the solenoid - "DØ_β") will be installed for run III. The tracking upgrade will allow DØ to tag b-jets from top decays, measure impact parameters for semileptonic b decays, and reduce conversion backgrounds using pulse height information from the silicon.

The silicon tracker (Fig. 11) is a hybrid consisting of a mixture of 'conventional barrel' and 'forward disk' topology and using a mixture of single- and double-sided silicon detector technology. The UCR group (Ellison, Heinson and Wimpenny) is playing a major role in the design and, together with LBL and Fermilab, will be responsible for its construction. The particular responsibilities of the UCR group are:

- Design of the E-disk and F-disk detectors, which form the main part of the disk detector system.
- R&D and evaluation of prototype F-disk detectors.
- Procurement, testing and installation of the E- and F-disk detectors.

Each F-disk is made up of 12 "wedge" detectors as shown in Fig. 12. From a technical point of view these double-sided wedge detectors are the most ambitious silicon devices. Mask design for the first F-disk prototype detectors has recently been completed at UCR and orders for detectors have been placed with S.I. (Norway) and Micron Semiconductor (UK).

The F-disk wedges are trapezoidal in shape with a height of 75 mm and a base width of 56 mm. There are 1024 readout strips on each side at a pitch of 50 μm. Each strip is AC-coupled using a SiO₂ dielectric and polysilicon resistors for biasing. The strips on the p-side are at -15° and those on the n-side are at +15°. This design allows the SVX-II front-end readout chips to be placed at the outer perimeter of the wedge, furthest from the beam. Fig. 13 shows the mask design for the S.I. prototype F-disk p-side.

We have estimated the effects of the radiation levels to which a nominal detector would be subjected for the conditions projected for collider runs I through III (1992 - 8) and have studied the effects on detector noise and bulk silicon doping concentration [14]. The maximum fluences expected have been calculated. For an integrated luminosity of 1 fb⁻¹ we expect a maximum charged particle fluence of 3.8 x 10¹³ cm⁻² and a neutron fluence of 1.2 x 10¹² cm⁻². Spiralling particles will increase the charged particle fluence by about a factor of 2. We conclude that the detectors are sufficiently radiation hard to operate beyond 2 fb⁻¹, corresponding to over 5 years of operation at a luminosity of 5 x 10³¹ cm⁻²s⁻¹. Test beam studies at Los Alamos National Laboratory have confirmed these conclusions [5].

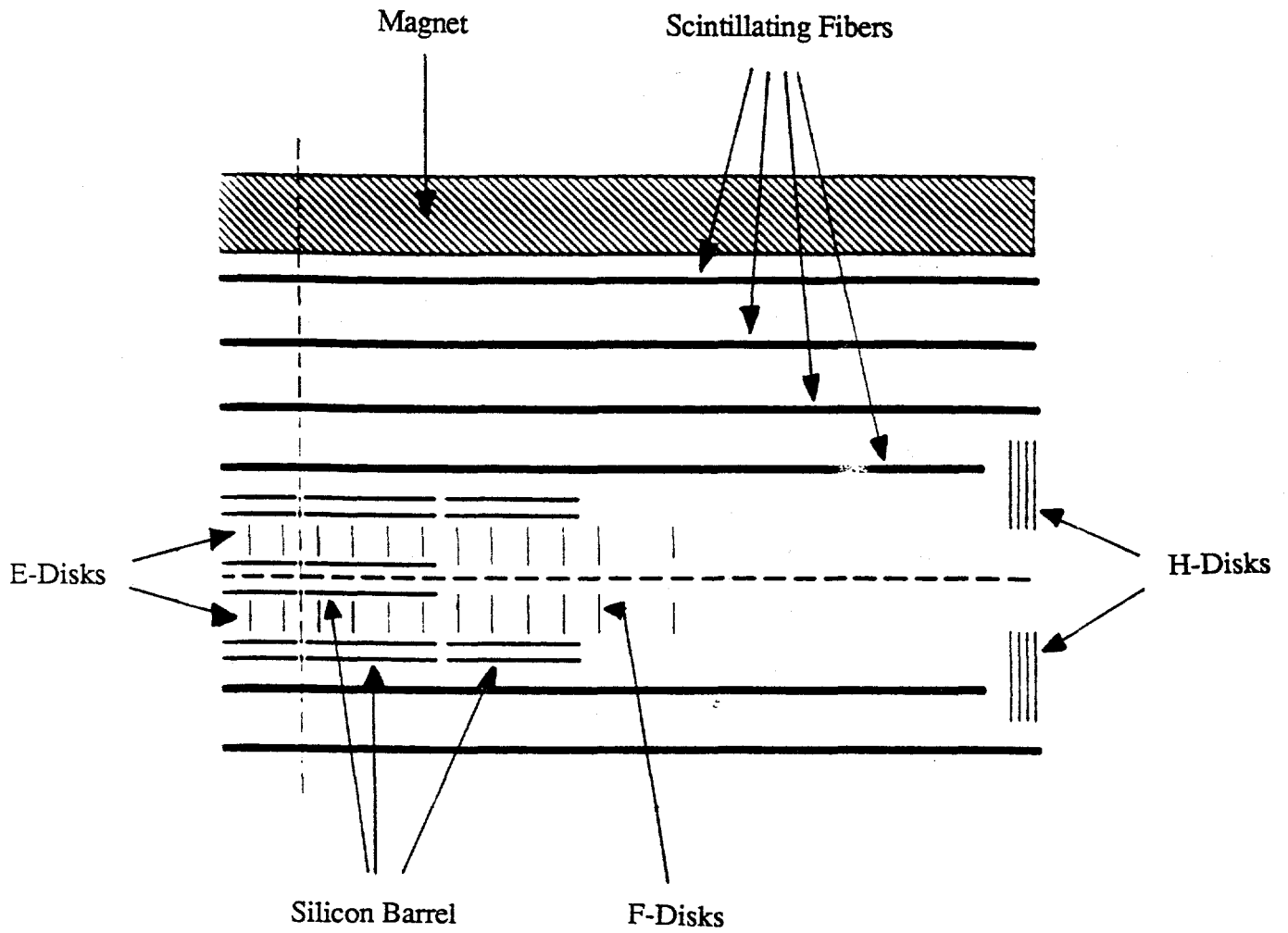


Fig. 11 Sketch of just over one quarter of the full $DØ\beta$ Upgrade Tracking System

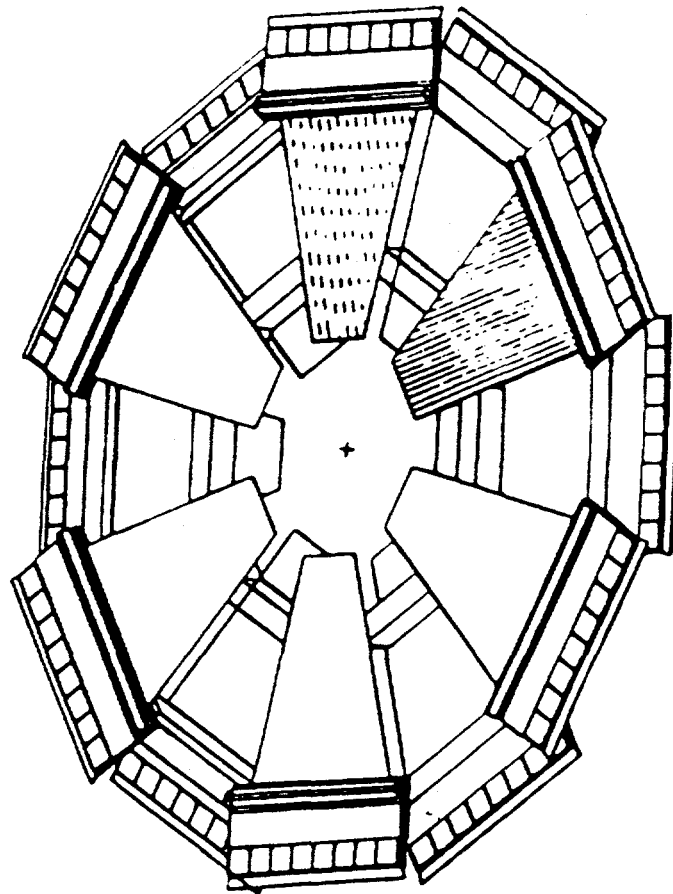


Fig. 12 Schematic view of an F-Disk, showing the 12 wedges and a support ring.

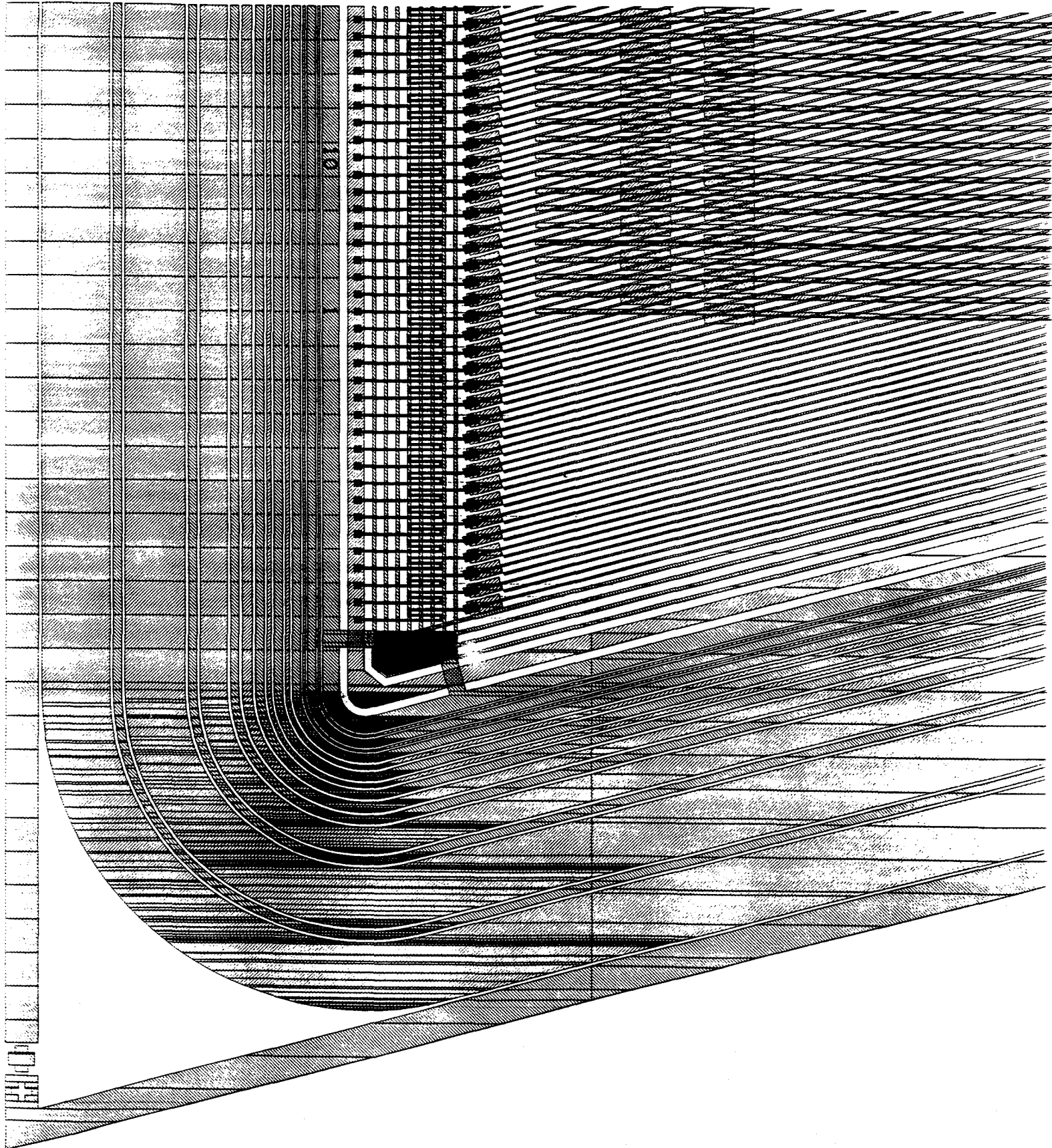


Fig. 13 A detail of the S.I. F-disk p-side mask design.

In preparation for testing of the F-disk prototype detector modules, we are setting up a readout system in the lab at UCR. It consists of two CAMAC modules, the SRS (SVX Readout Sequencer) and SDA (SVX Data Acquisition Module). The SRS is used to send control signals to the SVX chips and synchronize the SDA. The SDA contains an 8-bit flash ADC and a set of parallel memories. These memories accept the digitized pulse heights coming from the SVX chips as well as the associated chip ID and channel address. A VAXstation 3100 has been installed and is used with a SCSI CAMAC crate controller to control the readout system. To complete our setup, we are requesting funding support for a 1064 *nm* wavelength laser and a computer controlled x-y translation table, which are needed for detector module testing (see task A1 budget section). The laser is essential for testing and verifying detector modules. Due to the large number of modules to test, this cannot be done in a test beam. Over the next year, we plan to test four different designs of prototype detectors and to choose the final mask layout and fabrication technology, so that production of the first step upgrade can proceed on time.

References

- [1] DØ Upgrade Proposal, 18 October 1990.
- [2] DØ Upgrade, Responses to the Physics Advisory Committee, 18 June 1991, DØ Note 1148.
- [3] DØ Upgrade, Step I and Beyond, 20 May 1992, DØ Note 1421.
- [4] "Radiation Levels in DØ and Effects on Silicon Detectors", DØ Note 1155, July 1991, J. Ellison.
- [5] "Temperature Effects on Radiation Damage to Silicon Detectors", J.A. Ellison, J.K. Fleming, E. Reed, S.J. Wimpenny et al., UCR/SSC/92-01. Presented at the Sixth European Symposium on Semiconductor Detectors, Milan, February 24-26 1992. To be published in Nuclear Instruments and Methods.

1c SDC : PROTON-PROTON INTERACTIONS AT 20 TeV

1. Introduction

The Solenoidal Detector Collaboration (SDC) will build one of the two major detectors for the 20 TeV Superconducting Super Collider in Texas. UC Riverside joined SDC in mid 1989, and has taken an increasing role over the past three years. Our efforts are focussed through the Silicon Tracker group on designing and building the world's largest silicon detector, to be completed by 1998.

2. The SDC Silicon Tracker

The design of the SDC detector for the SSC [1,2] calls for a very large silicon tracking system [3,4] which will form the basis of the charged particle tracking at radii between 9.0 and 46.5 cm from the beam (Fig. 14). The total area of silicon is 16.94 m^2 and the system contains 6,481,920 readout channels. The design represents a significant step beyond any of the present generation of collider experiment silicon detectors. In March 1992, the Silicon Tracking Conceptual Design Report was released, which contains very detailed specifications of the performance goals for the system, and of the physical design of the detector and its readout system [5]. There are 122 physicists and engineers associated with this project, from 27 universities and laboratories in the United States, Japan, Italy, Great Britain and the Former Soviet Union. The group at UC Riverside is working very closely with the group at UC Santa Cruz, from where the whole project is coordinated and lead.

The tracker consists of $300 \mu\text{m}$ thick double-sided detectors with axial strips on one side and stereo strips on the other side. Pairs of such detectors with opposite stereo pitch are arranged in superlayers in a cylindrical barrel section and also in planar endcaps. The superlayers allow local hit association into segments that are then further associated into tracks. The intermediate angle detectors are spaced along the beam out to a distance of 2.58 m from the interaction point to allow good momentum measurement out to a pseudorapidity of $|\eta| \leq 2.5$.

The following section gives details of the UCR contribution to the SDC Silicon Tracker to date, and presents proposals of what we plan to do over the next few years.

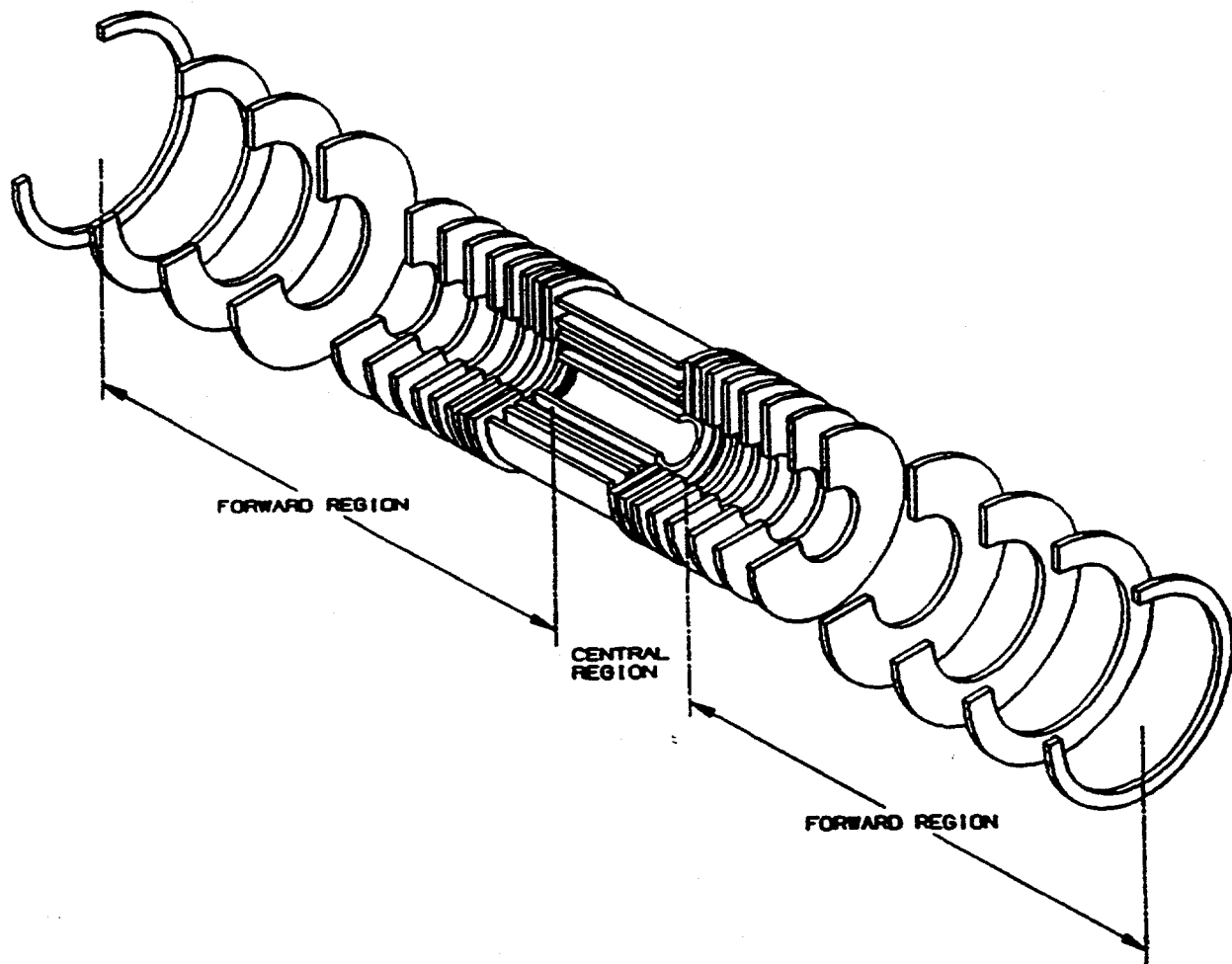


Fig. 14 The silicon detector array for SDC.

3. Detector R&D at UCR

The silicon detector laboratory at Riverside was set up in 1989 using UCR funding, with the purpose of studying silicon detectors and readout for trackers in the hadron collider environment. Since this time the facility has been continually evolving and has now doubled in size. It is equipped with a semiconductor probe station for testing prototype detectors, a clean room containing an ultrasonic wire bonder and various test and readout systems for evaluating the behavior of prototype detectors and the effects of radiation damage.

Detectors for SDC will have rather different designs to those for the DØ upgrade. This is due to the need for tracking within very high p_T jets (up to at least $p_T = 500$ GeV/c), the short time between beam crossings (16 ns) and the very large number of channels (and hence high total power dissipation) in the design. Consequently, the stereo angle of the detectors will need to be very small (≈ 10 – 20 mrad), readout will be digital and the cooling system will operate at a much lower temperature ($\approx 0^\circ\text{C}$).

Over the last three years, we have studied the damage caused by proton, photon and neutron radiation on silicon detectors using the LAMPF and LASREF facilities at Los Alamos National Laboratory. The aim of this work has been to determine the limit on the lifetime of the silicon tracker due to detector radiation damage effects and to study the effects on AC-coupled microstrip detectors. Our results [6-8] show that, over a nominal 10 SSC year running period, there is no serious degradation in the coupling capacitors on AC-coupled detectors and that polysilicon bias resistors are stable under a similar radiation exposure. Additional studies of bulk silicon effects using 1 cm^2 PIN diodes predict SSC detector lifetimes of around 10 years [7].

Our efforts are now divided between ongoing radiation damage studies and R&D work on the SDC silicon tracker forward disks. Another proton run is planned at LAMPF during September 1992. We will make further measurements, especially on the temperature dependence of annealing of the full depletion voltage. Our results from last year showed, for the first time, that the anti-annealing at 0°C is very much suppressed compared with room temperature operation (see Fig. 15). We also plan to study in more detail the effects of radiation on detector pulse height, pulse shape, and interstrip resistance and capacitance.

The group at UCR proposes to make a major contribution to the design and testing of the forward disks for the SDC tracker. At UCR, we will design the masks for the double-sided AC-coupled wedge detectors, and then evaluate the prototypes produced. There will be 8 different detector designs for the disks of the final detector, and once these designs are finalized, production will begin. There is a very tight schedule for this. We will be one of about 5 university and laboratory groups who will then test the detectors, each group being responsible for approximately 500 modules over about 2 years.

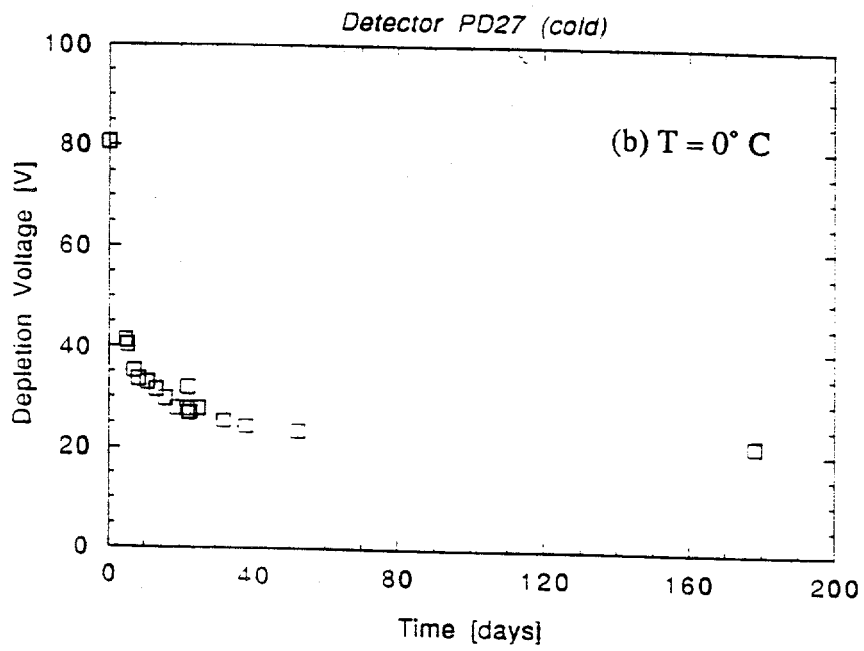
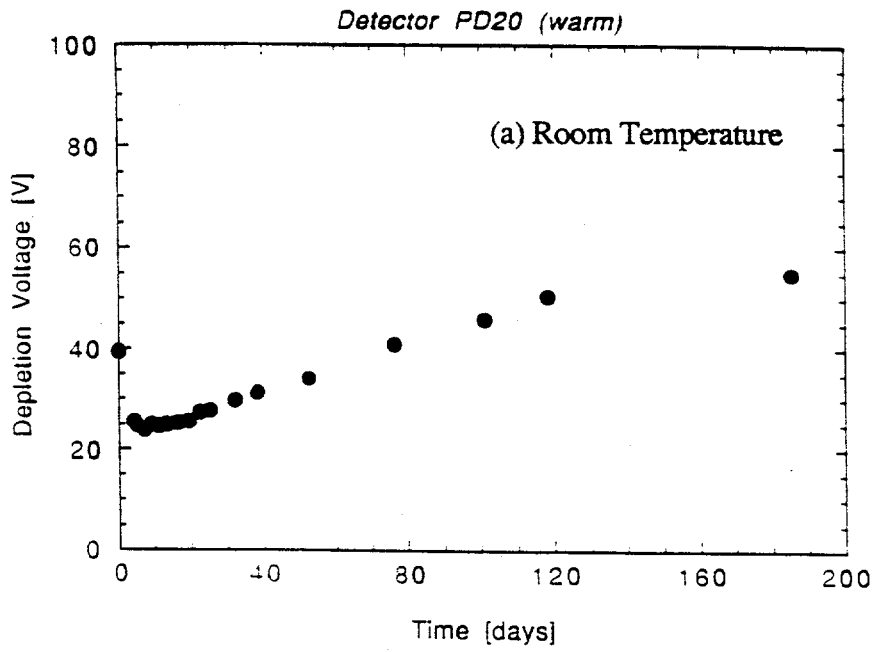


Fig. 15 Detector full depletion voltage vs. annealing time at (a) room temperature and (b) T = 0° C. The fluence was $\Phi \approx 8.5 \times 10^{13}$ protons cm⁻².

References

- [1] J. Ellison, S.J. Wimpenny et al., "Solenoidal Detector Collaboration Expression of Interest to Construct and Operate a Detector at the Superconducting Super Collider", May 24th 1990.
- [2] J. Ellison, S.J. Wimpenny et al., "Letter of Intent by the Solenoidal Detector Collaboration to Construct and Operate a Detector at the Superconducting Super Collider", November 30th 1990.
- [3] J. Ellison, S.J. Wimpenny et al., "SSC Detector Subsystem Proposal: Subsystem R&D Proposal to Develop a Silicon Tracking System", 1989.
- [4] J. Ellison, S.J. Wimpenny et al. "Subsystem R&D Proposal to Develop a Silicon Tracking System 1990-1991", 1990.
- [5] SDC Silicon Tracking Conceptual Design Report, J. Ellison, D. Joyce, C. Lietzke, S.J. Wimpenny et al., SDC-91-133.
- [6] J. Ellison, S.J. Wimpenny et al., "Study of Radiation Effects on AC-Coupled Silicon Strip Detectors", Proceedings of 2nd Conference on Advanced Technology and Particle Physics, Como, Italy, 1990, (to appear in Nucl. Phys. B).
- [7] J. Ellison, S. Jerger, C. Lietzke, S.J. Wimpenny et al., "Tests of Radiation Hardness of VLSI Integrated Circuits and Silicon Strip Detectors for the SSC Under Neutron, Proton and Gamma Irradiation", IEEE Trans. Nucl. Sci. **NS38** (1991) 269.
- [8] "Temperature Effects on Radiation Damage to Silicon Detectors", J.A. Ellison, J.K. Fleming, E. Reed, S.J. Wimpenny et al., UCR/SSC/92-01. Presented at the Sixth European Symposium on Semiconductor Detectors, Milan, February 24-26 1992. To be published in Nuclear Instruments and Methods.

At the heart of all calculations of hard scattering cross-sections are parameterizations of the parton distributions functions $q(x, Q^2)$, $\bar{q}(x, Q^2)$ and $g(x, Q^2)$. These, in turn, are derived from measurements of the Deep Inelastic Structure Functions $F_1(x, Q^2)$, $F_2(x, Q^2)$, and $F_3(x, Q^2)$ and it is on the reliability of these measurements on which the parton distribution functions depend.

In general the experimental data are in quite good agreement with the exception of the region of small Bjorken x ($x \leq 0.2$) where significant discrepancies exist. This is particularly unfortunate as this is the most important kinematic region for calculations pertaining to cross-sections at the Tevatron and SSC.

As a part of an ongoing study of the deep inelastic data have investigating four of the principal experimental datasets - the hydrogen and deuterium datasets of the EMC and BCDMS Muon Collaborations at CERN. It is the inconsistencies between these data which give rise to some of the largest uncertainties in the parton distributions.

The EMC and BCDMS have published high precision measurements on the structure function $F_2(x, Q^2)$ measured using hydrogen [1,2] and deuterium [3,4] targets. The same basic problems effect the data on both targets. For example Fig.16 shows a comparison of the published hydrogen data from which it can be seen that, in terms of their broad characteristics, the data agree. The Q^2 -dependence of $F_2(x)$ is similar for both experiments but when fitted results in significantly different results for Λ (Table 1). The x -dependence, however is significantly different and inconsistent with a simple normalization difference between the two experiments. This is inconsistent with the statistical and systematic errors quoted by the two groups.

We have studied the analysis methods used by the two groups in detail and find that there are several differences in both the theoretical input and methods used to extract F_2 . Careful studies of the treatment of the electromagnetic radiative corrections [5] and the calculations of the ratio $R = \sigma_L/\sigma_T$ [6] suggest that these may be responsible for some of the differences between the two sets of data.

To further investigate this we have re-analyzed the hydrogen and deuterium datasets using the same assumptions. We find that, after correction, the Q^2 -dependence of F_2 , and hence the values of Λ , are in very good agreement (see Table 1 and Fig. 17). The difference in the x -dependence persists and globally we find a normalization difference of 11% between the two datasets. To study this problem further we have also compared our results to those from the re-analyzed compilation of the SLAC electron data [7,8]. While there is little kinematical overlap with the two CERN groups the data provide an independent measure of the x -dependence of F_2 .

We have two versions of these data ; one using the results direct from the SLAC analysis (open squares) and the second using results re-extracted using our treatment of R [6] (solid points)

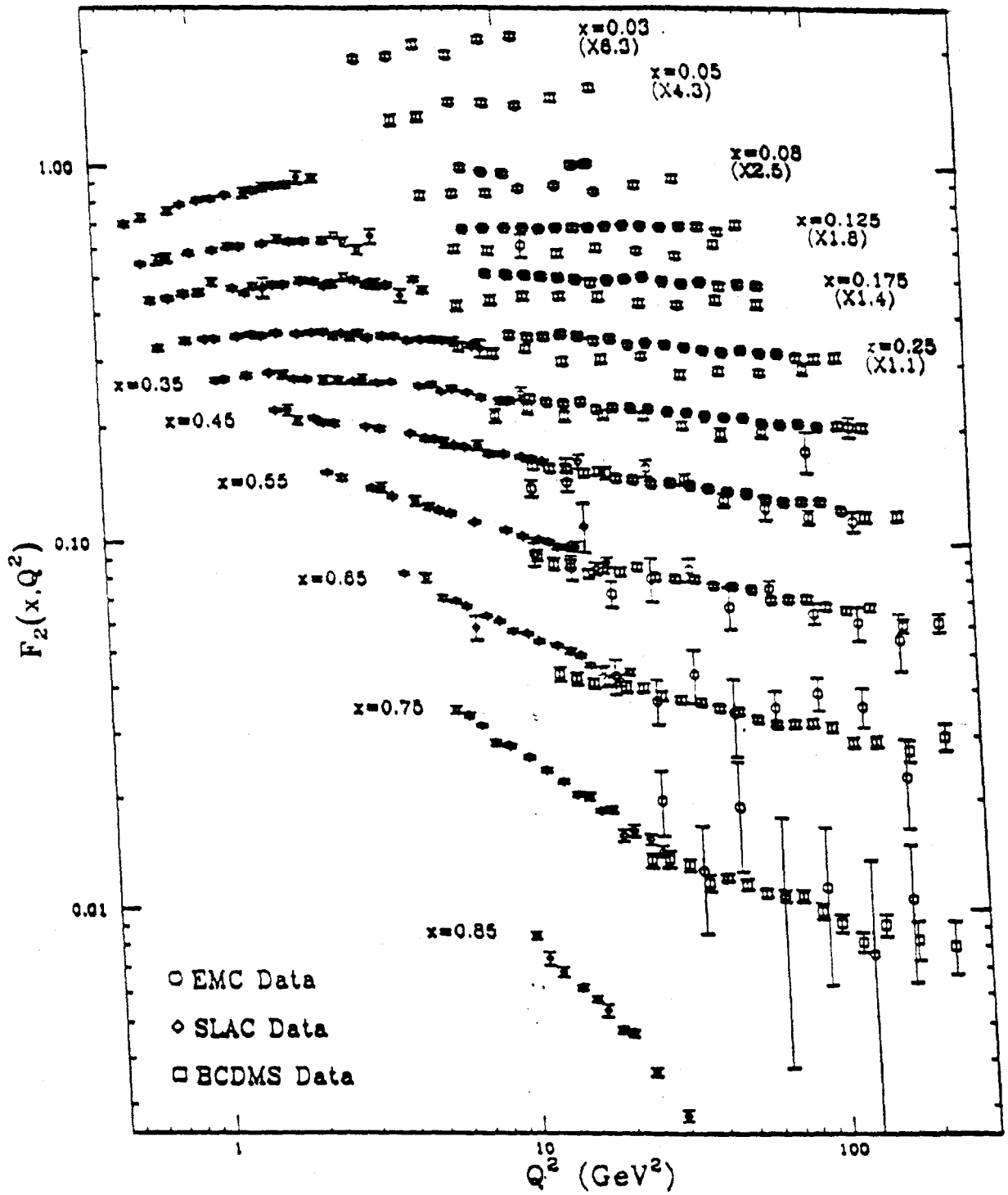


Fig. 16 Comparison of the Published EMC, BCDMS and SLAC data

TABLE 1

QCD Fit Results

QCD Fit	This Analysis	EMC[1]	BCDMS[2]
Leading Order Singlet	206^{+57}_{-50}	90 MeV	215 ± 27 MeV
Next to Leading Order Non-Singlet	209^{+78}_{-71} MeV	105 ± 101 MeV	214 ± 21 MeV

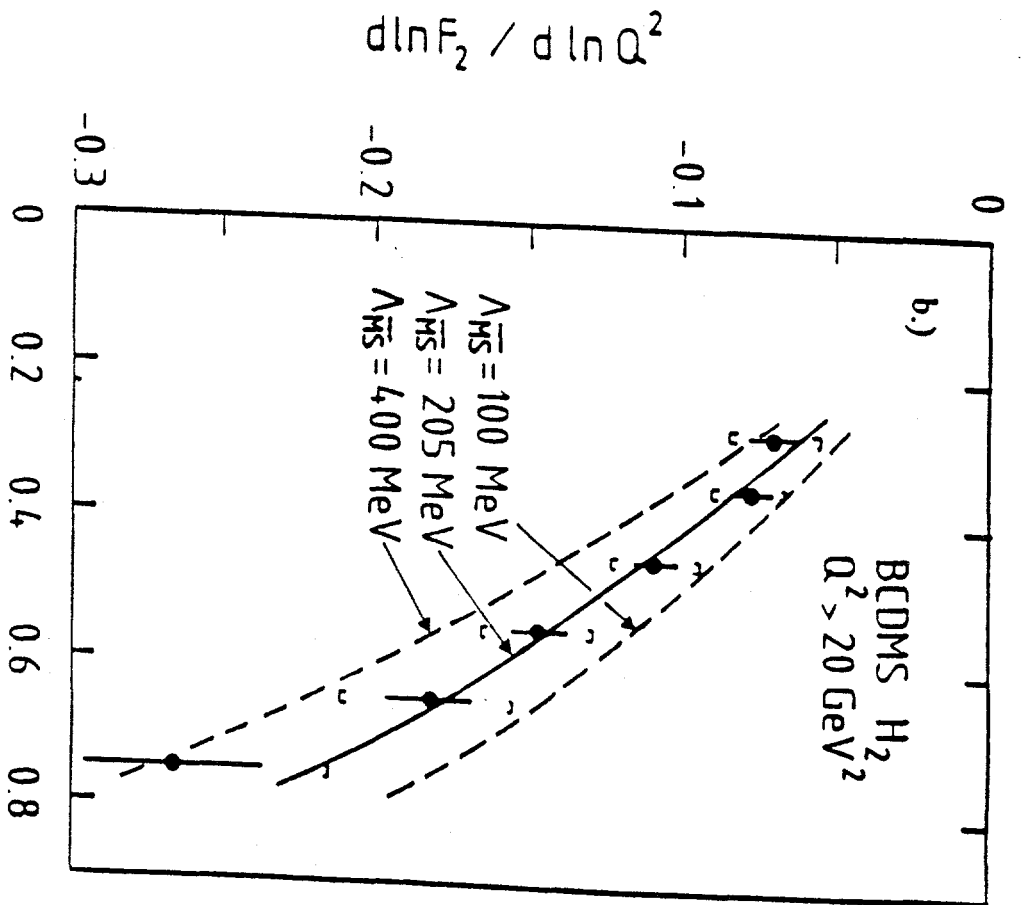
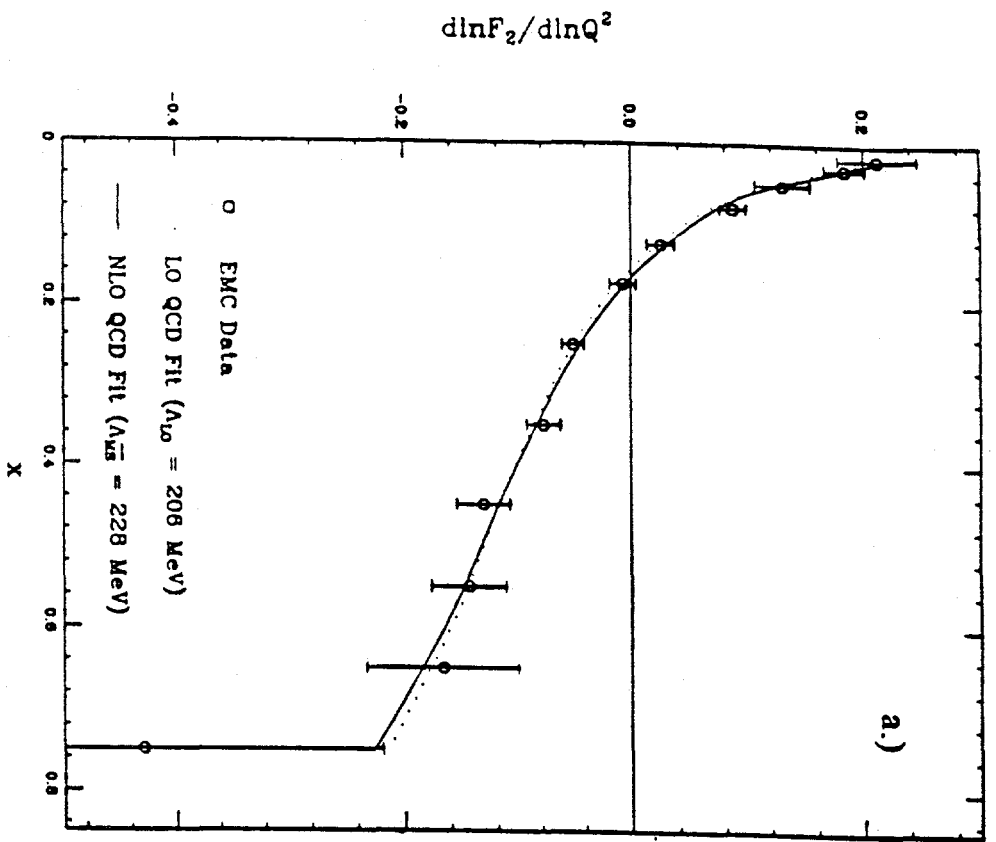


Fig. 17 Comparison of the data and the predictions of QCD
 a.) EMC Data (this analysis)
 b.) BCDMS Data [2].

which are compared to our results for EMC in Fig.18 and for BCDMS in Fig. 19. The agreement between the electron and muon datasets is good but further work is needed to see if the SLAC data is in better agreement with either set of muon data. On further study we find that the SLAC data are consistent with a constant normalization shift of 5.2 % with respect to EMC (Fig. 20) but that a single normalization shift cannot make the SLAC and BCDMS data agree (Fig. 20). The reason for the latter problem is not understood. Our final results, after correction for normalization differences are shown in Fig. 21 from which we conclude that reasonable consistency can be achieved between the three datasets provided that the same modelling is used for R and that differences in relative normalization are corrected for.

A parallel analysis of the deuterium data from SLAC, EMC, and BCDMS has led to essentially the same conclusions. We find that the Q^2 -dependence of F_2 for the EMC and BCDMS data are the same and lead to the same values of Λ , as were found from analysis of the hydrogen data. The x -dependent differences observed in the hydrogen data are also present in the deuterium results and remain similarly unexplained. Taking the SLAC data as reference we find that the EMC and BCDMS data differ in normalization by 8.2% with the EMC data requiring an upward re-normalization of 6.6% and the BCDMS data a downward re-normalization of 1.6%. A comparison of the three datasets from this analysis, after correcting for these effects, is shown in Fig. 22.

Results from these studies have been presented at the XXVth International Conference on High Energy Physics in Singapore [9] and the Joint International Lepton and Photon Symposium and Europhysics Conference on High Energy Physics in Geneva [10,11]. The data are now available in the Particle Data Group database and are in use in parton distribution studies by groups at Fermilab and RAL/Durham University in the United Kingdom.

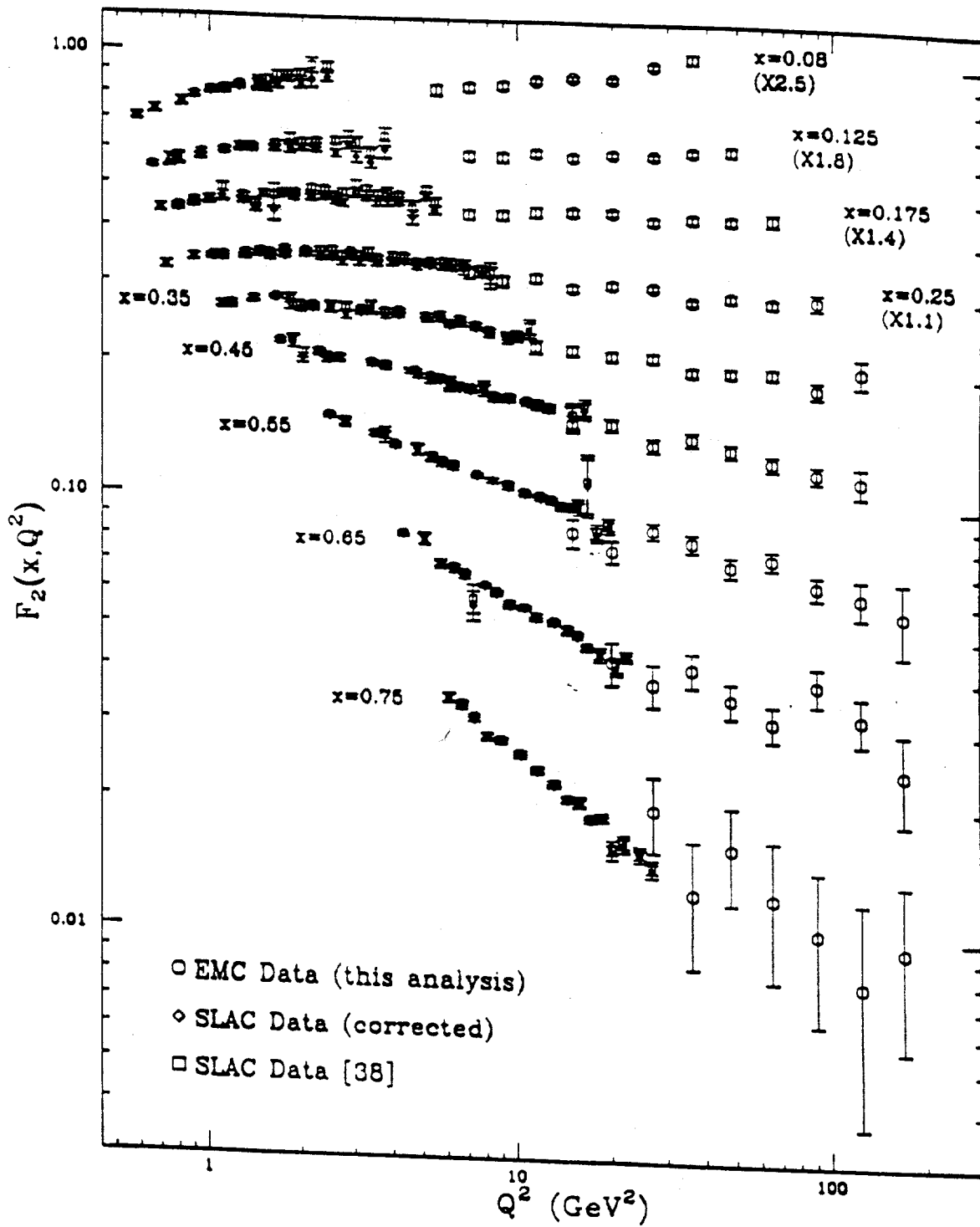


Fig. 18 Comparison of the SLAC and EMC Data (this analysis)

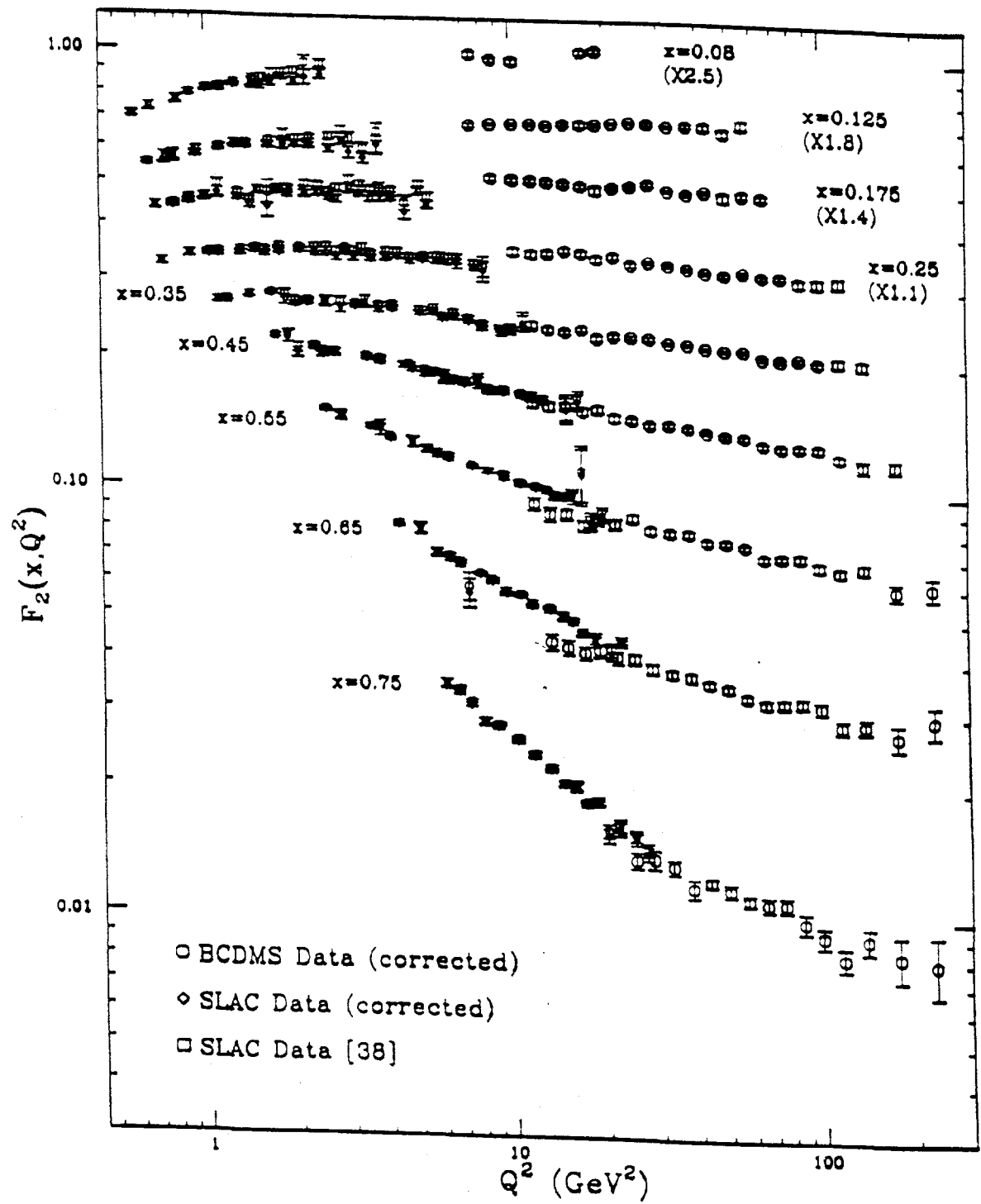


Fig. 19 Comparison of the SLAC and BCDMS Data (this analysis)

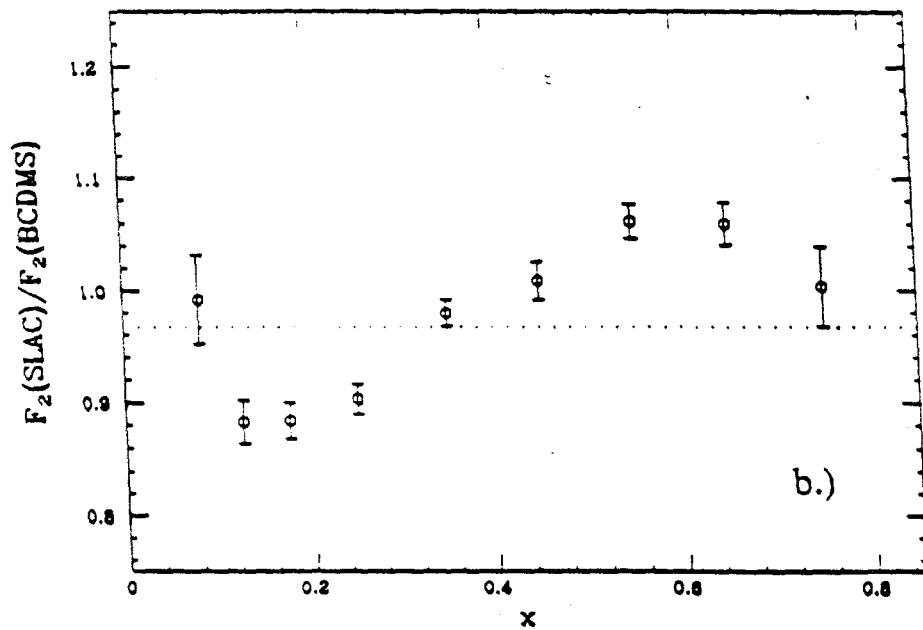
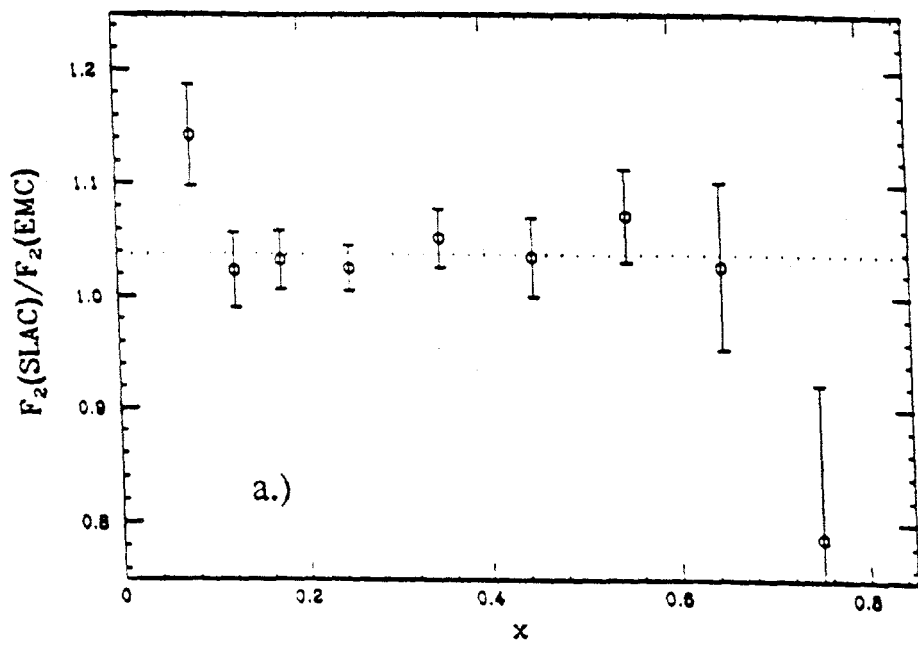


Fig. 20 Comparison of the x -dependences of the Ratio of SLAC and:

a.) EMC Data

b.) BCDMS data

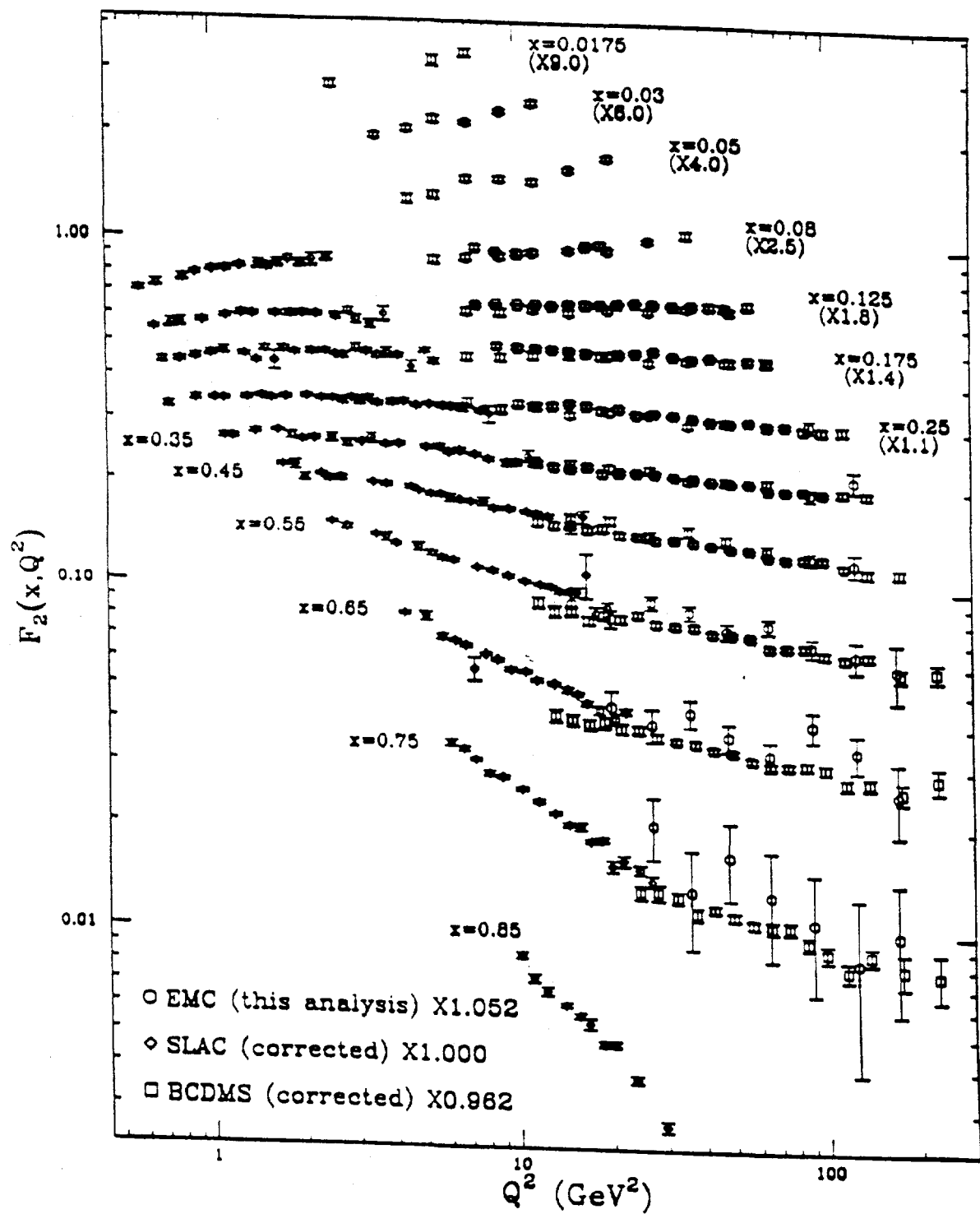


Fig. 21 Comparison of the EMC, BCDMS and SLAC data from this analysis

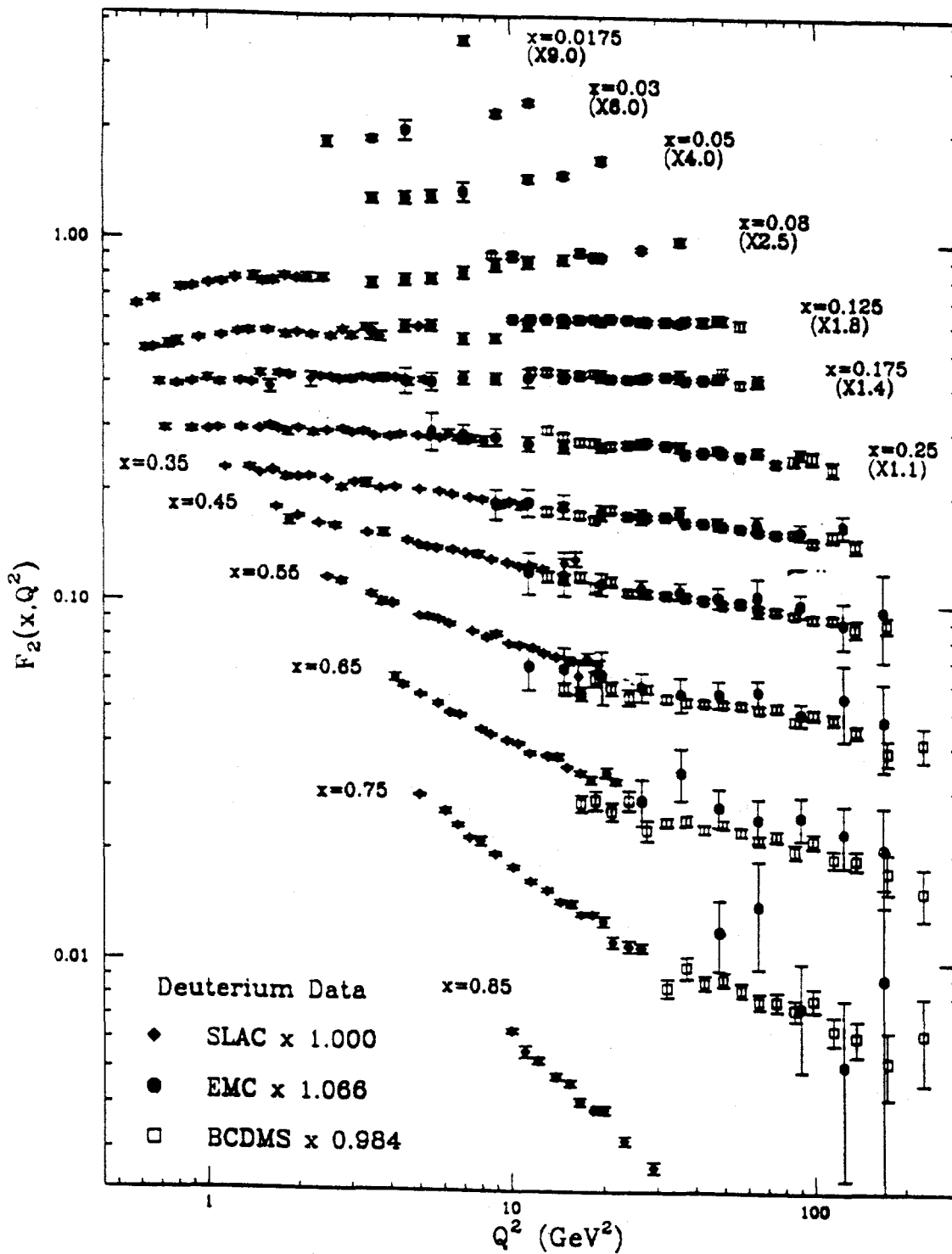


Fig. 22 Re-analyzed Deuterium Data

References

- [1] J.J. Aubert et al. (EMC Collaboration), Nucl. Phys. **B259**, 189, (1985).
- [2] A.C. Benvenuti et al.(BCDMS Collaboration), Phys. Lett. **B223** (1989) 485.
- [3] J.J. Aubert et al. (EMC Collaboration), Nucl. Phys. **B293** (1987) 740.
M. Arneodo et al. (EMC Collaboration), Nucl. Phys. **B333** (1990) 1.
M. Arneodo et al. (EMC Collaboration), to be submitted to Nucl. Phys. B, 1991.
- [4] A.C. Benvenuti et al (BCDMS Collaboration), CERN-EP/89-170, (1989).
- [5] C. Lietzke, S.J. Wimpenny, "A Comparison of the RadEMC and Bardin-Shumeiko Radiative Correction Programs", U.C. Riverside Report No. UCR/DIS-89-06, (1989).
- [6] K. Bazizi, S.J.Wimpenny, "A Study of the Properties of the Ratio $R=\sigma_L/\sigma_T$ ", U.C. Riverside Report No. UCR/DIS-90-04.
- [7] S. Dasu et al.(E139/E140 Collaboration), paper contributed to the International Europhysics Conference on High Energy Physics, Madrid, September 1989, University of Rochester Preprint No. UR-1119, 1989.
- [8] S. Rock, L.W. Whitlow, private communications.
- [9] K. Bazizi, T. Sloan, S.J. Wimpenny, "Comparison of Structure Function Measurements from Hydrogen and Deuterium". Proceedings of the 25th International Conference on High Energy Physics, Singapore, August 1990, World Scientific Publishing, 639-641 (1991).
- [10] S.J. Wimpenny, "A New QCD Analysis of the EMC Hydrogen and Deuterium Data". Proceedings of the Joint International Lepton and Photon Symposium and Europhysics Conference on High Energy Physics, Geneva, 25th July-1st August, 1991, World Scientific Publishing, 145-146 (1992).
- [11] K. Bazizi, S.J. Wimpenny, "A QCD Analysis of the Proton Structure Function $F_2(x, Q^2)$ ", UCR/DIS/91-03. Submitted to Joint International Lepton and Photon Symposium and Europhysics Conference on High Energy Physics, Geneva, 25th July-1st August, 1991.
K. Bazizi, S.J. Wimpenny, "A Comparative Study of Structure Function Measurements from Hydrogen and Deuterium", UCR/DIS/91-02. Submitted to Joint International Lepton and Photon Symposium and Europhysics Conference on High Energy Physics, Geneva, 25th July-1st August, 1991.

TASK A2

2.1 Task A2

2.1.1 Program

The physics program of Task A2 has been the systematic study of leptons and hadrons at e^+e^- colliders. The OPAL detector at LEP began taking data in 1989 and has now accumulated over 500,000 Z^0 s. Publications by the collaboration cover a broad spectrum of physics: the precision measurement of electroweak parameters, the first determination of the number of light neutrino generations by the method of single photon counting, the measurement of the running coupling constant of the strong interaction by several independent methods, the extension of the mass limit of the Higgs and other new particles, and a number of topics in heavy quark and tau physics. The continued exploitation of the rich physics potential of LEP and LEP200 will form the core of the UCR effort for the coming several years.

Conscious of the fact that the long term future of the field will involve hadron colliders, whether in the U.S. or in Europe, we are participating in the RD5 experiment at the CERN SPS to study muon triggering and momentum reconstruction in a strong magnetic field, the results of which will be of great utility in the design of the CMS detector currently being proposed for the LHC collider.

Several members of our group are also participating in an ongoing neutrino oscillation program LSND at Los Alamos which is expected to take data beginning in 1993. A small effort is proceeding at SLAC to publish papers based on the thesis topics of the last two UCR students to work on the TPC/ 2γ project.

2.1.2 Personnel

Ph.D. Physicists

M. Dittmar	Postgraduate Researcher
J.W. Gary	Assistant Professor
W. Gorn	Staff Research Associate
C.C.H. Jui	Postgraduate Researcher
J.G. Layter	Adjunct Professor
B.C. Shen	Professor
G.J. VanDalen	Professor
G.W. Wilson	Postgraduate Researcher

Graduate Students

S.L. Chu
E.G. Heflin
J.R. Letts
G. Moradkhanian

Summer Student

Y.R. Ryu

TASK B

Invited Talks 1991-1992

1991

1. January 21, 1991
California Institute of Technology, High Energy Seminar
"Hunting the Higgs with OPAL at LEP"
G.J. VanDalen
2. February 7, 1991
University of California at Riverside, Colloquium
"Low Energy Neutrino Experiments - Doing TeV Physics with MeV Neutrinos"
G.J. VanDalen
3. February 25, 1991
Department of Energy, Washington DC
"Determination of Electroweak Parameters at the Z with OPAL"
B.C. Shen
4. March 11, 1991
26th Rencontres de Moriond, Les Arc, France
"Tau Physics at LEP - Testing the Tau Lepton Universality"
M. Dittmar
5. March 13, 1991
Neutrinos, AstroPhysics and Cosmics Rays Workshop, UC San Diego
"The LSND Detector at Los Alamos"
G.J. VanDalen
6. March 1991
DOE Seminar
"Results from OPAL at LEP"
B.C. Shen
7. April 4, 1991
University of Maryland, College Park, Seminar
"Tau Physics with OPAL at LEP"
M. Dittmar
8. April 4, 1991
The 5th Spring School on Particles and Fields, Academia Sineca, Taiwan
"Precision Tests of the Electroweak Theory at the Z"
B.C. Shen

9. April 8, 1991
University of California, Riverside, Seminar
"Tau Physics with OPAL at LEP"
M. Dittmar
10. April 9, 1991
Dept of Physics and Astronomy, National Central Univ., Taiwan
"Study of Quantum Chromodynamics at the Z"
B.C. Shen
11. April 18, 1991
University of Michigan, Ann Arbor
"Recent Results on Tau Decays from the OPAL Detector at LEP"
K. Riles
12. April 20, 1991
Fermi National Accelerator Laboratory, Batavia
"Recent Results on Tau Decays from the OPAL Detector at LEP"
K. Riles
13. April 24, 1991
Korean Physical Society Meeting, Seoul, Korea
"Search for Close Mass Heavy Leptons with OPAL at LEP"
H. Oh
14. April 26, 1991
Korean Physical Society Meeting, Seoul, Korea
"Results from OPAL"
H. Oh
15. May 1991
National Central University, Taiwan, Colloquium
"Study of Quantum Chromodynamics at the Z⁰"
B.C. Shen
16. June 1991
University of Bonn, FRG, Seminar
"A Model Independent Observation of the String Effect and of Quark Gluon
Jet Differences at LEP"
J.W. Gary
17. July 1, 1991
University of Marseille, France
"Tau Physics with OPAL and LEP"
M. Dittmar

18. August 19, 1991
1991 APS/DPF Meeting, Vancouver, B.C.
"Review of Tau Physics at LEP"
K. Riles
19. September 3, 1991
University of California, Riverside
"Recent Tau results from OPAL"
K. Riles
20. September 1991
ICFA Workshop on Future e^+e^- Colliders, Saariselkä, Finland
"Prospects of SUSY Searches at High Energy Linear e^+e^- Colliders"
M. Dittmar
21. September 1991
Tibet University, China, seminar
"Recent Developments in High Energy Physics"
B.C. Shen
22. September 1991
University of Sichuan, China, seminar
"Current Status and Trends in Experimental Particle Physics"
B.C. Shen
23. September 1991
21st International Symposium on Multiparticle Dynamics, Wuhan, China
"Photon and Gluon Emission Processes at the Z^0 "
B.C. Shen
24. September 1991
21st International Symposium on Multiparticle Dynamics, Wuhan, China
"Double Pomeron Exchange in $p\bar{p}$ Interactions at CM Energy 630 GeV"
B.C. Shen
25. October 1991
International Workshop on Electroweak Physics Beyond the Standard Model,
Valencia, Spain
"A Measurement of Photon Radiation in Lepton Pair Events from Z Decays"
M. Dittmar
26. October 1991
Academia Sinica, Taiwan, seminar
"Photon Radiation and Gluon Emission at the Z^0 "
B.C. Shen

27. November 13, 1991
University of California at Los Angeles, Seminar
"Low Energy Neutrino Experiments - Doing TeV Physics with MeV Neutrinos"
G.J. VanDalen
28. November 15, 1991
Paul Scherrer Institute, Villigen, Switzerland
"A Measurement of Photon Radiation in Lepton Pair Events from Z Decays"
M. Dittmar

1992

29. February 10, 1992
University of California at Davis, seminar
"LEP Physics from the OPAL Vantage Point"
J.G. Layter
30. February 1992
California State University, Long Beach, Colloquium
"Z⁰ Physics and the Number of Families"
B.C. Shen
31. March 24, 1992
Photon-Photon '92 Conference, San Diego
Exclusive Production Session Chairman, Convener
J.G. Layter
32. April 27, 1992
California State University, Long Beach, Colloquium
"Low Energy Neutrino Experiments - Doing TeV Physics with MeV Neutrinos"
G.J. VanDalen
33. April 28, 1992
University of Montreal
"A Measurement of Photon Radiation in Lepton Pair Events from Z Decays"
M. Dittmar
34. April 28, 1992
University of California at Irvine, Seminar
"New Particle Searches at OPAL"
H. Oh
35. April 1992
American Physical Society Meeting, Washington D. C., Plenary talk
"QCD at LEP"
J.W. Gary

36. April 1992
Columbia University, Colloquium
"Some Aspects of LEP Physics, Present and Future"
B.C. Shen
37. May 1992
International Workshop on the Search for New Particles: Status and Prospects,
ICTP, Trieste
"Search for Rare Exotic Z Decays"
M. Dittmar
38. May 21, 1992
University of Trieste
"Measurement of Strange Baryon Production in Hadronic Z Decays"
M. Dittmar
39. July 13, 1992
22nd International Symposium on Multiparticle Dynamics, Santiago de Com-
postela, Spain
"Strange Baryon Production in e^+e^- Collisions"
B.C. Shen

Other Talks 1991 - 1992

1991

1. February 5, 1991
OPAL Weekly Meeting, CERN
"A Detailed Investigation of Radiative Lepton Pairs"
M. Dittmar
2. March 7, 1991
OPAL Plenary Meeting, CERN
"Status of Tau Polarization and Branching Ratio Analyses"
K. Riles
3. March 19, 1991
OPAL Monte Carlo Group Meeting, CERN
"Status of Hadron Calorimeter Monte Carlo Simulation"
K. Riles
4. April 19, 1991
Sung-Kyun-Kwan University, Seoul, Korea
"Results from OPAL"
H. Oh
5. April 24, 1991
APS Meeting, Washington D.C.
"Measurement of Tau to Muon Decay Parameters with the OPAL Detector at LEP"
B.P. O'Neill
6. April 24, 1991
APS Meeting, Washington D.C.
"Measurement of $B(\tau \rightarrow \pi\nu)$ and the Tau Polarization with OPAL at LEP"
C. Ho
7. April 24, 1991
APS Meeting, Washington D.C.
"A Direct Measurement of the Z Invisible Width by Single Photon Counting"
W.J. Larson
8. April 30, 1991
Kyung-Pook National University, Daegu, Korea
"Results from OPAL"
H. Oh

9. May 2, 1991
Kang-Leung National University, Kang-Leung, Korea
"Results from OPAL"
H. Oh
10. June 1991
OPAL Plenary Meeting, CERN.
"Monte Carlo Data Flow"
J.W. Gary
11. July 4, 1991
OPAL Analysis Meeting, CERN
"Summary of Tau Results from the Orsay Heavy Flavor Symposium"
K. Riles
12. October 1991
OPAL Physics Meeting
" α_s from AEEC - an Update"
J.W. Gary
13. November 1991
OPAL Physics Meeting
" α_s from AEEC - an Update"
J.W. Gary
14. December 4, 1991
OPAL QCD Workshop
"Analysis of Strange Baryon and Antibaryon Production in Hadronic Events
(Preliminary)"
J. Letts
15. December 1991
OPAL QCD Workshop, CERN
"An Update of Quark-Gluon Jet Differences"
J.W. Gary
16. December 1991
OPAL Plenary, CERN
"Strange Baryon Production in Hadronic Events"
M. Dittmar
17. December 1991
OPAL Plenary, CERN
"The String Effect with 1991 Data"
J.W. Gary

1992

18. February 6, 1992
OPAL Weekly Meeting, CERN
"Detailed Studies of Strange Baryon Production"
M. Dittmar
19. February 6, 1992
OPAL Weekly Meeting, CERN
"A Measurement of Inclusive Strange Baryon Production in Hadronic Z0 Decays"
J. Letts
20. April 9, 1992
OPAL Weekly Meeting, CERN
"A Measurement of Inclusive Strange Baryon Production in Hadronic Z0 Decays, Update"
J. Letts
21. April 20, 1992
APS Meeting, Washington D.C.
"Strange Baryon Production in Hadronic Z0 Decays"
J. Letts
22. May 1992
RD5 Group Meeting, CERN
"Muon Chamber Status"
J.G. Layter
23. May 7, 1992
Meeting on UC Participation in the CMS Experiment at LHC, UC Riverside
Convenor and Chairman
J.G. Layter
24. May 1992
OPAL Trigger Group Meeting, CERN
"Proposal for a highly efficient TOF trigger based on single-ended logic."
G.W. Wilson
25. June 22, 1992
OPAL Plenary Meeting, CERN
"The Status of the OPAL HPUX Cluster"
C.C.H. Jui

26. June 1992
OPAL Plenary Week, CERN
"Developments in the single photon analysis"
G.W. Wilson
27. June 23, 1992
OPAL Plenary Week, CERN
"Update of the Radiative Lepton Pair Paper Using 1990 and 1991 Data"
M. Dittmar
28. June 25, 1992
OPAL Plenary Week, CERN
"A Measurement of Inclusive Strange Baryon Production in Hadronic Z0 Decays, Update"
J. Letts
29. July 2, 1992
EAGLE Collaboration Meeting, CERN
"OPAL's Experience with HPUX Cluster"
C.C.H. Jui
30. July 13, 1992
Expanding Horizons Summer Student Program, UC Riverside
"How Many Types of Matter are There?"
G.J. VanDalen
31. July 16, 1992
LSND Collaboration Meeting, Los Alamos, NM
"OffLine Analysis Progress"
G.J. VanDalen

Publications 1991 - 1992

1991

1. M. Daoudi, W. Langeveld, J.G. Layter, W.T. Lin, B.C. Shen, G.J. VanDalen, *et al.* (TPC/Two-Gamma Collaboration), "Test of Spin Dependence in Charm-quark Fragmentation to D^* ", Phys. Rev. **D43** (1991) 29-33.
2. M. Dittmar, W. Gorn, E.G. Heflin, C. Ho, W.J. Larson, J.G. Layter, J. Ma, B.P. O'Neill, H. Oh, K. Riles, B.C. Shen, G.J. VanDalen, Y. Yang *et al.* (OPAL Collaboration), "A Study of Angular Correlations in 4-jet Final States of Hadronic Z^0 Decays", Zeitschrift f. Physik. **C49** (1991) 49-57.
3. M. Dittmar, W. Gorn, E.G. Heflin, C. Ho, W.J. Larson, J.G. Layter, J. Ma, B.P. O'Neill, H. Oh, K. Riles, B.C. Shen, G.J. VanDalen, Y. Yang *et al.* (OPAL Collaboration), "Searches for Neutral Higgs Bosons in e^+e^- Collisions at LEP", Zeitschrift f. Physik. **C49** (1991) 1-15.
4. M. Dittmar, W. Gorn, E.G. Heflin, C. Ho, W.J. Larson, J.G. Layter, J. Ma, B.P. O'Neill, H. Oh, K. Riles, B.C. Shen, G.J. VanDalen, Y. Yang *et al.* (OPAL Collaboration), "A Study of the Recombination Scheme Dependence of Jet Production Rates and of $\alpha_s(M_{Z_0})$ in Hadronic Z^0 Decays", Zeitschrift f. Physik. **C49** (1991) 375-384.
5. M. Dittmar, W. Gorn, E.G. Heflin, C. Ho, W.J. Larson, J.G. Layter, J. Ma, B.P. O'Neill, H. Oh, K. Riles, B.C. Shen, G.J. VanDalen, Y. Yang *et al.* (OPAL Collaboration), "Search for the Minimal Standard Model Higgs Boson in e^+e^- Collisions at LEP", Phys. Lett. **B253** (1991) 511-523.
6. M. Dittmar, W. Gorn, E.G. Heflin, C. Ho, W.J. Larson, J.G. Layter, J. Ma, B.P. O'Neill, H. Oh, K. Riles, B.C. Shen, G.J. VanDalen, Y. Yang *et al.* (OPAL Collaboration), "A Search for Lepton Flavour Violation in Z^0 Decays", Phys. Lett. **B254** (1991) 293-302.
7. M. Dittmar, W. Gorn, E.G. Heflin, C. Ho, W.J. Larson, J.G. Layter, J. Ma, B.P. O'Neill, H. Oh, K. Riles, B.C. Shen, G.J. VanDalen, Y. Yang *et al.* (OPAL Collaboration), "Measurement of the Cross Sections of the Reactions $e^+e^- \rightarrow \gamma\gamma$ and $e^+e^- \rightarrow \gamma\gamma\gamma$ at LEP", Phys. Lett. **B257** (1991) 531-540.
8. M. Dittmar, W. Gorn, E.G. Heflin, C. Ho, W.J. Larson, J.G. Layter, J. Ma, B.P. O'Neill, H. Oh, K. Riles, B.C. Shen, G.J. VanDalen, Y. Yang *et al.* (OPAL Collaboration), "A Model Independent Observation of the String Effect using Quark Tagging at LEP", Phys. Lett. **B261** (1991) 334-346.
9. M. Dittmar, W. Gorn, E.G. Heflin, C. Ho, W.J. Larson, J.G. Layter, J. Ma, B.P. O'Neill, H. Oh, K. Riles, B.C. Shen, G.J. VanDalen, Y. Yang *et al.* (OPAL

- Collaboration), "A Intermittency in Hadronic Decays of the Z^0 ", Phys. Lett. **B262** (1991) 351-361.
10. M. Dittmar, W. Gorn, E.G. Heflin, C. Ho, W.J. Larson, J.G. Layter, J. Ma, B.P. O'Neill, H. Oh, K. Riles, B.C. Shen, G.J. VanDalen, Y. Yang *et al.* (OPAL Collaboration), "A Study of Heavy Flavour Production using Muons in Hadronic Z^0 Decays", Phys. Lett. **B263** (1991) 311-324
 11. M. Dittmar, W. Gorn, E.G. Heflin, C. Ho, W.J. Larson, J.G. Layter, J. Ma, B.P. O'Neill, H. Oh, K. Riles, B.C. Shen, G.J. VanDalen, Y. Yang *et al.* (OPAL Collaboration), "A Search for Scalar Leptoquarks in Z^0 Decays", Phys. Lett. **B263** (1991) 123-134.
 12. M. Dittmar, W. Gorn, E.G. Heflin, C. Ho, W.J. Larson, J.G. Layter, J. Ma, B.P. O'Neill, H. Oh, K. Riles, B.C. Shen, G.J. VanDalen, Y. Yang *et al.* (OPAL Collaboration), "A Study of $D^{*\pm}$ Production in Z^0 Decays", Phys. Lett. **B262** (1991) 341-350.
 13. M. Dittmar, W. Gorn, E.G. Heflin, C. Ho, W.J. Larson, J.G. Layter, J. Ma, B.P. O'Neill, H. Oh, K. Riles, B.C. Shen, G.J. VanDalen, Y. Yang *et al.* (OPAL Collaboration), "The OPAL Detector at LEP", Nucl. Instr. and Meth. **A305** (1991) 275-319.
 14. M. Dittmar, W. Gorn, E.G. Heflin, C. Ho, W.J. Larson, J.G. Layter, J. Ma, B.P. O'Neill, H. Oh, K. Riles, B.C. Shen, G.J. VanDalen, Y. Yang *et al.* (OPAL Collaboration), "A Direct Measurement of the Z^0 Invisible Width by Single Photon Counting", Zeitschrift f. Physik **C50** (1991) 373-384.
 15. M. Dittmar, W. Gorn, E.G. Heflin, C. Ho, W.J. Larson, J.G. Layter, J. Ma, B.P. O'Neill, H. Oh, K. Riles, B.C. Shen, G.J. VanDalen, Y. Yang *et al.* (OPAL Collaboration), "Measurement of the Z^0 Line Shape Parameters and the Electroweak Couplings of Charged Leptons", Zeitschrift f. Physik **C52** (1991) 175-207.
 16. M. Dittmar, W. Gorn, E.G. Heflin, C. Ho, W.J. Larson, J.G. Layter, J. Ma, B.P. O'Neill, H. Oh, K. Riles, B.C. Shen, G.J. VanDalen, Y. Yang *et al.* (OPAL Collaboration), "A Measurement of the Electroweak Couplings of Up and Down Type Quarks Using Final State Photons in Hadronic Z^0 Decays", Phys. Lett. **B264** (1991) 219-232.
 17. M. Dittmar, W. Gorn, E.G. Heflin, C. Ho, W.J. Larson, J.G. Layter, J. Ma, B.P. O'Neill, H. Oh, K. Riles, B.C. Shen, G.J. VanDalen, Y. Yang *et al.* (OPAL Collaboration), "A Study of K_s^0 Production in Z^0 Decays", Phys. Lett. **B264** (1991) 467-475.

18. M. Dittmar, W. Gorn, E.G. Heflin, C. Ho, W.J. Larson, J.G. Layter, J. Ma, B.P. O'Neill, H. Oh, K. Riles, B.C. Shen, G.J. VanDalen, Y. Yang *et al.* (OPAL Collaboration), "A Direct Observation of Quark-Gluon Jet Differences at LEP", Phys. Lett. **B265** (1991) 462-474.
19. M. Dittmar, W. Gorn, E.G. Heflin, C. Ho, W.J. Larson, J.G. Layter, J. Ma, B.P. O'Neill, H. Oh, K. Riles, B.C. Shen, G.J. VanDalen, Y. Yang *et al.* (OPAL Collaboration), "Observation of J/ψ Production in Multihadronic Z^0 Decays", Phys. Lett. **B266** (1991) 485-496.
20. M. Dittmar, W. Gorn, E.G. Heflin, C. Ho, W.J. Larson, J.G. Layter, J. Ma, B.P. O'Neill, H. Oh, K. Riles, B.C. Shen, G.J. VanDalen, Y. Yang *et al.* (OPAL Collaboration), "Measurement of the Three-Jet Distributions Sensitive to the Gluon Spin in e^+e^- Annihilations at $\sqrt{s} = 91$ GeV", Zeitschrift f. Physik **C52** (1991) 543-550.
21. M. Dittmar, W. Gorn, E.G. Heflin, C. Ho, W.J. Larson, J.G. Layter, J. Ma, B.P. O'Neill, H. Oh, K. Riles, B.C. Shen, G.J. VanDalen, Y. Yang *et al.* (OPAL Collaboration), "Measurement of Branching Ratios and τ Polarization from $\tau \rightarrow e\nu\bar{\nu}$, $\tau \rightarrow \mu\nu\bar{\nu}$, and $\tau \rightarrow \pi(K)\nu$ Decays at LEP", Phys. Lett. **B266** (1991) 201-217.
22. M. Dittmar, W. Gorn, E.G. Heflin, C. Ho, W.J. Larson, J.G. Layter, J. Letts, J. Ma, B.P. O'Neill, H. Oh, K. Riles, B.C. Shen, G.J. VanDalen, Y. Yang *et al.* (OPAL Collaboration), "A Study of Bose-Einstein Correlations in e^+e^- Annihilations at LEP", Phys. Lett. **B267** (1991) 143-153.
23. M. Dittmar, W. Gorn, E.G. Heflin, C. Ho, W.J. Larson, J.G. Layter, J. Letts, J. Ma, B.P. O'Neill, H. Oh, K. Riles, B.C. Shen, G.J. VanDalen, Y. Yang *et al.* (OPAL Collaboration), "Decay Mode Independent Search for a Light Higgs Boson and New Scalars", Phys. Lett. **B268** (1991) 122-136.
24. M. Dittmar, J.W. Gary, W. Gorn, E.G. Heflin, C. Ho, W.J. Larson, J.G. Layter, J. Letts, J. Ma, B.P. O'Neill, H. Oh, K. Riles, B.C. Shen, G.J. VanDalen, Y. Yang *et al.* (OPAL Collaboration), "A Measurement of Photon Radiation in Lepton pair Events from Z^0 Decays", Phys. Lett. **B273** (1991) 338-354.
25. M. Dittmar, J.W. Gary, W. Gorn, E.G. Heflin, C. Ho, W.J. Larson, J.G. Layter, J. Letts, J. Ma, B.P. O'Neill, H. Oh, K. Riles, B.C. Shen, G.J. VanDalen, Y. Yang *et al.* (OPAL Collaboration), "Measurement of the τ Lepton Lifetime", Phys. Lett. **B273** (1991) 355-366.
26. S.-Y. Chu and B.C. Shen, "Can the Color Force be Used to Achieve Fusion?", Mod. Phys. Lett. **A6** (1991) 237-244.

27. M. Dittmar and 41 member working group, "*Physics Possibilities*", Report of the Working Group on High Luminosity at LEP, CERN 91-02 (1991) 69.
28. F. Boudjema, R. Casalbuoni, P. Chiappetta, D. Cocolicchio, M. Dittmar, F. Feruglio, B. Gavela (convener), "*Higgs and New Physics*", Report of the Working Group on High Luminosity at LEP, CERN 91-02 (1991) 88.
29. M. Dittmar and J.W.F. Valle, "*Heavy Singlet Neutral Leptons, Flavour and CP Violation on the Z Peak*", Report of the Working Group on High Luminosity at LEP, CERN 91-02 (1991) .
30. D. Cocolicchio and M. Dittmar, "*The Radiative and Hadronic Flavour-Changing Decays of the Z*", Report of the Working Group on High Luminosity at LEP, CERN 91-02 (1991) .
31. B.C. Shen, "*Recent Results from OPAL at LEP*", in Progress in High Energy Physics, Eds. W.-Y. P. Hwang *et al.*, North Holland (1990) 22-45.
32. M. Dittmar, "*The Future LEP Physics Program; Some Aspects of the Next Ten years*", in Progress in High Energy Physics, Eds. W.-Y. P. Hwang *et al.*, North Holland (1990) 89-105.
33. K. Riles, J.J. Gomez Cadenas, *et al.*, "*A Search for Elastic NonDiagonal Lepton Pair Production in e^+e^- Annihilation at $\sqrt{s} = 29 \text{ GeV}$* ", Phys. Rev. Lett. **66** (1991) 1007-1010.
34. K. Riles, "*Review of Tau Physics at LEP*", Proceedings of the 1991 Meeting of the Division of Particles and Fields, American Physical Society, Vancouver, British Columbia, (1991) 272-283.

1992

35. M. Dittmar, J.W. Gary, W. Gorn, E.G. Heflin, C. Ho, W.J. Larson, J.G. Layter, J. Letts, B.P. O'Neill, H. Oh, K. Riles, B.C. Shen, G.J. VanDalen, Y. Yang *et al.* (OPAL Collaboration), "*Properties of Multihadronic Events with a Final State Photon at $\sqrt{s} = M_{Z^0}$* ", Zeitschrift für Physik, **C54**, (1992) 193-209.
36. M. Dittmar, J.W. Gary, W. Gorn, E.G. Heflin, C. Ho, W.J. Larson, J.G. Layter, J. Letts, B.P. O'Neill, H. Oh, K. Riles, B.C. Shen, G.J. VanDalen, Y. Yang *et al.* (OPAL Collaboration), "*Measurement of the Average B Hadron lifetime in Z^0 Decays*", Phys. Lett. **B274** (1992) 513-525.
37. M. Dittmar, J.W. Gary, W. Gorn, E.G. Heflin, C. Ho, W.J. Larson, J.G. Layter, J. Letts, B.P. O'Neill, H. Oh, K. Riles, B.C. Shen, G.J. VanDalen, Y. Yang *et al.* (OPAL Collaboration), "*Measurement of B^0 - \bar{B}^0 Mixing in Hadronic Z^0 Decays*", Phys. Lett. **B276** (1992) 379-392.

38. M. Dittmar, J.W. Gary, W. Gorn, E.G. Heflin, C. Ho, W.J. Larson, J.G. Layter, J. Letts, B.P. O'Neill, H. Oh, K. Riles, B.C. Shen, G.J. VanDalen, Y. Yang *et al.* (OPAL Collaboration), "An Improved Measurement of $\alpha_s(M_{Z^0})$ Using Energy Correlations with the OPAL Detector at LEP", Phys. Lett. **B276** (1992) 547-564.
39. M. Dittmar, J.W. Gary, W. Gorn, E.G. Heflin, C. Ho, W.J. Larson, J.G. Layter, J. Letts, B.P. O'Neill, H. Oh, K. Riles, B.C. Shen, G.J. VanDalen, Y. Yang *et al.* (OPAL Collaboration), "A Search for Free Gluons in Hadronic Z^0 Decays", Phys. Lett. **B278** (1992) 485-494.
40. M. Dittmar, J.W. Gary, W. Gorn, E.G. Heflin, C. Ho, W.J. Larson, J.G. Layter, J. Letts, B.P. O'Neill, H. Oh, K. Riles, B.C. Shen, G.J. VanDalen, Y. Yang *et al.* (OPAL Collaboration), "Test of CP Invariance in $e^+e^- \rightarrow Z^0 \rightarrow \tau^+\tau^-$ and a Limit on the Weak Dipole Moment of the τ Lepton", Phys. Lett. **B281** (1992) 405-415.
41. M. Dittmar, J.W. Gary, W. Gorn, E.G. Heflin, C. Ho, W.J. Larson, J.G. Layter, J. Letts, B.P. O'Neill, H. Oh, K. Riles, B.C. Shen, G.J. VanDalen, Y. Yang *et al.* (OPAL Collaboration), "Evidence for b-flavoured Baryon Production in Z^0 Decays at LEP", Phys. Lett. **B281** (1992) 394-404.
42. M. Dittmar, M. Arignon *et al.*, "The Trigger System of the OPAL Experiment at LEP", Nucl. Instr. and Meth., **A313** (1992) 103-125.
43. S.A. Abel, M. Dittmar, H. Dreiner, "Testing Locality at Colliders via Bell's Inequality?", Phys. Lett. **B280** (1992) 304-312.
44. K. Riles, T. Barklow *et al.*, "A Search for Production of the Final States $\tau^+\tau^-e^+e^-$, $\tau^+\tau^-\mu^+\mu^-$, and $\tau^+\tau^-\pi^+\pi^-$ in e^+e^- Collisions at $\sqrt{s}=29$ GeV", Phys. Rev. Lett. **68** (1992) 13-16.

Publications Submitted

1. M. Dittmar, J.W. Gary, W. Gorn, E.G. Heflin, C. Ho, W.J. Larson, J.G. Layter, J. Letts, B.P. O'Neill, H. Oh, K. Riles, B.C. Shen, G.J. VanDalen, Y. Yang *et al.* (Aleph, Delphi, L3 and OPAL Collaborations), "Electroweak Parameters of the Z^0 Resonance and the Standard Model", CERN-PPE/91-232 (20 December 1991), submitted to Phys. Lett. B.
2. M. Dittmar, J.W. Gary, W. Gorn, E.G. Heflin, C. Ho, W.J. Larson, J.G. Layter, J. Letts, B.P. O'Neill, H. Oh, K. Riles, B.C. Shen, G.J. VanDalen, Y. Yang *et al.* (OPAL Collaboration), "A Global Determination of $\alpha_s(M_{Z^0})$ at LEP", CERN-PPE/92-18 (6 February 1992), submitted to Zeit. für Physik.

3. M. Dittmar, J.W. Gary, W. Gorn, E.G. Heflin, C. Ho, W.J. Larson, J.G. Layter, J. Letts, B.P. O'Neill, H. Oh, K. Riles, B.C. Shen, G.J. VanDalen, Y. Yang *et al.* (OPAL Collaboration), "A Measurement of Electron Production in Hadronic Z^0 Decays and a Determination of $\Gamma(Z^0 \rightarrow b\bar{b})$ ", CERN-PPE/92-38 (6 March 1992), submitted to *Zeit. für Physik*.
4. M. Dittmar, J.W. Gary, W. Gorn, E.G. Heflin, J.G. Layter, J. Letts, H. Oh, K. Riles, B.C. Shen, G.J. VanDalen, *et al.* (OPAL Collaboration), "A Test of Higher Order Electroweak Theory in Z^0 Decays to Two Leptons with an Associated Pair of Charged Particles", CERN-PPE/92-57 (14 April 1992), submitted to *Phys. Lett. B*.
5. M. Dittmar, J.W. Gary, W. Gorn, E.G. Heflin, J.G. Layter, J. Letts, H. Oh, K. Riles, B.C. Shen, G.J. VanDalen, *et al.* (OPAL Collaboration), "A Measurement of the τ Topological Branching Ratios at LEP", CERN-PPE/92-66 (23 April 1992), submitted to *Phys. Lett. B*.
6. M. Dittmar, J.W. Gary, W. Gorn, E.G. Heflin, J.G. Layter, J. Letts, H. Oh, K. Riles, B.C. Shen, G.J. VanDalen, *et al.* (OPAL Collaboration), "A Study of Two-Particle Momentum Correlations in Hadronic Z^0 Decays", CERN-PPE/92-89 (29 May 1992), submitted to *Phys. Lett. B*.
7. M. Dittmar, J.W. Gary, W. Gorn, E.G. Heflin, J.G. Layter, J. Letts, H. Oh, K. Riles, B.C. Shen, G.J. VanDalen, G.W. Wilson, *et al.* (OPAL Collaboration), "Inclusive Neutral Vector Meson Production in Hadronic Z^0 Decays", CERN-PPE/92-116 (7 July 1992), submitted to *Zeit. für Physik*.
8. M. Dittmar, J.W. Gary, W. Gorn, E.G. Heflin, J.G. Layter, J. Letts, H. Oh, K. Riles, B.C. Shen, G.J. VanDalen, G.W. Wilson, *et al.* (OPAL Collaboration), "A Measurement of Strange Baryon Production in Hadronic Z^0 Decays", CERN-PPE/92-118 (13 July 1992), submitted to *Phys. Lett. B*.
9. M. Dittmar, J.W. Gary, W. Gorn, E.G. Heflin, J.G. Layter, J. Letts, H. Oh, K. Riles, B.C. Shen, G.J. VanDalen, G.W. Wilson, *et al.* (OPAL Collaboration), "A Measurement of the Forward-Backward Charge Asymmetry in Hadronic Decays of the Z^0 ", CERN-PPE/92-119 (14 July 1992), submitted to *Phys. Lett. B*.
10. M. Dittmar, J.W. Gary, J.G. Layter, K. Riles, G.J. VanDalen, *et al.*, "The Detector Simulation program for the OPAL Experiment at LEP", CERN-PPE/91-234 (December 1991), submitted to *Nucl. Instr. and Meth.*
11. W. Gorn, B.P. O'Neill, *et al.*, "The Data Acquisition System of the OPAL Detector at LEP", CERN-PPE/92-xxx (July 1992), submitted to *Nucl. Instr. and Meth.*

12. W. Gorn, G.J. VanDalen *et al.*, "*Muon-neutrino Carbon Charged-Current Interaction Near the Muon Threshold*", submitted to Phys. Rev. C.
13. M. Dittmar, "*Testing the Tau Lepton*", to appear in the Proceedings of the 26th Rencontres de Moriond, Electroweak and Unified Theories, Les Arcs, France, 10-17 March 1991.
14. M. Dittmar, "*A Measurement of Photon Radiation in Lepton Pair Events from Z^0 Decays*", to appear in the Proceedings of the International Meeting on Physics Beyond the Standard Model, Valencia, Spain, October 2-5 (1992).
15. M. Dittmar, "*The Search for Rare Exotic Z^0 Decays*", to appear in the Proceedings of the International Workshop on Search for New Elementary Particles, ICTP, Trieste, May 20-22 (1992).

2.2 OPAL at LEP

In this section of the report, we present first the progress made in the operation of LEP and in measuring the beam energy. Subsequently we summarize the improvements to the OPAL detector, both new hardware and refinements to the online and offline environments. The remainder of the section will outline some of the principal physics results which OPAL has obtained.

2.2.1 LEP Performance

LEP performance in 1991 was impressive by almost any standard but that of the expectations of the experimenters. The "million Z's per year" still stands as a distant goal. Nevertheless there was significant improvement in luminosity and in uniformity of luminosity for the four experiments. Equally important was the achievement of precise energy measurement by resonance depolarization which has lowered the energy uncertainty by a factor of nearly three. The energy is now determined by a direct measurement and no longer depends on a precarious structure of correction factors as did the previous energy value. An unexpected surprise was the discovery that, however well the energy is measured on the average, it may be different in different interaction regions.

Luminosity

LEP did achieve a significant increase in integrated luminosity during 1991, 18.651 pb^{-1} compared to 12.235 pb^{-1} in 1990. Part of the increase was due to the 40 additional days of operation in 1991, but the average integrated luminosity per day increased from 77 pb^{-1} in 1990 to 158 pb^{-1} last year. While these two statements appear to be contradictory, it must be remembered that these numbers represent the "theoretical luminosity," based on measured beam intensity. It was known in 1990 that the theoretical luminosity largely overestimated the actual luminosity, and this problem was traced to beam-beam effects, prompting a change in the "operating point" for 1991. The 1991 theoretical luminosity figure is a reasonable approximation to the delivered luminosity, but the 1990 number must be derated by about 33%, which has been done in Figure 2.1.

Large differences between the luminosities seen by the four detectors, in 1990 amounting to nearly 25%, were traced to quadrupole misalignment. This was remedied in large part for 1991, and the differences were less than 5%. Unfortunately, OPAL is now the lowest of the four, and the measured luminosity delivered to OPAL was 16.6 pb^{-1} . Approximately two thirds of this amount was on the Z^0 peak and the remainder at 880 MeV increments above and below. (The value of this increment was dictated by the presence of depolarizing resonances, as we discuss below.)

Regardless of the peak luminosity one can achieve, the integrated luminosity depends on the average luminosity, which involves the factor η , the "availability" for physics, effectively the efficiency of operation. As we discussed in last year's report, this efficiency is simply $\eta = t_{phys}/(t_{phys} + t_{reload})$. It was hoped that a major boost in integrated luminosity would result from reductions in t_{reload} during the past year, but this was not the case. The running efficiency of the OPAL detector however improved from 78% in 1990 to 86% last year, so OPAL was able to collect 352,000 multihadrons during the period, for a grand total of over 500,000 for the two years.

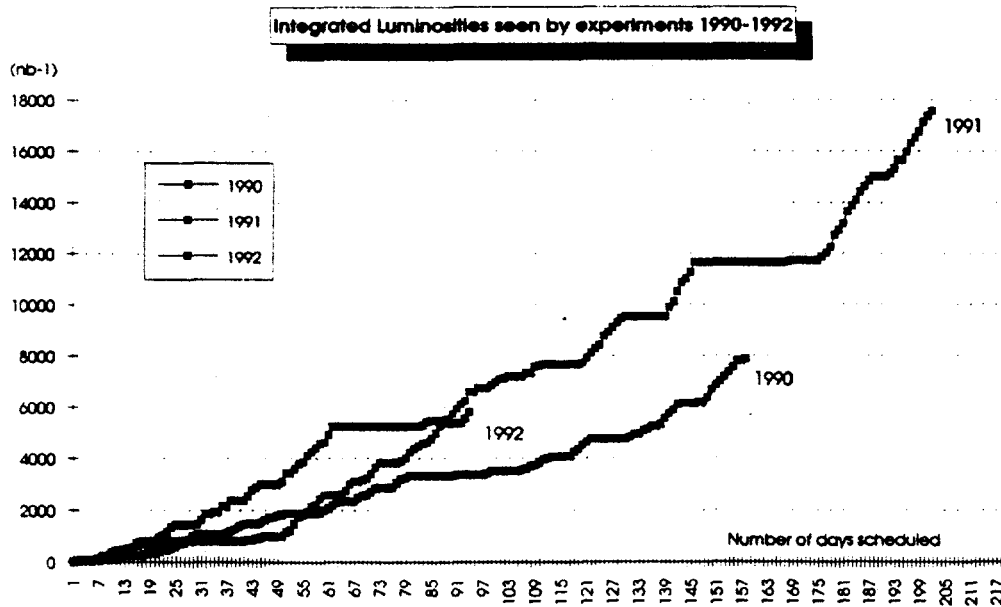


Figure 2.1: Theoretical integrated luminosity versus time for three years of LEP operations.

Polarization

During the last machine development run of 1990, a hurried measurement seemed to indicate the presence of transverse polarization of the beams. The importance of the existence of polarization for a precise determination of the beam energy led to a more serious effort during 1991, which has recently been described in a report by the LEP staff [1].

In the absence of closed orbit distortions, one expects the beams to reach the Sokolov-Ternov limit of 92.4% in a characteristic time of 310 minutes at a beam energy of 46 GeV. However, there are closed orbit distortions. A computer program SITF calculates the polarization to be expected on the basis of all known first order

effects as a function of the "spin tune" ν_s , the number of spin precessions in one turn around the ring, given by

$$\nu_s = \frac{g_e - 2}{2} \frac{E_{beam}}{m_e c^2}$$

Its proportionality to beam energy is the key to the method. The program predicts a polarization of approximately 20% for a spin tune of 105.5. The study attempted to measure the actual polarization at this value of the tune.

The experimental technique is to measure the vertical profile of a pulse of circularly polarized light from a Nd-YAG laser after it has been backscattered off the beam by spin-dependent Compton scattering. The amount of vertical deviation of the pulse $\Delta\langle Y \rangle$ relative to its position when the light is unpolarized is given by the relation

$$\Delta\langle Y \rangle = \kappa \xi P_e$$

where κ is the analyzing power of the polarimeter, ξ is the helicity of the polarized light; and P_e is the transverse polarization of the beam. The result of the measurement is a polarization on the order of 10%. Second order effects evidently reduce the predicted polarization by about a factor of two, but this is still sufficient to permit depolarization to be observed.

Resonant depolarization is produced by exciting the beam with an oscillating magnetic field generated by a vertical kicker magnet. This exciting field is thus perpendicular to the beam axis and situated in the plane of the ring. If the frequency of the resulting spin kick is in phase with the spin precession, a resonance condition occurs. Electron spins are coherently swept away from the vertical direction, and polarization disappears.

In practice, the exciting field is scanned over a frequency range around the fractional part of the spin tune, δ_s . If the scanning range includes the resonance point, the polarization level drops precipitously to zero, as shown in Figure 2.2. In some cases the polarization goes to negative values, corresponding to a spin flip. In any case, knowledge of the fractional part of the spin tune is generally sufficient to fix the beam energy. Uncertainties arise because of the discrete step size of the scan, and also because the "mirror frequency," $1 - \delta_s$, also gives rise to depolarization.

The correction to the so called "Field Display" energy obtained by resonance depolarization agrees surprisingly well with the "brute force" method described in detail in last year's report, but with an uncertainty over three times smaller:

$$E_{beam} = E_{FD} \times [1.0 - (7.4 \pm 0.6) \times 10^{-4}].$$

During 1991 the method was attempted at only one spin tune value. It is assumed that it will work as well at other values of the energy scan, which were chosen in fact to lie in the vicinity of resonances. In the meantime, other problems have arisen, as we discuss below.

Center of Mass Energy at I6

Already in 1990 it was apparent that OPAL's result for the mass of the Z^0 was some 20 MeV below that of the other experiments. Since this difference amounted to only two standard deviations, it was not a cause for worry, but it did lead some to ask if it pointed to some deeper misunderstanding of machine behavior. During 1991 the difference persisted and became more statistically significant. It then provoked a serious investigation of the problem. The startling result was that misalignment of the accelerating cavities could indeed lead to different effective center of mass energies in different interaction regions.

In order to establish OPAL's case, members of the group made exhaustive examinations of possible causes not related to the beam energy. The first candidate was the possibility of a spurious scan point in the OPAL data. Fits made dropping various combinations of points consistently led to the same low value for the mass. The next possibility was the fitting program ZFITTER. In the course of producing the combined LEP result on the Z^0 parameters, OPALites applied their program to the ALEPH data and reproduced their answer to within 1 MeV. Although OPAL has always considered its multihadron selection to be particularly robust, it nevertheless explored a completely new selection procedure and again arrived at the same low value. Still another avenue dealt with the luminosity. A correction must be made for the $Z^0 - \gamma$ interference. If the correction is not made, there is indeed a mass shift of approximately 15 MeV, but in the wrong direction. Armed with these null results, OPAL took its case to the machine physicists.

The only scenario consistent with all the facts was that the electrons and positrons would get a higher acceleration entering the OPAL region and a lower acceleration on leaving. This would leave the results of the other experiments intact and would also not affect the various methods of determining the beam energy, which measure an average value. The explanation involves the fact that two accelerating frequencies are present in the copper cavities, both near the 352 MHz fundamental machine frequency, but differing by twice the crossing frequency, about 90 kHz. To ensure equal acceleration of the beam particles entering and leaving the interaction point, the cavity spacing should be given by $d_0 = n \frac{c}{f_0}$ where f_0 is the simple average of the two relevant frequencies. In OPAL the cavities are spaced with a value appropriate for the lower frequency rather than the average. Beam particles enter the cavities too early and get too large a kick, and leave too late and get a compensating smaller acceleration. This is shown schematically in Figure 2.3.

The effect can in principle be evaluated and corrected, but the correction involves detailed LEP operational parameters. The preferred OPAL solution is a realignment of the cavities, a step the machine people are willing to consider. Since the beginning of this year OPAL has not issued updated mass values pending a satisfactory resolution of the question.

16 Sept. 1991

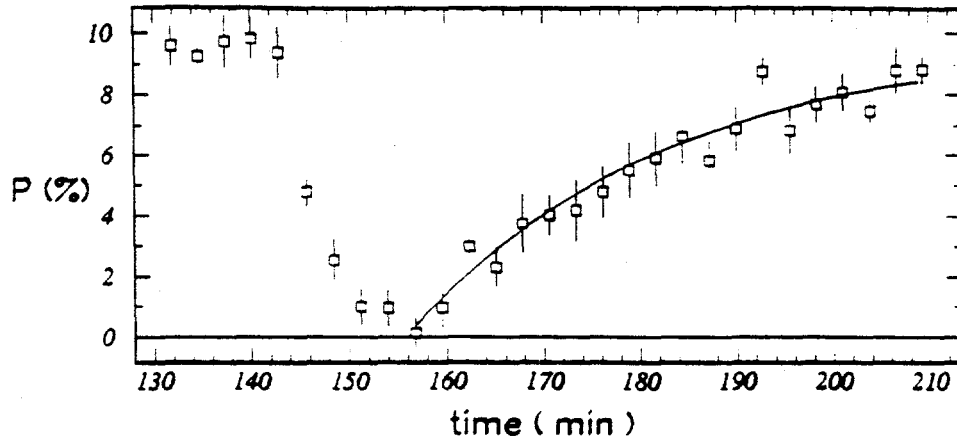


Figure 2.2: Polarization signal showing first a stable polarization region in the neighborhood of 10%, then a rapid depolarization as the exciting field is applied, and finally the asymptotic rise to the earlier stable level. The fitted curve indicates a characteristic time of 35 ± 10 minutes.

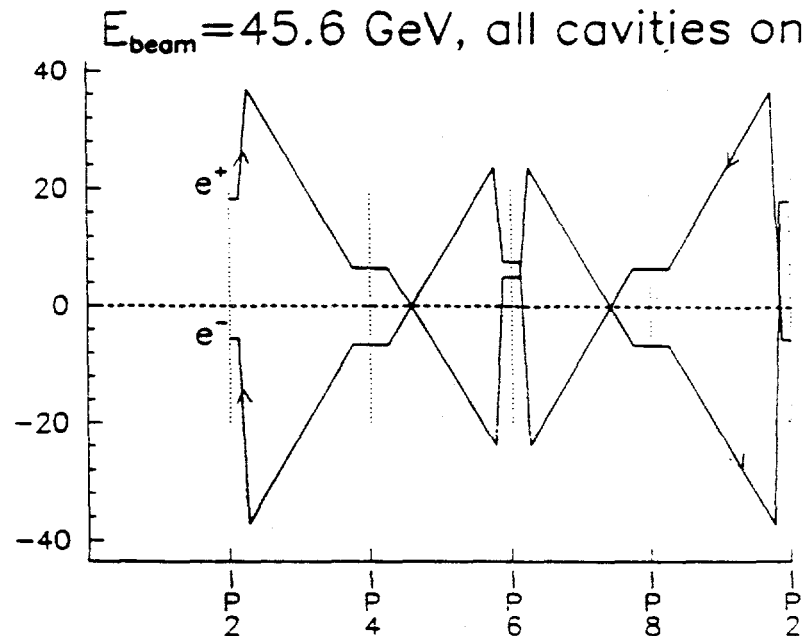


Figure 2.3: Energy of the particle beams relative to the nominal energy at the various interaction regions. A net energy shift is observed at points 2 and 6.

LEP Running Plans

LEP still plans to introduce 8-on-8 bunch running sometime in 1992, but improved beam instrumentation is required to bring this step to reality. The so called 90 degree lattice, necessary for LEP 200 running, is now operational but peak luminosities have not passed 6×10^{30} . Transverse alignment of beam elements is seen to be deteriorating. Misalignments on the order of 140 microns have been seen, nearly five times the design values. This affects beam dispersion and seems to be worsening.

In spite of the massive financial perturbation resulting from the unfavorable judgment in the contract dispute with the LEP construction consortium, CERN still expects to have superconducting cavities in sufficient quantities to reach W^+W^- threshold in 1994, which will mark the beginning of the LEP 200 era. Some delays have been experienced in the delivery of the initial complement of cavities, but there is optimism that the lost time can be recouped. Although short term scheduling for LHC continues unchanged, there are too many uncertainties in the long term prospects to merit comment at this time.

2.2.2 The OPAL Detector

OPAL surpassed all the other LEP detectors in number of Z^0 s collected during the 1991 run period, logging nearly 352,000 multihadron events. This came about largely from the detector's very high uptime of 86%, up from 78% in 1990, which in turn was due to the persistence of the data acquisition group in isolating the sources of deadtime in several detector components.

During 1991 the new silicon strip vertex detector was incorporated into OPAL, and approval was given for the construction of a Si-W luminosity monitor, to be ready for the 1993 running period, that is designed to give 0.1% precision in the luminosity measurement. Performance of the current OPAL luminosity monitor has continued to improve during this year. Major upgrades were made to the online data acquisition system, and all subdetectors are capable of taking data in a regime of 8×8 bunches. Continual improvements are being made in the hadron calorimeter electronics to increase efficiency and reliability and to extend monitoring capabilities. Computing farms keep proliferating, and OPAL, led by the Riverside group, has begun assembling a Hewlett-Packard based farm which will provide extensive Monte Carlo capacity. Finally a proposal is made to improve time-of-flight triggering.

Silicon Strip Vertex Detector

The first phase of the OPAL silicon strip vertex detector was installed during the 1990-1991 shutdown and became fully operational by June of 1991. This version has two layers of single-sided strips giving information in the r - ϕ plane. The silicon wafers, developed in conjunction with Micron in the U.K., incorporate the "Foxfet" transistor which provides dynamic biasing resistance. The MX5 multiplexor chip, originally planned for the phase two version, was available by June and showed an improved signal to noise ratio over the earlier MX3 chip. The high voltage system for the Si vertex detector was manufactured in Italy under the supervision of Dr. William Gorn of UCR.

A large initial calibration effort was necessitated by the fact that the extreme thinness of the detector made it subject to distortion from gravitational sag and torques applied during insertion over the beampipe. The detector as installed began to match the precision of the test bed versions at the end of the running period. In one typical physics application, a significant improvement is obtained in the impact parameter resolution for dilepton events, as shown in Figure 2.4. Information from the Si vertex detector is now regularly used in standard reconstruction routines. The phase one version of the chamber will remain in place throughout 1992. Two-sided strips providing z coordinate information will be installed during the 1992-1993 shutdown.

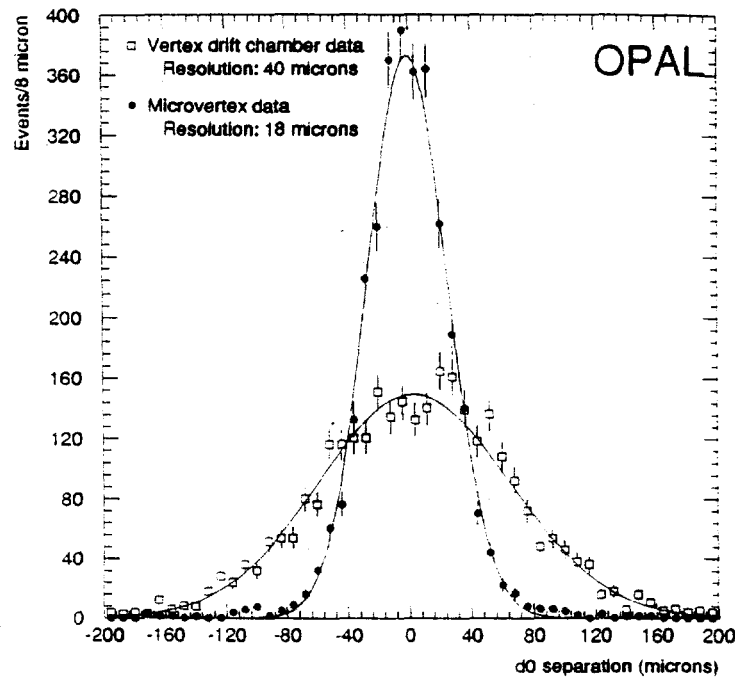


Figure 2.4: Resolution in the impact parameter for dilepton events with and without the information from the Si vertex detector.

Current Luminosity Precision

The OPAL Forward Detector was initially felt to be far inferior to those of the other LEP detectors. However, persistent attention to all the sources of uncertainties has reduced the overall experimental uncertainty in the luminosity determination to below 1%. The current level of the systematic errors from all sources is presented in Table 2.1.

Si-W Luminosity Monitor

As LEP begins to reach statistics of one million Z^0 s per year, it will become necessary to push the luminosity determination down to a precision on the 0.1% level. Even the most heroic efforts of the OPAL luminosity group will not be able to achieve this with the current forward detector for the simple reason that it does not see enough of the forward bhabha cross section to collect sufficient statistics. This is the motivation for the silicon-tungsten luminosity monitor, approved for construction at the end of last year by the LEP Committee and the CERN REsearch Board.

The position of this new detector element relative to the existing luminosity monitor is shown in Figure 2.5. Its fiducial region will lie between 25 and 60 milliradians, and consequently it will see a cross section of 70 nb, sufficient to achieve the desired precision. The Si-W detector, whose innermost radius is only 6 cm from the beam it-

Source of Error	Uncertainty [%]
Inhomogeneity in tube chambers	0.5
Pitch of tubes	0.4
Survey (with drift chambers)	0.2
Data statistics	0.2
Monte Carlo statistics	0.1
Calorimeter coordinates	0.1
Distance to interaction point	0.1
Trigger efficiency	< 0.1
Tube chamber inefficiency	< 0.1
Overall	0.7

Table 2.1: Preliminary estimate of systematic errors in the absolute luminosity determination for 1991

self, will consist of 18 layers of silicon wafers interleaving precisely machined tungsten slabs for a total of 22 radiation lengths. The wafers in each layer will be divided into r - ϕ pads of 2.5 mm radial pitch and 11.25° azimuthal segmentation, a total of 30,720 channels. Readout will use the AMPLEX chip, developed at CERN for a variety of silicon detectors. Scheduling is tight to have this detector ready for installation during the 1992-1993 shutdown, but so far it is still on course.

Data Acquisition

The most significant development in the OPAL data acquisition system for 1991 was the migration of the higher level functions of the filter and the online event reconstruction from VME 68000 class CPUs to the more flexible HP (Apollo) DN10000 machines. The overall configuration is shown schematically in Figure 2.6.

The function of the filter is to verify the hardware trigger and to classify the events into physics categories such as multihadronic or leptonic. The existence of such a process in the acquisition chain makes it possible to use loose hardware triggers with high and easily measurable efficiencies, but which also contain relatively high background levels. The filter is able to reject such backgrounds, and with current trigger implementations, approximately 35% of the triggered events are rejected at

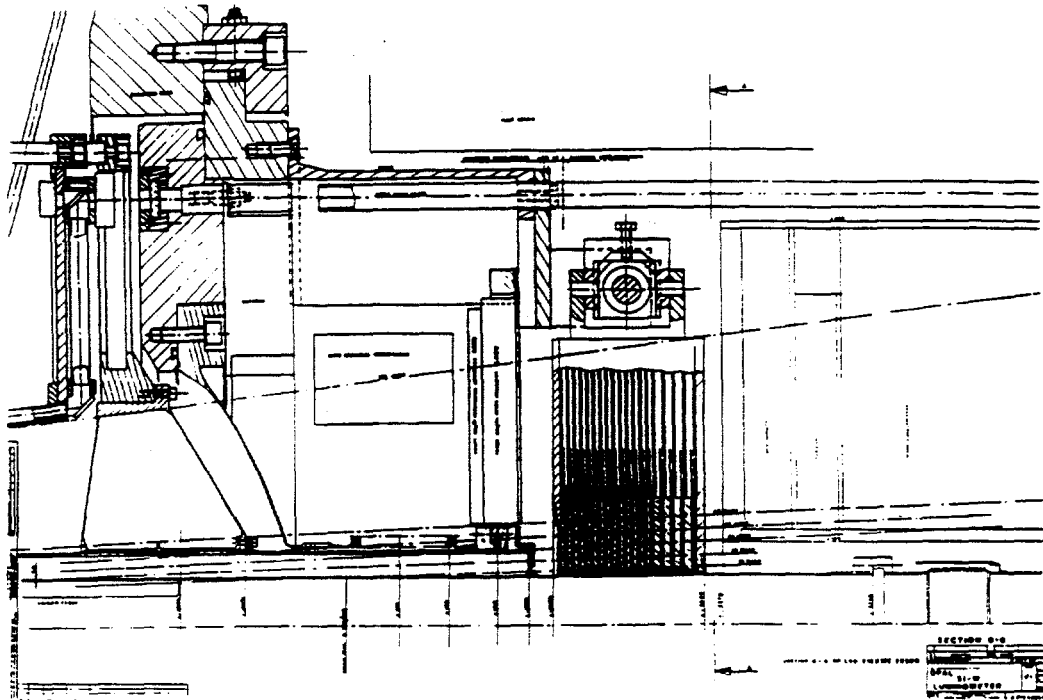


Figure 2.5: The position of the Si-W luminosity monitor relative to the existing forward detector.

this level. The filter also carries out data compression on accepted events and writes them to an optical disk buffer where they await the reconstruction step, which can thus run asynchronously.

In the initial OPAL proposal, the online event reconstruction was to be carried out by specially built 370/E emulators. Unfortunately, event size and algorithmic complexity outstripped the capacity of the emulators before they were ever installed, so the online reconstruction step was simply skipped prior to 1991 and the task postponed to the offline analysis phase. The advent of powerful and modular RISC processors such as the DN10000s, together with the introduction of the optical disk buffer, made it possible finally to recover online reconstruction capability. Running asynchronously with data taking, the processors can wait for the necessary calibration data to become available from the front end VME processors before beginning the reconstruction step. By taking advantage of the rundown in luminosity during a fill, the DN10000s can easily keep pace with the average data rate and so make fully reconstructed events available for offline analysis within 90 minutes of the event triggers.

A comprehensive paper discussing the OPAL trigger was published during the past year[2], consequently this topic will not be treated here.

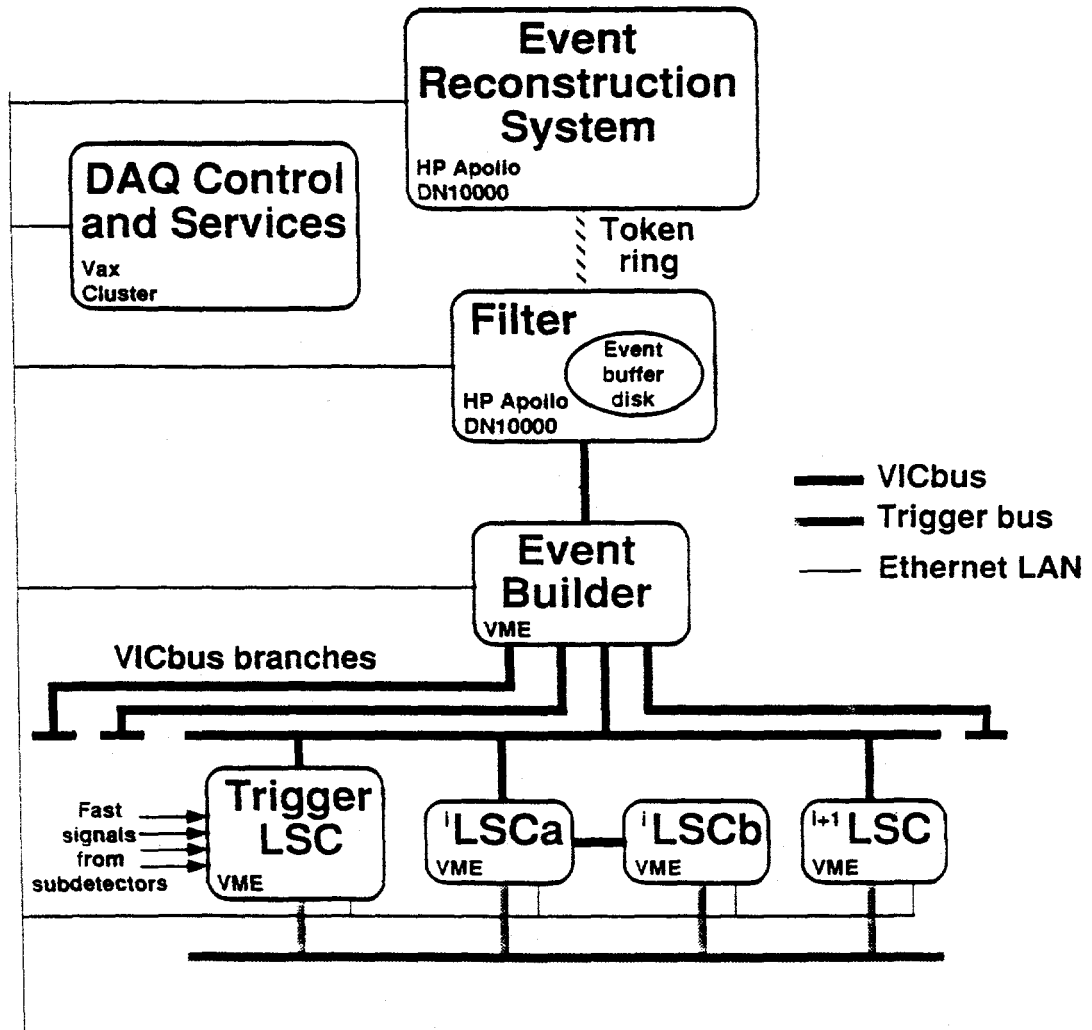


Figure 2.6: Schematic of the OPAL data acquisition system

Hadron Calorimeter

During the past year, there were two major upgrades of the OPAL Hadron Calorimeter Strips data acquisition system, (along with numerous small improvements). These consisted of the introduction of a second processor board in each readout crate, and the buffering of the data during readin.

The addition of a second processor follows an OPAL-wide decision to attempt to increase data throughput and eliminate the costly tails in the deadtime distributions of the various subdetectors. The second processor allows a division of processing responsibility: one board deals with the frontend readout while the second board does the event formatting and monitoring. The arrangement obviously increases throughput simply because of the increase in computing power. It also completely eliminates the deadtime tails, which were due entirely to interrupts from the local area network. In the new configuration the network is connected directly to the new processor and hence never interrupts the old processor doing the frontend readout. The addition of this second processor necessitated a significant rewrite of the data acquisition system, as well as the related monitoring system. The result has been the complete elimination of the tails in our deadtime distribution, without any degradation of the previous high reliability of the acquisition system.

The buffering of the readin was done in order to cope with any foreseeable increase in LEP luminosity. Prior to this year, the strips acquisition had an average deadtime of about 4ms, i.e., 1ms less than the design maximum for all subdetectors as set down when the OPAL data acquisition system was first specified. Since that time, LEP has come up with a scheme to greatly increase its luminosity. Should this scheme be implemented, the OPAL subdetectors will be required to reduce their deadtimes in order that the overall OPAL deadtime remain acceptably low.

By introducing a frontend data buffer, we are now able to accept a second event and hold it in the front end while we are still processing the first event. This lowers our deadtime to the 0.8 ms it takes to read in the frontend buffer, a five-fold reduction. Thanks to these two upgrades, the Hadron Calorimeter Strips should be able to take data under any currently anticipated running conditions at LEP.

UCR Monte Carlo RISC Farm for OPAL

Monte Carlo simulation plays a direct and essential role in the extraction of the physics content from data for nearly all studies at high energy facilities. With the large size and complexity of present day detectors, the Monte Carlo method is the most tractable, if not the only, means to address such basic questions of analysis as detector performance, acceptance and resolution.

The Monte Carlo simulation of the Z^0 decay event samples for the experiments at LEP is and will continue to be a major challenge for the experimental groups. This is not only because of the complexity of the detectors, but also because of the

very large data samples being collected. The OPAL detector contains many different subdetector units. Furthermore, there exists passive material in the form of the beam pipe, magnet coil, cables, pressure vessels and other elements. The OPAL simulation program is as a consequence very CPU intensive: a single multihadronic Z^0 decay generated with OPAL simulation requires approximately 8 minutes on a 5 mips machine, the standard CERN IBM/168 unit. (This is roughly equivalent to 14 minutes per event on a VAX 3600 station with 16 Mbyte memory.) So called "smear mode" simulations, which bypass the detailed step-by-step simulation of detector response by using parametrizations, are not adequate for the precision measurements of OPAL. An additional problem is that previously generated events become obsolete. For example, events generated in 1989 and 1990 do not have a simulation of the silicon microvertex detector, which was installed for 1991.

The experimental data sample at the end of 1991 stood at about 500,000 multihadronic events, with an additional 500,000 or more expected before the end of 1992. In planning the Monte Carlo resources, the capacity to generate many simulated samples, each with more statistics than the experimental one, must be envisioned in order that systematic studies for the physics analyses can be performed and that different physics event generators can be used. It is also desirable to incorporate improved simulations of detector elements as expeditiously as possible. Thus utilization of the OPAL data sample to its full potential requires the capacity to generate millions of fully simulated events on a reasonably short time scale. This is far in excess of the capacity that has been available heretofore.

UCR is at the forefront of the OPAL Collaboration in addressing and implementing a solution to this problem. We have purchased a network of nine HP workstations to be dedicated to event simulation, based on the new generation of reduced instruction set computers (RISC). These computers are designed around the relatively new "Precision-Architecture" (PA) chip sets developed by Hewlett Packard, and offer performance of up to 57 mips, roughly an order of magnitude faster than a Vaxstation 3100, at a cost approximately equivalent to the price of the latter when originally introduced. The computing power of these machines is far greater, relative to their purchase and maintenance costs, than what is available with other commercial devices.

Currently, OPAL has in operation a cluster of 10 HP-PA workstations, and another 8 are on order. These are configured in a single cluster with system file service from a single "boot-node." Figure 2.7 shows a schematic of the anticipated cluster configuration. When all 18 machines are installed, the total CPU power of the HP cluster will roughly equal that of the existing VAX cluster and of the older Apollo workstations combined. The FDDI protocol (which also works over ordinary ethernet hardware) will provide a high-speed link to the CERN central computing facility, while the cluster itself will occupy the existing ethernet in the OPAL building at CERN. It is also possible to install cluster clients elsewhere within the CERN site using the same server. The RD5/CMS group currently operates a client HP-720 over

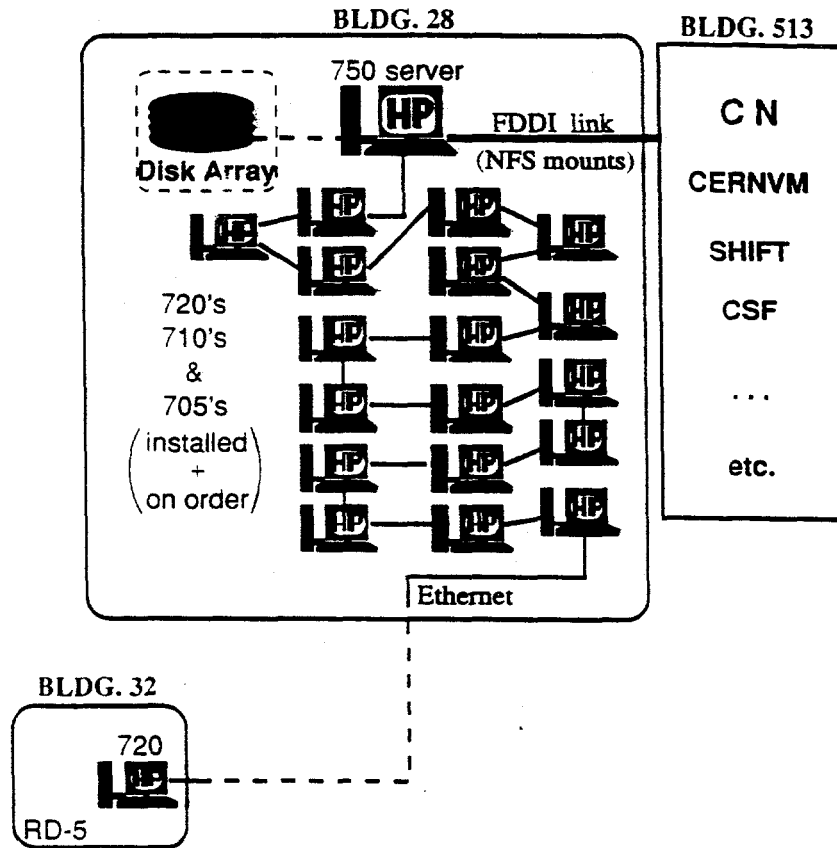


Figure 2.7: Configuration of the OPAL RISC Farm

a kilometer away from the cluster server.

We are now setting up this Monte Carlo cluster for OPAL with UCR resources and personnel to be used for system management. A UCR postdoc (Jui) and student (Chu) are now working on this project in conjunction with a faculty member (Gary). Tests show that we can produce approximately 1,000 multihadron events per day on each machine. The initial goal is to generate about 10,000 multihadron events per day on the cluster, which should allow us to bridge the current lag between the time the data is collected and the time when a Monte Carlo sample to simulate it has been created. In addition, for the first time in OPAL's history, we should be able to generate large samples of Monte Carlo events with several different multihadron generators to better understand and reduce systematic errors. This UCR RISC cluster will constitute a major contribution to the OPAL data analysis program over the next few years.

TOF Improvements

The OPAL time-of-flight (TOF) counters, being scintillators, are ideally suited for triggering functions. As they have been used thus far in OPAL, the TOF counters

are always used in two-ended mode, i.e., there must be a coincidence of signals from both ends of the scintillator bar for a hit to be registered. Since the bars are nearly 7 meters long, particles passing near one end are frequently missed since the light does not trigger the photomultiplier on the other end. This results in a loss of efficiency as a function of polar angle. Unfortunately, the function is neither simple nor general since it depends on details of the construction of each scintillator bar, but it varies roughly between 0.97 and 0.78 with an average of 0.92.

To address this problem, Dr. Graham Wilson, who has recently joined the UCR group and who was responsible for the TOF system in his previous position with the Saclay group, has devised a method of bringing the single-ended response of the scintillator bar into coincidence with other detector elements making up the theta-phi matrix (TPM) to result in a trigger element, TPTTTO, which would be essentially independent of polar angle in the barrel region and have an efficiency of 97%. The additional rate from such a trigger would be at a level of 0.1 Hz. The basic idea of his scheme is shown in Figure 2.8

The beauty of Dr. Wilson's proposal is that it makes use of previously unused output spigots on mixer modules ("melangeurs") already forming part of the trigger and so can be implemented quite cheaply for the remainder of 1992. An extension of this idea for 1993 to provide a loose pretrigger together with the current tight trigger function would require additional fanouts at somewhat higher cost. The necessary items are:

- 320 Lemo cables (40 ns) from constant fraction discriminators to mixers
- 40 Lemo cables (20 ns) from mixers to TPIN/TPOUT (These generate theta-phi matrix outputs.)
- 40 8-way CAMAC mixer modules (A few modules already exist.)
- 2 TPIN/TPOUT modules

The total cost of these items is approximately \$18,000.

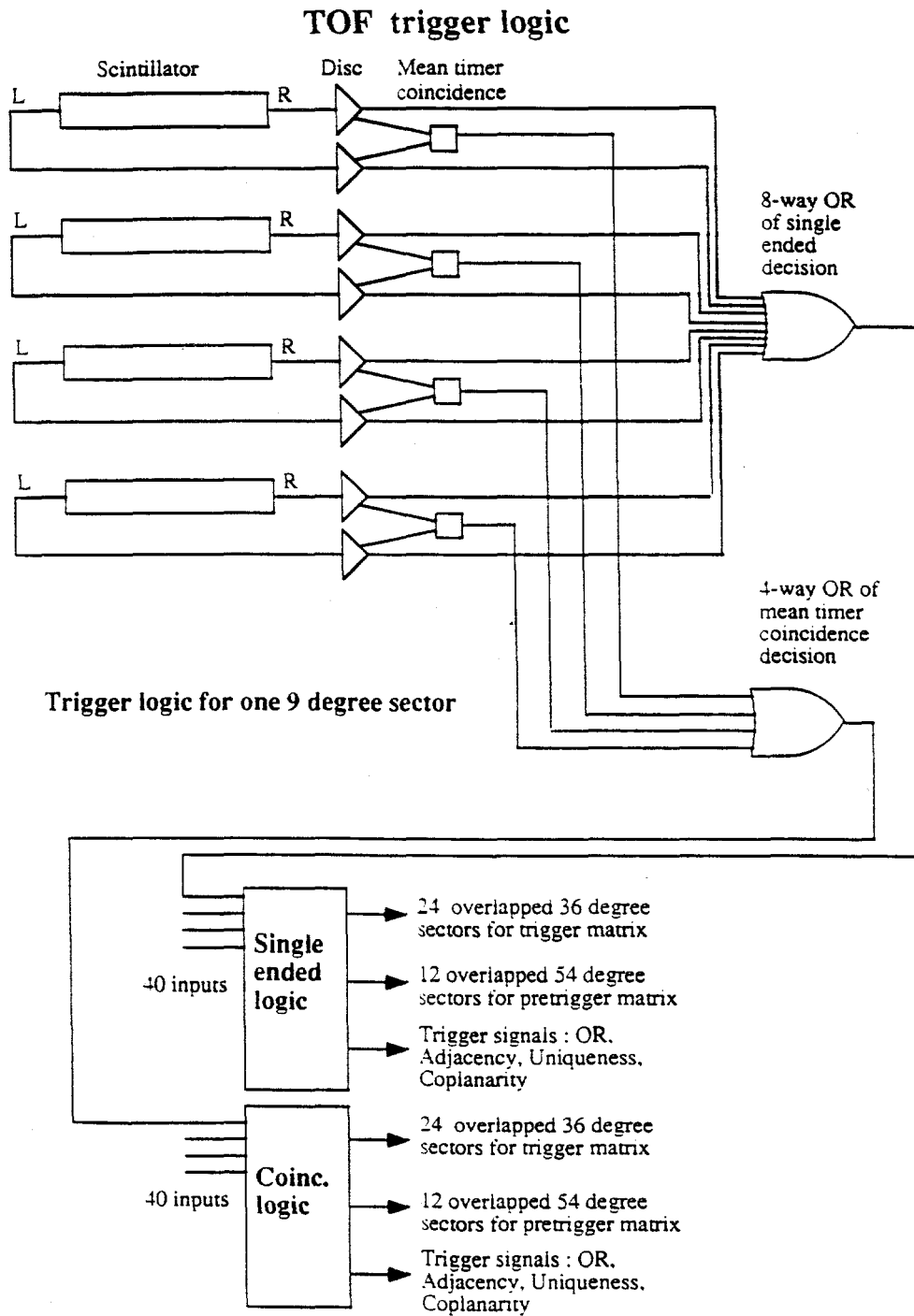


Figure 2.8: Schematic diagram for the single ended TOF trigger

2.2.3 Electroweak Studies at the Z^0

Within the framework of the Standard Model, M_Z , the mass of the Z^0 boson, the massive neutral carrier of the electroweak field, is a fundamental parameter. Its precise determination, in conjunction with the knowledge of the fine structure constant α and the Fermi coupling constant G_F leads to well defined predictions for the couplings of the Z^0 to all fermions. Since these couplings, as well as the mass of the Z^0 , are measured to high precision at LEP, comparison with predictions provides a stringent test of the Standard Model and places bounds on the allowed ranges of M_t and M_H .

We update OPAL's determination of electroweak parameters from Z^0 decays to reflect the line shape and lepton forward-backward asymmetry measurements performed with the 1991 data set, combined with our published measurements based on the 1990 data set. Preliminary results based on these data were presented at the 1992 Aspen Winter Conference [3]. Improved calibrations have allowed the inclusion of a part of our data set which was not used for the results presented at Aspen. The results presented here benefit from much improved systematic uncertainties in the event selection analyses, which are now essentially final. Since the 1991 luminosity analysis is however not yet final, we do not update our published value for the hadronic pole cross section.

The Relative Luminosity Measurement

The relative luminosity measurement for the 1991 data set was described in an earlier document [3]. The point-to-point relative luminosity error was dominated by (small) fill-to-fill fluctuations in the energy calibration of the Forward Detector calorimeter. This error scaled as $0.2\%/\sqrt{N_{\text{fills}}}$ where N_{fills} is the number of fills at each energy point. Since N_{fills} was always at least five, the systematic uncertainty in the relative luminosity was less than 0.1% at any one of the scan points and therefore negligible compared to the statistical uncertainty.

The Hadronic Decay Channel

In our previous publication [4], the criteria used to select hadronic Z^0 decays were based on energy clusters in the electromagnetic calorimeter and the charged track multiplicity. The accuracy of the acceptance calculation for this selection was limited by a 0.3% systematic uncertainty due to modelling of hadronisation. For the 1991 data, energy clusters in the forward detector calorimeter were also used in order to increase the geometrical acceptance and therefore reduce the sensitivity to the fragmentation model. Furthermore, invariant mass cuts were used to further reduce background contamination, in particular from $Z^0 \rightarrow \tau^+\tau^-$ decays.

The following five requirements defined a multihadron candidate:

- The total multiplicity of charged tracks and clusters in the electromagnetic calorimeter was at least 12.
- The sum of the total energy in the lead glass and one third of the total energy in the forward detector was at least 9% of the center-of-mass energy.
- An energy imbalance along the beam direction was less than 75% of the visible energy.
- The sum of the invariant masses of the two hemispheres defined by the thrust axis was required to be larger than 3.5 GeV.
- The charged track multiplicity in both of the thrust hemispheres was at least 2.

The acceptance of the event selection was determined to be 99.48% with a statistical error of 0.02% for the JETSET Monte Carlo events with the 1990 OPAL detector configuration. For the 1991 configuration, which differed mainly by the installation of a Silicon micro-vertex detector and an additional small diameter beam pipe, the acceptance was found to be $(0.03 \pm 0.02)\%$ higher, resulting in a Monte Carlo acceptance estimate of $(99.51 \pm 0.03)\%$.

The main contamination in the hadronic data sample came from $\tau^+\tau^-$ and two-photon multihadronic events. For $\tau^+\tau^-$ events, a background fraction of $0.17 \pm 0.01\%$ was estimated by using Monte Carlo events generated with the KORALZ program, which reproduced the real data distributions reasonably well. The small differences observed between data and Monte Carlo in the invariant mass distributions were taken into account in the estimate of the systematic uncertainty. The background from two-photon processes was estimated from the data by measuring the ratio of the numbers of the events with high and low $R_{vis}^{EC} \equiv \sum E_{clus}/\sqrt{s}$ and the ratio of the numbers of events with high and low $R_{bal}^{EC} \equiv |\sum (E_{clus} \cdot \cos \theta)| / \sum E_{clus}$ as functions of the beam energy. This resulted in a background estimate of 0.064 ± 0.017 nb, corresponding to approximately 0.2% at the peak energy point.

The effect of uncertainties resulting from modelling of fragmentation was investigated in two ways. We compared the acceptance calculated using the JETSET model with that obtained using the HERWIG model with a set of optimized parameters determined by OPAL and observed a difference of 0.06%. We also repeated the acceptance calculation with the JETSET model varying the optimised parameters of the model by one standard deviation. This resulted in an acceptance change of $(0.09 \pm 0.03)\%$. The differences revealed by these two studies were added in quadrature to give a total systematic error due to the fragmentation model of 0.11%. The total number of events selected by these cuts for the 1991 data set was 314498.

The Leptonic Decay Channels

The increased data sample collected in the 1991 LEP run allowed the systematic studies described in [4] to be repeated with increased precision and a number of new studies were performed. This, together with the continuous improvements made in both the performance and understanding of the OPAL detector, is reflected in the greatly reduced systematic errors. In the following three sections we describe briefly the most significant improvements for each lepton channel.

The e^+e^- Channel

For this analysis, electron pair events were required to lie within the angular range $|\cos \theta| < 0.70$. The dominant systematic error quoted in [4] was due to the uncertainty in determining the edge of the geometrical acceptance. We studied the possible effects of local distortions in the reconstructed electromagnetic calorimeter cluster position, the effect of an event vertex displacement, and the consistency of the θ -measurement using calorimeter clusters with that using charged tracks. Furthermore, a comparison was made of the accepted numbers of events for samples obtained by imposing the geometric acceptance cuts on the θ of the e^- , on the θ of the e^+ , or a random mixture of both. From these studies, the error on the edge of the acceptance was reduced to 0.3%.

The sign of the charge of the particles was determined from the tracks in the central detector. A fraction ($\approx 2\%$) of the events had the same sign measured for both of the tracks. For these events, an alternative method of charge determination was adopted, using the acoplanarity between the two calorimeter clusters of e^+e^- pair. With this method the correct charge assignment could be made for approximately 95% of events in the sample, independent of the tracking information. In this way we could use all the $e^+e^- \rightarrow e^+e^-$ events for the asymmetry measurement without selectively rejecting the same sign pairs, thus avoiding any possible bias. We assign an uncertainty of 0.003 on the asymmetry measurement for electron pairs.

The $\mu^+\mu^-$ Channel

Z^0 decays to muon pairs were selected within the angular range $|\cos \theta| < 0.95$. The main improvement to the selection criteria since our previous publication [4] was to tighten the cut on the number of charged tracks seen in the central detector. After applying algorithms to recognize tracks incorrectly split in the reconstruction and photon conversions, events were required to contain not more than three tracks. In our previous analysis these algorithms were not applied and events were allowed to contain as many as five tracks.

In order to check the predicted background from $Z^0 \rightarrow \tau^+\tau^-$ we studied distributions in visible energy, acoplanarity and acolinearity, that discriminated between $Z^0 \rightarrow \mu^+\mu^-$ and the backgrounds. For example, we made a selection of muon pair events with a large acoplanarity that could not be explained by the presence of a

radiated photon. Combining the 1990 and 1991 OPAL data samples we found 184 such events. This compared well with the Monte Carlo prediction of 175 events, of which 24 were due to $Z^0 \rightarrow \mu^+\mu^-$ and 151 to $Z^0 \rightarrow \tau^+\tau^-$. (This number represented 61% of the total predicted $Z^0 \rightarrow \tau^+\tau^-$ background in the final sample.) As a result of these checks we estimated a background of $1.15 \pm 0.15\%$ from $Z^0 \rightarrow \tau^+\tau^-$.

The forward-backward asymmetry was calculated using an unbinned maximum likelihood fit to the angular distribution. This was checked by simply counting the number of forward and backward events. Additional checks were performed by varying the cuts on the quality of central detector tracks used in the asymmetry measurement. We also tried using only positive tracks, only negative tracks, or using a track of randomly chosen charge to measure the asymmetry. As a result of these checks we assigned an uncertainty of 0.003 on the asymmetry measurement for muon pairs.

The $\tau^+\tau^-$ Channel

Z^0 decays to tau pairs were selected within the angular range $|\cos\theta| < 0.90$ using criteria that remained unchanged since our last publication [4]. Most of the systematic errors assigned to the selection cuts decreased due to the increased statistics of the available data and Monte Carlo samples. The uncertainty in the determination of the edge of the acceptance, which had been one of the dominant systematic errors, was reduced to 0.39%. We estimated an uncertainty of 0.003 on the asymmetry measurement for tau pairs.

The LEP Energy Calibration

As we have discussed in the earlier section on LEP, a precise calibration of the LEP energy scale based on the technique of resonant depolarization of a transversely polarized electron beam, as well as a detailed study of the properties of the LEP magnets and R.F. system, was achieved in 1991. At the same time it has become apparent that the geometry of the LEP radio-frequency accelerating cavities introduces significant shifts in the centre-of-mass energy at the four experimental intersection regions. Because of this, the energy scale at the OPAL intersection region differs by 15 ± 2 from the energy determined by the resonant depolarization measurement. For the results presented below the center-of-mass energies include the correction for this effect.

The uncertainty in the overall energy scale, $(\Delta E/E)^{abs}$ was reduced from $\pm 22 \times 10^{-5}$ in 1990 to $\pm 5.7 \times 10^{-5}$ for the data taken during the energy scan around the Z^0 resonance in 1991. The energy of the data taken before the polarization calibration had a larger uncertainty of $(\Delta E/E)^{abs} = \pm 20 \times 10^{-5}$. To combine the statistics of 1990 and 1991 we therefore imposed the constraint that both data sets give the same value for M_Z ; technically this was achieved by inflating the global centre-of-mass error for the 1990 data to $\Delta E^{abs}(1990) = \pm 200$ MeV which means that this energy scale was in effect a free parameter on the scale of precision of the 1991 measurements.

Determination of Electroweak Parameters

The fitting procedure for line-shapes and lepton asymmetries was described in our previous publications [4] and remained essentially unchanged. The theoretical parametrizations of the total and differential cross section of the $e^+e^- \rightarrow \text{hadrons}$, $e^+e^- \rightarrow \mu^+\mu^-$, $e^+e^- \rightarrow \tau^+\tau^-$ and the contribution of s -channel diagrams to $e^+e^- \rightarrow e^+e^-$ were based on the program ZFITTER [5]. For the e^+e^- channel, complicated by the presence of t -channel exchange diagrams, we used the program ALIBABA [6] to describe the contributions from the t -channel and from the s - t interference, with an uncertainty of 0.5% as assigned by the authors, and added them to the s -channel cross-sections calculated by ZFITTER.

Our results are based on a model independent approach to describe the experimental data. The parameters derived in the model independent framework were determined using a χ^2 minimization procedure taking into account the full covariance matrix of the data.

Without photonic corrections the pure Z^0 contribution to the hadronic cross section can be parametrized based on a Breit-Wigner line-shape with a width depending on the squared centre-of-mass energy, s .

$$\sigma(s) = \sigma_{\text{had}}^{\text{pole}} \frac{s\Gamma_Z^2}{(s - M_Z^2)^2 + \frac{s^2}{M_Z^2}\Gamma_Z^2}$$

$\sigma_{\text{had}}^{\text{pole}}$ represents the hadronic pole cross section as $\sqrt{s} = M_Z$ in the absence of initial state photon radiation and M_Z and Γ_Z are the Z^0 mass and width. Small additional contributions from γ exchange and the Z^0 - γ interference term were calculated within the SM framework.

For the leptonic differential cross section we used a generalization of the improved Born approximation [7]:

$$\begin{aligned} \frac{2s}{\pi\alpha^2} \frac{d\sigma}{d\cos\theta}(e^+e^- \rightarrow l^+l^-) &= \left| \frac{1}{1 - \Delta\alpha} \right|^2 (1 + \cos^2\theta) \\ &+ 4\text{Re} \left\{ \frac{2}{1 - \Delta\alpha} \chi(s) \left[C_{\gamma Z}^s(1 + \cos^2\theta) + 2C_{\gamma Z}^a \cos\theta \right] \right\} \\ &+ 16|\chi(s)|^2 \left[C_{ZZ}^s(1 + \cos^2\theta) + 8C_{ZZ}^a \cos\theta \right] \end{aligned}$$

with:

$$\chi = \frac{G_F M_Z^2}{8\pi\alpha\sqrt{2}} \frac{s}{s - M_Z^2 + is\Gamma_Z/M_Z}$$

Here α is the electromagnetic coupling constant, and G_F is the Fermi constant.

The C parameters may equivalently be written in terms of effective vector and axial-vector coupling constants, \hat{g}^v and \hat{g}^a , and four factors $\kappa_{\gamma Z}^s, \kappa_{\gamma Z}^a, \kappa_{ZZ}^s$ and κ_{ZZ}^a , which are equal to 1 in the improved Born approximation but are introduced here to allow for a more general approach:

$$\begin{aligned} C_{\gamma Z}^s &= \kappa_{\gamma Z}^s \hat{g}_e^v \hat{g}_l^v \\ C_{\gamma Z}^a &= \kappa_{\gamma Z}^a \hat{g}_e^a \hat{g}_l^a \\ C_{ZZ}^s &= \kappa_{ZZ}^s (\hat{g}_e^{a^2} + \hat{g}_e^{v^2}) (\hat{g}_l^{a^2} + \hat{g}_l^{v^2}) \\ C_{ZZ}^a &= \kappa_{ZZ}^a \hat{g}_e^a \hat{g}_l^a \hat{g}_e^v \hat{g}_l^v \end{aligned}$$

The subscripts 'e' and 'l' denote electron and lepton coupling constants, respectively, where 'l' stands for either electron, muon or tau leptons. The first term in the equation for the leptonic differential cross section arises from pure QED photon exchange, the second term describes the $Z^0 - \gamma$ interference, indicated by the subscripts ' γZ ' on the C or κ parameters, and the last term arises from s -channel Z^0 exchange, indicated by the subscripts ' ZZ '. Effects from higher order virtual corrections are accounted for by including the QED vacuum polarization factor $\Delta\alpha$, by introducing an s dependence to the Z^0 width in the propagator, and by using effective vector and axial-vector couplings denoted by \hat{g}^v and \hat{g}^a .

Figure 2.9 shows the corrected cross sections for the leptonic and hadronic channels, while Figure 2.10 gives the forward-backward asymmetries as a function of \sqrt{s} for the leptonic channels.

OPAL

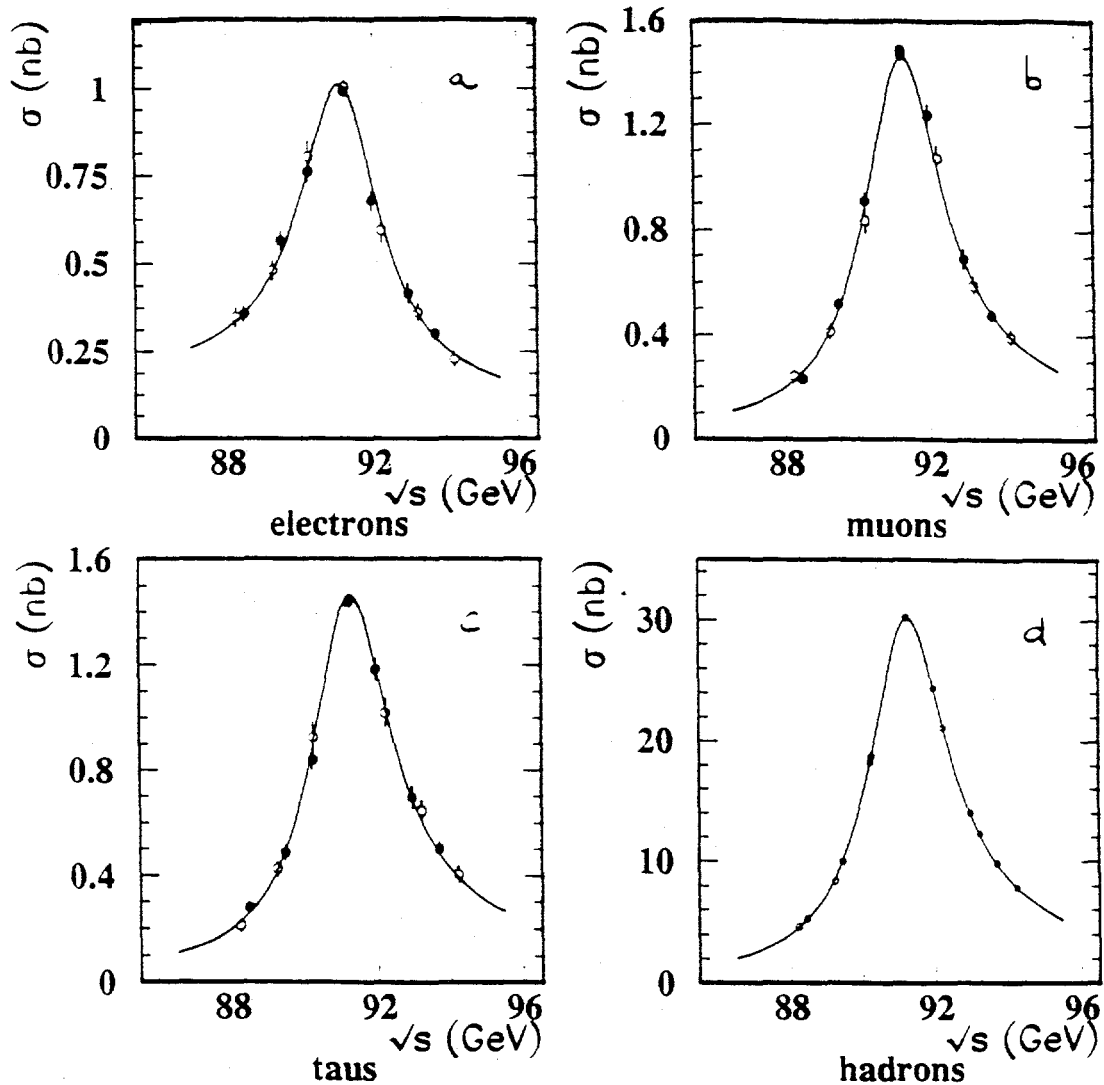


Figure 2.9: Cross sections as functions of center of mass energy for:
 a) $e^+e^- \rightarrow e^+e^-$, integrated over $|\cos\theta_{e^-}| < 0.7$ and corrected for efficiency with the geometrical acceptance;
 b) $e^+e^- \rightarrow \mu^+\mu^-$, corrected for acceptance;
 c) $e^+e^- \rightarrow \tau^+\tau^-$, corrected for acceptance;
 d) $e^+e^- \rightarrow \text{hadrons}$, corrected for acceptance.
 The solid lines are the results of the fit to the combined e^+e^- , $\mu^+\mu^-$, $\tau^+\tau^-$ and hadronic data described in the text. The solid points show the 1991 data and the open points the 1990 data.

OPAL

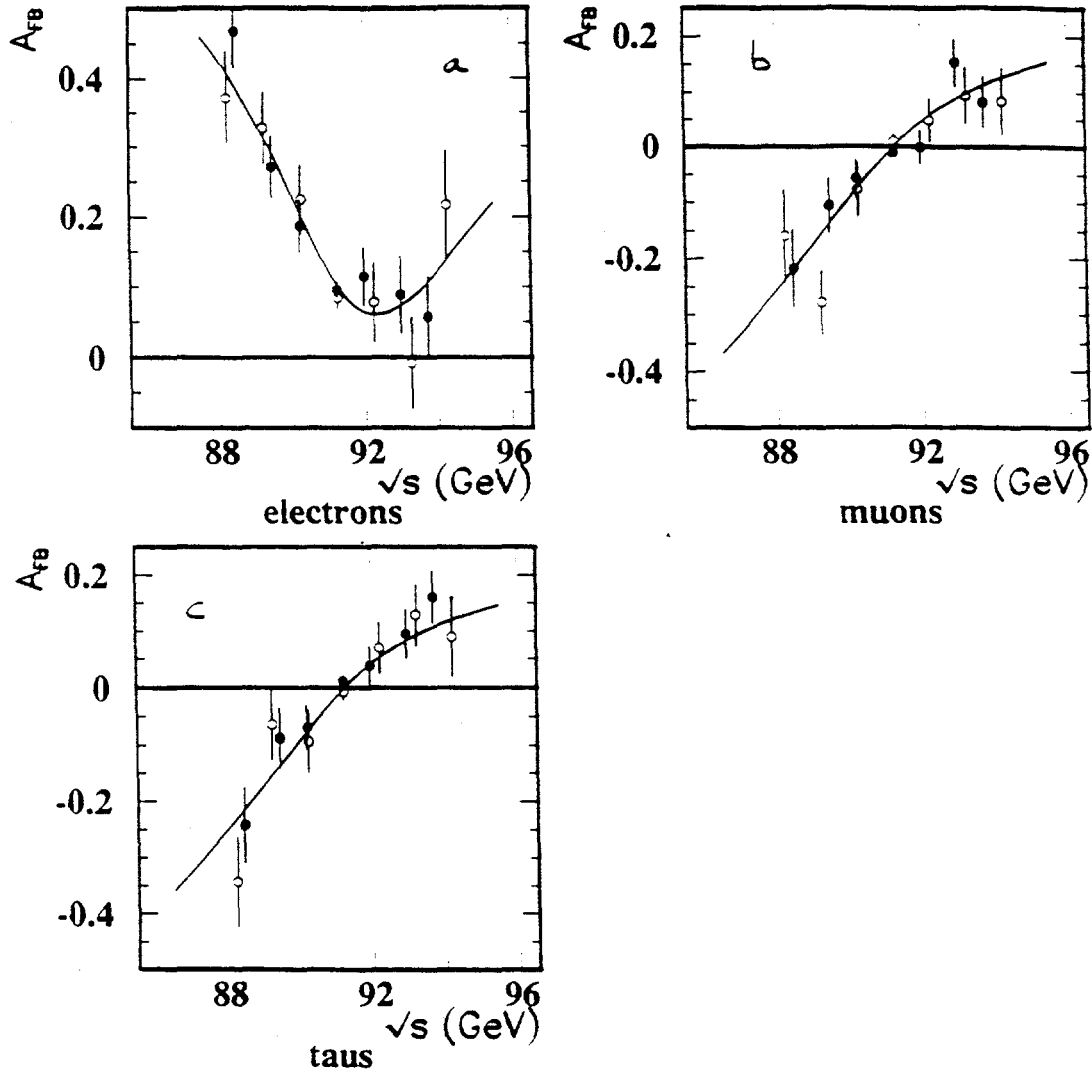


Figure 2.10: Forward-backward charge asymmetries for:

- a) $e^+e^- \rightarrow e^+e^-$, within $|\cos \theta_{e^-}| < 0.7$;
- b) $e^+e^- \rightarrow \mu^+\mu^-$, within $|\cos \theta| < 0.95$;
- c) $e^+e^- \rightarrow \tau^+\tau^-$, within $|\cos \theta| < 0.90$.

The solid lines are the results of the fit to the combined e^+e^- , $\mu^+\mu^-$, $\tau^+\tau^-$ and hadronic data described in the text.

We perform a 15 parameter fit to the combined data set of hadronic and leptonic cross-sections and the lepton forward-backward asymmetries with the mass, M_Z , and width, Γ_Z , of the Z^0 , the hadronic pole cross section, $\sigma_{\text{had}}^{\text{pole}}$, and the 4 C parameters for each lepton species, $C_{\gamma Z}^s$, $C_{\gamma Z}^a$, C_{ZZ}^a and C_{ZZ}^s , as free parameters. From this set of parameters we obtain the values shown in Table 2.2 for M_Z , Γ_Z , the ratios $R_l = \Gamma_{\text{had}}/\Gamma_l$ and the forward-backward asymmetry at the peak, $A_{\text{FB}}^0(l) = 3 \hat{g}_e^v \hat{g}_l^v / ((\hat{g}_e^{v^2} + \hat{g}_e^{a^2})(\hat{g}_l^{v^2} + \hat{g}_l^{a^2}))$. These quantities are essentially independent of the overall normalization. Figure 2.11 shows the one- σ contours in the R_l - A_{FB}^0 plane for each lepton species and the combined result assuming lepton universality. The results are consistent with lepton universality and the Standard Model within the errors.

	without lepton universality	with lepton universality	SM prediction
R_e	21.01 ± 0.26		
R_μ	20.65 ± 0.18		
R_τ	21.16 ± 0.25		
R_l		20.87 ± 0.13	$20.75^{+0.02}_{-0.04}$
$A_{\text{FB}}^0(e)$	-0.002 ± 0.012		
$A_{\text{FB}}^0(\mu)$	0.0047 ± 0.0076		
$A_{\text{FB}}^0(\tau)$	0.0165 ± 0.0082		
A_{FB}^0		0.0076 ± 0.0048	$0.014^{+0.08}_{-0.03}$
M_Z [GeV/ c^2]	$91.181 \pm 0.007 \pm 0.006$	$91.180 \pm 0.007 \pm 0.006$	input
Γ_Z [GeV]	$2.483 \pm 0.011 \pm 0.005$	$2.483 \pm 0.011 \pm 0.005$	$2.487^{+0.031}_{-0.017}$

Table 2.2: Results of the model independent fits to the lepton pair cross-sections and forward-backward asymmetries and the hadronic cross section measurements. The second error quoted on M_Z and Γ_Z is due to the uncertainty of the LEP energy. In the last column we give the Standard Model value for each parameter assuming $M_{\text{top}}=150$ GeV, $M_H=300$ GeV and $\alpha_s(M_Z^2) = 0.12$. The error quoted with the SM prediction reflects variations of M_{top} in the interval $50 \leq M_{\text{top}}$ (GeV) ≤ 230 and M_H in the interval $50 \leq M_H$ (GeV) ≤ 1000 .

Imposing lepton universality we obtain

$$R_l = \frac{\Gamma_{\text{had}}}{\Gamma_l} = 20.87 \pm 0.13$$

and

$$A_{\text{FB}}^0(l) = 0.0076 \pm 0.0048.$$

For the interpretation of the measured R_l value in terms of α_s , we use QCD corrections to quark final states computed to third order in α_s , [8] and include quark-mass

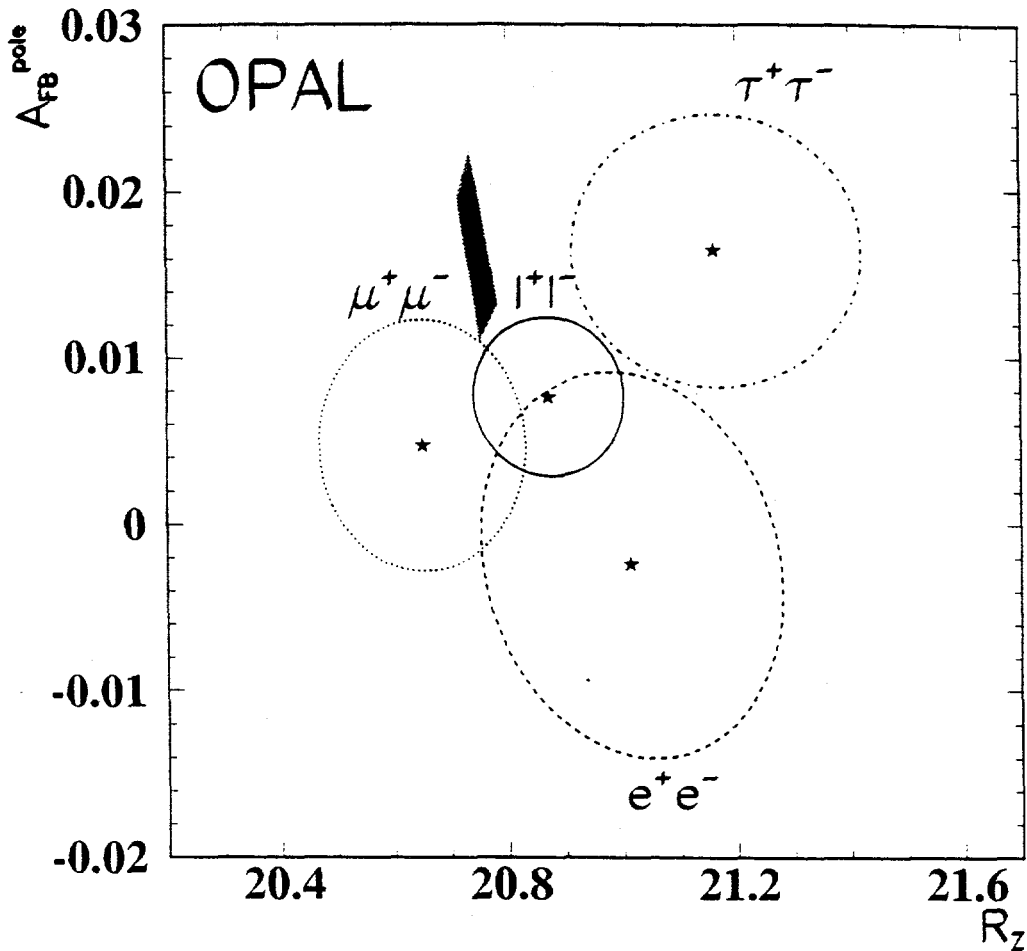


Figure 2.11: One sigma contour lines in the $R_l - A_{\text{FB}}^0$ plane for each lepton species and for all leptons assuming lepton universality.

dependent corrections [9]. From the measured value of R_l we derive a value for the strong coupling constant α_s of:

$$\alpha_s(M_Z^2) = 0.138 \pm 0.020$$

for $M_{\text{top}}=150$ GeV and $M_{\text{H}}=300$ GeV. The uncertainty introduced by varying the top quark and the Higgs boson masses is negligible. This result is consistent within its errors with results obtained from jet rates, event shapes and energy-energy correlations [10].

2.2.4 Combined LEP Results

The four LEP experiments are providing measurements of unprecedented precision of the Z^0 resonance and decay parameters to permit a better understanding of both

the strong and electroweak interactions. To go even further in constraining the Standard Model, the four collaborations have agreed to present combined results for the parameters derived from the hadronic and leptonic line shapes as well as from the leptonic forward-backward asymmetry [11].

The question of method was considered by a working group comprising members of each of the collaborations, asking in particular if it was sufficient to perform a weighted average of the fit parameters directly. This method is correct if the errors are sufficiently Gaussian, and if the common systematic errors are treated properly, i.e. subtracted quadratically before averaging the results, and then included in the final error. The procedure has been checked by comparing the averaged results to those derived from combined fits to the measured cross sections and asymmetries of the four experiments. The maximum deviation for any parameter between the two sets of results was less than one tenth of the uncertainty in that parameter and is therefore negligible. Studies have shown that interpretation of the fit results is not sensitive to details of the correlation matrix used, and that the average correlation matrix adequately describes the combined parameters.

The values determined by averaging the four sets of parameters and using the average correlation matrix are given in Table 2.3. These are based on the collaborations' results at the time of the Aspen meeting. Clearly the recent findings on differences in the center of mass energy values in the different regions will affect the results.

Parameter	Average Value
M_Z (GeV)	91.175 ± 0.021
Γ_Z (GeV)	2.487 ± 0.010
σ_{had}^0 (nb)	41.33 ± 0.23
R_e	20.91 ± 0.22
R_μ	20.88 ± 0.18
R_τ	21.16 ± 0.23
Γ_e (MeV)	83.20 ± 0.55
Γ_μ (MeV)	83.35 ± 0.86
Γ_τ (MeV)	82.76 ± 1.02
$\text{Br}(Z^0 \rightarrow e^+e^-)$ (%)	3.345 ± 0.020
$\text{Br}(Z^0 \rightarrow \mu^+\mu^-)$ (%)	3.351 ± 0.034
$\text{Br}(Z^0 \rightarrow \tau^+\tau^-)$ (%)	3.328 ± 0.040

Table 2.3: Average LEP line shape parameters.

It is perhaps worth remarking that the uncertainties given in these LEP-wide results are not that much better than those given earlier in the updated table of OPAL results. Clearly the results give ample justification to the assumption of lepton

universality. On that assumption one can obtain another series of average values, given in Table 2.4.

Parameter	Average Value
R_l	20.89 ± 0.13
Γ_{had} (GeV)	1.740 ± 0.012
Γ_l (MeV)	83.24 ± 0.42
$\text{Br}(Z^0 \rightarrow \text{hadrons})$ (%)	69.93 ± 0.31
$\text{Br}(Z^0 \rightarrow l^+l^-)$ (%)	3.347 ± 0.013
A_{FB}^0	0.0138 ± 0.0049
$g_{V_l}^2$	$(1.16 \pm 0.41) \times 10^{-3}$
$g_{A_l}^2$	0.2493 ± 0.0013
$g_{V_l}^2/g_{A_l}^2$	0.0047 ± 0.0017
Γ_{inv} (MeV)	498 ± 8
Γ_{inv}/Γ_l	5.985 ± 0.095
N_ν	3.00 ± 0.05

Table 2.4: Average LEP line shape parameters assuming lepton universality.

For a given value of M_Z the Standard Model predictions for the quantities Γ_Z , Γ_l , and A_{FB}^0 can be calculated. They are sensitive to M_t and M_H through radiative corrections. The top quark mass dependence is dominated by an M_t^2 term in the region of interest and is large compared to the sensitivity of the measurements. The Higgs mass effect is logarithmic and small, so at present no useful conclusions can be drawn about the Higgs mass. The variations in the χ^2 values of the fits for Γ_Z , σ_h^0 , $g_{V_l}^2$, and $g_{A_l}^2$ as a function of M_t are shown in Figure 2.12 both for LEP data only and for LEP data with additional inputs from the SPS collider and neutrino results.

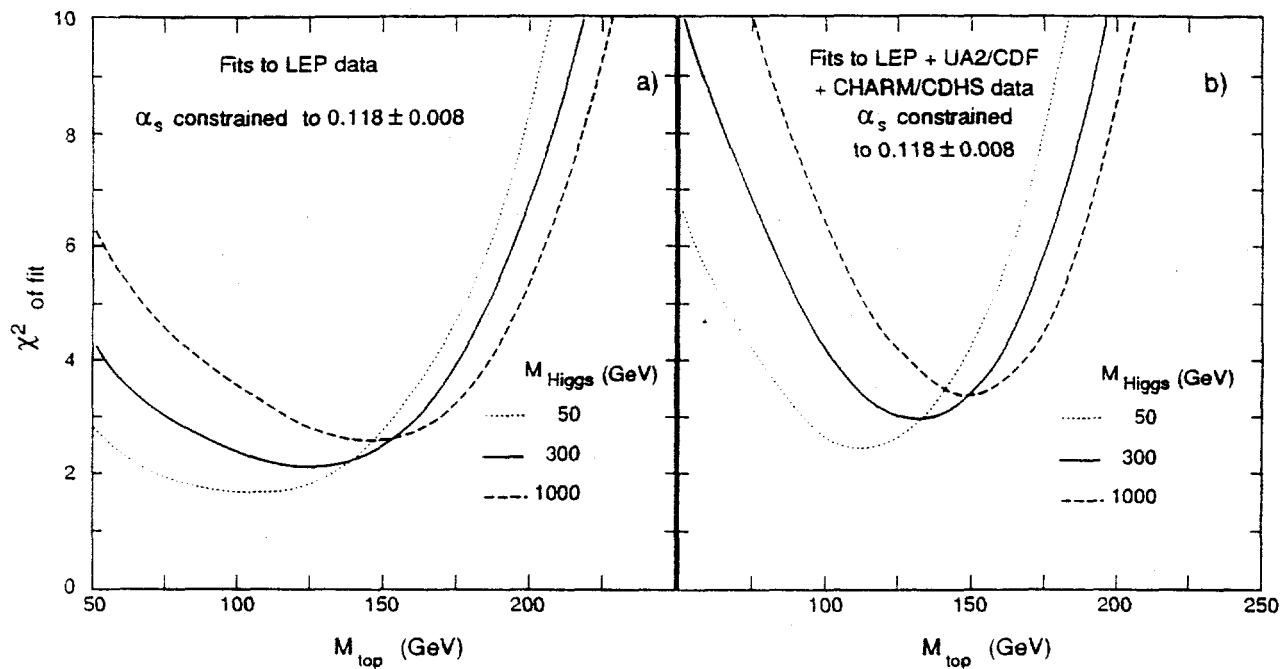


Figure 2.12: χ^2 as a function of M_t from a fit to a) LEP data with three degrees of freedom and b) LEP data and $p\bar{p}$ collider and ν data with five degrees of freedom.

2.2.5 QCD and Hadronic Final States

LEP offers many advantages relative to previous e^+e^- colliders for the study of Quantum Chromodynamics (QCD). The larger center-of-mass energy results in smaller theoretical uncertainties, because the value of the strong coupling constant α_s is smaller which makes the unknown higher order corrections less important. The uncertainty from hadronization is also smaller for LEP's larger energy, because its importance scales like $1/E_{c.m.}$. Detailed information about the hadronic final state, such as correlations in momentum between particles or production rates of different hadron species, provide tools with which to probe hadronization from a phenomenological standpoint. Large data statistics and excellent detector capabilities have made QCD and hadronization important and prolific areas of study for OPAL. Within OPAL, UCR has played a leading role in initiating, organizing and performing these studies. We summarize some of the recent QCD and hadronization work from OPAL and UCR in the following.

α_s from the Energy Energy Correlation Asymmetry Σ_{AEEC}

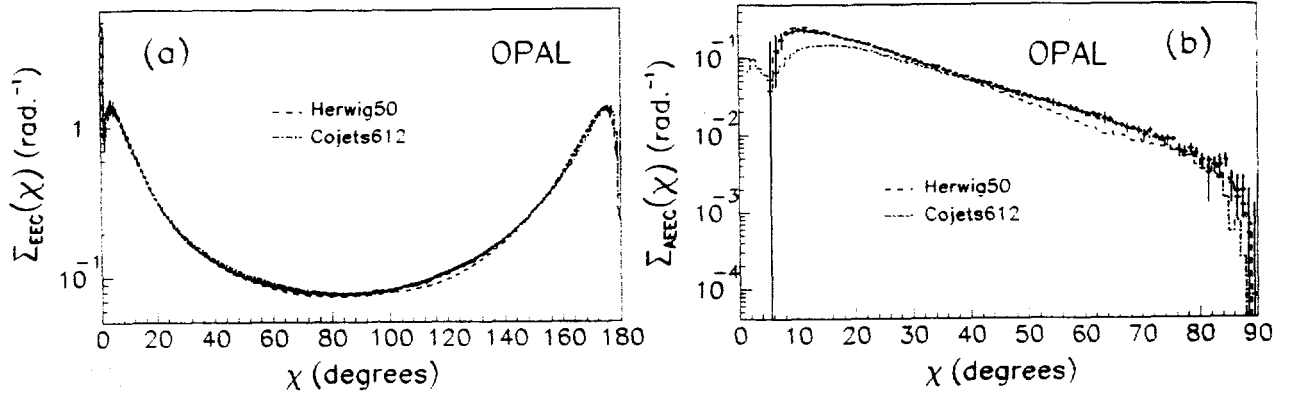


Figure 2.13: Measured (a) Σ_{EEC} and (b) Σ_{AEEC} distributions, compared to the predictions of the Herwig (dashed) and Cojets (dot-dashed) Monte Carlos.

The energy energy correlation asymmetry Σ_{AEEC} is constructed from the energy energy correlation function $\Sigma_{EEC}(\chi)$ [12]. This later distribution is defined using the angle χ_{ij} between two particles i and j in a multihadronic event:

$$\Sigma_{EEC}(\chi) = \frac{1}{\Delta\chi \cdot N_{events}} \sum_{N_{events}} \int_{\chi-\Delta\chi/2}^{\chi+\Delta\chi/2} \sum_{i,j} \frac{E_i E_j}{E_{vis.}^2} \cdot \delta(\chi' - \chi_{ij}) d\chi' ;$$

E_i and E_j are the energies of particles i and j ; $E_{vis.}$ is the sum over the energies of the observed particles in the event; $\Delta\chi$ is the angular bin width. The distribution

is summed over all events in the sample under study. Two-jet events contribute to Σ_{EEC} at values of χ near 0° and 180° . For events with three or more jets, the Σ_{EEC} distribution is populated at $\chi \approx 0^\circ$ and at central values of χ . The energy energy correlation asymmetry $\Sigma_{AEEC}(\chi)$ [12] is defined to be the asymmetry in the Σ_{EEC} distribution around the value $\chi = 90^\circ$:

$$\Sigma_{AEEC}(\chi) = \Sigma_{EEC}(180^\circ - \chi) - \Sigma_{EEC}(\chi) .$$

The subtraction this equation leads to cancellation of the two-jet component and of theoretical and experimental errors which contribute symmetrically to Σ_{EEC} . As a consequence, one obtains an experimental observable with unusually small systematic uncertainties, leading to an accurate determination of α_S .

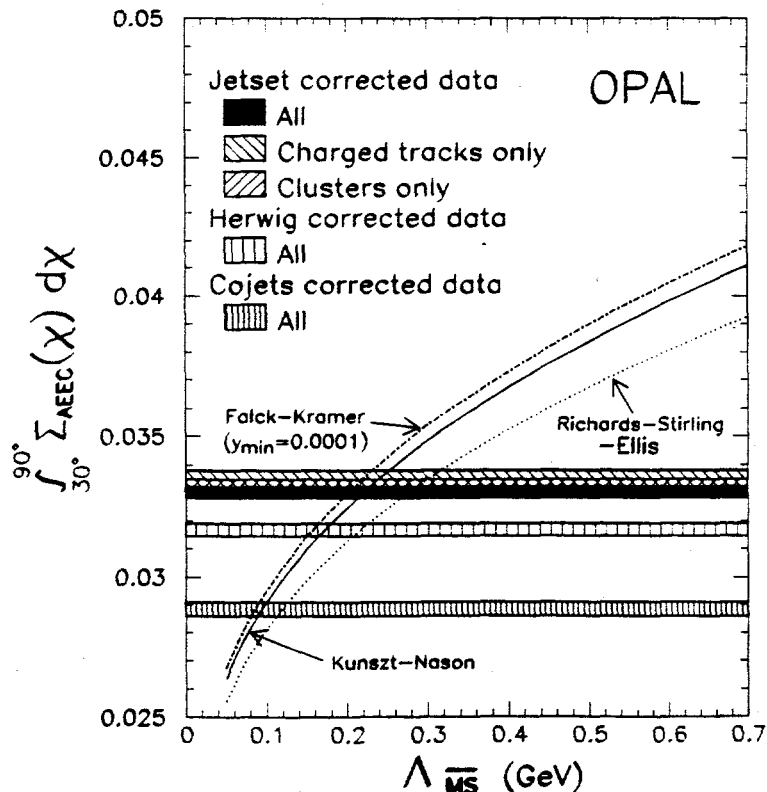


Figure 2.14: The values obtained for the measured Σ_{AEEC} distribution after it is integrated from $\chi = 30^\circ$ to $\chi = 90^\circ$, using various parton shower models for the corrections, as indicated (the final result uses Jetset). Shown as a function of $\Lambda_{\overline{MS}}$ are the predictions of several analytic calculations.

A high precision measurement of α_S at the Z^0 peak was undertaken by OPAL in 1991 [13], using the energy energy correlation asymmetry. This analysis was entirely a UCR effort. Unprecedented attention was paid to the different experimental and theoretical uncertainties, relative to what had been done in previous energy correlation studies. For example, it was discovered that a widely used theoretical calculation

based on Monte Carlo event generation was erroneous, if used with a small value of the renormalization scale μ for the argument of $\alpha_S(\mu)$. We were thus able to explain, in part, a discrepancy between our result and a result from another LEP experiment which used this erroneous calculation. The end result was one of the most accurate determinations of α_S to be produced from LEP and from e^+e^- collisions, using a single experimental distribution.

The measured energy correlation data Σ_{EEC} and Σ_{AEEC} from OPAL are shown in figure 2.13. Also shown are the predictions of several QCD calculations, using different assumptions about the hadronization. The small bin width of 1° emphasizes the large statistics and the excellent angular resolution of OPAL. The final result is summarized in figure 2.14, which shows the fully corrected data in comparison to different theoretical predictions. The theoretical curves are analytic calculations valid to exact 2nd order in perturbation theory, expressed in terms of $\Lambda_{\overline{MS}}$ instead of α_S ($\Lambda_{\overline{MS}}$ and α_S are equivalent to each other as long as the renormalization scale is specified). For α_S , this analysis yields

$$\alpha_S(M_{Z^0}) = 0.118 \pm 0.001 (\text{stat.}) \pm 0.003 (\text{exp.syst.}) \begin{matrix} +0.009 \\ -0.004 \end{matrix} (\text{theor.syst.}) ,$$

which is therefore a measurement with about 6% accuracy. The error is dominated by the theoretical systematic uncertainties. Figure 2.14 also indicates the result if only the charged tracking chamber or if only the electromagnetic calorimeter of OPAL is used: the excellent agreement between the results from these two independent measuring devices illustrates the smallness of the experimental error.

Global Determination of α_S

One way to reduce the theoretical systematic error on α_S , such as that present for Σ_{AEEC} , is to introduce many variables into the analysis. Unknown higher order corrections, which now constitute the largest source of uncertainty in the value of α_S , are different for different variables. By simultaneously studying many different variables in a "global analysis" of α_S , one can constrain the theoretical error by finding the range of α_S values which is compatible with all the measurements. OPAL has recently published such a global determination of α_S [14], with important contributions from UCR. Using second order theory (as for the Σ_{AEEC} analysis discussed above), this analysis includes global event shape variables, jet production rates and energy correlations. The study also includes theoretical calculations valid to beyond second order, based on the Modified Leading Logarithm Approximation (MLLA), which are available for a few of the event shape and jet rate distributions. The MLLA sums up the contributions of collinear and soft gluon radiation to all orders; these terms are then grafted to the exact second order expressions. Furthermore, complete third order calculations have recently become available for the hadronic branching fractions of the Z^0 and of the τ lepton. Analyses based on these third order calculations were also included in the OPAL publication. The OPAL study contains the first published

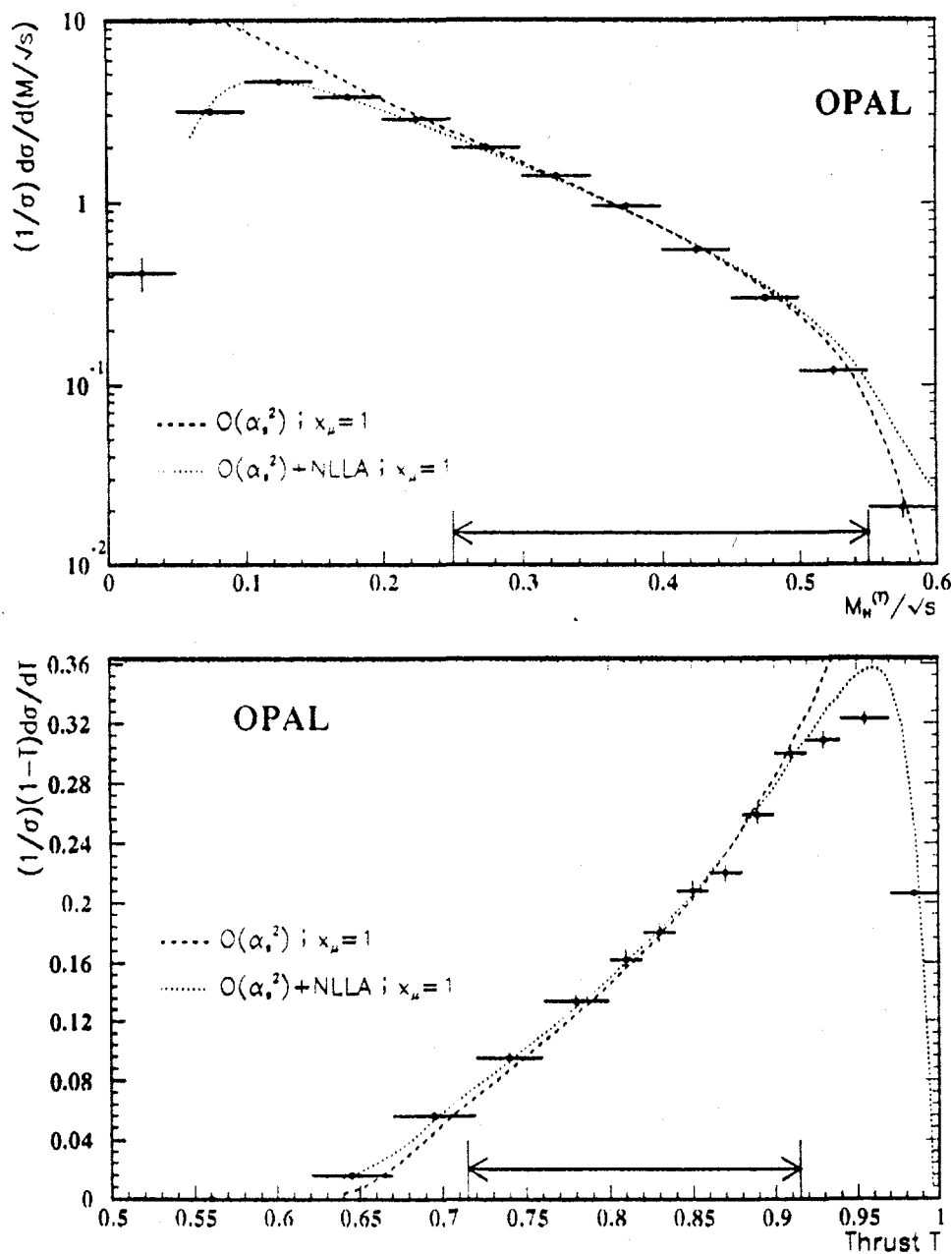


Figure 2.15: Measured distributions of $M_H^{(T)}$ and T , compared with fits to the $\mathcal{O}(\alpha_s^2)$ and to the resummed $\mathcal{O}(\alpha_s^2) + \text{MLLA}$ calculations, with a renormalization scale factor $x_\mu = 1$ in both cases. The ranges over which the fits were performed are indicated by the arrows.

experimental results using some of these new MLLA and third order expressions. The OPAL publication also presents the first analysis of planar triple energy correlations (PTC) from LEP.

As an example, Figure 2.15 shows the measured distributions of two global event shape variables, the heavy jet mass M_H and thrust T [15], in comparison to the pure 2nd order (dashed line) and the 2nd order plus MLLA (dotted line) calculations. The importance of the new MLLA results is clear, in that it extends the range of validity of the perturbative calculations into the two-jet region (low M_H or high T values), relative to the pure 2nd order results, as shown.

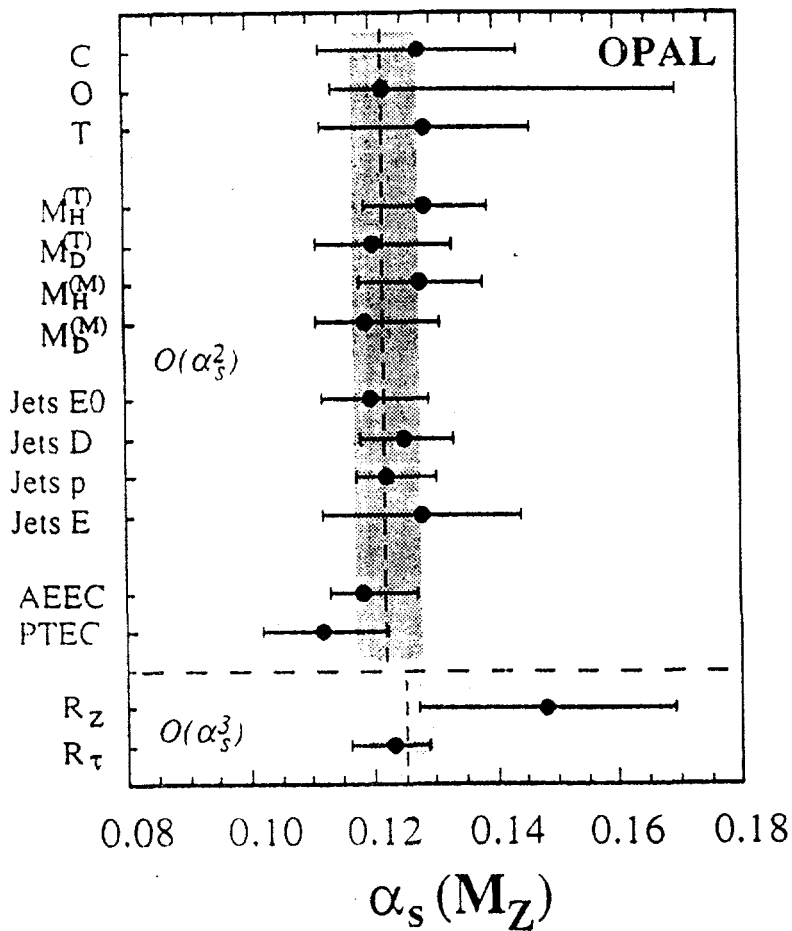


Figure 2.16: Compilation of final results of $\alpha_s(M_Z)$. The top shaded band corresponds to the weighted average of $\alpha_s(M_Z) = 0.122^{+0.006}_{-0.005}$ from the measurements in $\mathcal{O}(\alpha_s^2)$, and the bottom shaded band to $\alpha_s(M_Z) = 0.125 \pm 0.006$ from the two $\mathcal{O}(\alpha_s^3)$ results.

The α_S values obtained for the 15 different variables included in our study are summarized in figure 2.16. In second order, the final, combined result is

$$\alpha_S(M_{Z^0}) = 0.122^{+0.006}_{-0.005} ,$$

where the error includes all experimental and theoretical uncertainties. This final result is shown by the shaded band in the upper part of figure 2.16. The good agreement between the α_S values from the 13 different distributions studied at second order constitutes an important test of perturbative QCD at the Z^0 peak. For the second order plus MLLA calculations, we obtain

$$\alpha_S(M_{Z^0}) = 0.122^{+0.003}_{-0.006} ,$$

while in third order (shown in the bottom part of figure 2.16), the final result is

$$\alpha_S(M_{Z^0}) = 0.125 \pm 0.006 .$$

The good agreement between these three measurements based on different orders of perturbation theory, suggests that terms beyond third order may not be too important.

Two Particle Momentum Correlations

Another recent study from OPAL [16] concerns the momentum correlations between two charged particles within an event. This extends our work based on the single inclusive momentum distribution [17] and is the first such study to be published from LEP and, indeed, in e^+e^- annihilations. UCR contributed in an important way to this analysis by setting up and providing assistance with the different Monte Carlo generators (a essential element of this work) and by helping with the analysis strategy.

Figure 2.17 shows the two particle correlation data from OPAL in comparison to some QCD Monte Carlo predictions. The two particle correlations are expressed in terms of the combinations $\xi_1 + \xi_2$ or $\xi_1 - \xi_2$, where $\xi_i = \ln(1/x_p)_i$ with $(x_p)_i = 2p_i/E_{c.m.}$ is a theoretically favored way to study the momentum distribution p_i of a particle i , with $i = 1$ or 2 in this case. In figure 2.17, the Monte Carlo calculations are based on coherent parton branchings, which means that interference effects are included for gluon radiation from a quark or for gluon splitting into two gluons or into a quark and an antiquark. A considerably worse representation of the data is obtained if these interference effects are not included in the calculations. Thus our study lends evidence for the relevance of the coherence terms. The OPAL study also includes a comparison of QCD analytic calculations to the data. These analytic calculations incorporate the coherence phenomenon but make no correction for hadronization, instead relying on the conjecture of Local Parton Hadron Duality (LPHD) [18]. LPHD states that the momentum distribution of soft hadrons should reflect the underlying momentum distribution of soft gluons, to within an overall normalization factor. A rather poor

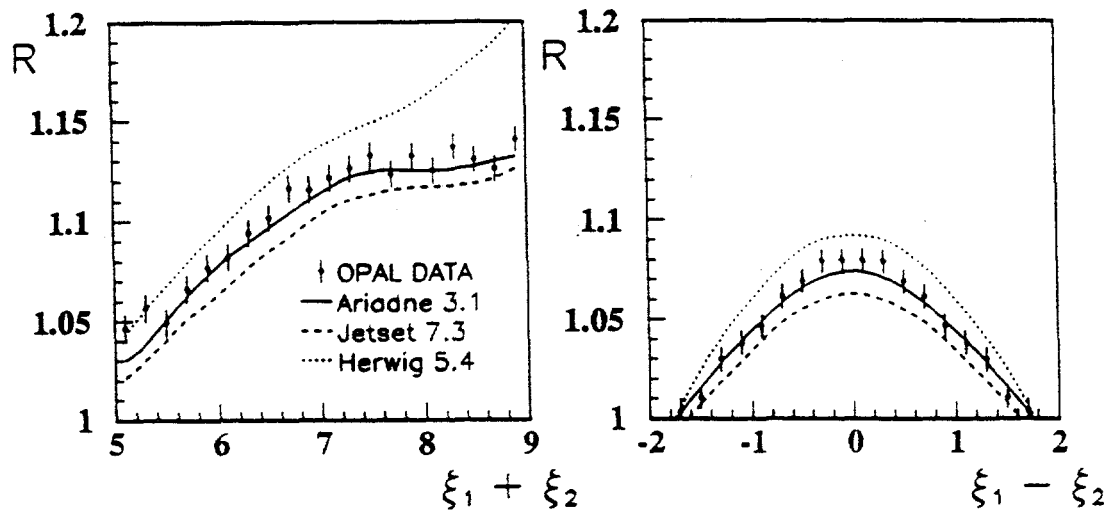


Figure 2.17: Comparison of two particle correlation data with the coherent parton shower models Ariadne (solid), Jetset (dashed) and Herwig (dotted).

representation of the data is obtained in this case, however, suggesting that LHPD may be somewhat simplistic and that detailed modeling of the hadronization is needed to describe the data.

Neutral Vector Mesons

OPAL has recently published a study of neutral vector meson production in hadronic Z^0 decays [19], which presents the first published cross sections from LEP for the $\phi(1020)$ and $K^*(892)^0$ mesons. Again, UCR contributed by providing Monte Carlo assistance and help with the analysis strategy. A number of unexpected features were uncovered by this study. For example, the ϕ rate was discovered to be considerably smaller than expected, based on the predictions of Monte Carlo generators tuned to lower energy e^+e^- data (the rate was measured to be 0.086 ± 0.017 ϕ mesons per event, compared to predictions of 0.190 and 0.115 from the popular Jetset and Herwig Monte Carlos, respectively). This implies that there is still much uncertainty in the models as to how the multiplicities of specific particle types are determined and how they change with energy.

Figure 2.18 shows the OPAL measurements of the differential cross sections for ϕ and K^{*0} in comparison to different Monte Carlo curves.

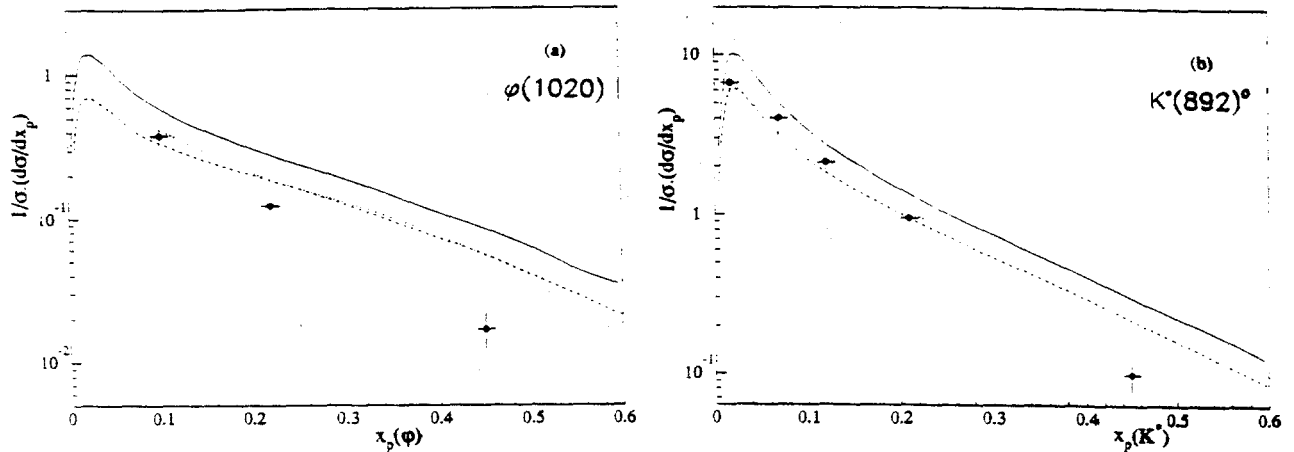


Figure 2.18: Differential cross sections for (a) $\phi(1020)$ and (b) $K^*(892)^0$ production; the solid curves indicate the predictions of Jetset with default parameters, the dotted curves give the Herwig predictions and the dashed curves show Jetset after tuning to this data.

Quark-Gluon Jet Differences

OPAL has pioneered work at LEP on the subject of quark and gluon jet structure. New techniques have been developed in order to tag quark and gluon jets and to compare their properties. These studies have been entirely a UCR effort. There has recently been an update [20] to the published OPAL result [21].

Gluon jets in three-jet events are identified by anti-tagging them using leptons from the semi-leptonic decay of charm and bottom quarks. Only symmetric three-jet events are selected, for which the angle between the gluon and the highest energy jet is the same as the angle between the highest energy and the other jet. A sample of events with the same geometry but without lepton identification is also studied. In this sample, the quark-jet purity is 50% (by construction). It is constituted of a normal mixture of quark flavors and hadron decays at the Z^0 peak. The properties of the quark jets are obtained by removal of the effect of the gluon contamination from this "normal mixture" sample, using the gluon jets measured in the tagged sample. The quark and gluon jets so obtained have the same energy and event environment, allowing their properties to be compared directly and in a model independent manner. Unlike earlier studies of quark and gluon jet differences, there is no need to use a Monte Carlo calculation to establish the experimental signal.

Figure 2.19 (a) shows the average energy value dE/dn of particles versus the azimuthal angle ψ in the three-jet event plane. The histogram in figure 2.19 (a)

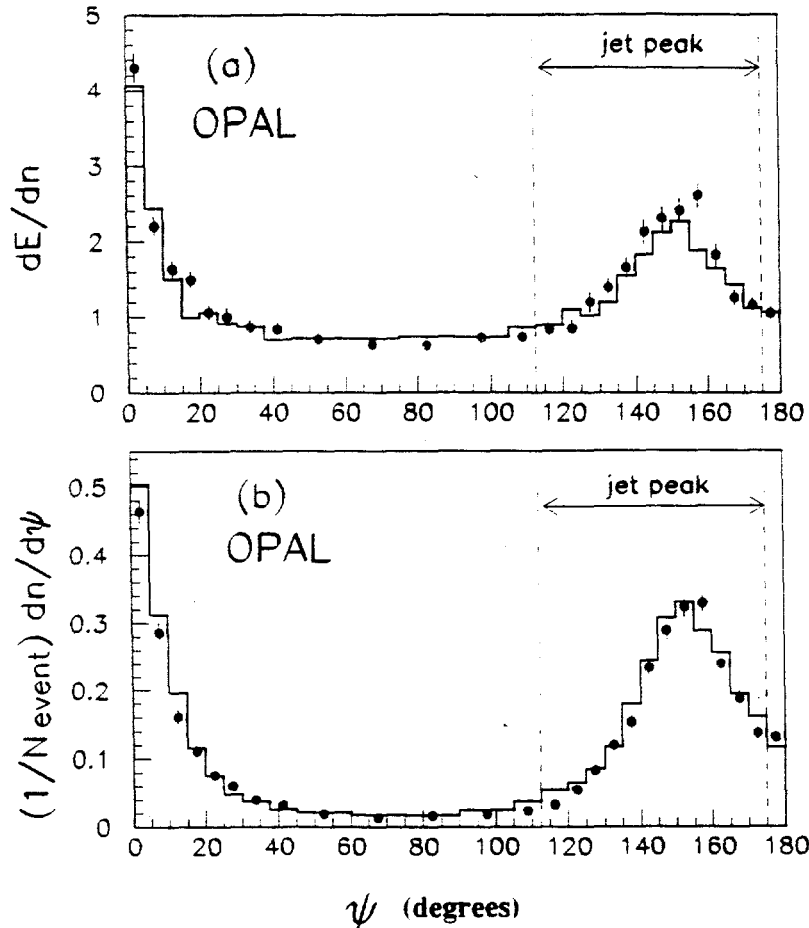


Figure 2.19: (a) The mean particle energy dE/dn versus the azimuthal angle ψ in the three-jet event plane. The histogram shows the distribution for the gluon jet side of the lepton tagged events. The solid points show the quark jet side of events with a normal mixture of quark flavors and hadron decays at the Z^0 peak. (b) The inclusive multiplicity distribution $(1/N_{event}) dn/d\psi$ versus ψ . The histogram and points with errors are defined as in (a).

shows dE/dn versus ψ for the lepton tagged sample, starting at the highest energy jet axis $\psi \equiv 0^\circ$ then proceeding through the gluon jet at $\psi \approx 150^\circ$ to stop halfway around the event plane at $\psi = 180^\circ$. The points with errors in figure 2.19 (a) show the normal mixture data after subtraction of the gluon content; the points with errors for $\psi \approx 150^\circ$ therefore show the normal mixture quark jet under study. It is clear that the mean particle energy value of the gluon jets (histogram) is systematically smaller than it is for the quark jets (points with errors) in the jet peak region. We therefore observe that gluon jets yield a softer particle energy spectrum than quark jets, in agreement with the expectations of QCD.

The inclusive multiplicity distribution versus ψ , or $(1/N_{event}) dn/d\psi$, is shown in figure 2.19 (b). These data are plotted like those of figure 2.19 (a). The histogram for

$\psi \approx 150^\circ$ shows the gluon jets while the solid points show the normal mixture quark jets. It is seen that the particle multiplicity of gluon jets is systematically larger than that of quark jets in the jet peak region, i.e. the histogram is above the points with errors for all but two of the thirteen bins in this region. The mean particle multiplicity value $\langle n \rangle$ of the jets is obtained by integrating the distributions in figure 2.19 (b) over the jet peaks. The ratio of mean multiplicity from the gluon to the quark jets is found to be

$$\frac{\langle n \rangle_{gluon}}{\langle n \rangle_{quark}} = 1.061 \pm 0.026$$

where the error is statistical only. The differences seen in this direct comparison of quark and gluon jets are therefore not large, but are systematically quite clear.

Strange Baryon Production in Hadronic Events

The production dynamics of mesons (bound quark antiquark states) and baryons (bound states of three quarks) were previously studied in jets at center of mass energies of about 30 GeV at the PETRA and PEP e^+e^- storage rings. These studies were limited by statistics but could show that with the introduction of diquarks into the fragmentation models and several free parameters the various identified baryons could be described.

Experiments at LEP have each collected about 500,000 hadronic Z^0 decays. Thus, about an order of magnitude more hadronic events can now be used to study details of baryon production dynamics in jets. With the additional factor of 10 more data expected during the coming years, we hope to obtain a precise picture of baryon and meson production in jets.

Our main interest is to obtain an experimental answer to the following questions:

1. What is the relative abundance of baryons with different spin and strangeness?
2. How is the baryon number conserved in jets?
3. How is the spin and the strangeness of baryons compensated?
4. Can one observe differences of baryon production for quark and gluon jets?
5. How are the electroweak effects on the primary quarks transmitted to mesons and baryons?

A first publication has just been submitted to Physics Letters B containing measurements of Λ , Ξ^- , $\Sigma(1385)^\pm$, $\Xi(1530)^0$ and Ω^- cross sections.

Selection of the Different Strange Baryons

The Λ can be identified by its decay into $p\pi^-$ with a branching ratio of 64%. Due to its relatively long lifetime, a very strong rejection of combinatorial background is

achieved by selecting particle combinations with secondary vertices which are clearly displaced from the main vertex. In addition, the good ionisation measurement dE/dx in the jet chamber permits a further strong background suppression.

Two methods are used to select Λ 's. The first is optimized to obtain very good mass resolution and a small systematic error. Here both tracks used to identify the Λ decay must have associated z-chamber measurements, which limits the polar angle to $|\cos\theta| < 0.7$. This method is used to derive the Λ cross section and results in a narrow, almost Gaussian Λ mass peak above a small background as shown in Figure 2.20 a). The mass obtained from a Gaussian fit to the peak, $1.1155 \text{ GeV} \pm 0.06 \text{ MeV}$, is in excellent agreement with the Particle Data Group value of 1.1156 GeV . The second method is optimized for high efficiency, which it achieves by dropping the z-chamber requirement and extending the polar angle range to $|\cos\theta| < 0.9$. The Λ s reconstructed by this method are used to identify the other baryon species.

The different distributions of the geometrical variables used to select Λ 's have been compared and very good agreement between data and Monte Carlo is found. Several sources of systematic errors have been studied and after adding all errors in quadrature the overall systematic error is found to be 5.6% for the Λ yield per hadronic event. The dominant errors are the uncertainty of the background estimation and of the cut simulation (4%).

Ξ^- decays essentially entirely to $\Lambda\pi^-$, and Ω^- to ΛK^- with a branching ratio of 67.8%. These signals appear clearly in Figures 2.20 b) and c). For the identification of Ξ^- and Ω^- , the wrong charge combination provides an excellent method to determine the remaining background.

The $\Sigma(1385)^\pm$ and $\Xi(1530)^0$ decay strongly with branching ratios of 88% to $\Lambda\pi^\pm$ and 67% to $\Xi^-\pi^+$, respectively. This latter signal is observed in Figure 2.20 d). Because of the prompt decay, no additional secondary vertex cuts are possible to reduce the combinatorial background.

Results of the Baryon Measurements

The differential cross sections $(1/N_{had})dn/dx_E$ for $\Lambda, \Xi^-, \Sigma(1385)^\pm$ and $\Xi(1530)^0$ are shown in Figure 2.21 together with the Jetset Monte Carlo values normalized to the measured yield per hadronic event. The Λ momentum spectrum is softer than the corresponding one from Jetset: the data are roughly 20% lower for x_E above 0.2. The momentum spectrum of Λ 's in the Herwig Monte Carlo is very similar to the Jetset one.

After integrating the measured differential cross section and adding the fractions predicted by Jetset for the unobserved momentum ranges, the following total yields per hadronic Z^0 decay are obtained:

- $\Lambda, \bar{\Lambda}/\text{event} = 0.351 \pm 0.003 \text{ (stat)} \pm 0.019 \text{ (syst)}$
- $\Xi^-, \bar{\Xi}^+/\text{event} = 0.0206 \pm 0.0011 \text{ (stat)} \pm 0.0019 \text{ (syst)}$

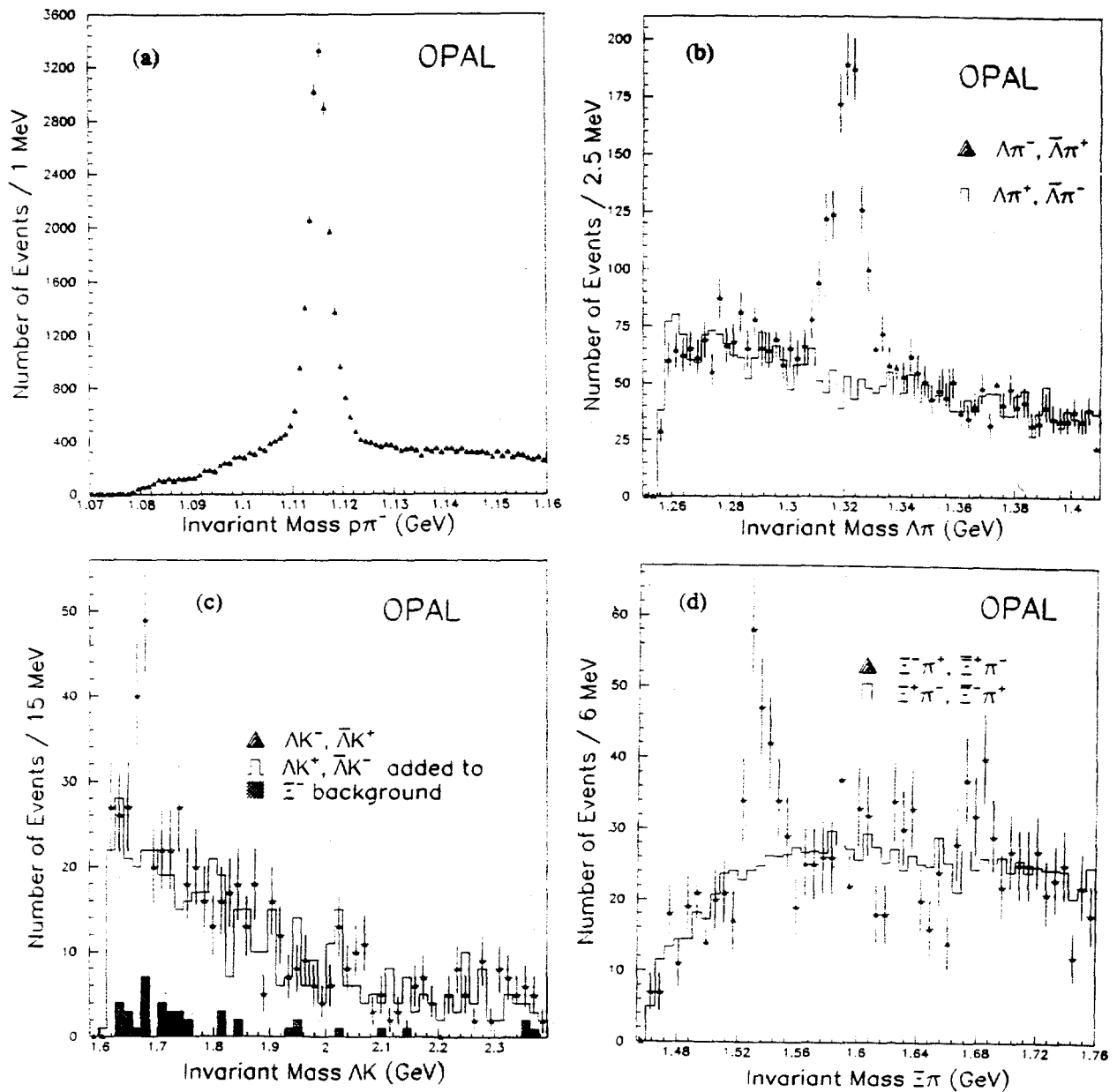


Figure 2.20: a) Λ signal seen in the invariant mass of $p\pi^-$; b) Ξ^- signal seen in the invariant mass distribution for $\Lambda\pi^-$. The histogram shows the wrong charge combination $\Lambda\pi^+$. c) Ω^- signal seen in the invariant mass distribution for ΛK^- . The histogram shows the wrong charge combination ΛK^+ . d) $\Xi(1530)^0$ signal seen in the invariant mass distribution for $\Xi^-\pi^+$. The histogram shows the distribution obtained using wrong charge combination Ξ^+ paired with π^- .

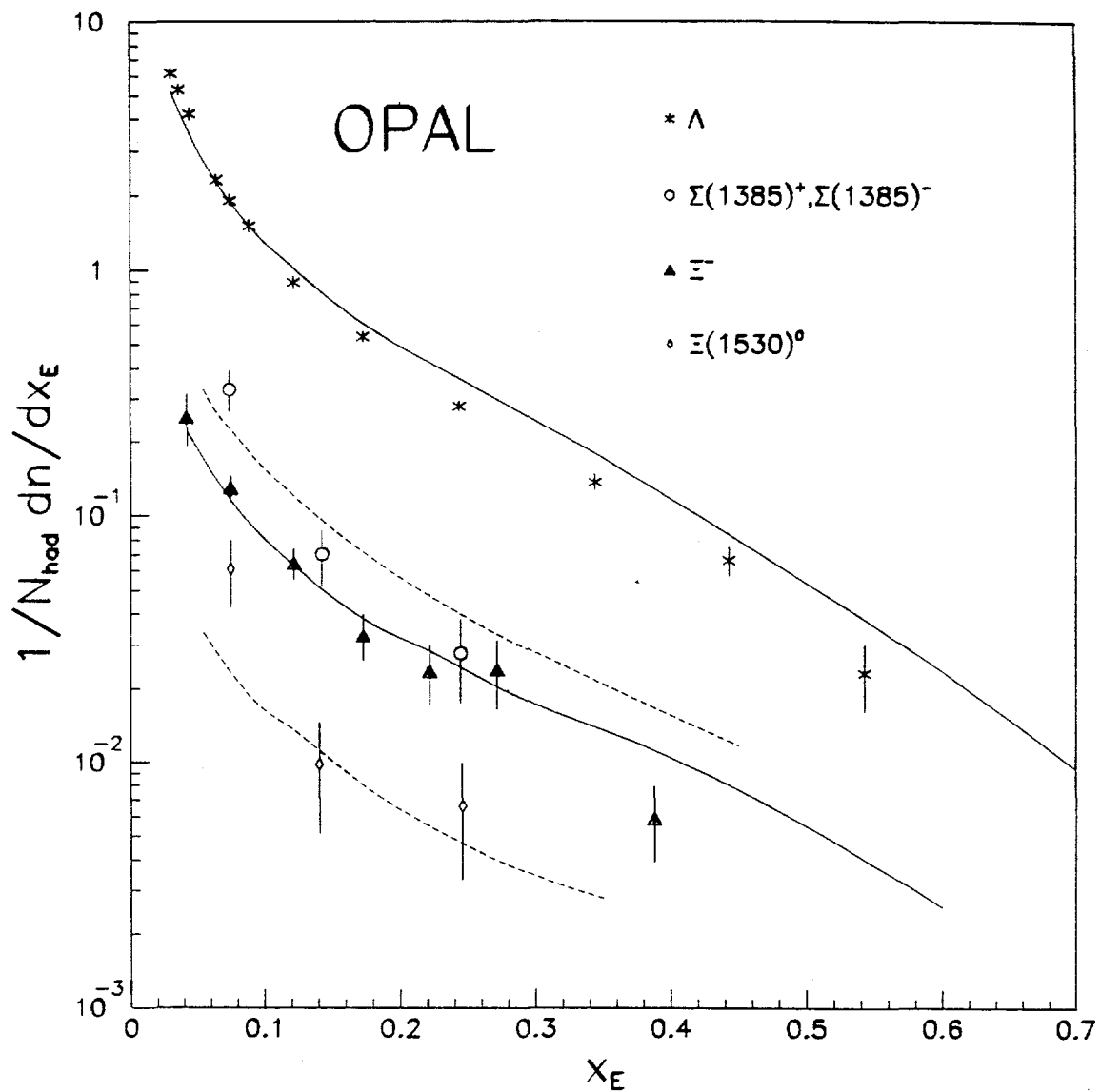


Figure 2.21: Differential cross sections $1/N_{had} dn/dx_E$ for Λ , $\Sigma(1385)^\pm$, Ξ^- , and $\Xi(1530)^0$. The curves show the respective Monte Carlo differential cross sections from JETSET. Very similar differential cross sections are obtained with the HERWIG Monte Carlo program.

- $\Sigma(1385)^\pm, \bar{\Sigma}(1385)^\pm/\text{event} = 0.0380 \pm 0.0038(\text{stat}) \pm 0.0049 (\text{syst})$
- $\Xi(1530)^0, \bar{\Xi}(1530)^0/\text{event} = 0.0063 \pm 0.0010(\text{stat}) \pm 0.0010 (\text{syst})$
- $\Omega^-, \bar{\Omega}^+/\text{event} = 0.0050 \pm 0.0012(\text{stat}) \pm 0.0009 (\text{syst})$

To test baryon production models via diquarks, we use the Jetset Monte Carlo. Within this diquark scheme, several parameters are relevant to baryon production:

- the diquark to quark ratio (qq/q),
- the strange to non-strange quark ratio (s/d),
- the strange diquark suppression factor $(su/ud) \times (d/s)$,
- the spin 1 diquark parameter $\frac{1}{3}(qq_1/qq_0)$, and
- the popcorn parameter.

Table 2.5 shows the baryon yields obtained using Jetset with its default parameters, $qq/q = 0.1$, $s/d=0.3$, $(us/ud) \times (d/s)=0.4$, $\frac{1}{3}(qq_1/qq_0)=0.05$ and 50% popcorn probability. The strange octet baryons are described within 20%. A simple change

particle	number/event (OPAL)	LUND default	LUND tuned	HERWIG default	HERWIG tuned
$n_{charged}$	21.4 ± 0.43	21.3	21.3	20.9	21.1
K^0	2.10 ± 0.14	2.16	2.15	2.07	2.12
Λ	0.351 ± 0.019	.383	0.351	0.427	0.352
Ξ^-	0.0206 ± 0.0020	.0272	0.0209	0.062	0.046
$\Sigma(1385)^\pm$	0.0380 ± 0.0062	.0743	0.0684	0.136	0.115
$\Xi(1530)^0$	0.0063 ± 0.0014	.0053	0.0048	0.0307	0.0216
Ω^-	0.0050 ± 0.0015	.00072	0.00044	0.0095	0.0054

Table 2.5: Inclusive particle yields in the data, this measurement (the statistical and systematic errors are added in quadrature). The values for $n_{charged}$ and K^0 are taken from [22] and [23]. The predictions are from the LUND and HERWIG Monte Carlo programs with default parameters. To describe the octet baryons the extra strangeness suppression value for diquarks has been changed from the default (0.4) to 0.3 describe the octet baryons. For the HERWIG model the cluster mass parameter has been changed to 3.32 to describe the Λ yield.

of the $(us/ud) \times (d/s)$ parameter to 0.3 ± 0.03 results in a good description of the K^0 , Λ , and Ξ^- rates, as shown in Table 3. However, the decuplet baryons are not well

described. The corresponding baryon rates within the Herwig Monte Carlo version 5.0 are also shown in Table 3. Even after tuning the cluster mass parameter from its default value of 3.5 to 3.32 ± 0.05 , the other baryons differ by up to a factor of three from the measured values.

To investigate how the different decuplet baryon rates can be described, we have performed further studies. In these studies the parameter s/d was fixed to 0.285 (to describe our measured K^0 yield and the parameter qq/q was unchanged from the default value of 0.1 since it describes the measured K^0 and Λ yields. The other three parameters, which mainly determine the relative baryon production rates, have been varied over a wide range.

The popcorn parameter defines the probability to form an additional meson between a baryon-antibaryon pair. Two additional parameters exist within the popcorn scheme as implemented in Jetset. These additional parameters regulate the strangeness suppression if a meson is produced between the baryon antibaryon pair. Their default values lead to an extra strange meson and baryon suppression. According to the current model, the spin information of the remaining antiquark is lost for the subsequent antibaryon when a meson is produced between the two baryons. On the basis of simple spin counting, the production of decuplet antibaryons is therefore less suppressed.

To simplify the comparison of the results for the strangeness and spin suppression diquark parameters, the popcorn model has been modified to have identical strange quark treatment for the different popcorn values. To do so, the two additional parameters within the popcorn scheme have been changed from the default value of 0.5 to 1. Table 2.6 gives a summary of results. The parameters, $(su/ud) \times (d/s)$ and the $\frac{1}{3}(qq_1/qq_0)$ have been varied to give agreement with the octet baryons and either the $\Sigma(1385)^\pm$ (column 1 of each popcorn value) or the $\Xi(1530)^0$ (column 2 of each popcorn value) yield. It has not been possible to describe the Ω^- yield by this approach.

From these studies one finds that the diquark parameters are strongly correlated and can only be estimated with good accuracy for a fixed value of the popcorn parameter. We also find that the ratios of the inclusive yields for Ξ^-/Λ and $\Xi(1530)^0/\Sigma(1385)^\pm$ or $\Omega^-/\Xi(1530)^0$ cannot be varied independently within the current model. For all studied parameters, these ratios are in disagreement with the measurement, as shown in Figure 2.22 a) and b). For a more sophisticated and conclusive study of diquark models, more measurements of other baryon species and also of correlations are clearly needed.

After having finished the first paper on inclusive baryon production, we are investigating now in detail the correlation mechanism of baryon antibaryon pairs. We expect with this study to obtain a much more detailed knowledge of the quark flow during the fragmentation process. Of further interest will be the study of how the strange quark inside the baryon is compensated. It will thus be a study of baryon-meson-antibaryon final states. Clearly these measurements will benefit from the improved

statistics expected during the coming years.

	data	popcorn=0%		popcorn=50%		popcorn=100%	
$us/ud \times d/s$		0.20	0.28	0.18	0.25	0.15	0.20
$\frac{1}{3} \times qq_1/qq_0$		0.04	0.15	0.012	0.08	0.008	0.05
K^0	2.10 ± 0.14	2.11	2.11	2.12	2.11	2.11	2.10
Λ	0.351 ± 0.019	.365	.356	.366	.353	.358	.342
Ξ^-	0.0206 ± 0.0020	.0191	.0205	.0213	.0214	.0197	.0201
$\Sigma(1385)^\pm$	0.0380 ± 0.0062	.0374	.0862	.0382	.0886	.0385	.0815
$\Xi(1530)^0$	0.0063 ± 0.0014	.0019	.0054	.0027	.0065	.0026	.0055
Ω^-	0.0050 ± 0.0015	.0001	.0006	.0003	.0009	.0003	.0006

Table 2.6: Inclusive yields, this measurement and LUND Monte Carlo tuned to get agreement with either the $\Sigma^\pm(1385)$ (first column for each popcorn value) or the $\Xi^0(1530)$ measurement (second column).

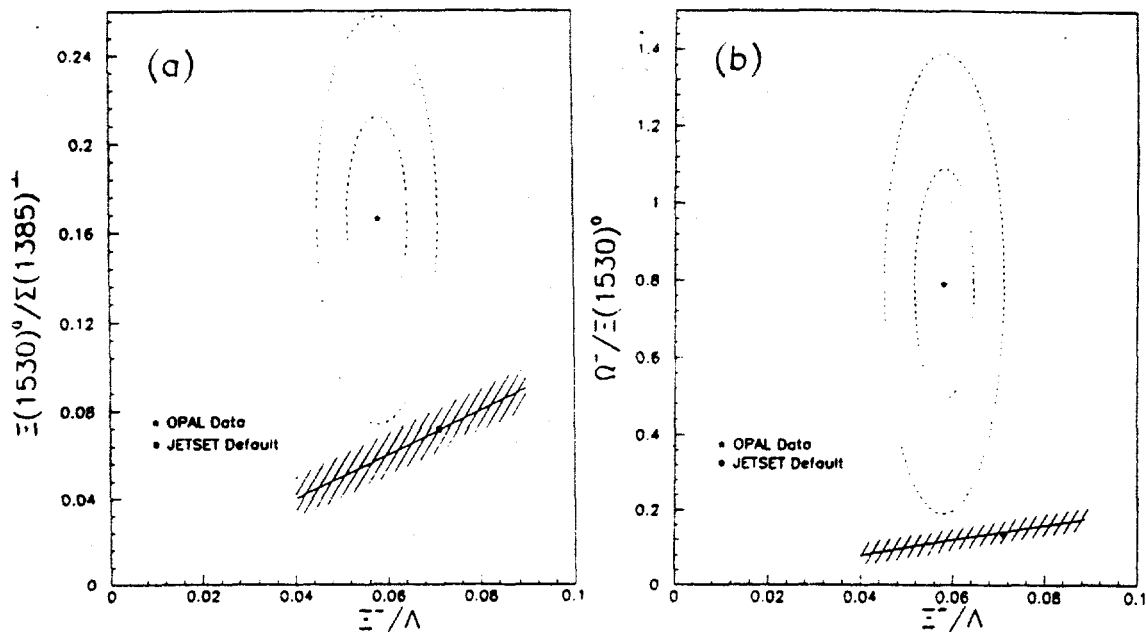


Figure 2.22: a) The ratio of the decuplet baryons $\Xi(1530)^0/\Sigma(1385)^\pm$ versus the ratio of the octet baryons Ξ^-/Λ , b) The ratio of the decuplet baryons $\Omega^-/\Xi(1530)^0$ versus the ratio of the octet baryons Ξ^-/Λ , In each case the value from the data is represented by the (\star) and that from the Monte Carlo by the (\bullet). For the Monte Carlo the shaded area shows ratios obtained within reasonable parameter changes.

2.2.6 Studies of Events with Photons

The observation of single photon events can be used to measure the cross-section for the production of weakly interacting particles. This method uses a photon radiated from the initial state to tag the otherwise invisible final state. This method was first suggested by Ma and Okada [24]. At LEP energies, this topology is expected to be dominated by Z^0 decays to invisible particles. Within the Standard Model these particles can only be light-mass neutrinos. An accurate measurement of the single photon cross-section can thus provide a measurement of the effective number of light-mass neutrino generations.

Photon radiation from initial and final states and radiative decays is well described by quantum electrodynamics. Nevertheless, there is considerable interest in the study of radiative lepton pairs in e^+e^- collisions at the Z^0 . A higher yield in radiative tau pair events alone could indicate anomalous magnetic properties of the tau. No direct searches for three body Z^0 decays into a photon and a pair of leptons have been performed so far. The events with hard initial state radiation allow a measurement of the cross section at energies between 60 GeV (TRISTAN) and the Z^0 .

Neutrino counting

The first measurement of the Z^0 invisible width by single photon counting was published by OPAL in 1990 based on 5.3 pb^{-1} integrated luminosity [25]. The result was $\Gamma_{inv} = 0.50 \pm 0.07 \pm 0.03 \text{ GeV}$ corresponding to $N_\nu = 3.0 \pm 0.4 \pm 0.2$ light neutrino generations. The analysis of the 1991 data is currently being finalized by a team led by Dr. Graham Wilson of UCR with assistance from UCR graduate student Edward Heflin. The combined 1990-1991 data set contains about 20 pb^{-1} in scans around the Z^0 . Further work and the increased statistics have led to a better understanding of the background sources and to much reduced systematic errors on the acceptance. An example of this is shown in Figure 2.23 comparing momentum and angular distributions of barrel electrons with Monte Carlo predictions for signal and background.

The energy spectrum of the observed single photon candidates is shown in Figure 2.24 for center-of-mass energies at and above the Z^0 peak (1991 data) together with the expectation from the $e^+e^- \rightarrow \nu\bar{\nu}\gamma$ Monte Carlo. A paper draft will be presented to the OPAL Collaboration before the end of the summer.

Photon Radiation in Lepton Pair Events

A study of lepton pair events in which there was an initial hard photon appeared in September 1991. [27], This study, so far unique at LEP, extended a method developed earlier for a search for supersymmetry to identify the different types of lepton pairs in a very model independent way. The amount of photon radiation in different lepton pair events could thus be directly counted and compared with each other. For very

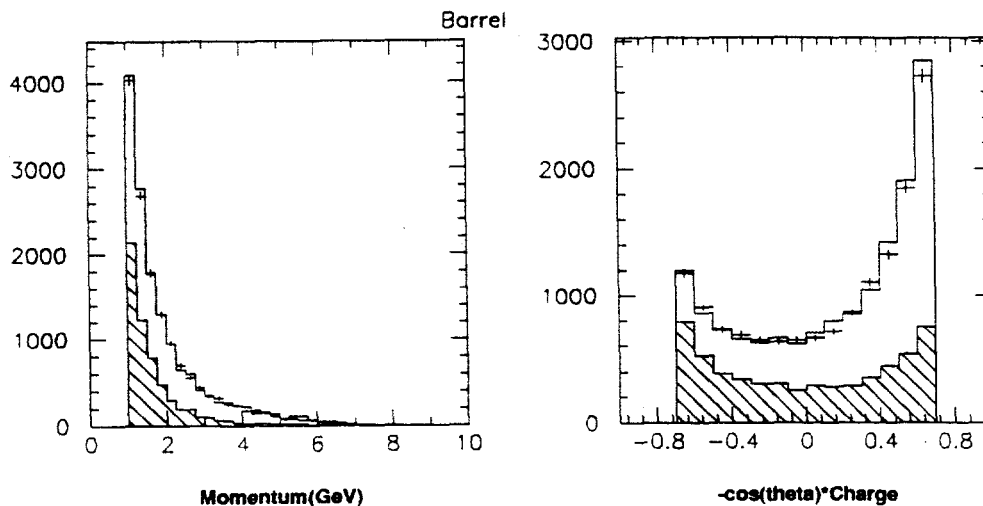


Figure 2.23: *Left:* The observed momentum spectrum and *Right:* the angular distribution of single electron events compared with Monte Carlo expectations. The shaded histograms show the contribution from two photon reactions, while the open histograms are from radiative Bhabha events. The points with error bars are the data.

small angles between the photon and the closest lepton, the lepton masses are important, while for larger separation angles identical photon yields are expected. Even though this is a standard QED prediction, such a detailed comparison had never been performed before. No deviations from QED expectations were found and very stringent limits on exotic radiative Z^0 decays could be obtained. We are currently working on an update of this measurement and some of the new results using the full 90 and 91 statistics are given in table 1.

In the same letter we have published our findings from using $\mu^+\mu^-\gamma$ events with hard initial state radiation to obtain a cross section for μ pair production in the so far unknown center-of-mass energies between TRISTAN and LEP. The method is to search for acollinear events with very little observed electromagnetic energy. The missing energy is assumed to be a photon radiated along the beam line. Its energy can be determined from the kinematics of the event. After cutting on the total energy of the event to eliminate two-photon events, we are left with 19 events with an effective centre-of-mass energy between 60 GeV and 84 GeV and an average energy of 75 GeV. The values obtained using the full 1990 and 1991 statistics agree with the Standard Model expectations as shown in Figure 2.25 and in the following table.

The above measurements close the window on observing new physics in the lepton pair sector until about a million or more Z^0 decays are obtained.

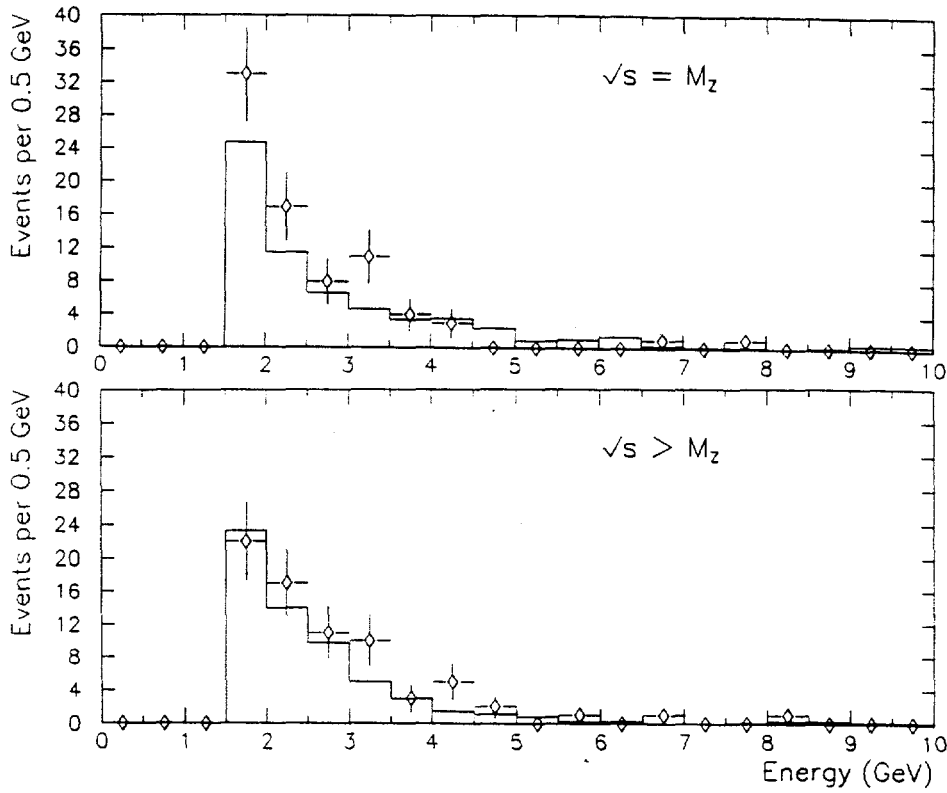


Figure 2.24: The E_γ spectrum for selected single photon events on and above the Z^0 peak. The histogram shows the expectation for 3 neutrino generations.

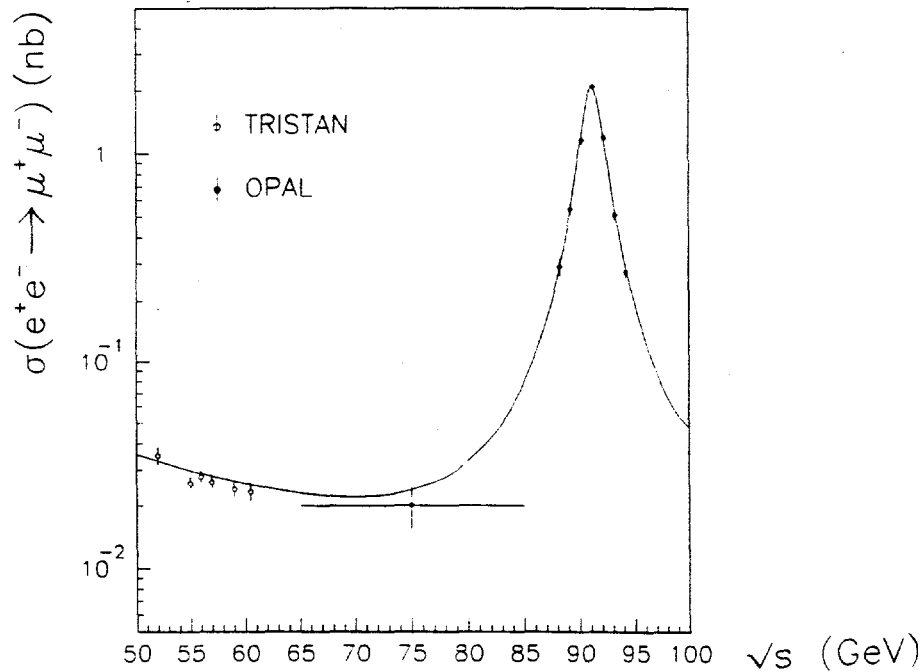


Figure 2.25: The measured cross sections for e^+e^- annihilation into $\mu^+\mu^- \gamma$ events are shown from TRISTAN to LEP energies.

Data on peak			
$Z \rightarrow \ell^+\ell^-\gamma$	$e^+e^-\gamma$	$\mu^+\mu^-\gamma$	$\tau^+\tau^-\gamma$
$N_{\ell^+\ell^-}^{coll}$	12724	11044	9289
N_γ (Data)	412	385	361
N_γ (MC)	407 ± 20.9	353 ± 17.8	316 ± 10.5
$N_\gamma/N_{\ell^+\ell^-}^{coll}$ (Data) ($\times 10^{-2}$)	3.2 ± 0.16	3.5 ± 0.18	3.9 ± 0.20
$N_\gamma/N_{\ell^+\ell^-}^{coll}$ (MC) ($\times 10^{-2}$)	3.2 ± 0.2	3.2 ± 0.2	3.4 ± 0.1
Limits for $Z \rightarrow \ell^+\ell^-\gamma$			
limit N_γ^{extra} (95% c.l.)	45	71	83
$BR(Z \rightarrow \ell^+\ell^-\gamma)$ limit	2.44×10^{-4}	3.77×10^{-4}	5.24×10^{-4}

Table 2.7: The numbers of collinear lepton pair events and the number of events with isolated photons and x_γ above 0.02 in the data and the Monte Carlo on the Z^0 peak. The resulting 95% confidence level limits for the possible photon excess and the calculated Z^0 branching ratio limits for anomalous three body Z^0 decays.

$\sqrt{s'}(GeV)$	40-60	60-70	70-78	78-84	$\langle \sqrt{s'} \rangle = 75$
$N_{\text{measured}}^{\text{events}}$	3	6	6	7	19
$N_{\text{expected}}^{\text{events}}$	2.4	4.7	7.7	10.3	22.7
$\sigma_{\text{Born}}^{\text{expected}}$ (pb)	36	23	23	36	24
σ_{measured} (pb)	$45 \pm_{18}^{34}$	29 ± 12	17.9 ± 7.3	24.5 ± 9.2	20.1 ± 4.6

Table 2.8: Observed and expected number of acollinear $\mu^+\mu^-$ events for the different effective dilepton center-of-mass energies $\sqrt{s'}$ and the corresponding cross sections.

2.2.7 Studies of $\tau^+\tau^-$ Pair Production and Decay

During the past year several independent and sometimes antagonistic approaches in the selection and analysis of taus have been brought together in a common effort. This was the work of Dr. Keith Riles, of UCR who headed the OPAL Tau Working Group before his departure at the end of the year. The Working Group is in the process of finalizing updated analyses of the topological branching ratios and of polarization in the rho channel. A separate Lifetime Working Group continues to refine its measurement of the tau lifetime. Members of the UCR group are continuing their study of lepton flavor violation, in which significant limits on tau decays have already been published by OPAL.

Topological Branching Ratios

This measurement deals with the inclusive branching ratios of the τ lepton to final states containing one, three and five charged particles (1, 3 and 5-prong decays). It is based on a high statistics sample of $e^+e^- \rightarrow \tau^+\tau^-$ events collected using the OPAL detector, at center-of-mass energies between 88.2 and 94.2 GeV, during the 1990 and 1991 LEP running periods. At these energies it is possible to obtain an extremely clean sample of τ decays with minimal bias against any particular decay mode. This, combined with the good tracking and particle identification capabilities of the OPAL detector, makes possible a precise measurement of the topological branching ratios of the τ lepton.

The main interest in this measurement stems from the so-called "missing decay mode" problem. Previous measurements of τ decays [31] suggest an inconsistency between the inclusive 1-prong branching ratio ($86.1 \pm 0.3\%$) and the sum of the 1-prong exclusive branching ratios ($< 80.2 \pm 1.4\%$ where theoretical constraints are used to limit poorly measured channels) [32, 33]. The discrepancy, as determined using this technique, is not entirely resolved by averaging more recent branching ratio measurements [34, 35, 36]. However, evidence against such a "missing decay mode" is provided in analyses of all known exclusive decay modes performed by CELLO[38] and ALEPH[34]. ALEPH, for example, set a limit on the branching ratio of new photonic decays to be less than 3.4% at 95% *CL*. Discrepancies also exist between the measurements of the inclusive branching ratios. For example, the HRS collaboration measures an inclusive 1-prong branching ratio of $86.4 \pm 0.3 \pm 0.3\%$ [37] while the CELLO collaboration reports a value of $84.9 \pm 0.4 \pm 0.3\%$ [38].

Selection of $e^+e^- \rightarrow \tau^+\tau^-$ events

The procedure used to select τ pair events is very similar to that described in previous OPAL publications [40, 41]. The distinctive signature of a τ pair event is two almost back-to-back jets of one or more charged particles, often accompanied by neutral hadrons or photons. Each jet is accompanied by "missing energy" from the

production of one or more neutrinos.

There are four main backgrounds to consider. The first two are $e^+e^- \rightarrow e^+e^-$ and $e^+e^- \rightarrow \mu^+\mu^-$ events, which can be identified by the presence of two very high-momentum, back-to-back charged particles with the full center-of-mass energy, E_{CM} , deposited in the electromagnetic calorimeter for $e^+e^- \rightarrow e^+e^-$ and with very little ECAL energy for $e^+e^- \rightarrow \mu^+\mu^-$. Hermeticity of the calorimeter ensures correct identification of $e^+e^- \rightarrow e^+e^-\gamma$ and $e^+e^- \rightarrow \mu^+\mu^-\gamma$ events which have been a troublesome background for some previous experiments. A third background to $e^+e^- \rightarrow \tau^+\tau^-$ events comes from $e^+e^- \rightarrow q\bar{q}$ (multihadronic) events. This background is less significant at LEP than at lower-energy experiments because the particle multiplicity in $e^+e^- \rightarrow q\bar{q}$ events increases with E_{CM} , while for τ decays it remains constant. So as to minimize the bias against 1-5 and 3-3 topology events somewhat looser cuts are used to eliminate multihadrons than in the general τ pair selection. Finally, a fourth background comes from two-photon processes $e^+e^- \rightarrow (e^+e^-)X$ where the final-state electron and positron escape undetected at low angles and the system X is misidentified as a low-visible-energy τ pair event. The contribution to the background from these processes is small because they lack the enhancement to the cross-section from the Z^0 resonance and because the visible energy of the two-photon system is in general much smaller than that from a τ pair event. Other potential backgrounds arising from cosmic rays and single-beam interactions can be suppressed with straightforward requirements on TOF, on the location of the primary event vertex and on event topology. An estimate of residual backgrounds is given in Table 2.9.

The consequence of the naturally reduced backgrounds to $e^+e^- \rightarrow \tau^+\tau^-$ at LEP is that high purity can be attained without sacrificing selection efficiency or strongly biasing for or against certain τ decay modes. This substantially reduces the systematic uncertainties in the branching ratio measurements introduced by the event selection.

These selection criteria were applied to all the data collected during 1990 and 1991, where the detector components important to the analysis were fully operational, to give a sample of 3794 τ pair candidate events for the 1990 run and 8913 events for the 1991 run. From Monte Carlo studies [42] the selection efficiency was estimated to be $57.1 \pm 0.2\%$. This corresponds to an efficiency of 92.0% within the $|\cos\theta| < 0.7$ angular acceptance. The efficiency for selecting events with a 1-3 topology is slightly greater than that for events with a 1-1 topology because of the cuts necessary to eliminate $e^+e^- \rightarrow e^+e^-$ and $e^+e^- \rightarrow \mu^+\mu^-$ events. Within the Monte Carlo statistical errors there is no significant bias against events with a 3-3 or 1-5 topology.

Monte Carlo studies of $e^+e^- \rightarrow e^+e^-$ [43], $e^+e^- \rightarrow \mu^+\mu^-$ [42], $e^+e^- \rightarrow q\bar{q}$ [44] and $e^+e^- \rightarrow (e^+e^-)X$ [45] events give the residual backgrounds shown in table 2.9. The total background is found to be $1.9 \pm 0.7\%$ of the total number of events.

Measurement of the τ branching ratios

In this analysis the τ topological branching ratios are measured using an unfolding technique. The migration of events from one topology to another caused by tracking

inefficiencies, photon conversions and K_S^0 decays are taken into account using the Monte Carlo simulation of the detector [39]. The inclusive 1, 3 and 5-prong branching ratios are determined from a simultaneous fit to the numbers of events with each measured topology. Four possible true event topologies are considered here: 1-1, 1-3, 3-3 and 1-5. The corrected number of events in each class, N_{kl} , is related to the measured number of events with an i - j topology, n_{ij} , by

$$n_{ij} - n_{ij}^B = \sum_{kl} \epsilon_{kl \rightarrow ij} f_{kl} N_{kl}$$

where n_{ij}^B is the estimated non- τ background, f_{kl} is the bias introduced by the event selection and $\epsilon_{kl \rightarrow ij}$ is the probability of a τ pair event with a "true" k - l topology resulting in a measured i - j topology. The inclusive branching ratios, B_1 , B_3 and B_5 , are then given by

$$N_{kl} = (2 - \delta_{kl}) B_k B_l N_{tot}$$

where N_{tot} is the total number of τ pair events. Of the 71 events eliminated by restricting the fit to these topologies ≈ 58 correspond to background from $e^+e^- \rightarrow q\bar{q}$ events. This method has the advantage that it is independent of the integrated luminosity measurement and the overall efficiency of the τ pair selection and so gives a smaller systematic error on the branching ratio measurement than if the absolute number of events in each topology were used.

The inclusive branching ratios of the τ lepton to one, three and five charged particle final states are measured to be $B_1 = 84.48 \pm 0.27(stat) \pm 0.23(sys)\%$, $B_3 = 15.26 \pm 0.26 \pm 0.22\%$ and $B_5 = 0.26 \pm 0.06 \pm 0.05\%$ respectively. These measurements have been obtained from a fit where $B_1 + B_3 + B_5$ is constrained to equal one. While the measurements of B_1 and B_3 are highly correlated, the measurement of B_5 is relatively independent of B_1 and B_3 . The measured 5-prong branching ratio is in agreement with the 1990 Particle Data Group world average [31]. However, the measured 1-prong branching ratio is lower than the world average by more than three standard deviations while the 3-prong branching fraction is correspondingly higher than the average value. The errors on these measurements are of comparable size to those on the 1990 world averages. The 1-prong measurement confirms the result obtained by the CELLO collaboration [38] which also gave a 1-prong branching ratio which was significantly smaller than previous measurements. It is also in agreement with the results obtained by other LEP experiments [34]. The significance of the "missing decay mode" effect as determined by the OPAL 1-prong branching fraction and the sum of average exclusive branching ratios [31] is less than three standard deviations. A four standard deviation effect was reported in reference [31]. While this result is not sufficient by itself to entirely resolve the problem it does go some way towards reducing the size of the effect.

The τ polarization measurement

Last year OPAL presented results on polarization measured from the electron, muon, and pion(kaon) decays of the tau. We summarize these results briefly: From a sample of 3308 $e^+e^- \rightarrow \tau^+\tau^-$ events with an estimated background of 1.9%, 964 $\tau \rightarrow e\nu\bar{\nu}$, 903 $\tau \rightarrow \mu\nu\bar{\nu}$, and 309 $\tau \rightarrow \pi(K)\nu$ candidates were found. The average τ polarization at the Z^0 resonance was measured to be -0.01 ± 0.09 from an analysis of the momentum spectra of the electron, muon, and pion candidates, implying that the ratio of vector to axial vector couplings of the τ to the Z^0 is $v_\tau/a_\tau = 0.01 \pm 0.04$. The measurements of the average polarizations in the forward and backward hemispheres lead to the efficiency-corrected, forward-backward polarization asymmetry $A_{pol}^{FB} = -0.22 \pm 0.10$, implying for the electron couplings to the Z^0 the ratio $v_e/a_e = 0.15 \pm 0.07$. Since these values for the tau and electron couplings are consistent with one another, we assume lepton universality to derive $v/a = 0.05 \pm 0.04$ and a value for the weak mixing angle of $\sin^2 \bar{\theta}_W = 0.237 \pm 0.009$, with no ambiguity introduced by the relative signs of v and a .

Two measurements are made from an analysis of the $\tau^\pm \rightarrow \rho^\pm \nu_\tau$ decay. The first is the branching fraction for this mode:

$$B(\tau \rightarrow \rho \nu_\tau) = 0.234 \pm 0.009(\text{stat.}) \pm_{0.009}^{0.010}(\text{syst.})$$

This value is in very good agreement with the world average, and we will not discuss it further here. The second is a measurement of the τ polarization itself. The τ polarization is dependent on the vector and axial couplings between the Z^0 and τ^\pm , which in turn are dependent on $\sin^2 \theta_W$ in the Standard Model. By measuring this we can test lepton universality and obtain a measurement of $\sin^2 \bar{\theta}_W$, the effective electroweak mixing angle in the improved Born approximation.

There are several features unique to the case of $\tau^\pm \rightarrow \rho^\pm \nu_\tau$. Since this is the most likely τ decay mode, it potentially has the largest sample size for polarization studies. Along with $\tau^\pm \rightarrow \pi^\pm \nu_\tau$, this mode is thought to be the most sensitive for polarization measurements. However, the background for the $\tau^\pm \rightarrow \rho^\pm \nu_\tau$ is inherently much more difficult to remove than is the background for modes earlier studied because at LEP energies all the τ decay products tend to be highly collimated, making it very difficult to resolve the individual particles in the ρ^\pm decay.

Selection of τ -pairs

The data are from the 1990 run, pass 3 (ROPE 312). The Monte Carlo data are 50k events from the Tokyo group, generated with KORALZ 3.7 and run through GOPAL123/ROPE312. Preselection of $\tau^+\tau^-$ events follows the standard procedure within the τ polarization working group. This is summarised here:

The data are required to meet the usual detector and trigger status requirements. Good charged tracks are defined by cuts on the distance of closest approach, the

number of hit wires, and minimum transverse momentum. Good clusters are defined by minimum energies, different for barrel and endcaps.

A “cone analysis” is carried out to select τ pair candidates. All charged tracks and ECAL clusters in the event are listed in decreasing order of their energy. The highest-energy track/cluster is taken to define a cone direction, and then the list is searched for the next-highest energy track or cluster within 35° of the cone. When it is found, the momenta are added together to define a new cone direction. Then the procedure is repeated until no new tracks or clusters can be added to the cone. New cones are further defined, until all tracks and clusters in the event have been accounted for. Events are required to have exactly two cones, with an acolinearity of less than 15° . Each cone must have at least one charged track and at least 1% of the LEP beam energy. The average $|\cos\theta|$ of the two cones must satisfy $|\overline{\cos\theta}| < 0.68$ (this requirement eliminates 41% of all τ -pair data).

Cosmic rays are eliminated by cuts on time of flight and distance of closest approach. Multihadrons are rejected by cuts on the number of good charged tracks and total number of good ECAL clusters. Bhabha scattering events are rejected with cuts on total ECAL and track energies. Two-photon cuts are aimed at eliminating events with very little observed (“visible”) energy, which is defined by summing the energy in all tracks and clusters. Charged tracks are assumed to be pions for this calculation. Events are rejected if they have two muon candidates, where a muon candidate must satisfy track quality requirements and be associated with hits in one of the external detectors.

As estimated from our simulated data, the preselection requirements identify $\tau^+\tau^-$ pairs with $54.7 \pm 0.7\%$ efficiency (59% from the acceptance requirement alone, as stated above). The final sample contains a contamination of $1.9 \pm 1.0\%$ non- τ pair events, broken down in Table 2.10.

Selection of $\tau^\pm \rightarrow \rho^\pm \nu_\tau$

Our requirements are designed to select events where the final-state π^+ and π^0 are well separated spatially in the detector. Tracks and clusters are examined within a decay cone of half-angle 0.3 rad around the direction of the cone as calculated in preselection. This is defined by the angular spread from the direction of the τ decay cone of the final-state π^+ and photons, where the photons are required to have at least 2.0 GeV of energy to be consistent with a “neutral cluster threshold” We require there to be only one good charged track inside the cone. This greatly reduces background from τ decay modes with 3 or 5 charged particles. Events are required to have either one or two neutral ECAL clusters inside the cone, where a neutral cluster is unassociated with the good charged track and must have at least 2.0 GeV of raw energy.

The cone mass M_{cone} is calculated as the magnitude of the sum of all four-momenta in the event. We require that this mass be consistent with that of a ρ meson: $0.55 < M_{\text{cone}} < 0.95$ GeV. This reduces the background from $\tau^\pm \rightarrow \pi^\pm(2\pi^0)\nu_\tau$ decays and

other hadronic modes. The cone mass distribution is shown after all other cuts for data and Monte Carlo in Figure 2.26, left.

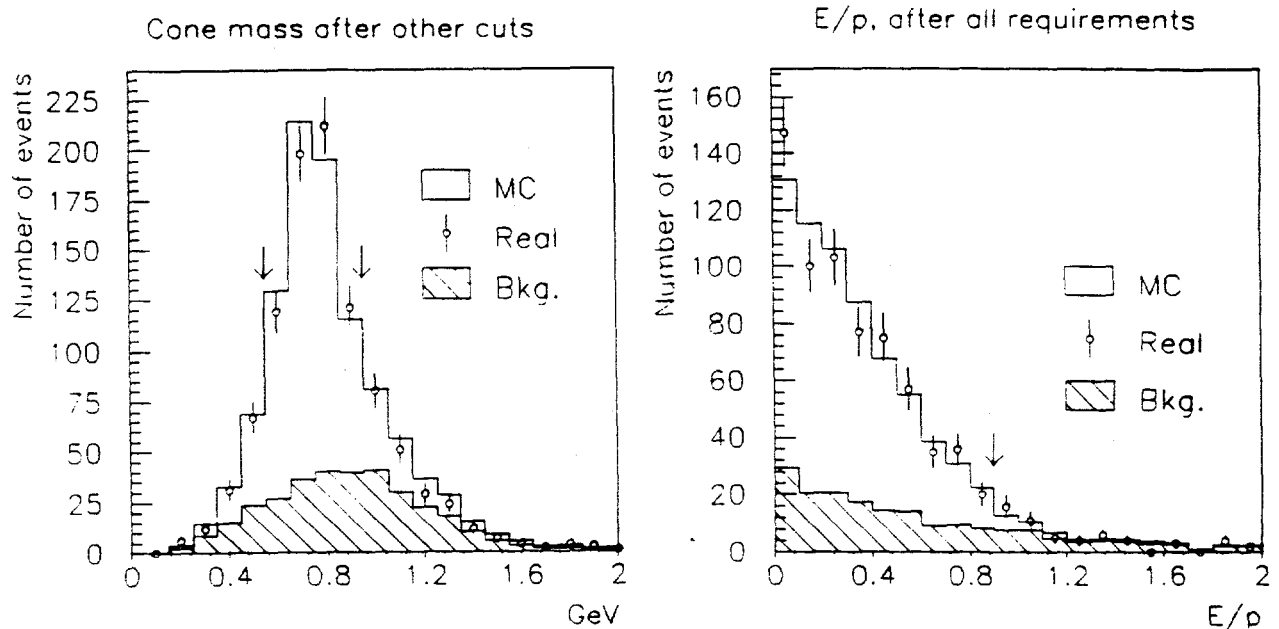


Figure 2.26: *Left:* Cone mass, data and Monte Carlo. *Right:* E_{ass}/P_{ctrk} , data and Monte Carlo. The arrow represents the cut position.

To further reduce the background from $\tau^\pm \rightarrow \pi^\pm(2\pi^0)\nu_\tau$ and $\tau^\pm \rightarrow \pi^\pm(\geq 3\pi^0)\nu_\tau$ modes, we also require that the energy in the cluster associated with the charged track satisfy $E_{ass}/P_{ctrk} < 0.9$. The aim of this requirement is to discard events which have more than one π^0 , where the neutral cluster from a π^0 may overlap with that from the charged track. The E/p distribution is shown after all other cuts for data and Monte Carlo data in Figure 2.26, right.

After making all these requirements, the selection efficiency for $\tau^\pm \rightarrow \rho^\pm\nu_\tau$ decays is $32.7 \pm 0.8\%$. The background after all cuts is $21.8 \pm 1.5\%$. The main sources of background are listed in table 2.11.

τ Polarization



Decay angles in $\tau^\pm \rightarrow \rho^\pm \nu_\tau$

The origins and theoretical estimates for the τ polarization itself are discussed in reference [29]. Here only the measurement aspects are discussed. The mean τ polarization (P_τ) is extracted by fitting the theoretical angular distribution of τ decay products to the measured distribution. There are two possibilities here. One is to fit only the distribution in $\cos \theta^*$, the scattering angle of the ρ in the rest frame of the τ (see diagram above). This gives

$$\frac{1}{N} \frac{dN}{d \cos \theta^*} = \frac{1}{2} (1 + \alpha P_\tau \cos \theta^*)$$

where α derives from differing contributions for different ρ helicity states, and is equal to

$$\alpha = \frac{M_\tau^2 - 2M_\rho^2}{M_\tau^2 + 2M_\rho^2}$$

This is of the same form as the angular distribution for the decay $\tau^\pm \rightarrow \pi^\pm \nu_\tau$, except for the factor of α . What we see is that the opposing contributions from the different ρ polarization states lessen the sensitivity to P_τ (assuming the ρ to have point mass, $\alpha = 0.46$). For this reason it has conventionally been thought that these decays were inferior to the $\tau^\pm \rightarrow \pi^\pm \nu_\tau$ decay as a method of measuring the τ polarization. However, there is a second method of measuring the τ polarization: one can make use of the fact that the ρ decays via $\rho^\pm \rightarrow \pi^\pm \pi^0$ and fit the decay distribution as a function of $\cos \theta^*$ and $\cos \psi$, where ψ is the decay angle of the π^\pm in the center-of-mass frame of the ρ (see reference [30]). The relevant distribution in this case is

$$\begin{aligned} W(\theta, \psi) = & \frac{3}{8(m_\tau^2 + 2m_\rho^2)} [(1 + P_\tau) \sin^2 \psi [(m_\tau \sin \eta \cos \frac{\theta^*}{2} - m_\rho \cos \eta \sin \frac{\theta^*}{2})^2 + m_\rho^2 \sin^2 \frac{\theta^*}{2}] \\ & + (1 - P_\tau) \sin^2 \psi [(m_\tau \sin \eta \sin \frac{\theta^*}{2} + m_\rho \cos \eta \cos \frac{\theta^*}{2})^2 + m_\rho^2 \cos^2 \frac{\theta^*}{2}] \\ & + 2(1 + P_\tau) \cos^2 \psi (m_\tau \cos \eta \cos \frac{\theta^*}{2} + m_\rho \sin \eta \sin \frac{\theta^*}{2})^2 \\ & + 2(1 - P_\tau) \cos^2 \psi (m_\tau \cos \eta \sin \frac{\theta^*}{2} - m_\rho \sin \eta \cos \frac{\theta^*}{2})^2] \end{aligned}$$

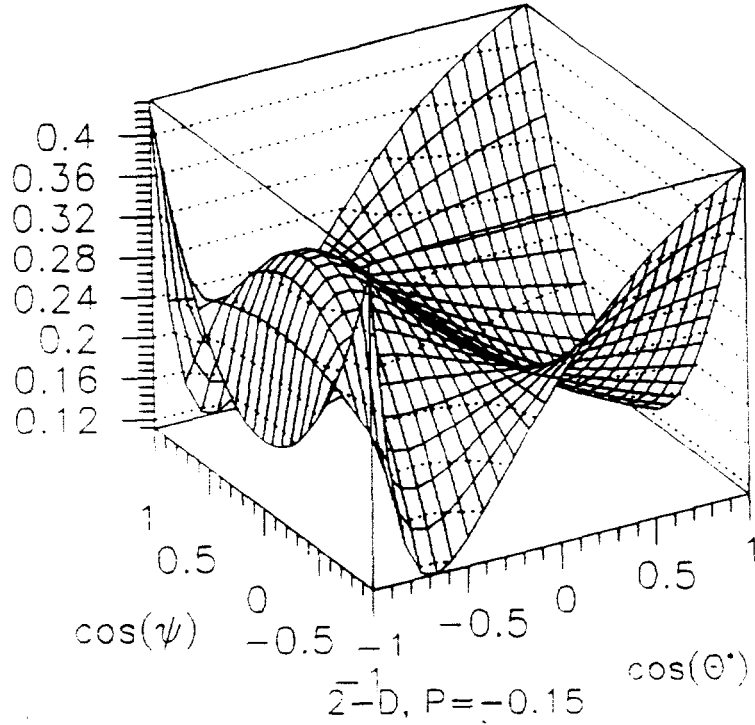


Figure 2.27: Two-dimensional angular distribution of $\tau^\pm \rightarrow \rho^\pm \nu_\tau$ decays, for $P_\tau = -0.15$, the default value in the Monte Carlo. Plotted on the vertical axis is $1/N d^2 N / d \cos \theta^* d \cos \psi$

where η represents an angle of Wigner rotation and is given by

$$\cos^2 \eta = \frac{m_\tau^2 - m_\rho^2 + (m_\tau^2 + m_\rho^2) \cos \theta^*}{m_\tau^2 + m_\rho^2 + (m_\tau^2 - m_\rho^2) \cos \theta^*}$$

This distribution, along with that for $\cos \theta^*$ alone, is plotted in Figure 2.27 for $P_\tau = -0.15$ (the expected value in the Standard Model).

To measure the polarization, the decay angles are calculated and the resulting distributions fit to the theoretical function above. The angles $\cos \theta^*$ and $\cos \psi$ are given by

$$\cos \theta^* = \frac{2M_\tau^2}{M_\tau^2 - M_\rho^2} \left(\frac{E_\rho}{E_{beam}} \right) - \frac{M_\tau^2 + M_\rho^2}{M_\tau^2 - M_\rho^2}$$

and

$$\cos \psi = \frac{M_\rho}{(M_\rho^2 - (M_{\pi^+} + M_{\pi^0})^2)^{1/2}} \frac{2E_{\pi^+} - E_\rho}{P_\rho}$$

where E_{beam} is the energy of the colliding e^- , with $E_\tau \simeq E_{beam}$.

Data are binned in a two-dimensional distribution in $\cos \theta^*$ and $\cos \psi$ (5×4 bins). Corrections are then made to the data on a bin-by-bin basis to recover the actual distributions from those measured. The final result from the polarization measurements

is

$$P_2 = -0.17 \pm 0.10 \pm 0.08 \quad (\chi^2/D = 16.8/17)$$

Forward-Backward polarization Asymmetry

The forward-backward polarization asymmetry is obtained by calculating separately the τ polarization in the forward ($\cos \theta_{\tau^-} > 0$) and backward ($\cos \theta_{\tau^-} < 0$) hemispheres, then taking

$$A_{FB}^{pol} = \frac{1}{2}(P_F - P_B) \left(\frac{3 + c^2}{4c} F_{eff} \right)$$

where $c = |\cos \theta|_{max}$ is the acceptance ($c=0.68$ here), P_F and P_B are the polarization results from using data only in these hemispheres. The factor F_{eff} is a small correction term arising from integrating the Born cross-section for τ -pair production over θ , taking into account efficiency variations. We calculate $F_{eff} = 0.98 \pm 0.02$.

The measured values of these parameters are

$$P_F = -0.24 \pm 0.15 \pm 0.08$$

$$P_B = -0.09 \pm 0.15 \pm 0.08$$

where the systematic error on each measurement is taken to be that from the mean polarization measurement above. The polarization asymmetry is then

$$A_{FB}^{pol} = -0.09 \pm 0.13 \pm 0.05$$

The statistical error on the polarization asymmetry is obtained by propagating the statistical errors through from the individual polarization measurements. The systematic error is obtained assuming that the error on the polarization in each hemisphere is the error on their difference, plus a contribution from δF_{eff} .

It is convenient to define variables λ_e and λ_τ in terms of the vector and axial coupling constants:

$$\lambda_e \equiv \frac{2(v_e/a_e)}{1 + (v_e/a_e)^2} = -\frac{4}{3} A_{FB}^{pol}$$

$$\lambda_\tau \equiv \frac{2(v_\tau/a_\tau)}{1 + (v_\tau/a_\tau)^2} = -P_\tau$$

Given a measurement of λ , we calculate v/a , from which we obtain $\sin^2 \bar{\theta}_W$ using

$$\frac{v}{a} = 1 - 4 \sin^2 \bar{\theta}_W$$

From the τ polarization we have $\lambda_\tau = 0.17 \pm 0.13$, yielding

$$v_\tau/a_\tau = 0.09 \pm 0.06 \quad \text{and} \quad \sin^2 \bar{\theta}_W = 0.228 \pm 0.015$$

From the polarization asymmetry we have $\lambda_e = 0.12 \pm 0.19$, yielding

$$v_e/a_e = 0.06 \pm 0.10 \quad \text{and} \quad \sin^2 \bar{\theta}_W = 0.235 \pm 0.025$$

These measurements are combined with previous OPAL results[28] (see Table 2.12). From the polarization, we calculate $\lambda_\tau = 0.07 \pm 0.06$, yielding $v_\tau/a_\tau = 0.03 \pm 0.03$. From the polarization asymmetries (also in Table 2.12) we calculate $\lambda_e = 0.23 \pm 0.09$, or $v_e/a_e = 0.12 \pm 0.05$. This provides a check on lepton universality.

Assuming lepton universality, the individual forward and backward polarization asymmetry measurements can also be combined, using the equations

$$P_F = -\lambda \left(1 + \frac{3c}{3 + c^2} F_{eff}^{-1} \right)$$

and

$$P_B = -\lambda \left(1 - \frac{3c}{3 + c^2} F_{eff}^{-1} \right)$$

$P_F = -0.24 \pm 0.15 \pm 0.08$ gives $\lambda = 0.15 \pm 0.09 \pm 0.05$ using the $\tau^\pm \rightarrow \rho^\pm \nu_\tau$ measurement alone, and $P_B = -0.09 \pm 0.15 \pm 0.08$ implies $\lambda = 0.23 \pm 0.38 \pm 0.20$. To combine these numbers, each is weighted by its statistical error alone. This gives $\lambda = 0.15 \pm 0.08$, yielding $v/a = 0.08 \pm 0.04$ and $\sin^2 \bar{\theta}_W = 0.230 \pm 0.010$.

Combining all OPAL forward and backward polarization measurements (see Table 2.13), we have $\lambda_{OPAL} = 0.11 \pm 0.05$. This gives $v/a = 0.057 \pm 0.025$ and $\sin^2 \bar{\theta}_W = 0.2358 \pm 0.0063$.

Search for Lepton Flavor Violation in Z^0 Decays

A letter "A Search for Lepton Flavor Violation at LEP", [55], written primarily by UCR authors Dittmar and Shen, appeared about a year before similar studies from other experiments at LEP were finished. This first direct search for flavor changing Z^0 decays improved indirect limits from τ decays by more than a factor two. We are currently working on an update of this paper and expect to obtain new interesting results when more than a million total Z^0 decays are collected with OPAL.

Background	Contamination(%)
$e^+e^- \rightarrow q\bar{q}$	1.0 ± 0.3
$e^+e^- \rightarrow e^+e^-$	0.3 ± 0.3
$e^+e^- \rightarrow \mu^+\mu^-$	0.5 ± 0.5
$e^+e^- \rightarrow (e^+e^-)X$	0.1 ± 0.1
Total	1.9 ± 0.7

Table 2.9: Estimated background contaminations in the 12707 τ pair candidate events. The errors include both statistical and systematic uncertainties.

Background	Contamination (%)
$e^+e^- \rightarrow e^+e^-$	0.2 ± 0.2
$e^+e^- \rightarrow \mu^+\mu^-$	0.8 ± 0.9
$e^+e^- \rightarrow q\bar{q}$	0.7 ± 0.3
$e^+e^- \rightarrow e^+e^-X$	0.2 ± 0.2
Total	1.9 ± 1.0

Table 2.10: Contamination in τ -pair sample

Background decay mode	Fraction of candidates (%)
$\tau^\pm \rightarrow \pi^\pm(2\pi^0)\nu_\tau$	16.06 ± 1.35
$\tau^\pm \rightarrow (K^*)^\pm\nu_\tau$	1.54 ± 0.21
$\tau^\pm \rightarrow (K^\pm, \pi^\pm)\nu_\tau$	1.32 ± 0.03
$\tau^\pm \rightarrow \pi^\pm(\geq 3\pi^0)$	1.90 ± 0.71
$\tau^\pm \rightarrow \mu^\pm\bar{\nu}_\mu\nu_\tau$	0.46 ± 0.05
$\tau^\pm \rightarrow e^\pm\bar{\nu}_e\nu_\tau$	0.50 ± 0.06
Total	21.78 ± 1.54

Table 2.11: Sources of background in selected data

Mode	P_τ	A_{FB}^{Pol}
$\tau^\pm \rightarrow e^\pm \bar{\nu}_e \nu_\tau$	$+0.03 \pm 0.13$	-0.18 ± 0.14
$\tau^\pm \rightarrow \mu^\pm \bar{\nu}_\mu \nu_\tau$	-0.10 ± 0.15	-0.21 ± 0.17
$\tau^\pm \rightarrow \pi^\pm \nu_\tau$	-0.04 ± 0.11	-0.22 ± 0.13
$\tau^\pm \rightarrow \rho^\pm \nu_\tau$	-0.17 ± 0.13	-0.09 ± 0.14
Combined	-0.07 ± 0.06	-0.17 ± 0.07

Table 2.12: OPAL polarization and polarization asymmetry measurements

Mode	P_F	P_B	λ_{comb}
$\tau^\pm \rightarrow e^\pm \bar{\nu}_e \nu_\tau$	$-0.12 \pm 0.14 \pm 0.08$	$+0.16 \pm 0.14 \pm 0.08$	$+0.05 \pm 0.09 \pm 0.05$
$\tau^\pm \rightarrow \mu^\pm \bar{\nu}_\mu \nu_\tau$	$-0.27 \pm 0.16 \pm 0.10$	$+0.07 \pm 0.16 \pm 0.10$	$+0.15 \pm 0.10 \pm 0.06$
$\tau^\pm \rightarrow \pi^\pm \nu_\tau$	$-0.22 \pm 0.11 \pm 0.07$	$+0.09 \pm 0.11 \pm 0.07$	$+0.11 \pm 0.07 \pm 0.04$
$\tau^\pm \rightarrow \rho^\pm \nu_\tau$	$-0.24 \pm 0.15 \pm 0.08$	$-0.09 \pm 0.15 \pm 0.08$	$+0.15 \pm 0.09 \pm 0.05$
Combined	-0.21 ± 0.08	$+0.06 \pm 0.08$	$+0.11 \pm 0.05$

Table 2.13: OPAL forward and backward polarization measurements

2.2.8 Searches

Many different searches have been performed at LEP for signatures characteristic of new particles. In particular, searches have been made for the Higgs boson in minimal Standard Model form and for supersymmetric extensions, for fourth generation leptons, excited leptons, and leptoquarks. However the very impressive agreement between the predictions of the Standard Model and the measured lineshape of the Z^0 leaves very little room for new physics at LEP, and in fact no evidence for new physics has been reported. We update briefly the status of some of the searches that have been performed.

Minimal Standard Model Higgs

The main focus of attention of Higgs searches has been in the high mass region. Here one makes use of the Bjorken process, followed by the decay of the Higgs boson to heavy particles, either $b\bar{b}/c\bar{c}$ or $\tau^+\tau^-$, and the decay of the Z^{0*} to all possible fermion-antifermion pairs. Distinctive signatures with significant branching ratios are $H^0 \rightarrow b\bar{b}/c\bar{c}$ and $Z^{0*} \rightarrow \nu\bar{\nu}$, the missing energy channel; $H^0 \rightarrow b\bar{b}/c\bar{c}$ and $Z^{0*} \rightarrow e^+e^-$ or $\mu^+\mu^-$, the isolated lepton channel; and the $\tau\tau$ -jet-jet channel, in which either the Higgs or the Z^{0*} contributes the $\tau^+\tau^-$ pair. The search strategy in each of these channels is optimized for a mass reach from 25 to beyond 50 GeV/c^2 . Concretely, as the supposed Higgs mass increases, its decay would change appearance from a monojet to a pair of jets. Analysis of the full event sample of 494,000 hadronic Z^0 decays leads to mass limit of 52.6 GeV/c^2 at the 95% confidence level. The combined effect of the various channels is shown in Figure 2.28.

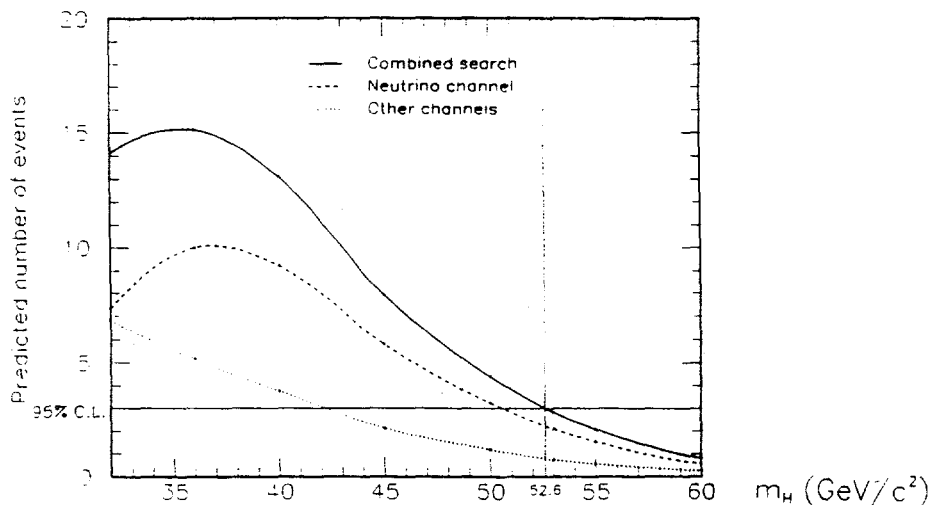


Figure 2.28: The number of expected Higgs boson events for various masses. The horizontal line shows the number of events required for a 95% C.L. limit, and the vertical line shows the new limit at 52.6 GeV/c^2 .

In another paper published during the past year, OPAL closed the missing "window" in its exclusion region between twice the muon mass and $3 \text{ GeV}/c^2$ by determining the expected signal for all possible final states in this mass region.

Minimal Supersymmetric Model Higgs

In a more general case, two Higgs doublets are considered and the Higgs sector contains five physical Higgs bosons. A popular theory with such a Higgs sector is supersymmetry (SUSY). In the minimal SUSY Model (MSSM) one of the Higgs doublets couples to up-type fermions only, while the other couples only to down-type fermions, thus preventing flavor-changing neutral currents. Of the two neutral scalar Higgs bosons in this model, one (h^0) must be lighter than the Z^0 , while the other must be heavier than the Z^0 . There is also a charged Higgs pair which has to be heavier than the W , and a neutral CP-odd or pseudoscalar Higgs (A^0) which has to be heavier than the h^0 but can be lighter than the Z^0 and might therefore also be accessible to experiments running near the Z^0 resonance. In this model, two independent parameters are needed to specify the Higgs sector. There are two common choices for these parameters: i) $\tan \beta = v_2/v_1$, the ratio of the vacuum expectation values of the doublets, and m_{h^0} , the mass of the lightest Higgs; and ii) m_{h^0} , and m_{A^0} , the mass of the pseudoscalar Higgs.

This reasonably straightforward extension to the two Higgs doublet situation was somewhat complicated by the introduction of one-loop corrections. [56] These modify the mass relationships so that m_{h^0} can be greater than m_Z and greater than m_{A^0} . Thus one must consider the decays $Z^0 \rightarrow Z^* A^0 A^0$ and $Z^0 \rightarrow Z^0 A^0 A^0$ if $m_{h^0} > 2m_{A^0}$. Although the OPAL Higgs group has worked out the consequences of these relationships in terms of the original interpretation of the one-loop corrections [56], other theorists have suggested that this point of view is incorrect and that different relationships hold. The question awaits clarification from the theorists.

Doubly Charged Higgs Production

Introduction The existence of a doubly-charged Higgs boson ($H^{\pm\pm}$) is a novel feature of some models that extend the Standard Model to allow small neutrino mass [46, 47, 48], or that explore different possibilities for the Higgs sector [49]. Since the $H^{\pm\pm}$ does not couple to quarks, there are three modes by which the $H^{\pm\pm}$ can decay: by Yukawa couplings to like-sign lepton pairs ($H^{\pm\pm} \rightarrow \ell_1^\pm \ell_2^\pm$, where $\ell_{1,2} = e, \mu, \tau$), by the weak decay mode ($H^{\pm\pm} \rightarrow H^\pm W^\pm$), or by the Higgs decay mode ($H^{\pm\pm} \rightarrow H^\pm H^\pm$ and $H^\pm H^\pm H^0$). In this study it has been assumed that the $H^{\pm\pm}$ decays solely via Yukawa couplings to like-sign lepton pairs because of the large value of the mass of singly-charged Higgs bosons.

The leptonic decay mode of the $H^{\pm\pm}$ gives rise to final states containing four charged leptons. The large coupling of the $H^{\pm\pm}$ to the Z^0 and the distinctive four-

lepton final state make LEP a promising place to search for the doubly-charged Higgs boson. If the $H^{\pm\pm}$ decays dominantly to same-sign lepton pairs with a coupling constant less than 10^{-7} , the $H^{\pm\pm}$ will have a lifetime that is long enough for it to decay well away from the interaction point.

Neglecting radiative corrections, the expression for the Z^0 partial width for decays into $H^{\pm\pm}$ pairs (following [50]) is:

$$\Gamma(Z^0 \rightarrow H^{++}H^{--}) = \frac{G_F M_Z^3}{6\pi\sqrt{2}} (I_3^L - Q \sin^2 \theta_W)^2 \left(1 - \frac{4M_H^2}{M_Z^2}\right)^{\frac{3}{2}},$$

where M_Z is the mass of the Z^0 boson, $\sin^2 \theta_W$ is the electroweak mixing parameter, G_F is the Fermi coupling constant and m_{h^0} , Q , I_3^L are the mass, charge and third component of weak isospin respectively of the $H^{\pm\pm}$. The value of I_3^L is model dependent, and can take any of the three possible values 1, 0 or -1 . Note that this width would correspond to a sizeable fraction of the total Z^0 width (comparable to $\Gamma(Z^0 \rightarrow \mu^+\mu^-)$ for low mass $H^{\pm\pm}$).

The exclusion region for the process $Z^0 \rightarrow H^{++}H^{--} \rightarrow \ell_1^+ \ell_2^+ \ell_3^- \ell_4^-$ ($\ell = e, \mu, \tau$) for short-lived $H^{\pm\pm}$ is labeled as 'A' in Figure 2.29. It extends from the $H^{\pm\pm} \rightarrow \ell_1^\pm \ell_2^\pm$ threshold to an upper limit of $45.6 \text{ GeV}/c^2$, primarily determined by the falling cross section for $Z^0 \rightarrow H^{++}H^{--}$. The boundary of the excluded region at small Γ_H in the four-lepton, short $H^{\pm\pm}$ lifetime search is determined by the efficiency of the four-track cut since, as Γ_H decreases, the $H^{\pm\pm}$ lifetime increases, and the fraction of events passing this cut falls. The exclusion zone is shown for both $I_3^L = \pm 1$ and $I_3^L = 0$.

The search for long-lived $H^{\pm\pm}$ includes the final states where one, or both, of the $H^{\pm\pm}$ escape the jet chamber without decaying. In this case, the mass range extends from twice the electron mass to an upper limit of $45.6 \text{ GeV}/c^2$. The upper Γ_H boundary of the excluded region is determined by the $H^{\pm\pm}$ lifetime: as Γ_H increases, the $H^{\pm\pm}$ lifetime decreases, and with it the likelihood that one of the $H^{\pm\pm}$ fully traverses the tracking chamber without decaying. The excluded region in the (m_{h^0}, Γ_H) plane for this channel is labeled as 'B' in Figure 2.29.

Heavy Leptons

UCR postdoc Heungmin Oh is preparing a publication which will describe a general search in Z^0 decays for pair production of a new heavy charged particle with mass M that decays to a lighter, invisible partner of mass $M_{invis} \equiv M - \delta M$ and conventional hadrons and leptons. Depending on the partner masses, these events may be characterized by low visible energy and large missing momentum or, in the case of near degeneracy of the partner masses, by extremely low visible energy. The primary aim is extending the search sensitivity to the case of near degeneracy in mass for a large range of heavy charged particle masses. The paper will also provide a standard template – in terms of partial width times acceptance – for setting limits on other exotic particles with possibly suppressed couplings.

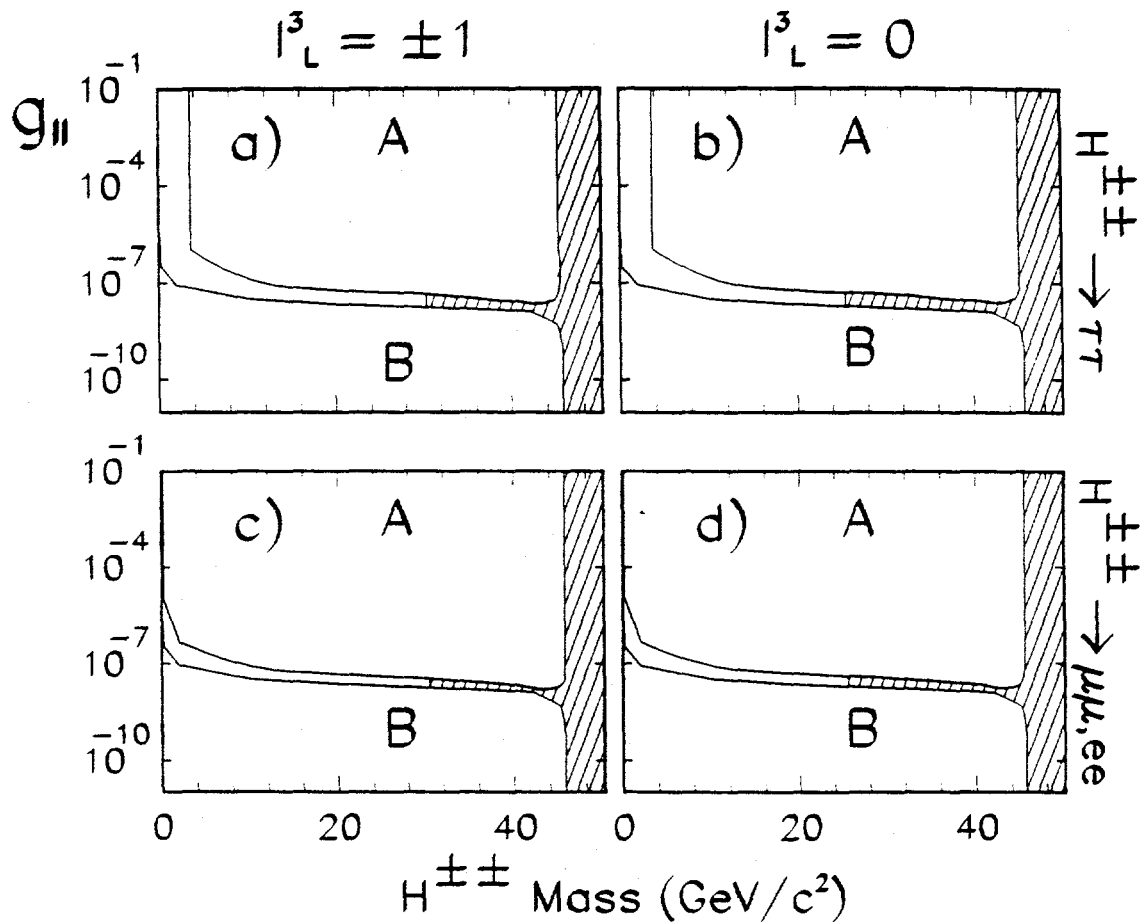


Figure 2.29: The $H^{\pm\pm}$ exclusion regions in the m_{h^0} - $\Gamma_{||}$ plane. The unhashed zones show the regions excluded at the 95% confidence level. The regions labeled by 'A' are excluded by the search for the short-lived $H^{\pm\pm}$. Those labeled by 'B' (which extend down to $\Gamma_{||} = 0$) are excluded by the search for the long-lived $H^{\pm\pm}$. $H^{\pm\pm}$ with mass less than $25.5 \text{ GeV}/c^2$ ($I_3^L = 0$) or $30.4 \text{ GeV}/c^2$ ($I_3^L = \pm 1$) are excluded by measurements of Γ_Z , as indicated by the dotted lines.

The search is based on two independent methods: The first method, which differs little from those used in previous conventional searches, looks for events with missing energy and missing momentum transverse to the beam without requiring particle identification. The second method relies instead upon the identification of highly acoplanar events with two charged particles, exactly one of which is an electron. This method is effective in searching for events with extremely low visible energy that would otherwise be hidden by two-photon backgrounds and where conventional search techniques prove to be insensitive.

The search results could be translated in terms of a fourth generation charged heavy lepton doublet model where the neutrino is allowed to be massive. For the case of a massless neutrino, a charged lepton is excluded at the 95% confidence level in the mass range 5-44.3 GeV/c^2 . For a mass splitting $\approx 0.5 \text{ GeV}/c^2$, the excluded range is 10-20 GeV/c^2 , as shown in Figure 2.30

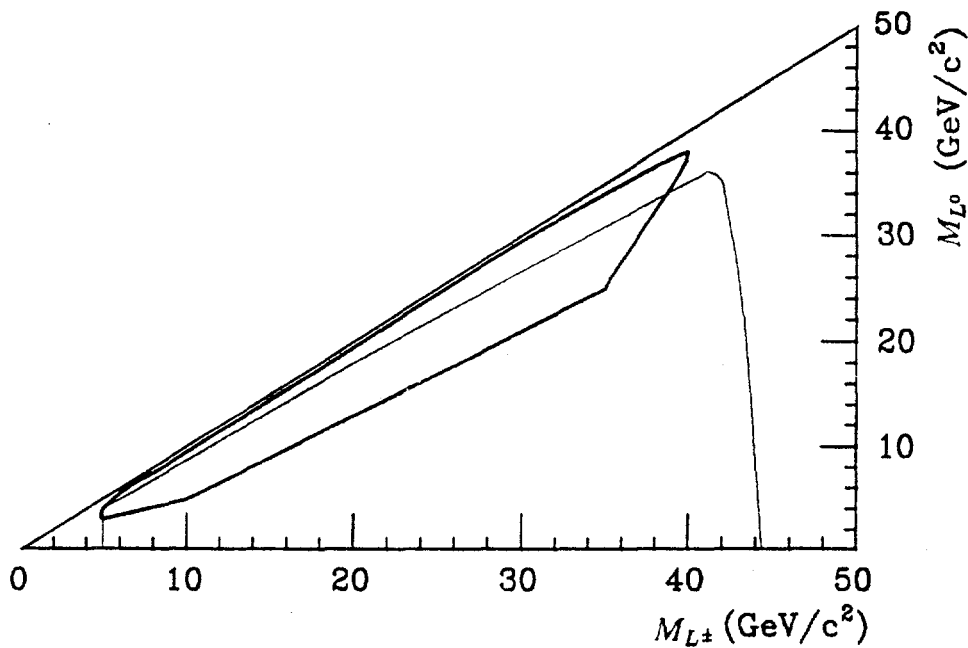


Figure 2.30: Exclusion contours at 95% confidence level in the (M_{L^\pm}, M_{L^0}) mass plane. The thin line is the mass limit from the missing p_T and E_{vis} analysis. The area surrounded by the thick line is excluded by the $L^+L^- \rightarrow e\bar{e}$ search.

2.2.9 Personnel

The OPAL experiment at LEP is the major project of our group, and our responsibilities include operation of the Hadron Calorimeter strip system, residual responsibilities for the time-of-flight electronics, maintenance and development of online data acquisition and offline reconstruction software, and physics analysis.

The physicists participating in OPAL are M. Dittmar, J.W. Gary, W. Gorn, C.C.H. Jui, J.G. Layter, B.C. Shen, G.J. VanDalen, and G.W. Wilson. Graham Wilson replaces Keith Riles who has obtained a tenure track position at the University of Michigan. Graham was previously at Saclay where he had responsibility for the time-of-flight system. Charles Jui has recently completed his thesis working on the MEGA detector at Los Alamos.

Four graduate students W.J. Larson, C. Ho, H. Oh, and B.P. O'Neill, completed their Ph.D. research during the past year. Among the current students, E.G. Heflin is planning to finish during this coming academic year, and J.R. Letts the following year. S.L. Chu has recently moved to CERN to begin his research project. G. Moradkhanian will work at SLAC during the summer and fall to complete the TPC/ 2γ papers. He expects to join the OPAL experiment at CERN during 1993.

2.3 The Compact Muon Solenoid (CMS) at LHC

One of the most fundamental questions to be answered in the next decade is the physics origin of the electroweak symmetry breaking and how the particles acquire their masses. Within the minimum version of the Standard Model, spontaneous symmetry breaking through the Higgs mechanism leads to the existence of a spin zero particle, the Higgs boson H . The searches carried out at LEP have found no evidence for the Higgs up to a mass of 45 GeV. With LEP200 the search will have a sensitive range up to the mass of the Z^0 . Recent work involving members of the UCR theory group indicates that, on the basis of very general arguments, there may exist an upper bound in the neighborhood of $800 \text{ GeV}/c^2$ for the Higgs boson mass. Therefore, the search for the Higgs boson will be the most important physics goal of the next generation of colliders.

The UCR group is seeking to participate in the construction and exploitation of the Compact Muon Solenoid (CMS) detector which is currently being planned for the Large Hadron Collider (LHC) at CERN. We do this in the belief that LHC, because it will be constructed in the LEP tunnel at a much lower cost than SSC, will almost inevitably enjoy a several year window of exclusivity in the search for the Higgs boson. We therefore feel that it is incumbent on American groups that have the possibility of doing so to participate in the CERN endeavor so that American physicists have a significant involvement in this important next step. Given the UCR group's long involvement at CERN and the presence at CERN of a large fraction of our personnel in conjunction with the OPAL experiment, we feel it only natural and logical that our efforts be directed to the LHC.

Physics Potential of CMS

In final states with four muons, the produced Higgs can decay into two real Z^0 's if the Higgs mass is greater than twice the Z^0 mass. For the Higgs mass between 130 GeV and $2M_{Z^0}$, the Higgs decays into one real Z^0 and one virtual Z^0 . The main background consists of $Z^0 Z^0$ continuum:

$$pp \rightarrow \mu^+ \mu^- \mu^+ \mu^- X$$

and a non-resonant part for which at least one muon pair does not arise from a Z^0 . [57] In this case the dominant contributions are pair-produced top quarks and $Z^0 b\bar{b}$:

$$pp \rightarrow \tau^+ \tau^- X \text{ or } Z^0 b\bar{b} X \rightarrow \mu^+ \mu^- \mu^+ \mu^- X.$$

The invariant mass distributions of the four muons are shown in Figure 2.31 for the background in comparison with the Higgs signal for masses of 200, 400, and 700 GeV. A center of mass energy of 16 TeV, corresponding to that of the LHC, is assumed. The requirements of $p_T > 20 \text{ GeV}/c$ and pseudo-rapidity less than 2.5

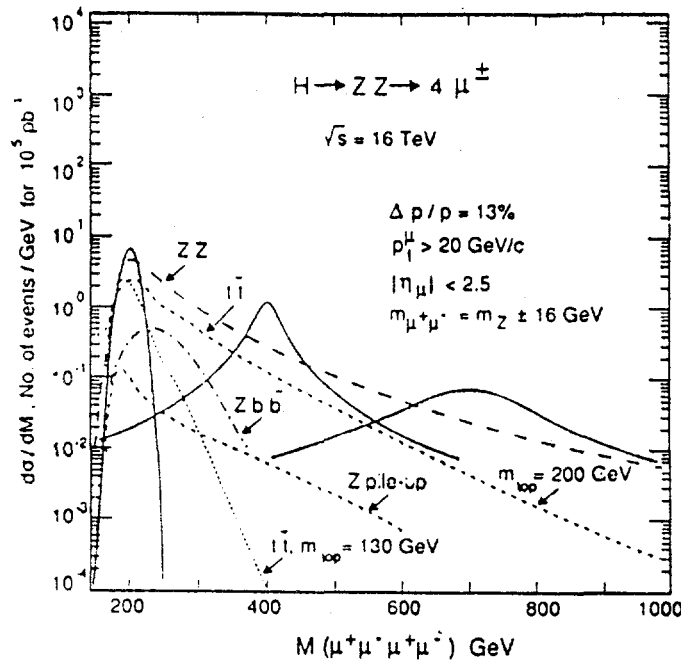


Figure 2.31: Higgs signal in the $H \rightarrow ZZ \rightarrow 4\mu^\pm$ channel, and $4\mu^\pm$ backgrounds, assuming 15% resolution.

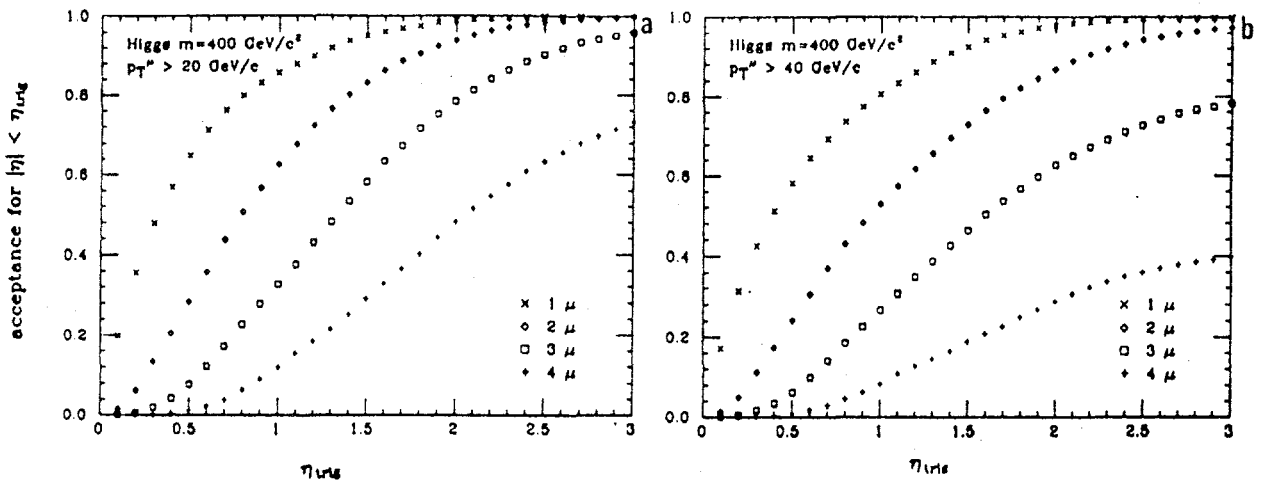


Figure 2.32: Acceptance for detecting the Higgs boson through the process $H^0 \rightarrow Z^0Z^0 \rightarrow \mu^+\mu^-\mu^+\mu^-$ when n muons ($n = 1, 2, 3, 4$) are detected in the pseudorapidity region $|\eta| \leq \eta_{trig}$. The p_T cut applied for all muons is 20 GeV/c (a) and 40 GeV/c (b).

for each muon and the requirement for muon pair masses within 16 GeV of the Z^0 reduce the non-resonant background well below the resonant Z^0Z^0 background. The assumed momentum resolution of 15% achievable with 3 m of iron magnetized to 1.8 T is adequate to resolve the signal from the background except for the very low mass region. However, using the reconstructed muon momenta from the constraint that the muon pair mass be that of the Z^0 mass greatly improves the resolution in the low mass region.

The acceptances of muons in rapidity and transverse momentum are also important design parameters for a collider detector in addition to good momentum resolution. The acceptance for a Higgs boson decaying into four muons is given as a function of rapidity in Figure 2.32. For high-mass Higgs particles which are centrally produced, the chosen rapidity interval of $|\eta| < 3$ and a p_T cut of 10 GeV/c presents little detection loss. For low-mass Higgs a larger acceptance in rapidity would be desirable. However, the muon trigger becomes increasingly difficult in the forward direction because of the rapidly increasing particle densities. There are also further demands on detector capabilities in the identification and momentum measurement of the muons at large rapidities.

The guiding idea of the CMS detector is that an efficient trigger can be constructed utilizing the topological properties of tracks in a strong magnetic field to efficiently reject muons from secondary decays and hadronic punchthrough. The principle is shown in Figure 2.33 which presents a segment of a conceivable CMS detector, on which is superimposed a muon track. The angle α in the figure is related to the transverse momentum of the track. Requiring a coincidence between "Station 1" and "Station 2" would discriminate against hadronic punchthrough.

The CMS project is not yet approved by the LHC committee, but then neither is any other LHC experiment. At a meeting at Evian, France, this past March, the CMS presentation was extremely well received and is considered very likely to be approved before the end of 1993. The UCR group is participating in the formulation of a Letter of Intent which will be submitted in the early fall.

Research and Development Activity

During 1991, UCR took part in the main R&D project associated with the CMS detector, the RD5 experiment set up in the North Area at the CERN SPS, which studies a number of questions which are crucial to the successful use of muon triggers in such a detector: the rate of muons from hadron punchthrough and decays, the efficiency of triggering using transverse momentum cuts, and the precision in momentum reconstruction required for identifying the Higgs. This short term program (scheduled for two to three years) uses the P2 test beam at the CERN SPS. The apparatus to be used for the experiment is illustrated schematically in Figure 2.34

Inasmuch as the cryogenic system for the EHS magnet was not available for the 1991 runs, the RD5 experiment did not really mimic a section of the CMS detector.

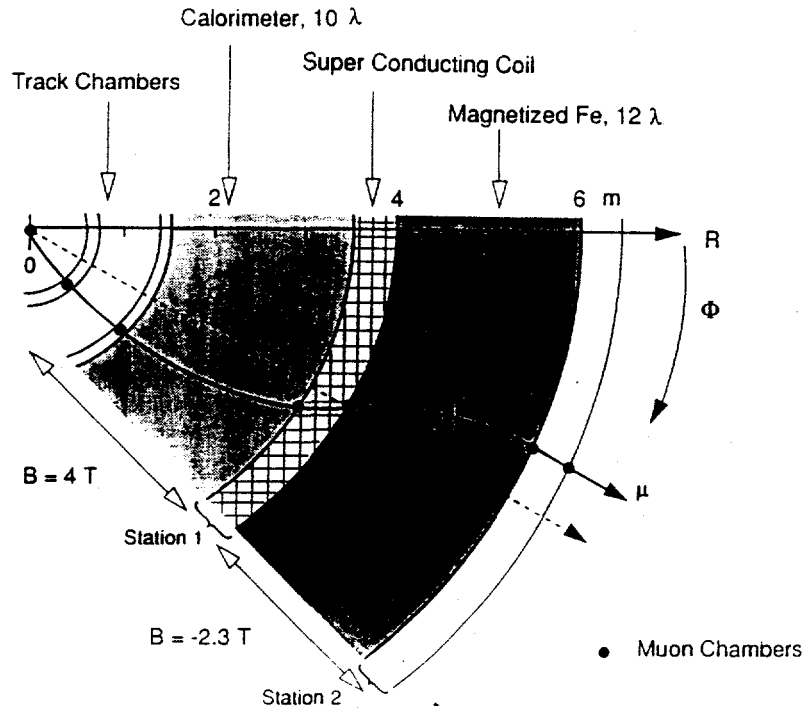


Figure 2.33: Transverse view of the Compact Muon Solenoid detector with superimposed particle trajectory.

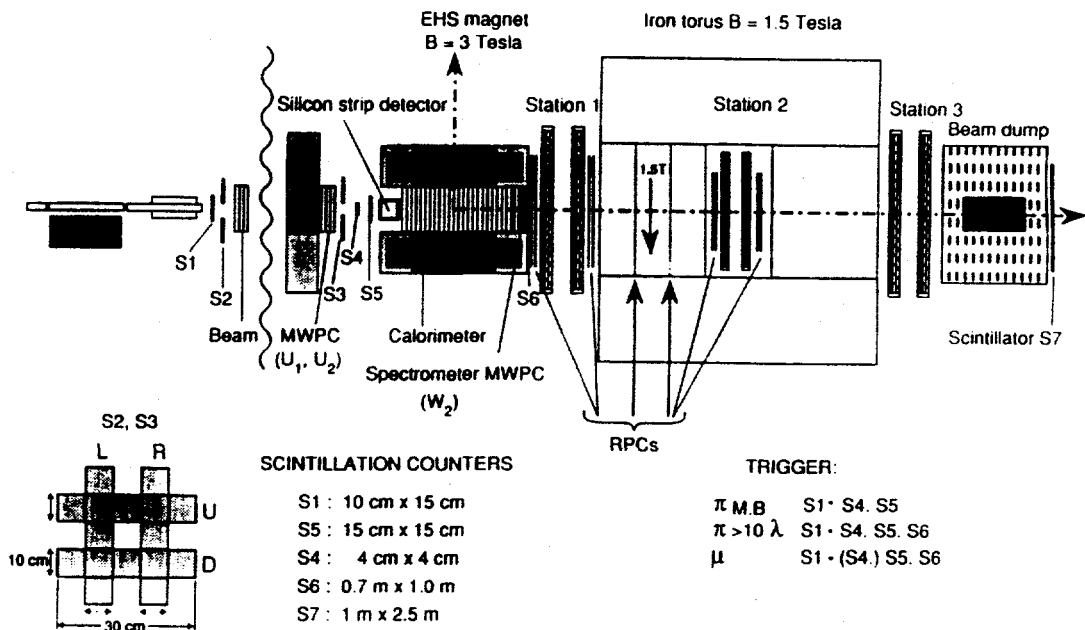


Figure 2.34: Plan view of the experimental setup of the RD5 project.

Consequently last year's running period was largely a shakedown of the various detector elements and the combined readout system. Nevertheless, valuable information on hadronic punchthrough was obtained from the runs which lasted about three weeks.

The honeycomb strip chamber (HSC), developed by the NIKHEF group [58], is one of the candidates for a low cost, large area chamber for muon detection. The cells are hexagonal in shape and are fabricated from mylar sheets on which copper strips have been laid down. The strips are perpendicular to the axis of the hexagonal cells, and an anode wire is strung at the center of each cell. Strip spacing is approximately 4 mm and the hexagonal cell diameter is roughly 1 cm. The chambers run at voltages between 1500 and 1800 V in an Ar-CO₂ gas mixture. Both the strips and the wires can be read out to give two-dimensional information.

In the RD5 setup, the HSCs are located inside the EHS magnet, and are interleaved with slabs of stainless steel of varying thicknesses, for a total of about 9 interaction lengths. This constitutes a tracking calorimeter or TRACAL as it is called. The chambers functioned adequately during the summer tests, although some difficulties were experienced in obtaining a suitable operating point, not surprising for a new technology. Eventually the HSC display provided clear visual distinction between penetrating muons and showering hadrons. Evaluation of the intrinsic resolution of the strips required careful correction for the effect of multiple scattering in the steel. A result of 80 μ was obtained.

Resistive Plate Chambers, or RPCs [59], are intended to be low cost detector elements capable of producing a fast timing signal. They are made easily and cheaply from high resistance plastic sheets, in this case bakelite, coated with graphite over their outer surfaces, which are held apart by 2 mm spacers to constitute a gas gap. The construction is shown in Figure 2.35. Signal pickup is accomplished by wide aluminum strips applied over the graphite layer and separated from it by a thin sheet of PVC. The gas is a mixture of argon, n-pentane, and freon, and a voltage of 7.1 kV is applied between the graphite layers.

Because of their construction, the chambers have only very coarse spatial resolution, on the order of 8 mm. Their advantage lies in their very fast time response of about 5 ns, quite comparable with scintillators at a small fraction of their cost. The idea would be to interleave these chambers with more precise but slower chambers so that the latter would have a local t_0 for each hit point. The RD5 tests confirmed the time and space resolution, and also showed that the single hit efficiency is between 96% and 99% depending on the beam intensity. It was also found that for chambers with a low resistivity, 100 K Ω , the efficiency degraded only at beam intensities of 100 Hz/cm², while chambers with five times this resistivity experienced efficiency falloff at only half the intensity. One also sees a broadening of the cluster size at high muon momentum, a consequence of electromagnetic showering of the muons.

One of the aims of RD5 is to study the hadron punchthrough and the behavior of muons produced in hadron showers from secondary pion or kaon decays in an absorber, with and without magnetic field. Reliable punchthrough data are necessary for the

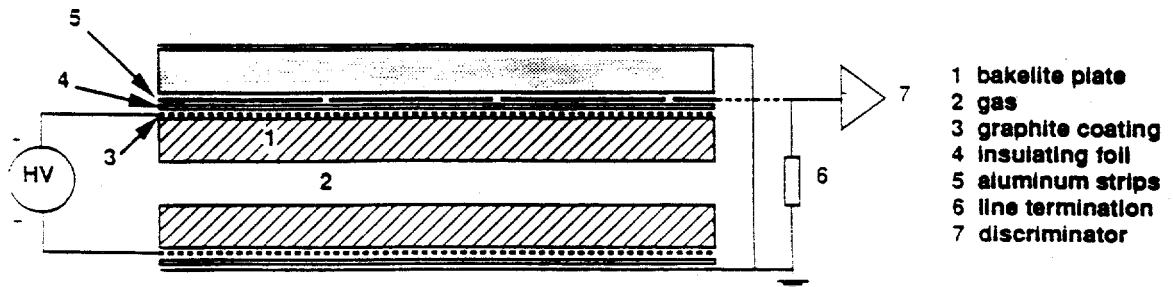


Figure 2.35: Section through a Resistive Plate Chamber

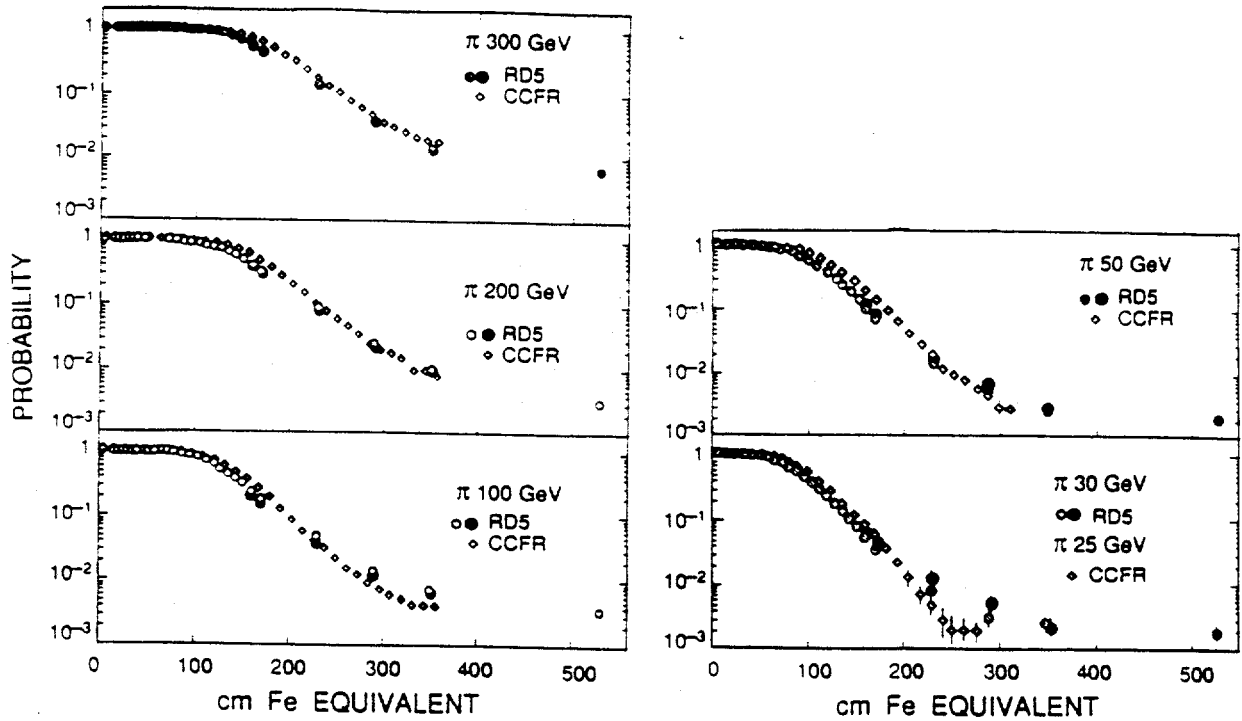


Figure 2.36: Punchthrough probability for various beam momenta. The CCFR results [60] are shown as circles.

construction of muon triggers which allow a fast and efficient cut on the transverse momentum of muons produced at the LHC.

Two methods were used to evaluate the punchthrough from the data. The first more simple-minded method defined the punchthrough probability at a given depth as the ratio of the number of events with at least one hit in a detector element at that depth to the total number of incoming beam particles. The second more sophisticated method used information from all possible detector elements to define the punchthrough probability in terms of the probability that a given configuration of detector hits would be realized at a given depth. This method allowed information on chamber noise and efficiency to be incorporated in a natural way. In a great victory for the simple-minded approach, the two methods give nearly identical answers, as shown in Figure 2.36 where the punchthrough probabilities obtained for various beam momenta are presented.

An accurate punchthrough measurement at large absorber depths requires the elimination of any muon contamination in the pion beam. The two methods use various combinations of information from the TRACAL and the RPCs to separate beam muons from shower muons. Even so, the residual muon contamination begins to be dominant at about 20λ , corresponding to distances greater than 330 cm in Figure 2.36. Efforts will be made in the 1992 running to beat down this residual contamination further with upstream veto counters.

A estimate of the trigger efficiency as a function of muon momentum was also made. The muon entrance angle was given by the beam monitor chambers, and the exit angle using two planes of RPCs with a level arm of 81 cm. The fraction of tracks rejected by different angular cuts is shown in Figure 2.37 as a function of muon momentum. It is clear that momentum cuts up to 50 GeV/c can be achieved in this configuration.

UCR Participation

The Riverside group participated in the installation and preparation of the muon chambers. This involved dismounting the chambers, with their associated high voltage supplies and readout electronics, from the UA1 experiment and reassembling them in place at the SPS North Hall. Members of the group developed a very successful system for monitoring and control of the high voltage supplies for the chambers. Online monitoring of the chamber signals was carried out by the Aachen group who originally constructed the chambers, and who modified existing UA1 programs for this purpose. The members of the Riverside group who were involved were W. Gorn, J.G. Layter, B.C. Shen, Y. Yang, and a graduate student.

Further runs during 1992 will incorporate several new detector prototypes which are candidates for use in CMS. These include a "wall-less" drift chamber developed by the Aachen group, tube chambers of a type used in the ZEUS detector at HERA developed by the Padua group, "cathode strip chambers" developed by a BNL team

and their associates which are being considered for the GEM detector, a new generation of silicon strip detectors being proposed by the Finnish groups, and possibly gaseous microstrip detectors, although these are also the object of another dedicated DRDC experiment. In addition, it is expected that the EHS magnet will be available for the runs this year.

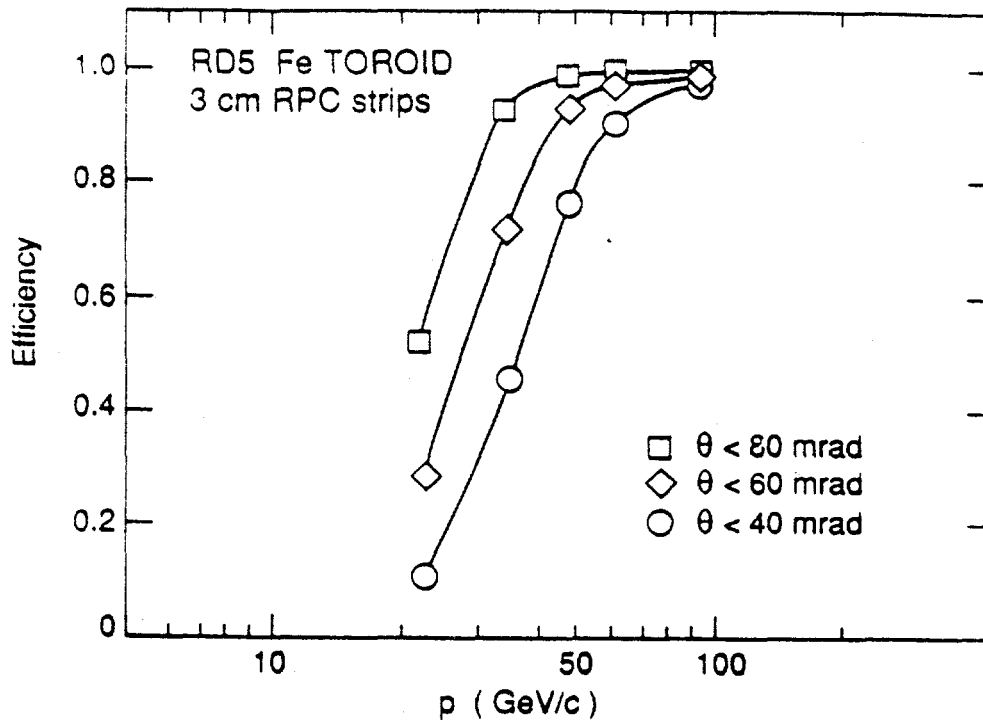


Figure 2.37: Fraction of tracks rejected by different angular cuts, corresponding to 30, 40, and 50 GeV/c momentum cuts, as a function of the muon momentum.

2.4 Neutrino Physics at LAMPF

Neutrino interactions have been used throughout the development of particle physics to study a wide range of fundamental questions including the nature of the electroweak interaction, lepton number conservation, and as a probe of cosmology. Low energy neutrinos, such as those available at LAMPF, offer significant advantages in testing the fundamental properties of the neutrinos themselves. In the decade of the 80's a series of experiments at LAMPF have measured neutrino interactions at low energies. Since 1982 several members of our group, notably William Gorn and Gordon VanDalen, have participated in an experiment at LAMPF which established significant limits in the search for neutrino oscillations [61] and measured neutrino scattering cross sections [62].

We are now collaborating in a new program which is a natural successor to the previous experiment, and serves as a logical next step in the entire LAMPF neutrino program. The primary goal of the experiment is to search for neutrino oscillations to the levels of 10^{-2} eV² in mass difference and 2×10^{-4} in mixing. This greatly extends the range explored by accelerator based searches.

The new experiment, called the Large Scintillation Neutrino Detector, or LSND, will consist of 200 tons of dilute mineral oil-liquid scintillator located near the LAMPF beam stop neutrino source. The primary focus of LSND is neutrino oscillations, although a range of related neutrino interactions will also be investigated. The collaboration of 33 physicists from LAMPF and 5 universities prepared a proposal which has been approved with the highest ranking by the Los Alamos PAC [63]. An expanded collaboration began construction in 1990-91, and data acquisition with the complete detector will begin in spring of 1993.

2.4.1 The Detector

The detector is similar to a large water Cerenkov device but with better angular, position, and energy resolution due to more light collected from scintillation, and the improvements in Cerenkov imaging from higher index of refraction, longer radiation length, and lower density of mineral oil compared to water. The expected energy, position and angular resolutions for a 45 MeV electron are $< 5\%$, < 25 cm, and $< 15^\circ$ respectively. Protons are identified by the absence of a Cerenkov cone, and neutrons will be tagged by the 2.2 MeV photon from neutron absorption on a free proton. The superb event timing and vertex reconstruction allows us to separate neutrino induced events from pion decay in flight, decay at rest, and cosmic ray backgrounds using the 200 MHz fine structure in the LAMPF beam.

The proposed detector is shown in Figure 2.38. It consists of a cylindrical tank of dilute mineral-oil-based liquid scintillator approximately 6 m in diameter by 9 m long with an active mass of 200 tons. The 1200 9" photomultiplier tubes cover 28% of the surface area of the tank with sensitive photocathode.

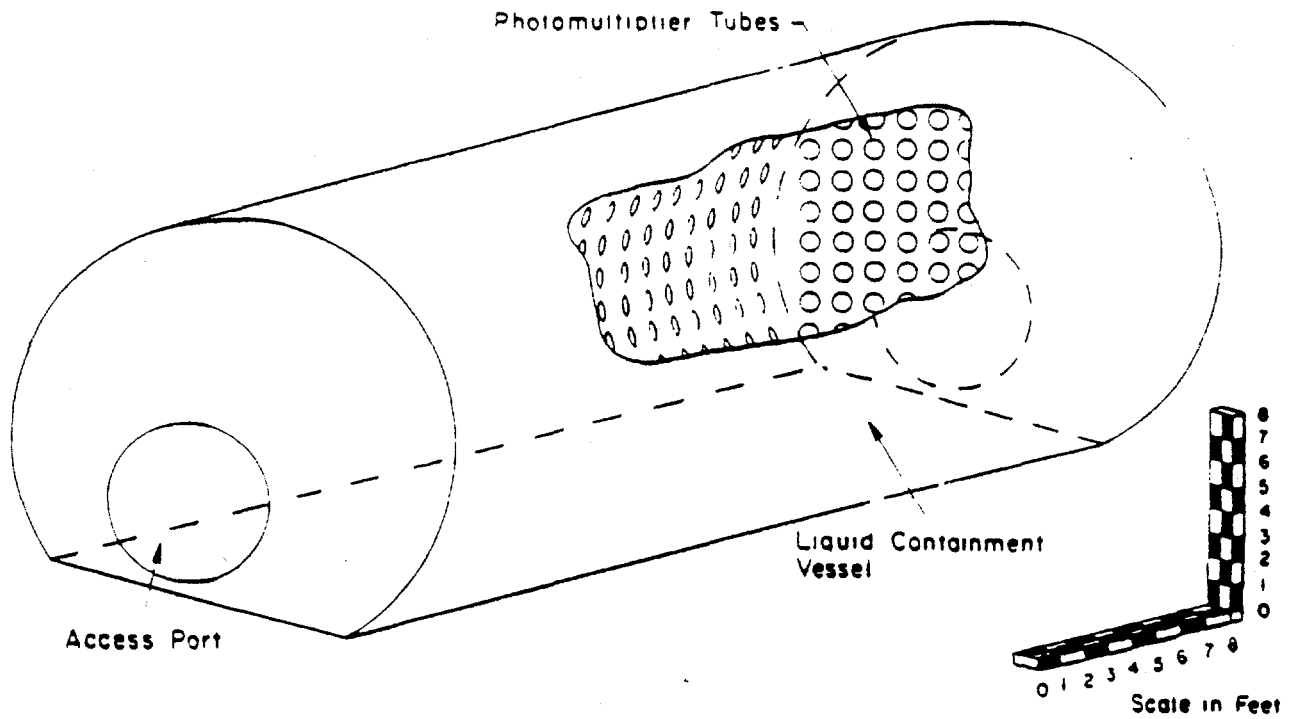


Figure 2.38: Schematic view of the LSND detector

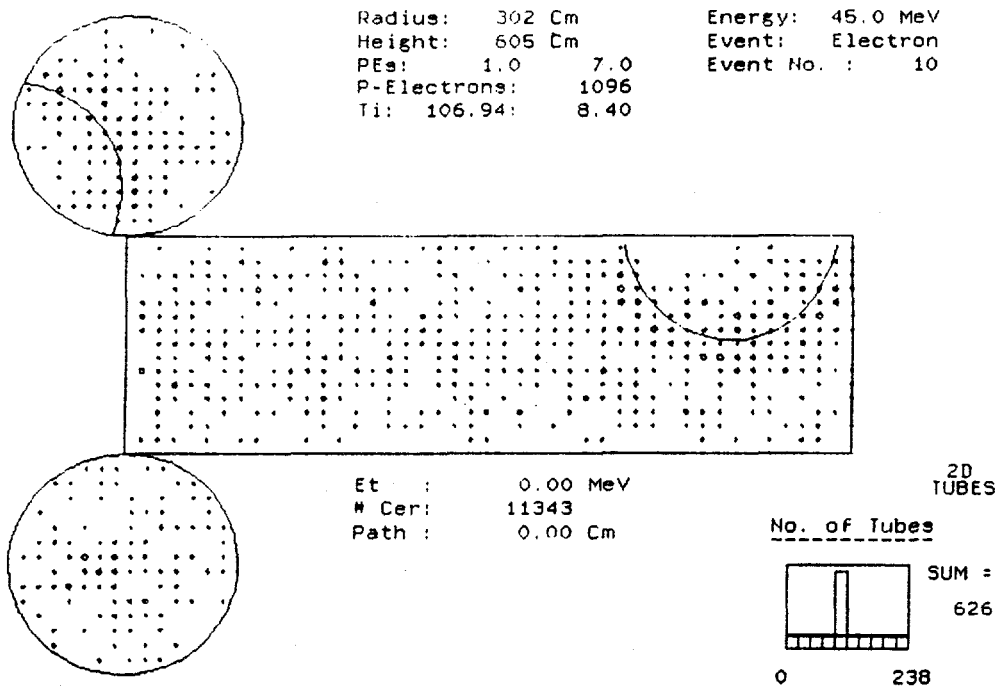


Figure 2.39: Monte Carlo event seen in the detector.

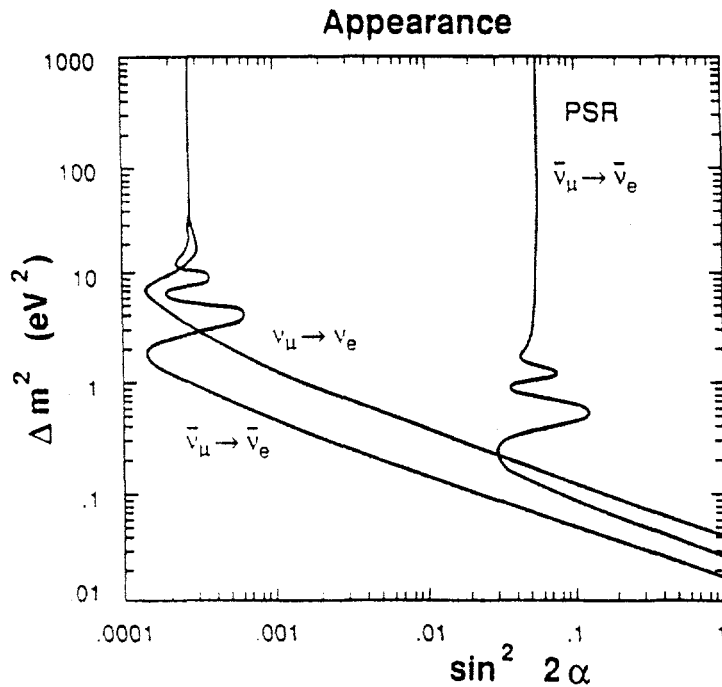


Figure 2.40: Limiting oscillation curve in the Δm^2 versus $\sin^2 2\theta$ parameter space for accelerator experiments.

Figure 2.39 shows a typical 45 MeV electron event generated by the Monte Carlo. Each number corresponds to a hit photomultiplier tube and equals the number of photoelectrons. The detector cylinder has been unrolled to clearly show the phototube hit pattern. Note that the location of the Cerenkov ring can be seen by eye.

2.4.2 The Physics

LSND does two largely independent neutrino oscillation experiments with similar sensitivities that can be performed concurrently. Simply stated, one experiment looks for high-energy ν_e ($80 < E_\nu < 200$ MeV) produced by conversion to ν_e of the ν_μ from the decay-in-flight component of the beam-dump neutrino beam. Simultaneously, another experiment looks for low-energy $\bar{\nu}_e$ produced by conversion of $\bar{\nu}_\mu$ ($40 < E_\nu < 53$ MeV) from the decay-at-rest component of the same beam. In each experiment the incident beam, the event signature, and the backgrounds are different. Consequently, with similar sensitivities as shown in Figure 2.40, the two experiments (plus the PSR experiment) provide important redundancy in addition to significantly wider coverage of the $\Delta m^2 - \sin^2 2\theta$ space than all previous accelerator searches for $\nu_\mu \rightarrow \nu_e$ ($\bar{\nu}_\mu \rightarrow \bar{\nu}_e$) oscillations combined.

There are many other physics objectives that can be pursued with the liquid scintillator detector. Searching for $\bar{\nu}_\mu \rightarrow \bar{\nu}_e$ oscillations is equivalent to searching for the lepton number violating decay $\mu^+ \rightarrow e^+ \nu_\mu \bar{\nu}_e$. The $\nu C \rightarrow \nu C^*$ (15.11 MeV γ) neutral-current reaction, one of the only neutrino-nuclear neutral-current reactions that can be easily observed, will be measured to approximately 10% accuracy. The

rare decays $\pi^0 \rightarrow \nu\bar{\nu}$ and $\eta \rightarrow \nu\bar{\nu}$, followed by $\nu_e C \rightarrow e^- N$, can be searched to sensitivities of about 10^{-6} and 10^{-4} , respectively, with very little background because the neutrinos from these decays are extremely energetic. These decays are forbidden for massless Weyl neutrinos and can proceed only if neutrino states of both chiralities exist or if lepton number is not conserved. We shall also measure the $\nu_e C$ and $\nu_\mu C$ charged-current scattering cross sections and the νe elastic scattering cross section to approximately 10 – 15% accuracy. These measurements would test present theories of neutrino-nucleus scattering and provide an estimate of $\sin^2\theta_W$.

2.4.3 Personnel

Construction of the LSND began in 1990-91 and continues into 1992-93. Data acquisition with the LAMPF beam should begin in 1993. UC Riverside is heavily involved in the data acquisition computing hardware and software. This will draw heavily on the very successful OPAL data acquisition system.

B. Shen and G. VanDalen will devote a fraction of their research time to the LSND project. A one-year grant from DOE Nuclear Sciences supports two research students (W. Strossman and K. McIlhaney) and the expenses associated with UCR participation in LSND for 1992-93. A post-doc will be hired with university funds.

2.5 TPC/ 2γ at PEP

The UCR group has participated actively in the TPC/ 2γ experiment at PEP since the inception of the program. A large number of paper have been published on the study of leptons and quarks based on data taken between 1983 and 1987. A total of five students have completed their Ph.D. research on the TPC/ 2γ experiment. Willis Lin and Mourad Daoudi, who received their Ph.D.'s in the Spring and Fall of 1990, are the most recent.

Unfortunately, our hope for high luminosity running of PEP came to an end when it was announced by Burton Richter on Nov.1, 1991 that PEP would not be operated at SLAC for at least one year. The TPC/ 2γ Collaboration decided subsequently to discontinue the operation of the detector. Nevertheless, the data accumulated so far is still quite valuable for a number of physics topics and is available for the groups involved in the experiment. It should be noted however that the window of opportunity for utilizing these data is rapidly closing since the CLEO experiment at CESR has 1.4 fb^{-1} in hand and is presently building up its analyzing power in the area of two-photon physics.

Consequently we are stepping up our efforts to bring to publication results obtained earlier by Lin and Daoudi. This work is being carried out by Layter and Shen together with a new student Garen Moradkhanian, who has spent a part of the summer at SLAC becoming familiar with the analysis programs. It is to be hoped that Lin will also be able to participate in this effort. Only a modest amount of support is needed for computing, communication and travel for this work.

2.6 Budget Justification

The proposed budget of Task A2 for the 93-94 contract year is designed to maintain and continue the research activities at the current level.

Our share of the common operations cost of OPAL is 80,000 SwF for 1993. This is equivalent to \$60,000, estimated at the exchange rate of 1.34 SwF to the dollar. We have included this amount under the item OPAL Operational Upgrades. For the TOF trigger improvement we request an amount of \$18,000 for the electronics and cables needed. We have not requested funds within this budget for any equipment support associated with RD5 or CMS.

The personnel at the Ph.D. level for the 1993-94 contract year will remain basically at the same level as for the current period. Dr. Graham Wilson joined our group as a Postgraduate Researcher in February 1992 replacing Keith Riles, who left in December 1991 to assume a faculty appointment at University of Michigan. Dr. Charles Jui joined us in April 1992 with the understanding that half of his salary will be supported by the University.

The graduate students we have had on contract during the 1992 contract year include: Altice, Heflin, Larson, Letts, Moradkhanian, Oh, Strossman, and Ryu. Moradkhanian and Ryu are summer students who plan to carry out their graduate research on the OPAL experiment. Larson and Oh, who are partially supported, are finishing the remaining work on their research for the final version of a paper or thesis. Altice has chosen to pursue a career in industry upon receiving his M.S. Strossman is working on the neutrino experiment LSND and will be supported by a grant from DOE Nuclear Science.

Heflin and Letts are proceeding well with their research. Heflin is expected to complete his thesis and other requirements within the 1992-93 academic year. Letts is expected to finish sometime during the following academic year. Moradkhanian, who is currently analyzing TPC data, will go to CERN at the beginning of 1993 and work on the OPAL experiment. Ryu, who still has graduate course requirements to fulfill, will work again in the summer months to begin his research in OPAL. Therefore, the students we will have for the 1993-94 contract year are Heflin, Letts, Moradkhanian. We anticipate accepting a new student to replace Altice and another student when Heflin leaves the group.

The 1992-93 contact year has been very difficult for us financially because of the increase in OPAL running costs, inflation and the eroding exchange rate. We would not have been able to manage if we did not receive generous support from the University. The University provided part of the summer salaries of Shen and VanDalen in consideration of their services respectively as Associate Dean and Chairperson during the academic year. The University also provided some salary support for research personnel for our group. In the area of computing, the University provided computer hardware as part of the startup support for Gary, which makes up the HP UNIX cluster of workstations for the OPAL Monte Carlo work. It also provided one HP

workstation for the analysis of RD5 data and for the design of CMS detector through Monte Carlo simulation.

The budget requested for the 1993-94 contract year represents the very bare minimum. While there is practically no change in personnel, both at the Ph.D. level and in graduate students, our salary burden has increased because of the decreased support from the University as a result of the large State budget deficit. In addition, both Shen and VanDalen will not receive summer salary support from the University when they complete their terms of administrative services on June 30, 1993. The increase in the OPAL operations costs is compounded by the devaluation of the dollar.

Bibliography

- [1] "Measurement of LEP Beam Energy by Resonant Depolarization," CERN-PPE/92-49.
- [2] OPAL Collaboration, M. Arignon *et al.*, Nucl. Inst. and Meth. in Phys. Res. **A313** (1991) 275.
- [3] OPAL Physics Note PN-051.
- [4] OPAL Collaboration, Zeit. Phys. **C52** (1991), 175.
- [5] D. Bardin, *et al.*, Comp. Phys. Comm. **59** (1990) 303;
D. Bardin, *et al.*, Z. Phys. **C44** (1989) 493;
D. Bardin, *et al.*, Nucl. Phys. **B351** (1991) 1;
D. Bardin, *et al.*, Phys. Lett. **B229** (1989) 405.
D. Bardin, *et al.*, CERN-TH 6443/92 (May 1992)
- [6] Bhabha line shape program ALIBABA, W. Beenakker, *et al.*, Nucl. Phys. **B349** (1991) 323.
- [7] M. Consoli and W. Hollik, Z Physics at LEP1, CERN 89-08, ed. G. Altarelli, *et al.*, Vol 1 (1989) 7.
- [8] S.G. Gorishny, A.L. Kataev and S.A. Larin, Phys. Lett. **B259** (1991) 144.
- [9] K.G. Chetyrkin and J.H. Kühn, Phys. Lett. **B248** (1990) 359, W.J. Marciano, Phys. Rev. **D29** (1984) 580.
- [10] M.Z. Akrawy, *et al.*, CERN-PPE/92-18 (Feb. 1992), submitted to Z. Phys. C
- [11] The LEP Collaborations: ALEPH, DELPHI, L3 and OPAL, CERN-PPE/91-232.
- [12] C.L. Basham *et al.*, Phys. Rev. Lett. 41 (1978) 1585; Phys. Rev. **D17** (1978) 2298.
- [13] OPAL Collab., P.D. Acton *et al.*, Phys. Lett. **B276** (1992) 547.

- [14] OPAL Collab., P.D. Acton et al., CERN-PPE/92-18.
- [15] the definition of these variables is given in Z. Kunszt, P. Nason, G. Marchesini and B.R. Webber, "QCD" in "Z Physics at LEP 1", CERN 89-08, vol. 1, eds. G. Altarelli, R. Kleiss and C. Verzegnassi (Geneva 1989).
- [16] OPAL Collab., P.D. Acton et al., CERN-PPE/92-89.
- [17] OPAL Collab., M.Z. Akrawy et al., Phys. Lett. B247 (1990) 617.
- [18] D. Amati and G. Veneziano, Phys. Lett. B83 (1979) 87;
Ya.I. Azimov et al., Z. Phys. C27 (1985) 65.
- [19] OPAL Collab., P.D. Acton et al., CERN-PPE/92-116.
- [20] J.W. Gary, "An update of the OPAL study on quark-gluon jet differences,"
OPAL internal physics note OPAL-PN063 (1992).
- [21] OPAL Collab., G. Alexander et al., Phys. Lett. B265 (1991) 462.
- [22] T. Sjöstrand, Comp. Phys. Comm. **39** (1986) 347 and CERN-TH.6488/92.
- [23] L3 Collaboration, B. Adeva et al, Phys. Lett. **B259** (1991) 119.
- [24] E. Ma and J. Okada, Phys. Rev. Letters **41** (1978) 287.
- [25] M.Z. Akrawy, et al., Zeitschrift fuer Physik **C50** (1991) 373-384.
- [26] M.Z. Akrawy, et al., Phys. Lett. **B240** (1990) 261-270.
- [27] P.D. Acton et al., Phys. Lett. **B273** (1991) 338-354.
- [28] G. Alexander, et al., Phys. Lett. **B266** (1991) 201-217.
See also OPAL Physics note PN026.
- [29] S. Jadach et al., "Z Physics at LEP1," CERN 89-08, ed. G. Altarelli et al., Vol. 1(1989)235-265
- [30] "Tau decays as polarization analysers," André Rougé, Invited talk given at the Workshop on Tau Lepton Physics, Orsay, France, (1990)
- [31] Particle Data Group, J.J. Hernandez et al., Phys. Lett. **239B** (1990), pVI.14.
- [32] B.C. Barish and R. Stroynowski, Phys. Rep. **157** (1988) 1.
- [33] T.N. Truong, Phys. Rev. **D30** (1984) 1509.
F.J. Gilman and S.H. Rhie, Phys. Rev. **D31** (1985) 1066.
K.G. Hayes and M.L. Perl, Phys. Rev. **D38** (1988) 3351.

- [34] ALEPH Collaboration, D. Decamp *et al.*, CERN-PPE/91-186 (1991), submitted to *Z.Phys. C*.
L3 Collaboration, B. Adeva *et al.*, *Phys. Lett.* **B265** (1991) 451.
- [35] ARGUS Collaboration, H. Albrecht *et al.*, DESY/91-084, July 1991.
- [36] K. Riles, *Proceedings of Particles and Fields 91, Vol. 1*, Univ. of British Columbia, Vancouver, August 1991.
- [37] HRS Collaboration, S. Abachi *et al.*, *Phys. Rev.* **D40** (1989) 902.
- [38] CELLO Collaboration, H.J. Behrend *et al.*, *Phys. Lett.* **B222** (1989) 163.
CELLO Collaboration, H.J. Behrend *et al.*, *Z.Phys.* **C46** (1990) 537.
- [39] J. Allison *et al.*, *Comp. Phys. Comm.* **47** (1987) 55;
D. R. Ward, *Proceedings of the MC'91 Workshop*, NIKHEF, Amsterdam, 1991.
J. Allison *et al.*, CERN-PPE/91-234 (1991), to be published in *Nucl. Instr. and Meth.*
- [40] OPAL Collaboration, G. Alexander *et al.*, *Z. Phys.* **C52** (1991) 175.
- [41] OPAL Collaboration, G. Alexander *et al.*, *Phys. Lett.* **B266** (1991) 201.
- [42] S. Jadach, J.H. Kuhn, and Z. Was, *Comp. Phys. Comm.* **64** (1991) 275; TAUOLA.
S. Jadach, B.F.L. Ward, and Z. Was, *Comp. Phys. Comm.* **66** (1991) 276; KORALZ, Version 3.7.
- [43] M. Böhm, A. Denner and W. Hollik, *Nucl. Phys.* **B304** (1988) 687;
F.A. Berends, R. Kleiss, W. Hollik, *Nucl. Phys.* **B304** (1988) 712; BABAMC.
- [44] T. Sjöstrand, *Comp. Phys. Comm.* **39** (1986) 347; JETSET.
- [45] R. Bhattacharya, J. Smith, G. Grammer, *Phys. Rev.* **D15** (1977) 3267;
J. Smith, J.A.M. Vermaseren, G. Grammer, *Phys. Rev.* **D15** (1977) 3280.
- [46] G. B. Gelmini and M. Roncadelli, *Phys. Lett.* **B99** (1981) 411.
- [47] R. N. Mohapatra and J. D. Vergados, *Phys. Rev. Lett.* **47** (1981) 1713.
- [48] V. Barger, H. Baer, W. Y. Keung and R. J. N. Phillips, *Phys. Rev.* **D26** (1982) 218.
- [49] J. F. Gunion, H. E. Haber, G. L. Kane, and S. Dawson, *The Higgs hunter's guide*, (Addison-Wesley, 1990)

- [50] J. A. Grifols, A. Mendez, and G. A. Schuler, *Modern Physics Letters* **A4** (1989) 1485.
- [51] M. L. Swartz, *Phys. Rev.* **D40** (1989) 1521.
- [52] D. Chang and W. Keung, *Phys. Rev. Lett.* **62** (1989) 2583;
F. Hoogeveen, *Z. Phys.* **C44** (1989) 259.
- [53] Mark II Collaboration, M. Swartz et al., *Phys. Rev. Lett.* **64** (1990) 2877.
- [54] F. A. Berends and R. Kleiss, *Nuclear Physics* **B260** (1985) 32.
- [55] P. Acton, et al., *Phys. Lett.* **B254** (1991) 293-302.
- [56] J. Ellis, G. Ridolfi, F. Zwirner, CERN-TH.5946/90,
H.E. Haber and R. Hempfling, SCIPP-90/41,
R. Barbieri and M. Frigeni, IFUP-TH 2/91.
- [57] M. Della Negra, et al., CERN/DRDC/90-36.
- [58] H. van der Graaf, *Nucl. Instr. and Meth. in Phys. Res.* **A307** (1991) 220.
- [59] R. Santonico and R. Cardarelli, *Nucl. Instr. and Meth. in Phys. Res.* **A187**
(1981) 337,
R. Cardarelli, et al., *Nucl. Instr. and Meth. in Phys. Res.* **A263** (1988) 20.
- [60] F.S. Merritt et al., *Nucl. Instr. and Meth. in Phys. Res.* **A245** (1986) 27.
P.H. Sandler et al., *Phys. Rev.* **D42** (1990) 759.
- [61] T. Dombek, et al., *Phys. Lett.* **B194** (1987) 591.
- [62] D. Koetke et al., submitted to *Phys. Rev. C*.
- [63] X. Q. Lu, et al.. LSND Proposal, Los Alamos Meson Physics Facility, 1989.

Task B: Theory

a) Introduction

The High Energy Physics Theory Program at UC Riverside has continued to be active and productive in the past year. Since July 1991, there have been 19 completed research papers (UCRHEP-T81 to UCRHEP-T99). They are listed under **Publications** (Section c) together with 11 other papers which were listed in last year's report as yet to be published but are now published. Of the 24 papers with definite publication information, 7 are in letter journals: 3 in Phys. Rev. Lett., 2 in Phys. Lett. B, and 2 in Mod. Phys. Lett. A; and 3 others are in the Rapid Communications section of Phys. Rev. D.

The Theory Group has consisted mainly of E. Ma (Professor), J. Wudka (Assistant Professor), H. Kikuchi (Postgraduate Researcher since September 1991), J. Pantaleone (Postgraduate Researcher until October 1991), T. V. Duong and K. McIlhany (Graduate Student Research Assistants). Mr. McIlhany has now joined the experimental high-energy physics group of Prof. VanDalen, but 2 other students (J. Perez and M. Roy) are expected to join us in October 1992.

In Section b) the research activities of the Theory Group since July 1991 are discussed. In Section c) there is a list of completed or published papers since July 1991. In Section d) travel activities of the group are described and visitors to Riverside noted. In Section e) there is a list of personnel and there are statements concerning their needs. In Section f) the future research plans of Ma and Wudka are outlined.

b) Research Program

Since July 1991, E. Ma has completed 9 papers for publication. They are described briefly below.

It was observed by CLEO some time ago that the $\Upsilon(4S)$ had an unexpectedly large rate of decay into high-momentum J/ψ 's. This effect was subsequently dismissed as background fluctuation, but perhaps it is not entirely absent, only that it is present at a reduced level. If so, it may be interpreted as coming from the mixing of a 4-quark state with the $\Upsilon(4S)$. E. Ma, J. Pantaleone, and S. Uma Sankar proposed in Paper 12 that this 4-quark state is of the form $(bq)(\bar{b}q)$ where $q = u$ or d , such that bq forms a tightly bound color-sextet spin-zero diquark.

In a short note (Paper 16), E. Ma, S. Pakvasa, and S. F. Tuan pointed out that if the

apparent τ lifetime discrepancy is due to the mixing of a fourth generation of leptons containing a massive neutral lepton instead of a light neutrino, there is a window of opportunity for the decay of the Z boson into it and ν_τ or the corresponding charged lepton and τ at the level of 10^{-5} in branching fraction.

Current electroweak precision measurements of M_Z , $\sin^2 \theta_W$, etc. tend to prefer negative values of the oblique radiative parameters, S and T , relative to their standard-model expectations. E. Ma and P. Roy proposed in Paper 17 to consider the addition of colorless fermions in the anomaly-free combination of two doublets $(N_1, E)_L$, $(E^c, N_2)_L$, and one singlet N_{3L} , which are contained in some supersymmetric or E_6 extensions of the standard model. It was found that negative S and T were possible from the 3×3 Majorana mass matrix of the neutral fermions, but S can never be negative enough to be of order -1 .

Returning to the τ lifetime problem, it was proposed by X. Li and E. Ma over 10 years ago (Phys. Rev. Lett. 47, 1788 (1981)) before any such data were published that $e - \mu - \tau$ universality was only an accidental approximate symmetry analogous to flavor $SU(2)$ and $SU(3)$. A specific gauge model based on $U(1) \times SU(2)_1 \times SU(2)_2 \times SU(2)_3$ was constructed and it was predicted that the τ lifetime should be longer than what it would be in the standard model, in agreement with what is now observed. In Paper 21, X. Li and E. Ma show also that this model is consistent with other precision electroweak measurements, and in particular it contributes negatively to the ρ parameter measured at the Z peak. Paper 28 is a much more detailed account with updated experimental results.

In Papers 23 and 24, E. Ma discussed the above model in 2 conference proceedings with some additional numerical work both before and after new data from LEP on the τ lifetime and leptonic branching fractions and data from BEPC on m_τ . The discrepancy expressed by $\xi - 1$ has gone from 0.027 ± 0.012 to 0.015 ± 0.008 .

In Paper 26, E. Ma speculated on m_t and m_H . Assuming the vanishing of the standard-model quadratic divergence and its local variation with mass scale in the absence of the QCD coupling, it was deduced that $m_t \simeq 117 \text{ GeV}$ and $m_H \simeq 183 \text{ GeV} \simeq 2M_Z$.

In Paper 27, T. V. Duong and E. Ma discuss the possible decay of the Z boson into scalar particles. This may be important for multi-Higgs models because some of the physical scalar particles may be required to be light or even massless from symmetry considerations. For illustration, a recent model by E. Ma (Paper 9) of the 17 keV neutrino is used for specific calculations.

Since July 1991 José Wudka has completed six papers for publication, which are summarized below.

In an invited talk by J. Wudka presented at the *Topical Conference on Precise Electroweak Measurements*, (Santa Barbara, CA 21-23 Feb. 1991) it was pointed out that in many instances the basic rationale for predicting the magnitude of effects from physics underlying the standard model was flawed. It was emphasized that a sound approach was to study this problem using effective lagrangians and examples of the subsequent modifications to previously published predictions were given. This approach was expanded and carefully spelled out at the talk presented at the *Int. Workshop on Electroweak Symmetry Breaking*, in Hiroshima, Japan (1991) (paper 19). This has been a topic of interest in the community, though some confusion still remains regarding a consistent way of doing loop calculations within this approach. To fill this gap a sample calculation, where all the important points are illustrated, was performed (paper 30). These two publications summarize the effective lagrangian approach to physics beyond the standard model, both its philosophy and its calculational details.

In collaboration with H. Kikuchi, J. Wudka revisited the $U_A(1)$ problem (paper 22). They found that the assumption of instantons behaving as an *interacting* gas, where the leading long distance interactions are given by the η' exchange, provides a solution to this long-standing puzzle. They found that their results coincide, with those obtained using large N approximations, with the improvement that there is no need to introduce fictitious ghosts to alleviate problems with positivity.

In collaboration with M. Einhorn, J. Wudka studied the effects of heavy scalars on low energy observables in gauge theories (paper 29). They provided a general set of conditions which, when satisfied, will insure that all observables currently accessible to observation will receive negligible radiative corrections from heavy scalars. This is a well known effect in the standard model (the "screening theorem"). This investigation gives the generalization to an arbitrary gauge theory with an arbitrary scalar sector. As an application they studied an arbitrary (natural) left-right symmetric model, and determined that, in view of current experimental data, it must contain scalar excitations with masses of the same order as those of the right handed vector bosons.

In collaboration with M. Velkovsky, a student at UCR, J. Wudka studied the standard model in the case where the usual doublet is replaced by an arbitrarily large multiplet. They find that, just as is the case for simpler systems, the physical Higgs mass is set by the Fermi constant, even if the mass parameter in the Lagrangian is much larger than this scale. This

is of relevance for triviality issues pertaining the standard model. They also calculated the S , T and U parameters and found that, while T vanishes, both S and U can take arbitrary values.

In a talk presented at the *Workshop on High Energy Neutrino Astrophysics* (Univ. of Hawaii, Manoa, March 23–26, 1992) J. Wudka outlined the situations under which neutrinos can undergo left-right transitions in the presence of an intense gravitational field. These effects become of interest in the presence of a very massive black hole and could have an impact on the flux predictions for quasar neutrino astronomy.

Since July 1991, **Hisashi Kikuchi** has completed three papers for publication. They are described briefly below.

In order to estimate the baryon- and lepton-number non-conserving scattering amplitude in the standard model at high energy collision, one has to answer the question, that is, how can one extract the non-perturbative contribution from the perturbative one: more closely separated instanton–anti-instanton configurations become important for the estimation at the higher energy process, and they are hardly distinguishable from perturbative fluctuation. Developing the “new valley method” (Nucl. Phys. B369, 219, (1992)) which he has suggested in collaboration with H. Aoyama, H. Kikuchi showed how to evaluate the Borel function of the path-integral and how to separate the two different contributions in terms of the Borel transform (Phys. Rev. D45, 1240 (1992)). Although it is not included in the list of publication, the final version of this paper was completed at UCR.

In collaboration with J. Wudka, H. Kikuchi shed a new light on the $U(1)$ problem in QCD (Paper 22). It was found that the assumption of the existence of the interaction between instantons and η' -mesons, which is a natural consequence of the Adler-Bell-Jackiw anomaly and chiral condensation of QCD vacuum, induces effective mass to the propagation of η' in the instanton gas. This interacting instanton gas approach gives η' -mass formula consistent with that derived by $1/N$ -expansion and provides a more integrated view point than the ideal instanton gas approach.

Non-negligible instanton effect in favour of the resolution of the $U(1)$ problem naively leads one to another long-standing problem – strong CP problem. The equivalence of the chiral angle, the phase of the determinant of quark mass matrix, to the vacuum angle brings important constraints on looking into physics underlying the standard model. Although the equivalence has been taken for granted since the recognition of the problem in 1976, it has not been necessarily clear for massive quarks. H. Kikuchi studied the quark path-integral and clarifies the equivalence for arbitrary mass matrix elements (Paper 25).

c) Publications

The following list contains work published or completed by the Riverside Theory Group since July 1991.

1. UCRHEP-T62: "What if There is Really No Top?," E. Ma, in Proc. of 25th International Conference on High Energy Physics, Singapore, August (1990), edited by K. K. Phua and Y. Yamaguchi (South East Asia Theoretical Physical Association and the Physical Society of Japan), p. 806 (1991).
2. UCRHEP-T67: "Decaying Dirac Neutrinos," A. Acker, S. Pakvasa, and J. Pantaleone, Phys. Rev. D45, R1 (1992).
3. UCRHEP-T68: " $S_3 \times Z_3$ Model of Lepton Mass Matrices," E. Ma, Phys. Rev. D44, R587 (1991).
4. UCRHEP-T69: "Non-MSW Solutions to the Solar Neutrino Problem," J. Pantaleone, in Proc. of Trends in Astroparticle Physics, Santa Monica, California, November 1990, edited by D. Cline and R. D. Peccei, p. 356.
5. UCRHEP-T71: "Weak Neutrinos in Strong Gravity," J. Wudka, in Proc. of the 4th Mexican School of Particles and Fields, Oaxtepec, Mexico, December 1990, World Scientific, Singapore, 1992; p. 406.
6. UCRHEP-T72: "Adiabatic Phases and Group Theory," J. Wudka, J. Phys. A25, 2945 (1992).
7. UCRHEP-T73: "Gravitational Effects on Neutrino Oscillations," J. Wudka, Mod. Phys. Lett. A6, 3291 (1991).
8. UCRHEP-T74: "Variant of the $S_3 \times Z_3$ Model for the 17 keV Neutrino," T. V. Duong and E. Ma, Phys. Rev. D45, 2570 (1992).
9. UCRHEP-T77: "Custom-Designed Model of the 17 keV Neutrino," E. Ma, Phys. Rev. Lett. 68, 1981 (1992).
10. UCRHEP-T78: "Dirac Neutrino Helicity Flip in Dense Media," J. Pantaleone, Phys. Lett. B268, 227 (1991).
11. UCRHEP-T79: "Unified Description of Quark and Lepton Mass Matrices," E. Ma, in Proc. of the Second Winter School on Cosmology and Elementary Particles, Rio Piedras, Puerto Rico, (April 1991), edited by D. R. Altschuler et al. (World Scientific, Singapore, 1992), p. 267.

12. UCRHEP-T81: "Is there a Four-Quark State near the $B\bar{B}$ Threshold?", E. Ma, J. Pantaleone, and S. Uma Sankar, Phys. Rev. D 46, 463 (1992).
13. UCRHEP-T82: "Measuring $|V_{ub}|$ via Nonleptonic Decays of B Mesons," D. Choudhury, D. Indumati, A. Soni, and S. Uma Sankar, Phys. Rev. D45, 217 (1992).
14. UCRHEP-T83: "Quark and Lepton Masses from the Dynamics of Four-Fermion Interactions," B. R. Desai, Phys. Rev. Lett. 68, 3838 (1992).
15. UCRHEP-T84: "Dirac Neutrinos in Dense Matter," J. Pantaleone, Phys. Rev. D (in press).
16. UCRHEP-T85: " τ Non-Universality?", E. Ma, S. Pakvasa, and S. F. Tuan, Particle World 3, 27 (1992).
17. UCRHEP-T86: "Negative, Anomaly-Free, Oblique Radiative Corrections," E. Ma and P. Roy, Phys. Rev. Lett. 68, 2879 (1992).
18. UCRHEP-T87: "A Large N Standard Model," M. Velkovsky and J. Wudka, submitted to Phys. Rev. D.
19. UCRHEP-T88: "Effective Lagrangian Description of Precision Measurements or How to Parametrize Ignorance," M. B. Einhorn and J. Wudka, in Proc. of Workshop on Electroweak Symmetry Breaking, Hiroshima, Japan, November (1991).
20. UCRHEP-T89: "Neutrinos in the Mist", J. Wudka, in Proc. of the Workshop of High Energy Neutrino Astrophysics, Univ. of Hawaii, Manoa, March 23-26, 1992.
21. UCRHEP-T90: "Generation Nonuniversality and Precision Electroweak Measurements," X. Li and E. Ma, Phys. Rev. D (Rapid Communication, in press).
22. UCRHEP-T91: "Screening in the QCD Instanton Gas and the U(1) Problem," H. Kikuchi and J. Wudka, Phys. Lett. B (in press).
23. UCRHEP-T92: "Longer Tau Lifetime and Negative T," E. Ma, in Proc. of XXVII Rencontres de Moriond: Electroweak Interactions, Les Arcs, France, March (1992).
24. UCRHEP-T93: "Accidental Approximate Generation Universality and its Possible Verification," E. Ma, in Proc. of Beyond the Standard Model III, Ottawa, Canada, June (1992).
25. UCRHEP-T94: "Chiral Phase Dependence of the Massive Fermionic Path Integral," H. Kikuchi, submitted to Phys. Rev. D.
26. UCRHEP-T95: "Fixing the Top-Quark and Higgs-Boson Masses," E. Ma, Mod.

Phys. Lett. A (in press).

27. UCRHEP-T96: "Decay of the Z Boson into Scalar Particles," T. V. Duong and E. Ma, submitted to Phys. Rev. D.

28. UCRHEP-T97: "Gauge Model of Generation Nonuniversality Reexamined," X. Li and E. Ma, submitted to Phys. Rev. D.

29. UCRHEP-T98: "Screening of Heavy Scalars beyond the Standard Model," M.B. Einhorn and J. Wudka, submitted to Phys. Rev. D.

30. UCRHEP-T99: "Effective Lagrangian approach to precision measurements: the anomalous magnetic moment of the muon," C. Arzt and J. Wudka, submitted to Phys. Rev. D.

d) Travel and Consultants

E. Ma attended the First Linear Collider Workshop (Saariselka, Finland) in September 1991 and gave a talk on "Leptophilic New Z's." In December 1991, he attended the Workshop on the 17-keV Neutrino Question (Berkeley, California) and gave a talk on his "Custom-Designed Model of the 17-keV Neutrino." He then gave seminars at the University of California, Irvine in February 1992, and at Brookhaven National Laboratory in March, after which he attended the XXVIIIth Rencontres de Moriond: Electroweak Interactions (Les Arcs, France) and gave a talk. In April, he attended the SSC Symposium (Madison, Wisconsin), gave a talk and chaired a session, after which he visited McGill University (Montreal, Canada) and gave a seminar. Finally in June 1992, he attended the Beyond the Standard Model III Conference in Ottawa, Canada and gave a talk.

J. Wudka presented an invited lecture at the Workshop on High Energy Neutrino Astrophysics, Univ. of Hawaii, Manoa, March 23-26, 1992. He also gave invited seminars at Purdue University and at the University of Michigan, and attended the symposium celebrating Caltech's 100-th anniversary. He will be a participant at the Aspen Summer Institute (1992).

Visitors who gave high-energy theory seminars/colloquia include P. Roy (Tata Institute, Bombay), M. Einhorn (Santa Barbara), B. Grzadkowski (Davis), K. Choi (San Diego), D. Ng (North Carolina), J. Gunon (Davis), Z. Gao (Beijing), B. Haeri (Purdue), R. Volkas (Melbourne), T. Yanagida (Tohoku Univ., Sendai), X. He (Melbourne), N. Uraltsev (Notre Dame), and T. Vachaspati (Tufts). Three visitors spent up to 1 month each at Riverside to collaborate on research: P. Roy and X. Li with E. Ma, and J. Vidal with J. Wudka.

e) Personnel and Needs

Two faculty members are covered by this proposal: E. Ma (Professor) and J. Wudka (Assistant Professor), for whom 2 months of summer salary are requested. H. Kikuchi will continue to be Postgraduate Researcher (100%). Graduate Research Assistants will be T. V. Duong, J. Perez, and M. Roy.

Two foreign trips are planned, at about \$3,000 each, to conferences such as the European High Energy Physics Conference and the International Conference on Neutral Currents. Four domestic trips are planned, at about \$1,500 each, to conferences such as APS meetings and various other workshops and summer institutes yet to be announced. About \$2,000 is requested for visitors. A total of \$8,000 is needed for supplies and expenses.

f) Future Research Plans

In the immediate future, E. Ma plans to work on two projects. Together with X. Li (Institute of Theoretical Physics, Beijing), he will update further the phenomenological consequences of their gauge model of generation nonuniversality (Papers 21, 28), with special emphasis on rare K and B decays, as well as CP nonconservation. With the anticipated data from Brookhaven on K's and Cornell on B's in the next few years, their results will be useful in identifying key experimental observations which may signal support or go against the idea of generation universality as only an accidental approximate symmetry.

The 17-keV neutrino remains controversial experimentally. Theoretical interests, on the other hand, are considerable because there are important astrophysical and cosmological implications for any such massive neutrino even if its mixing with the electron neutrino is too small to be observed in beta decay. Building models to fit in a 17-keV neutrino helps one to focus on many of these issues, and may open up one's vision to a pattern of neutrino masses unencumbered by the usual prejudice of the quark mass matrices and the see-saw mechanism. E. Ma has been asked to write a Brief Review on this subject for Mod. Phys. Lett. A.

In the future J. Wudka intends to further most of the areas of investigation considered during this past year.

In a collaboration with M. Einhorn, J. Wudka will revisit a proposed gauge fixing condition of theirs which allowed many technical simplifications in their studies of the screening of heavy scalars in gauge theories. This gauge fixing condition has found other applications in the study of heavy quark effects and in the equivalence theorem. The point they wish to

investigate is the dependence of the effective action on the gauge parameter.

J. Wudka will investigate several aspects of the effective lagrangian approach to physics beyond the standard model, concentrating on the possible corrections to the anomalies stemming from these effects (with careful attention paid to the Adler-Bardeen theorem). In collaboration with M.A. Perez, J. Wudka will start to investigate the effects of physics beyond the standard model on processes involving scalars at the SSC and LHC.

He and H. Kikuchi will study various aspects of the $U(1)$ problem. In particular, they will investigate the condition under which canonical commutation relations can be applied to obtain anomalous sum rules in QCD.

In the area of neutrino physics J. Wudka is completing a publication with J. Vidal in the area of solar neutrinos. In this publication they respond to various criticisms levelled at a previous publication where the solar neutrino puzzle was explained on the basis of a small neutrino magnetic moment and the presence of a topological phase. They argue that these criticisms were unfounded and provide physical conditions under which their results will hold. Taking into account the recent data from Gallex, their results will provide a stringent upper bound on the neutrino magnetic moment.